

Geology of the Kroonstad
Kimberlite Cluster,
South Africa

Geoffrey H. Howarth

January 2010

Thesis submitted in fulfilment of the requirements for
the degree of Master of Science in the Department of
Geology, Rhodes University.

Abstract

The Cretaceous (133Ma) Kroonstad Group II Kimberlite Cluster is located approximately 200km south west of Johannesburg on the Kaapvaal Craton. The cluster is made up of six kimberlite pipes and numerous other intrusive dike/sill bodies. Three of the pipes are analysed in this study, which includes the: Voorspoed, Lace (Crown) and Besterskraal North pipes. These pipes were emplaced at surface into the Karoo Supergroup, which is comprised of older sedimentary rocks (300-185Ma) overlain by flood basalts (185Ma). At depth the pipes have intruded the Transvaal (2100-2600Ma) and Ventersdorp (2700Ma) Supergroups, which are comprised dominantly of carbonates and various volcanic units respectively. The pipes have typical morphology of South African pipes with circular to sub-circular plan views and steep 82° pipe margins. The Voorspoed pipe is 12ha in size and is characterised by the presence of a large block of Karoo basalt approximately 6ha in size at the current land surface. This large basalt block extends to a maximum of 300m below the current land surface. The main Lace pipe is 2ha in size with a smaller (<0.5ha) satellite pipe approximately 50m to the west. No information is available on the morphology of the Besterskraal North pipe as it is sub-economic and no mining has occurred. Samples from the Besterskraal North pipe were collected from the De Beers archives. The Kroonstad Cluster has been subjected to approximately 1750m of erosion post-emplacment, which has been calculated by the analysis of the crustal xenoliths with the pipe infill.

The hypabyssal kimberlite from the three pipes shows a gradational evolution in magma compositions, indicated by the mineralogy and geochemistry. The Lace pipe is the least evolved and has characteristics more similar to Group I kimberlites. The Voorspoed and Besterskraal North kimberlite are intermediately and highly evolved respectively. The gradational evolution is marked by an increase in SiO_2 and Na_2O contents. Furthermore the occurrence of abundant primary diopside, aegirine, sanidine, K-richterite and leucite indicates evolution of the magma. The root zones of the pipes are characterised by globular segregatory transitional kimberlite, which is interpreted to be hypabyssal and not the result of pyroclastic welding/agglutination. The hypabyssal transitional kimberlite (HKt) is characterised by incipient globular segregatory textures only and the typical tuffisitic transitional kimberlite (TKt) end member (Hetman et al. 2004) is not observed. The HKt contact with the overlying volcanoclastic kimberlite (VK) infill is sharp and not gradational.

The presence of HKt in the satellite blind pipe at Lace further indicates that the distinct kimberlite rock type must be forming sub-volcanically. The HKt is distinctly different at the Voorspoed and Lace pipes, which is likely a result of differing compositions of the late stage magmatic liquid. Microlitic clinopyroxene is only observed at the Lace HKt and is interpreted to form as a result of both crustal xenolith contamination and CO₂ degassing. Furthermore the HKt is intimately associated with contact breccias in the sidewall. The root zones of the Kroonstad pipes are interpreted to form through the development of a sub-volcanic embryonic pipe.

The volcanoclastic kimberlite (VK) infill of the Kroonstad pipes is not typical of South African tuffisitic Class 1 kimberlite pipes. The VK at Voorspoed is characterised by numerous horizontally layered massive volcanoclastic kimberlite (MVK) units, which are interpreted to have formed in a deep open vent through primary pyroclastic deposition. MVK is the dominant rock type infilling the Voorspoed pipe, however numerous other minor units occur. Normally graded units are interpreted to form through gravitational collapse of the tuff ring. MVK units rich in Karoo basalt and/or Karoo sandstone are interpreted to form through gravitational sidewall failure deep within an open vent. Magmaclasts are interpreted to form in the HKt during the development of an embryonic pipe and therefore the term autolith or nucleated autolith may be applied. Debate on the validity of the term nucleated autolith is beyond this study and therefore the term nucleated magmaclast is used to refer to spherical magmaclasts in the VK.

The emplacement of the Kroonstad pipes is particularly complex and is not similar to typical Class 1 tuffisitic kimberlites. However the initial stage of pipe emplacement is similar to typical South African kimberlites and is interpreted to be through the development of an embryonic pipe as described by Clement (1982). The vent clearing eruption is interpreted to be from the bottom up through the exsolution of juvenile volatiles and the pipe shape is controlled by the depth of the eruption (+/-2km) (Skinner, 2008). The initial embryonic pipe development and explosive eruption is similar to other South African kimberlites, however the vent is cleared and left open, which is typical of Class 2 Prairies type and Class 3 Lac de Gras type pipes. The latter vent infilling processes are similar to Class 3 kimberlites from Lac de Gras and are dominated at the current level by primary pyroclastic deposition.

Contents

Section 1. Introduction	1
1.1. Previous Work on the Kroonstad Kimberlite Cluster	4
1.1.1. Lace (Crown) Kimberlite	5
1.1.2. Voorspoed Kimberlite	7
1.1.3. Besterskraal North Kimberlite	8
1.2. Kroonstad Kimberlite Cluster Regional Geology	11
1.2.1. Ventersdorp Supergroup	12
1.2.2. Transvaal Supergroup	13
1.2.3. Karoo Supergroup	14
1.2.3.1. Dwyka Group	14
1.2.3.2. Ecca Group	15
1.2.3.3. Beaufort Group	16
1.2.3.4. Molteno, Elliott and Clarens Formations	17
1.2.3.5. Drakensberg Group	18
Section 2. Methodology	19
2.1 Terminology	19
2.2 Drill core sampling/logging	24
2.3 Petrographic modal analysis	26
2.4 Geochemistry	26
2.5 Mineral composition	27
2.6 Petrographic interest rating	27
Section 3. Geology of the Kroonstad Kimberlite Cluster	29
3.1 Lace (Crown) Kimberlite Pipe	30
3.1.1 Introduction	30
3.1.2 Group II Hypabyssal Kimberlite (HK) Sensu Stricto (Sample K2-1)	35
3.1.3 Hypabassal Transitional Kimberlite and Kimberlite Breccia (HKt/HKtB)	37
3.1.4 Volcaniclastic Kimberlite	51
3.1.4.1 Basalt-rich VKB (Samples K2-9 and K2-D)	52
3.1.4.2 Quartz-rich VKB (Samples K2-A and K2-B)	55
3.2 Voorspoed Kimberlite Pipe	57
3.2.1 Basalt Megablock	59
3.2.2 Distribution and Macroscopic Description of the Volcaniclastic Kimberlite	61
3.2.2.1 Initial Eruption Zone (IEZ)	61
3.2.2.2 Central Eruption Zone (CEZ)	67
3.2.3 Hypabyssal Kimberlite	72

3.2.3.1 Hypabyssal Sill (K1/111)	72
3.2.3.2 Hypabyssal Dikes	75
3.2.3.3 Other Hypabyssal Varieties	78
3.2.4 Hypabyssal Transitional Kimberlite Breccia (HKtB) and Contact Breccias	80
3.2.4.1 Hypabyssal Transitional Kimberlite Breccia (HKtB) (Sample 9/2)	80
3.2.4.2 Contact Breccias	83
3.2.5 Volcaniclastic Kimberlite	85
3.2.5.1 Upper-crustal Xenoliths	87
3.2.5.2 Basement Xenoliths	89
3.2.5.3 Magmaclasts	82
3.2.5.4 Interclast Material	95
3.2.6 Petrographic Descriptions of representative samples of the Massive Volcaniclastic Kimberlite (MVK) varieties	96
3.2.6.1 Type 1 (a) Massive Volcaniclastic Kimberlite (T1aMVK) (Sample 9-145)	97
3.2.6.2 Soft Massive Volcaniclastic Kimberlite (sMVK) (Sample 7/1; Skinner collection)	99
3.2.6.3 Atypical Massive Volcaniclastic Kimberlite (aMVK) (Sample 9-288)	100
3.2.6.4 Type 1 b Massive Volcaniclastic Kimberlite (T1bMVK) (Sample 3/1; Skinner collection)	102
3.2.6.5 Intermediate Massive Volcaniclastic Kimberlite (intMVK) (Sample 3/3; Skinner collection)	104
3.2.6.6 Type 2 Massive Volcaniclastic Kimberlite (T2MVK) (Sample 2/4; Skinner collection)	104
3.2.6.7 Fine grained bands (Sample 2-280)	107
3.2.6.8 Initial Eruption Zone (IEZ) Bedded Volcaniclastic Kimberlite (BVK) (Samples 10-90)	108
3.2.6.9 Central Eruption Zone (CEZ) Bedded Volcaniclastic Kimberlite (BVK) (Sample 3-67)	109
3.2.6.10 Massive Volcaniclastic Basalt Breccia Sample (10-36)	111
3.2.6.11 Massive Volcaniclastic Sandstone Breccia (Sample 8-1)	112
3.3 Besterskraal North Kimberlite	114
3.3.1 Introduction	114
3.3.2 Hypabyssal Kimberlite	114
3.3.3 Massive Volcaniclastic Kimberlite	122

Section 4. Mineral Chemistry and Bulk Rock Geochemistry of Selected Voorspoed and Lace Kimberlite Samples.....**124**

4.1 Introduction	124
4.1.1 Evolution of Group II Kimberlite Magma	125
4.2 Mineral Composition	126

4.2.1	Paragenesis of diopside, aegirine and phlogopite at the Kroonstad Cluster	127
4.2.2	Composition	130
4.2.2.1	Diopside	130
4.2.2.2	Aegirine	132
4.2.2.3	Phlogopite	133
4.2.2.4	Microlitic Clinopyroxene at Lace HKt and HKtB	133
4.2.3	Primary diopside-titanian aegirine at other localities	134
4.2.4	Primary diopside composition at Voorspoed	134
4.2.5	Aegirine at Besterskraal North Hypabyssal Kimberlite (HK)	135
4.2.6	Epitaxial growth of aegirine	136
4.2.7	Comparison with Mitchell (1995) Voorspoed data	138
4.2.8	Evolution of phlogopite in Group II kimberlite	138
4.2.9	Evolution of phlogopite at the Kroonstad Kimberlite Cluster	139
4.2.10	Mineralogical evidence for the evolution of the Voorspoed kimberlite	141
4.2.11	Comparison of primary diopside at Voorspoed with microlitic clinopyroxene compositions	141
4.3	Bulk Rock Geochemistry	144
4.3.1	Introduction	144
4.3.2	Major element geochemistry relative to Group I kimberlites	145
4.3.3	Unevolved and Evolved Group II Geochemistry	146
4.3.4	Contamination Index	148
4.3.5	Contamination of the Voorspoed and Lace kimberlites: Indicated by geochemistry	149
4.3.5.1	Voorspoed Kimberlite	149
4.3.5.2	Lace Kimberlite	150
4.3.6	Geochemistry of the Voorspoed and Lace kimberlites	150
4.3.6.1	Voorspoed kimberlite	150
4.3.6.2	Lace kimberlite	152
4.3.7	Evolution of the magma at the Kroonstad cluster	153
4.3.8	Geochemical evidence for fractional crystallisation	154
4.3.9	Geochemical variation at the Lace kimberlite	155
4.3.9.1	Geochemical variation of the HKtB: Crustal contamination	158
4.3.9.2	Geochemical variation of the HKt: CO ₂ degassing	159
4.3.10	Comparison with the Wesselton and Dutoitspan kimberlites	159
4.3.11	Implications for microlitic clinopyroxene compositions	162
4.4	Summary	162
4.4.1	Evolution of the magma	162
4.4.2	Microlitic clinopyroxene	163
Section 5. Interpretation and Discussion		165
5.1	Erosion estimate for the Kroonstad kimberlite cluster	165
5.1.1	Methodologies for estimating erosion	165

5.1.2	Karoo Supergroup xenolith correlation	166
5.1.2.1	Sandstone Xenoliths	166
5.1.2.2	Basalt Xenoliths	167
5.1.3	Erosion estimation	168
5.1.3.1	Method 1: Palaeo-stratigraphy of the Karoo Supergroup	168
5.1.3.2	Method 2: Difference in elevation	172
5.1.3.3	Method 3: Denudation rates post-emplacement	172
5.1.4	Margin of error for estimating erosion	173
5.1.5	Depth of contact between Hypabyssal and volcanoclastic kimberlite at Kroonstad and comparison with other South African pipes	175
5.2	Classification of Kimberlite Pipes	176
5.2.1	Morphology	177
5.2.2	Pipe infill	178
5.2.3	Magmaclast characteristics	179
5.2.4	Emplacement of the pipe classes	180
5.2.5	Classification of the Kroonstad kimberlite pipes	182
5.3	Emplacement of the root zone at the Kroonstad cluster	184
5.3.1	Root zone/embryonic pipe process in kimberlite emplacement	184
5.3.1.1	Review of the embryonic pipe model for emplacement of kimberlite pipes-Clement (1982)	185
5.3.1.2	Welding in kimberlites: An alternate explanation for the formation of transitional kimberlite	188
5.3.2	Contact breccias and hypabyssal transitional kimberlite (HKt): Review of literature	190
5.3.2.1	Contact breccias	190
5.3.2.2	Contact breccias at the Voorspoed and Lace pipes	193
5.3.2.3	Transitional kimberlite	193
5.3.2.4	Transitional kimberlite at the Kroonstad cluster	196
5.3.3	Pre-development of the embryonic pipe	197
5.3.3.1	Magma ascent to the near surface	197
5.3.3.2	Fractional crystallisation, differentiation and a staging chamber	198
5.3.4	Embryonic pipe model for the initial development of the Kroonstad pipes	199
5.3.4.1	Evidence for sub-volcanic origin from the Kroonstad cluster	199
5.3.4.2	Discussion on the term nucleated autolith/magmaclast	204
5.3.4.3	Features of the embryonic pipe (HKt/HKtB) at the Kroonstad cluster relevant to formation processes	205
5.3.5	Formation of the embryonic pipe	211
5.3.5.1	Formation of microlitic clinopyroxene and calcite in the groundmass of the Lace HKt	211
5.3.5.2	Stages in the development of the embryonic pipe	214
5.3.6	Summary of emplacement	221
5.4	Volcanoclastic Kimberlite	222
5.4.1	Volcanoclastic kimberlite emplacement-review of models	222
5.4.2	Volcanoclastic kimberlite infill at the Voorspoed pipe	225

5.4.2.1 Alteration of basalt xenoliths in the volcanoclastic infill: implications for formation temperatures	225
5.4.2.2 Country rock xenolith distribution relative to the original Stratigraphy	227
5.4.2.3 Horizontal layering and concentric zoning of the volcanoclastic Kimberlite	228
5.4.3 Formation of the pipe infill	229
5.4.3.1 Massive volcanoclastic kimberlite (MVK)	229
5.4.3.2 Massive volcanoclastic basalt breccia (MVBB) and massive volcanoclastic sandstone breccia (MVSB)	232
5.4.3.3 Bedded volcanoclastic kimberlite (BVK)	233
5.4.3.4 Fine grained volcanoclastic bands	234
5.4.3.5 Basalt megablock	235
5.4.4 Role of fluidisation in the formation of the MVK	236
5.4.5 Stages in the emplacement of the volcanoclastic kimberlite	238
5.4.6 Deposits overlying the current land surface	242
5.4.7 Volcanoclastic kimberlite at the Lace pipe	242
5.5 Economics of the Voorspoed and Lace kimberlites	244
5.5.1 Petrographic interest rating	244
5.5.2 Diamond distribution in the Voorspoed volcanoclastic kimberlite	246
Section 6. Summary and Conclusion	249
6.1 Further Work	252
Section 7. References	255
Appendix 1. Major element geochemistry	
Appendix 2. Trace element geochemistry	
Appendix 3. Mineral chemistry	
Appendix 4. Borehole logs for the Voorspoed Pipe	
Appendix 5. Correlation of Voorspoed Volcanoclastic kimberlite nomenclature	
Appendix 6. Borehole logs of the Lace kimberlite core sampled	
Appendix 7. Summary of Abbreviations used in the text.	
Appendix 8. Table of Samples List	

List of Figures

Section 1 Figures

- Figure 1.1** Location of the Kroonstad Kimberlite Cluster (KKC) relative to the major kimberlite provinces on the Kaapvaal Craton (pale brown), South Africa (grey). 2
- Figure 1.2** Plan view and cross section through the Lace pie from Clement (1982). The increase in diameter of the pipe with depth is not observed from the current mining plans. 6
- Figure 1.3** Original plan view of the Voorspoed pipe showing the distribution of the Karoo basalt and consequent/antecedent dikes. Diagram from Wagner (1914). 8
- Figure 1.4** Regional geology of the Kroonstad Kimberlite Cluster. HG: Halfway House Granite; Wits.Grp: Witwatersrand Supergroup; Ventersdorp Supergroup (Klip.Grp: Klipriversberg Group; Al.F: Allanridge Formation); Transvaal Supergroup (Hek.F: Hekpoort Formation; Das.F: Daspoort Formation); Karoo Supergroup (Vry.F: Vryheid Formation; Vol.F: Volksrust Formation; Norm.F: Normandien Formation; Dol.: Karoo Dolerite) and tc: tertiary cover. Black squares indicate kimberlite pipes. The Voorspoed and Lace pipes are labelled. See table 1. For regional country rock stratigraphy. See figure 1.1 showing the position of the Kroonstad Kimberlite Cluster (KKC) in South Africa. 9
- Figure 1.5** Distribution of the Ventersdorp Supergroup. Note the position of the Kroonstad Kimberlite Cluster (KKC). Diagram after van der Westhuizen et al. (2006). 11
- Figure 1.6** Distribution of the Transvaal Supergroup. Note the position of the Kroonstad Kimberlite Cluster (KKC). Diagram after Eriksson et al. (2006). 13
- Figure 1.7** Distribution of the Karoo Supergroup in the Kroonstad area. The Kroonstad kimberlite cluster is located approximately 200km to the south west of Johannesburg. Diagram after Catuneanu et al. (2005). 15
- Figure 1.8** Karoo Supergroup (Drakesnberg Group) basalt stratigraphy. Diagram from Hanson (2006). 17

Section 3 Figures

- Figure 3.1** Photograph of the Lace pit looking west. The competent rock in the wall is the satellite pipe outcropping in the pit. The pit has been open for over a hundred years and yet no caving of the satellite pipe has occurred indicating the highly competent nature. 31
- Figure 3.2** East-west cross-section of the Lace pipe showing the distribution of the internal geology to a depth of 780m from the current land surface. Pipe outlines based on the schematic diagrams at the Lace mine. Boreholes C6 and C7 are illustrated with depth of borehole given every 100m. Depths given on the left are depth below the surface. The main pipe is occupied by variable distribution of HKt /HKtB. Further detailed logging needs to be done to map the distribution of the HKt and HKtB. The satellite pipe is occupied by HKtB only. See appendix 6 for the borehole logs for hole C6 and C7. See appendix 7 for a full list of abbreviations used in the diagram and text. The HKt/HKtB is described in detail in section 3.1.3 and photomicrographs are shown in figure 3.4 – 3.7. See table 3.2 for a full list of samples from the Lace drill core. 32
- Figure 3.3** Photomicrographs of the hypabyssal kimberlite sensu stricto at the Lace pipe as described in 3.1.2 (sample K2-1 collected from the dump site). a) Highly altered olivine (Ol). Alteration is to green yellow serpentine and clay minerals and ultra fine opaques. b) Highly poikilitic interlocking phlogopite plates. Also note the darker red brown tetraferriphlogopite margin on the phlogopite. c) Poikilitic phlogopite plate with numerous inclusions of colourless serpentised melilite laths (MI). d) Poikilitic phlogopite plate with carbonatised dirty laths of melilite (MI) and abundant fine grained spherical altered monticellite and opaques. e) High power image showing abundant fine grained serpentised monticellite characterised by inclusions of opaques. f) Apatite (Ap) phenocryst laths in a base of yellow green clay minerals. Note the abundant inclusions of opaques. 33

Figure 3.4 Photomicrographs of coherent hypabyssal transitional kimberlite (HKt) from sample C6-713 in borehole C6 as shown in figure 3.2 and described in section 3.1.3. See table 3.1 for a modal analysis of this sample and table 3.2 for relative development of the HKt compared to the rest of the pipe. a) Highly clay mineralised olivine (Ol) phenocrysts in a groundmass of much finer grained kimberlite relative to sample K2-1. b) The development of fine grained microlitic clinopyroxene (D) around the margins of country rock xenoliths (CRX). Note the abundance of fine grained microlitic clinopyroxene throughout the groundmass and the presence of colourless apatite in the top right corner. c) Colourless apatite (Ap) lath in relation to pale yellow green fine grained microlitic clinopyroxene (D). d) Abundant fine grained microlitic clinopyroxene (D) in the groundmass of the rock. Note that microlitic clinopyroxene does not occur as inclusions within the phlogopite. 39

Figure 3.5 Photomicrographs from samples C6-706 (a-b) and C6-642 (c-d) from borehole C6 in figure 3.2. Both these samples are described in detail in section 3.1.3 and a modal analysis is given for C6-706 in table 3.1 and C6-642 in table 3.3. a) Clear development of a nucleated globule with a central kernel of an altered olivine (Ol) phenocryst. b) Non-poikilitic phlogopite (P) laths in a base of colourless calcite (C) and very fine grained grey microlitic clinopyroxene. c) Distinct large globule (4mm) without a central kernel between abundant green shale xenoliths. d) Development of globules (G) in a base of colourless calcite. Note the abundant green shale xenoliths, which are derived locally. See table 3.2 for relative development of the transitional kimberlite compared to the rest of the pipe. 42

Figure 3.6 Photomicrographs from sample C6-630 from borehole C6 as shown in figure 3.2. Detailed descriptions of this HKt are given in section 3.1.3 and a modal analysis of the sample is given in table 3.1. a) Development of abundant distinct globules (G) with central kernels of altered olivine phenocrysts. b) Similar development of abundant globules (G) with central kernels of either olivine or country rock xenoliths. Note the large globule (3mm) at the bottom of the photo with a carbonate CRX kernel. The region marked by the square is shown in photo d). c) High power image of the groundmass kimberlite within a globule showing abundant microlitic clinopyroxene laths in the matrix. Note the highly altered lath of melilite (Ml). d) High power image of the region indicated in b). Note the presence of a rim of fine grained grey microlitic clinopyroxene around the CRX central kernel. The kimberlite mantle around the CRX is composed of abundant phlogopite and minor opaques and highly altered melilite laths in a base of calcite and microlitic clinopyroxene. e) Photo of part of a globule with a central kernel of an altered olivine (Ol) phenocryst. The region indicated by the square is shown in photo f). f) High power image of the region shown in e). Note the abundant pervasive microlitic clinopyroxene, which has replaced the base and the non-poikilitic phlogopite phenocrysts. See table 3.2 for relative development of the transitional kimberlite compared to the rest of the pipe. 45

Figure 3.7 Photomicrographs of samples C6-597 (a), C6-552 (b) and C6-321 (c-d) from borehole C6 as shown in figure 3.2. HKt samples are described in detail in section 3.1.3. a) Contact breccia with no kimberlite component. The interclast is colourless calcite. b) CRX rich sample with abundant green and black shales with an interclast material of dominantly clay minerals and lesser kimberlite. c) Distinct globules forming in an interclast material of colourless calcite. d) Distinct large globules with an interclast material of clay minerals and lesser calcite. Note photos c-d is from the satellite pipe. See table 3.2 for relative development of the transitional kimberlite compared to the rest of the pipe. 47

Figure 3.8 Photomicrographs of the volcanoclastic kimberlite at the Lace pipe. a)-b) bVK, as described in section 3.1.4.1, showing abundant basalt xenoliths set in a fragmental interclast material. Note the kimberlite magmaclasts in a). c) qVK, as described in section 3.1.4.2, photo showing abundant quartz xenocrysts in the interclast material and large magmaclasts (Mg.Clast). d) Another example of qVK showing an irregular magmaclast and the presence of basalt xenoliths. 54

Figure 3.9 Plan view of the Voorspoed pipe showing the distribution of the basalt mega block at the surface, at 137m level and 250m level. Sections lines indicated on the diagram are shown in figure 3.10. Diagram from Clement (1982). 58

Figure 3.10 Cross-sections through the Voorspoed pipe showing the distribution of the basalt mega block. Section lines are indicated in figure 3.9. Diagram from Clement (1982). 59

Figure 3.11 Plan view of the Kamfersdam kimberlite pipe showing the distribution of a large floating reef. (Skinner and Marsh, 2004). 60

Figure 3.12 Plan view of the Voorspoed pipe showing the positions of boreholes and the distribution of the Central Eruption Zone (CEZ) (pale brown). The Initial Eruption Zone (IEZ) is the white area and underlies the basalt (grey). The section line aa-bb is shown in figure 3.14. Borehole logs created in this study for holes 2, 3, 9 and 10 are given in appendix 4. The rest of the logs are not given but De Beers logs were used to compare with the logs created in this study. Diagram modified after (Clement, 1982). 65

Figure 3.13 Photographs of representative samples from the IEZ MVKs. a) T1aMVK: Note the typical amygdaloidal basalt xenolith (B). b) Soft MVK: Note the spherical magmaclasts (M) and pitted edges of the core. c) Atypical MVK: Note the spherical and angular magmaclasts (M). Detailed petrographic descriptions of these rock units are given in section 3.2.6. 66

Figure 3.14 Cross-section aa-bb; (as indicated on figure 3.12) showing the interpreted distribution of internal geology at the Voorspoed pipe. The section is based on the geology logged in boreholes 2, 3, 9 and 10 as shown on the diagram and in appendix 4. Note the distribution of the central and initial eruption zones as indicated at the top of the section. The latter CEZ cross cuts the earlier formed IEZ. (HKt: transitional kimberlite; CB: contact breccia). See appendix 7 for a full list of abbreviations used in the diagram and text. Pipe outline modified after Clement (1982). 68

Figure 3.15 Photographs of the CEZ MVK samples. a) Type 1 b MVK. b) Intermediate MVK. c) Type 2 MVK. Note the colour variation between the T1bMVK and the intMVK and T2MVK. The latter varieties are clearly lighter in colour. The T2MVK contains abundant spherical magmaclasts with central kernels of either altered green olivine macrocrysts or country rock xenoliths. 70

Figure 3.16 Photomicrographs of the hypabyssal sill (K1/111, De Beers collection, appendix 8) as described in section 3.2.3.1. Modal analysis for this sample is given in table 3.4 a) Highly serpentinised olivine (Ol) phenocryst surrounded by non-poikilitic phlogopite. Also note the large diopside phenocryst (D). b) Non-poikilitic phlogopite laths showing minor evolution to red/brown tetraferriphlogopite margins. c) Clear colourless sanidine (S) segregation with inward protruding pyroxene. The sanidine is being altered by brown yellow clay minerals (Clay). Two pyroxenes are present: typical colourless diopside and light green overgrowths on the diopside of aegirine (A). d) Clear development of aegirine (A) overgrowth on a diopside (D) lath. In this case the clear segregation is calcite. 74

Figure 3.17 Photomicrographs from an internal hypabyssal dike (section 3.2.3.2) at the Voorspoed pipe (sample 4/1; Skinner collection, appendix 8). Modal analysis of the rock is given in table 3.4 a) Altered clay mineralised olivine (Ol) phenocryst surrounded by phlogopite. b) Non-poikilitic phlogopite phenocrysts showing some evolution to tetraferriphlogopite. c) High power image showing green aegirine overgrowths on colourless diopside (D) laths. d) Development of fine green aegirine overgrowths on a diopside (D) lath. 76

Figure 3.18 Photomicrographs from two rare hypabyssal varieties at the Voorspoed pipe (samples K1/154 and K1/135 respectively; De Beers collection). a) Diopside kimberlite containing abundant fine grained diopside and euhedral olivine (Ol) phenocrysts. b) Melilite-bearing kimberlite. Note the presence of abundant highly altered dirty looking carbonatised melilite (Ml) laths. 79

Figure 3.19 Core photos of the hypabyssal transitional kimberlite breccia (HKtB) at the Voorspoed pipe from borehole 9 at approximately 320m depth in the borehole. Note the abundant xenolith content in (a) and the presence of a large globule in (b). Also note the variation in xenolith content between the upper and lower cores in photo (b). Photomicrographs of the HKtB are given in figure 3.20 and modal analysis of a relatively xenolith poor sample (9/2) is given in table 3.4. 81

Figure 3.20 Photomicrographs of the hypabyssal transitional kimberlite breccia (HKtB) sample 9/2 (Skinner collection) from borehole 9 at 292m depth at the Voorspoed kimberlite. Refer to appendix 8 for a full list of the samples analysed in this study. Photos from the core are show in figure 3.19 and modal analysis for this sample (9/2) is given in table 3.4. a) Low power image showing incipient development of globules (G) in base of colourless calcite. b) Clear development of globules, which do not contain central kernels, in a base of colourless calcite. c) Higher powered image of the kimberlite groundmass showing highly clay mineralised olivine (Ol) phenocrysts, diopside (D) phenocrysts and phlogopite phenocrysts in a base of calcite and ultra fine grained phlogopite. d) High power image showing the ultra fine grained phlogopite base material. Note the hexagonal basal phlogopite sections marked with a P. Diopside (D) is also show. 82

Figure 3.21 Photographs of contact breccias observed in the borehole 10 at 260m and 270m depth at the Voorspoed pipe. a) Contact breccia is the sidewall shales at 270m in borehole 10. The bottom of the core is at

the bottom of the photo. Note the progressively decreasing intensity of fracturing. Calcite is infilling the fractures and no kimberlite is present. b) Narrow contact breccia zone at 260m depth directly overlying the contact breccia in a). The contact breccia has formed in a dolerite sill, which pre-dates the kimberlite intrusion. Note the calcite infilling a large void. 84

Figure 3.22 Cross-section aa-bb; (as indicated on figure 3.12) showing the interpreted distribution of internal geology at the Voorspoed pipe. Sections show the distribution of the dominant components of the MVK as discussed in section 3.2.5 and given in table 3.5 and 3.6. These sections are based on the geology logged in boreholes 2, 3, 9 and 10 as shown in appendix 4. 86

Figure 3.23 Photomicrographs of the dominant country rock xenoliths present within the volcanoclastic kimberlite. The top two are typical Karoo basalt xenoliths. Bottom left: a rare sandstone xenolith and bottom right: typical shale xenolith. 88

Figure 3.24 Photomicrographs of the typical basement xenoliths observed in the volcanoclastic infill. a) Chert-rich carbonate xenolith most likely from the Monte Cristo Formation of the Malmani Subgroup, Transvaal Supergroup. b) Quartzite xenolith. c) Exotic unidentified xenolith containing clinzoisite phenocrysts in a base of feldspar. d) Altered basement basalt xenolith from the Ventersdorp Supergroup. Note the distinct green colour relative to the basalt in figure 3.21. 91

Figure 3.25 Photomicrographs of typical magmaclasts in the volcanoclastic infill. a) Oval shaped clast containing no central kernel. The kimberlite is composed of two highly clay mineralised olivine phenocrysts, one clear colourless diopside phenocryst, abundant phlogopite laths and highly altered melilite laths in a base of calcite and clay minerals. b) Large spherical autoliths with a Karoo basalt central kernel. Note the ultra fine grained dark rim around the autoliths. c) Medium power image showing a relatively altered central kernel of basalt with a mantle of kimberlite containing olivine, diopside and phlogopite set in a fine grained dark base. Note the fine grained nature of the base relative to photographs e) and f). d) Fine grained autolith showing clear tangential alignment of phlogopite grains around a central kernel of olivine and phlogopite phenocrysts. e) Medium power image of an autolith sensu stricto showing clear flow alignment of the phlogopite grains. Note the coarse grained nature of the base relative to photo c). f) Typical irregular shaped autolith sensu stricto with a well crystallised base component. The autolith is comprised of abundant clear diopside and phlogopite laths in a base of calcite and serpentine. Note the lack of olivine. 95

Figure 3.26 Photomicrographs of representative samples of each of the MVK varieties. a) Type 1a MVK. b) Soft MVK. c) Atypical MVK. d) Type 1b MVK. e) Type 2 MVK. f) Intermediate MVK. Note the higher kimberlite proportion in e) and f). Also note the slightly higher basalt CRX proportion in photo d) and the lack of basalt CRX in photo c). 101

Figure 3.27 Core photo of the Type 2 MVK showing abundant highly altered carbonate xenoliths. 105

Figure 3.28 Photomicrographs of the resedimented volcanoclastic kimberlite infill. a) Low power image of the contact between typical MVK (bottom) and a fine grained RVK band (top) (Sample 2-280). b) RVK sample from the De Beers collection. Note the abundant quartz grains and rare kimberlite magmaclast (Sample location unknown). c) Fine grained top of a graded bed (Sample 10-90). d) Coarse grained equivalent to photo c) (Sample 10-90). 110

Figure 3.29 Photomicrographs of the massive volcanoclastic basalt and sandstone breccias. a) and b) show the basalt breccia (Sample 10-36). c) and d) show the sandstone breccia (Sample 8/1; Skinner collection). Note the still relatively abundant basalt xenoliths within the sandstone breccia. 112

Figure 3.30 Photomicrographs of the Type 1 hypabyssal kimberlite from samples K5/34 and K5/35. a) Coarse diopside (D) with distinct green overgrowth of aegirine (A). b) Medium power image showing diopside (D) and K-richterite (R). Note the distinct pleochroism of the K-richterite from brown to green. c) Photo showing finer grained diopside with a green overgrowth of aegirine in a base of clay minerals (Clay). Note the non-poikilitic phlogopite laths, which show evolution to tetraferriphlogopite. d) Highly clay mineralised olivine (Ol) phenocrysts surrounded by fine grained phlogopite laths. Note also the K-richterite (R) and diopside (D). 111

Figure 3.31 Photomicrographs of the Type 2 hypabyssal kimberlite from sample K5/9. a) Very fresh olivine (Ol) phenocrysts. b) Dark red brown highly poikilitic phlogopite plate. c) Light green brown K-richterite (K)

with colourless diopside (D). Note the feathery green margins. d) Diopside (D) phenocrysts with feathery overgrowths, which look more similar to the margins on the K-rich richterite in photo (c).....118

Figure 3.32 Photomicrographs of the CRX-rich hypabyssal kimberlite from sample K5/30-32. a) Large CRX surrounded by kimberlite with euhedral clay mineralised olivine (Ol) phenocrysts with abundant fine grained diopside. b) Photo showing clay mineralised olivine (Ol) phenocryst with distinct rim of fine grained phlogopite and distinct colourless rounded and highly altered leucite (L) phenocrysts. Note the leucite does not have rims of phlogopite. Fine grained diopside (D) is also particularly abundant. c) Typical example of the CRX-rich variety with abundant clay mineralised olivine (Ol) with rims of fine grained phlogopite and abundant fine grained diopside laths. d) Typical example with a large CRX present.....120

Figure 3.33 Photomicrographs of the volcanoclastic kimberlite at the Besterskraal kimberlite. a) Low power image showing the fragmental nature of the interclast material. Note the presence of two magmaclasts (mg.clast). b) Typical spherical magmaclasts. c) Typical magmaclasts. d) Basalt CRX as a central kernel in a relatively large magmaclasts.122

Section 4 Figures

Figure 4.1 Compositional variation of pyroxene at the Voorspoed kimberlite sample K1/114. Note the clear gap in compositions indicating that there is no gradational change from diopside (brown points) to aegirine (blue points).....131

Figure 4.2 Composition of phlogopite at Voorspoed sample K1/114. Note the complete lack of evolution to tetraferriphlogopite.....132

Figure 4.3 Compositions of evolved aegirine-rich clinopyroxene from Postmasburg, Sover North, Makganyene and Voorspoed plotted in the ternary system diopside (Di)- hedenbergite (Hd)- aegirine (Ae). Diagram from Mitchell (1995).134

Figure 4.4 Diagram illustrating epitaxis where in a) the volume of the liquid available to and edge or corner of the crystal is greater than at the side and b) volume of liquid available for a narrow crystal is even greater. Diagram after Winter (2001).136

Figure 4.5 Composition of phlogopite at the Voorspoed and Lace HK. Top and bottom left are compositions from Lace. Top and bottom right are from Voorspoed. Note the clear zonation trend of the phlogopite from Voorspoed in sample K1/111 but not in sample K1/110. The phlogopite analysed in this study (sample K1/114) is very similar to that of sample K1/110. Also note the trend of the phlogopite at Voorspoed to the highly evolved Besterskraal and Sover North phlogopite compositions. The composition of the phlogopite at Lace does not increase in TiO₂, which is characteristic of unevolved Group II kimberlites. Diagrams from Mitchell (1995).....140

Figure 4.6 Comparison of diopside and aegirine from Voorspoed (this study) with microlitic clinopyroxene data from Skinner and Scott (1979), Mitchell et al. (2009) and Lace (this study). Microlitic clinopyroxene plotted as open triangles are from Skinner and Scoot (1979) and Mitchell et al. (2009). Microlitic clinopyroxene from the Lace HKt plotted as open squares and the HKtB as green diamonds.142

Figure 4.7 Combination of Clement (1982) C.I. and the contamination technique used by Kjarsgaard et al. (2009) to indicate the degree of crustal contamination for the samples analysed at the Kroonstad cluster. Red squares: Lace dump samples (HKt); Orange triangles: Lace core samples (HKtB) and Blue diamonds: Voorspoed HK data from Roberts (1997) and this study.....149

Figure 4.8 Geochemical variation of the Lace and Voorspoed kimberlites. Lace Dump represents the HKt; Lace Core represents the HKtB. Group I and Group II kimberlite field from data presented by Fraser and Hawkesworth (1992), Mitchell (1995), le Roex et al. (2003), Becker and Le Roex (2006), Coe et al. (2008). Chemistry given as wt%. Blue diamonds: Voorspoed. Red Squares: Lace HKt. Red triangles: Lace HKtB....151

Figure 4.9 Variation diagram showing Ni vs. MgO, evidence for fractional crystallisation of olivine at Lace and Voorspoed. Note the trends away from olivine composition, although it seems likely that olivine is not the only

phase fractionating as the trend is not directly away from olivine. MgO given as wt% and Ni as parts per million.....	152
Figure 4.10 Geochemical variation diagrams showing trends interpreted to result from fractional crystallisation of olivine and possibly minor phlogopite. Red squares: Lace. Blue Diamonds: Voorspoed.....	155
Figure 4.11 Geochemical variation diagrams for the Lace kimberlite HKt (red squares) and Lace kimberlite HKtB (orange triangles). Note the composition of microlitic clinopyroxene plotted on the diagram. This is an average composition from all the Lace HKt microlitic clinopyroxene data. Trend 1 indicates crustal contamination. Trend 2 is interpreted to indicate CO ₂ degassing.	156
Figure 4.12 Geochemical variation diagrams for the Lace kimberlite HKt (red squares) and Lace kimberlite HKtB (orange triangles). Note the composition of microlitic clinopyroxene plotted on the diagram. This is an average composition from all the Lace HKt microlitic clinopyroxene data. Trend 1 indicates crystal contamination. Trend 2 is interpreted to indicate CO ₂ degassing. Note the sub-trends of crustal contamination in the bottom diagram.	157
Figure 4.13 Geochemical variation diagrams for the Wesselton and Dutoitspan kimberlites. Open symbols represent intrusive dike/sills (Clement, 1982) and root zone Hypabyssal kimberlite (Clement, 1982). Closed symbols represent TKB (Clement, 1982) and Nucleated Autoliths, closed circles, (Danchin et al. 1975). Note the composition of microlitic clinopyroxene plotted on the diagrams. Microlitic clinopyroxene data from Mitchell et al. (2009) for the Wesselton kimberlite.....	160
Figure 4.14 Compositional variation of microlitic clinopyroxene. Data from Skinner and Scott (1979) and Mitchell et al. (2009). Note the possible trend of increasing Na ₂ O and Al ₂ O ₃	161

Section 5 Figures

Figure 5.1 Ternary diagram showing point count results and Karoo Supergroup correlation for sandstone xenoliths from the Voorspoed and Lace pipe VK. Qm: Monocrystalline quartz; F: Feldspar and Lt: Lithic fragments. Diagram after Hanson (2006) and Howarth (2007).	166
Figure 5.2 Geochemistry variation diagrams showing the geochemistry and Karoo Supergroup correlation of the basalt xenoliths from the Lace and Voorspoed VK. Lesotho Formation fields from Marsh et al. (1997). Ventersdorp fields from Crow and Condie (1988). Lace: Red squares (data from Howarth, 2007). Voorspoed: Blue triangles (data from Roberts, 1997) and Blue diamonds (data from Hanson, 2006).	167
Figure 5.3 Palaeo-distribution of the Karoo basalt escarpment. Diagram from Hanson (2006). Note the Voorspoed pipe located between the 140-120 Ma and 90-75 Ma escarpments.	172
Figure 5.4 Schematic representations of the three pipe Class varieties. a) Class 2 Prairies Type Pipe; b) Class 3 Lac de Gras Type Pipe and c) Class 1 Tuffisitic Kimberlite Type Pipe. PK: Pyroclastic kimberlite; RVK: Resedimented volcanoclastic kimberlite; HK: Hypabyssal kimberlite; TK: Tuffisitic kimberlite and PTK: Pyroclastic equivalent of TK. Diagram from Scott Smith (2008a).	177
Figure 5.5 Simplified schematic illustration from Skinner (2008) showing the solidi ab for a water-saturated melt (i.e. Class 1 kimberlites) and cd for a CO ₂ saturated melt (i.e. Class 2 kimberlites). Diagram based on experimental work on peridotite by Wyllie (1987).	180
Figure 5.6 Schematic illustration of the Clement (1982) model for embryonic pipe development and near surface eruption of South African kimberlites. Note specifically the formation of contact breccias at the base of dolerite sills in the country rock. Diagram from Field and Scott Smith (1999).	186
Figure 5.7 Schematic illustration of a tunnel developed through a contact breccia at the De Beers pipe. Note the variation in kimberlite percentage, which gradually becomes nothing toward the end of the tunnel (right hand side). Diagram from Skinner (2008) after Clement (1982).	189
Figure 5.8 Composite model for the Gahcho Kue kimberlites. Diagram from Hetman et al. (2004).	192

Figure 5.9 Photomicrographs from the Lace kimberlite HKt/HKtB. a) the base of the HKt with no globular segregatory texture, although microlitic clinopyroxene is abundant (too fine grained to see at this scale). b) First development of globular segregatory texture, note the distinct large globular cored by a serpentinised olivine macrocryst in the bottom right corner. The base of the rock is a combination of serpentine and calcite. c) HKtB with abundant calcite in the base. Note the incipient development of globules cored by serpentinised olivine (centre left). d) Typical incipiently developed HKtB with an ultra fine base, which is often difficult to identify. e) Patchy distribution of ultra fine grey microlitic clinopyroxene in the HKtB. D: Microlitic clinopyroxene. f) Similar patchy distribution of ultra fine grey microlitic clinopyroxene indicated by D.	201
Figure 5.10 Photomicrographs of from the Voorspoed VK showing: a) aegirine laths within the nucleated globule shown in b). b) Nucleated globule with a basalt central kernel and coarse crystalline mantle. Aegirine is observed in the mantle as shown in a). c) Nucleated globule with basalt central kernel and relatively fine grained mantle with a dark brown turbid base. b) and c) show the two end member varieties as discussed in the text: section 5.3.4.2 below.	207
Figure 5.11 Simplified schematic illustration showing the formation of the embryonic pipe at the Kroonstad kimberlite cluster. Contact breccias become more extensive in spatial relation to more competent rock units such as the dolerite sill observed at Voorspoed. The contact at the base of the exsolving magma shows the depth at which Hypabyssal kimberlite with a coherent texture will be emplaced after eruption of the kimberlite pipe. The base of the Karoo basalt is at approximately 1400m from the original land surface and the base of the exsolving magma is at approximately 2000m.	217
Figure 5.12 Photomicrographs of basalt xenoliths from a) MVBB showing no alteration; b) BVK showing some degree of alteration indicated by the partially altered plagioclase; c) and d) typical MVK xenoliths showing relatively high degrees of alteration.	226
Figure 5.13 Illustration of mechanisms for infilling a kimberlite pipe. 1) collapse of surrounding extra crater deposits, 2) rock bursts/sidewall failure deep within the pipe and 3) deposition by primary pyroclastic process such as fall out from the column and column collapse. (Diagram from Brown et al. 2008c).	232
Figure 5.14 Illustration showing the failure of the crater rim and slumping of material back into an open vent. This model was developed for a 500-700m deep, cleared crater for Class 1 kimberlites. The tuff ring would be substantially bigger for the Kroonstad kimberlite where a +/-2km vent is cleared. Diagram after Skinner (2008).	235
Figure 5.15 Illustration of the crater excavation and subsequent crater infilling proposed for the formation of the Kroonstad kimberlite pipes. a) exsolution in the embryonic pipe produces cracking through to the surface induces decompression of the magma column; b) decompression related eruption clears a vent and deposits extra crater tuff ring and c) infilling of the pipe by three processes (A) primary pyroclastic deposition through either column collapse or explosive in-vent flows, (B) gravitational sidewall failure and (C) crater rim collapse.	240
Figure 5.16 Photomicrographs of the basalt-rich VKB at the Lace pipe. a) interclast material; note the complete absence of microlitic clinopyroxene relative to photo b). b) nucleated autolith; note the abundant high relief microlitic clinopyroxene.	243
Figure 5.17 Cross-section aa-bb through the Voorspoed pipe, as shown in figure 3.14, showing the distribution of the volcanoclastic kimberlite. This figure shows the percentage of kimberlite present within each of the volcanoclastic units. Kimberlite components include magmaclasts and xenocrysts. HKt: transitional kimberlite and CB: contact breccia.	247

List of Tables

Table 1.1 Regional country rock stratigraphy for the Kroonstad Cluster area.....	10
Table 2.1 Depth, bearing and depth of the Voorspoed boreholes logged and sampled in this study.	25
Table 3.1 Modal abundances of the HK and HKt kimberlites at Lace based on 500 point counts over a single thin section. (Ol: olivine; Phl: phlogopite; Mel: melilite; Mon: monticellite; Ap: apatite; Op: opaque spinel; Per: perovskite; Cal: calcite; Clay: Clay minerals; Ser: serpentine; CRX: country rock xenolith; Mc: microlitic clinopyroxene).....	37
Table 3.2. Summary table of the relative abundances of: microlitic diopside (Mcp _x), globular segregatory (Glob. Seg.) textural development and country rock xenolith (CRX) proportion in the Lace kimberlite hypabyssal transitional kimberlite and kimberlite breccia (HKt/HKtB). Refer to appendix 8 for a full list of all the samples analysed in this study. See section 3.1.3 for detailed descriptions of the samples and table 3.1 for modal analyses for selected samples. Samples labelled C6 are from borehole C6 (C7 from borehole C7) as shown in figure 3.2.....	38
Table 3.3 Modal abundances of the components for the HKtB at Lace based on 500 points counted per single thin section. (Kimb: kimberlite; CRX: country rock xenolith).....	46
Table 3.4 Modal abundances of the volcanoclastic kimberlite at the Lace pipe based on 500 points counted per single thin section. (Sed.: sedimentary; Mg.Clast: magmaclasts; Ol. in: olivine inside magmaclasts; Ol. out: olivine as xenocryst; Intercl. Mat.: interclast material; Kim: kimberlitic).....	52
Table 3.5 Modal abundances of the hypabyssal and transitional hypabyssal (9/2) kimberlite at the Voorspoed pipe. (Ol.: olivine; Phlog: phlogopite; Diop: diopside; Serp: serpentine; Clay: clay minerals; Sani: sanidine; Mel: melilite).	72
Table 3.6 Modal abundances of the major constituents for the MVK varieties at the Voorspoed pipe. (Sed: sedimentary; Mg.Clast: magmaclast; Ol. in: olivine within magmaclasts; Ol. out: olivine as xenocrysts; Kim: kimberlitic).....	99
Table 3.7 Modal abundances for the resedimented VK and the MVBB/MVSB kimberlites. (See table 3.5 for definition of acronyms).....	113
Table 3.8. Modal analysis results for the characteristic Besterskraal North HK types. Results given as percentage abundance of total rock volume. Samples are from the De Beers collection and locations within the pipe are unknown.....	115
Table 4.1 Representative compositions of diopside and aegirine from Voorspoed Sample K1/114 and microlitic clinopyroxene (Mcp _x) from the HKt (Sample K2-5) and HKtB (C7-713) from Lace. See appendix 3 for full tables of the compositions of the pyroxenes.....	128
Table 4.2 Structural formula on the basis of four cations and six oxygens.....	128
Table 4.3 Representative compositions of phlogopite from Voorspoed sample K1/114. See appendix 3 for full tables of compositions.....	129
Table 4.4 Structural formula based on 22 oxygens.....	129
Table 4.5 Comparison of composition of aegirine from Mitchell (1995) (1,2) and this study (Aeg. 187 and 239).....	137
Table 4.6 Structural formula on the basis of four cations and six oxygens for table 4.5.....	137
Table 4.7 Comparison of geochemistry of Average Group II kimberlite (Becker and le Roex, 2006); Unevolved Group II kimberlite (Mitchell, 1995) and Evolved Group II kimberlite (Mitchell, 1995).....	147

Table 5.1 Calculation of Karoo Supergroup sedimentary unit thinning rates and projected thicknesses used in erosion estimate method 1.....169

Acknowledgements

Firstly thanks must be extended to De Beers consolidated mines Ltd. as well as diamond corp. for allowing me to visit and sample the Voorspoed and Lace mines respectively. Furthermore De Beers must be thanked for partially funding this project and providing us with additional samples from all the Kroonstad cluster kimberlites.

Jock Robey is thanked for his assistance at the De Beers core stores in Kimberley and basically setting up all the boreholes I needed to examine.

John Hepple and his staff in the basement are thanked for their sample preparation and willingness to help with any problem.

Ashley Goddard is sincerely thanked for help with any and all admin issues I have had over the past two years.

Goonie Marsh, Barbra Kuhn and N.V. Chalapathi Rao need to be thanked for both XRF geochemical and microprobe mineral chemistry analysis as well as helping me interpret the data produced.

John Moore must be thanked for initially sparking my interest in kimberlite geology through my honours project on upper-crustal xenoliths within kimberlite pipes and for helping to develop this project over the course of the last two years.

Thanks must be extended to my parents for putting me up at varsity for the past six years. This M.Sc would never have been possible without their constant support and encouragement to do what I love.

My deepest gratitude must be extended to Mike Skinner for his endless help and encouragement. This project could not have happened if it was not for Mike's persistence with De Beers for samples and all the time he dedicated to helping me with the project. Thanks must also be made for the hours Mike spent going through drafts of this thesis and for many hours spent helping with the particularly difficult kimberlite petrology. Thank you.

Section 1. Introduction

The Kroonstad Group II Kimberlite (also known as orangeites; Mitchell, 1995) Cluster was emplaced into the stable Kaapvaal craton and is located 30km north-east of Kroonstad in the Free State Province of South Africa as shown in figure 1.1. The cluster contains six kimberlite pipes and a variety of hypabyssal intrusions, including both dikes and sills. The kimberlite pipes occur in a general trend from north-east to south-west. The six pipes are: Voorspoed, Lace (Crown), Besterskraal North, Normandien, Silverbank and Grootbosch. The latter three are small sub-economic pipes, which have not been mined and therefore no material is available for study. This study is focused on the Voorspoed and Lace kimberlites as they are active mines. Furthermore samples from the Besterskraal North kimberlite were made available by De Beers.

The Kroonstad kimberlite cluster (KKC) pipes are unique in South Africa as they are unlike the typical tuffisitic South African kimberlite, called Class 1 pipes by Skinner and Marsh (2004). The pipes are dominantly infilled with massive, matrix supported, poorly sorted, fragmental volcanoclastic kimberlite (massive volcanoclastic kimberlite: MVK). Refer to appendix 7 for a full list of abbreviations used in the text. Numerous MVK units are observed as horizontal layers deposited in a layer by layer sequence of pyroclastic eruption. The MVK is not typical tuffisitic kimberlite as described by (Clement and Reid, 1985). The root zones of the pipes are more typical of South African kimberlites, especially those described by Clement (1982) in the Kimberley area. Highly fragmented in situ country rock is observed in the sidewall deep within the pipes, which are characterised by a typical jigsaw fit texture similar to the contact breccias described in Kimberley by Clement (1982). An extensive root zone (Skinner, 2008) has only been intersected at the Lace pipe and is characterised by globular segregatory textured hypabyssal kimberlite. The development of the globular segregations is gradational from poorly developed at depth, which becomes better developed toward the surface. Microlitic clinopyroxene is present in this root zone, which also shows a gradual and patchy development. This texturally distinct rock is very similar to the transitional kimberlite described by Skinner and Marsh (2004) and Hetman et al. (2004).

The Voorspoed and Besterskraal North kimberlites have been noted to be part of the more geochemically evolved Group II kimberlites (Mitchell, 1995). This is evident by

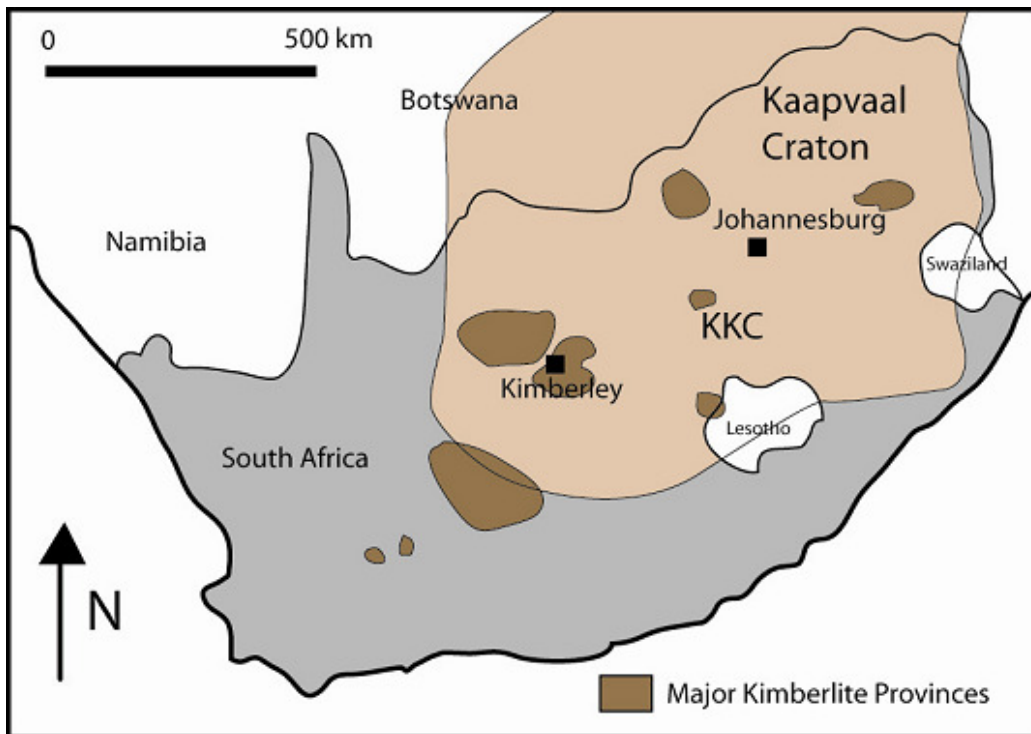


Figure 1.1 Location of the Koonstad Kimberlite Cluster (KCC) relative to the major kimberlite provinces on the Kaapvaal Craton (pale brown), South Africa (grey).

both petrographic investigation and geochemical analysis. Mineral chemistry of the selected Voorspoed pipe minerals is done to further illustrate the degree to which this evolution has occurred relative to the Besterskraal North Kimberlite. The Besterskraal North kimberlite is a rare example of a highly evolved Group II kimberlite, which contains minerals such as K-richrichterite, sanidine, leucite and aegirine (Mitchell, 1995). New geochemical analyses of the Lace kimberlite are presented for the root zone globular segregationary kimberlite. Some very interesting trends are observed, which are controlled by the modal abundance of microlitic clinopyroxene. Microlitic clinopyroxene forms in two ways: 1) magma contamination by xenoliths or 2) CO₂ exsolution (Mitchell et al. 2009). Therefore the geochemistry is likely also controlled by one of these mechanisms.

The emplacement of the Koonstad pipes is particularly complex. The early stages of emplacement are similar to the typical model for South African kimberlites of Clement (1982) however the later infilling of the pipe is very different from the typical South African kimberlite. A new model for the infilling of the Koonstad pipes needs to be proposed to account for the unique nature of the deposits in South Africa. The focus of this research is to

provide a detailed macro- and microscopic investigation into the geology of the Kroonstad kimberlites with specific interest in near-surface emplacement mechanisms.

Orangeite or Kimberlite

The discrimination of Group I and II kimberlites was first done on an isotopic basis by Smith (1983). Group II kimberlites are also known as orangeites as described by Mitchell (1995). The Kroonstad kimberlites have been classified as Group II kimberlites (orangeites) based on their micaceous nature and geochemical characteristics. No isotopic studies have been conducted for the Kroonstad kimberlites. Some discrepancies have been noted in the Kroonstad kimberlites with their classification as orangeites. The presence of abundant monticellite at the Lace kimberlites (as described in section 3) is more typical of Group I or so called archetypal kimberlites. Monticellite is not listed as an orangeite mineral and Mitchell (1995) clearly states that orangeites may be distinguished from kimberlites (Group I) by the absence of monticellite. The presence of melilite at the Kroonstad cluster (as described in section 3) is also anomalous with orangeites. Furthermore the presence of a suite of megacrysts in Group II kimberlites is extremely rare according to Mitchell (1995). The Lace kimberlite also contains abundant olivine megacrysts (as described in section 3), which again is more similar to Group I kimberlite. Skinner et al. (1994) shows that there are kimberlites in the Prieska area which are transitional between Group I and Group II isotope ranges. This indicates that there is no clear distinction between Group I and II kimberlites but rather that Group I and II kimberlites are end members to kimberlite magma compositions. Mineralogical variations also occur where kimberlites containing a typical Group I isotopic signature contain abundant phlogopite, which is more common of Group II kimberlites. Late stage dikes and plugs of hypabyssal kimberlite (HK) at the Koffiefontein Group I pipe are phlogopite rich (Naidoo et al. 2004) indicating a more Group II type mineralogy. Furthermore Clement (1982) describes phlogopite rich kimberlite in all the so called KIMFIK pipes. The KIMFIK pipes include the Wesselton, Bultfontein, De Beers, Du Toitspan and Finsch kimberlites. All of which are grouped as Group I kimberlites except for the Finsch kimberlite, which is Group II. Furthermore Group I kimberlites showing similarities to Group II (orangeites) are also noted on the Man Craton where abundant phlogopite kimberlite is described (Skinner, et al. 2004). The Majhgawan kimberlite in India is also likened to Group II or transitional type kimberlite (Chalapathi Rao, 2005) similar to the Prieska kimberlites. Furthermore Becker et al. (2007) show kimberlites near Kimberley (Leicester and Wimbeldon), which have isotopic and petrographic characteristics intermediate between

Group I and II kimberlites. It seems likely based on the gradational variation in both isotopic signature and mineralogy that orangeites are in fact kimberlites and not some other unique rock type as suggested by Mitchell (1995). Group II kimberlites represent a relatively rare end member composition of kimberlite magma.

In terms of emplacement mechanisms Group II kimberlites from South Africa are very similar to the typical Group I kimberlites. The Finsch kimberlite pipe contains abundant tuffisitic kimberlite characterised by pervasive microlitic diopside replacement and abundant serpentine as the base (Clement, 1982 and Fraser and Hawkesworth, 1992). The Finsch pipe is a typical Class 1 tuffisitic kimberlite as described by Field and Scott Smith (1999) and Skinner and Marsh (2004). Indicator minerals and mantle xenoliths present within the Group II kimberlites are also very similar to those observed in Group I kimberlites, which indicates a similar origin for the magmas (Skinner pers. comm.).

Therefore the author believes it to be reasonable to compare the Kroonstad Group II kimberlites to examples of Group I kimberlites worldwide and that Group II kimberlites should not be classified as something different to typical Group I kimberlites but rather a rare end member isotope composition of kimberlite magma.

1.1 Previous Work on the Kroonstad Kimberlite Cluster

Numerous authors have incorporated observations made at the Kroonstad Kimberlite Cluster (KKC) into journal publications and text books. However, a detailed study on the geology of the cluster has yet to be done. Phillips et al. (1999) has done Ar/Ar dating of the three largest pipes within the cluster. An average age of 133 Ma has been obtained. Individual ages are: Voorspoed (131.8 +/- 1.7 Ma), Lace (133.2 +/- 2.8 Ma) and Besterskraal North (133.5 +/- 3.5 Ma) (Phillips et al. 1999). Numerous internal De Beers reports are also available on the mineralogy of the different pipes, although these are not used in this section as they are adequately covered by the published literature. An internal report, done in 2004, by J. Stiefenhofer at the Voorspoed pipe led to the development of this thesis.

1.1.1 Lace (Crown) Kimberlite

The Lace (Crown) Kimberlite pipe is approximately 2ha in size and there is an apparent increase in diameter of the pipe with depth, pipe walls flare outward at approximately 350m as shown in figure 1.2 (Clement, 1982). This increased diameter has not been observed in the current model used by the Lace mine and therefore the validity of this statement is unclear. A smaller satellite pipe is also present to the west of the main pipe as shown in figure 1.2.

The earliest published literature from the Kroonstad kimberlite cluster (KKC) is from Merensky (1909), which documents his observations at the Lace (Crown) mine. The most important observation made by Merensky (1909); is the presence of two varieties of volcanoclastic rocks. The first is typical blue ground, as observed at most kimberlite pipes in South Africa and the second is kimberlite sandstone. Wagner (1914) observed only the blue ground kimberlite and not the kimberlite sandstone. The blue ground contains abundant foreign material (xenoliths) of (in decreasing order of abundance): Karoo basalt, white sandstone, pink sandstone, diabase (dolerite) and granite (Wagner, 1914). Wagner (1914) further estimates that <10% of the rock is kimberlite material. The kimberlite sandstone is a rock cemented by sandstone (quartz) but contains angular fragments of dolerite, andesitic rock (most likely Karoo basalt), shale, quartzite and kimberlite components (Merensky, 1909). Clement (1982) has not noted the two varieties of volcanoclastic rocks but has described the matrix of the rock as crystallinoclastic, indicating the almost clastic nature. The only other example of crystallinoclastic kimberlite observed in Southern Africa is from the Dokolwayo kimberlite in Swaziland (Hawthorne et al. 1979). This crystallinoclastic kimberlite at Lace has been documented in this study along with the typical 'blue ground' kimberlite.

The mineralogy of the hypabyssal kimberlite (HK) at the Lace pipe has been documented by Wagner (1914) and Mitchell (1995). These authors both describe the kimberlite as typical micaceous kimberlite, which is known as Group II kimberlite. Wagner (1914) describes a sample obtained from a dike to the south of the pipe where relatively fresh kimberlite can be sampled from the surface. The dike is comprised of olivine, phlogopite, augite, apatite, perovskite and iron ore (opaque spinels) which has been both serpentinised and carbonatised. The augite described here is a pale yellow pyroxene, which has been analysed by Mitchell (1995) and found to be diopside, not augite. The mineralogy at Lace has similarly been

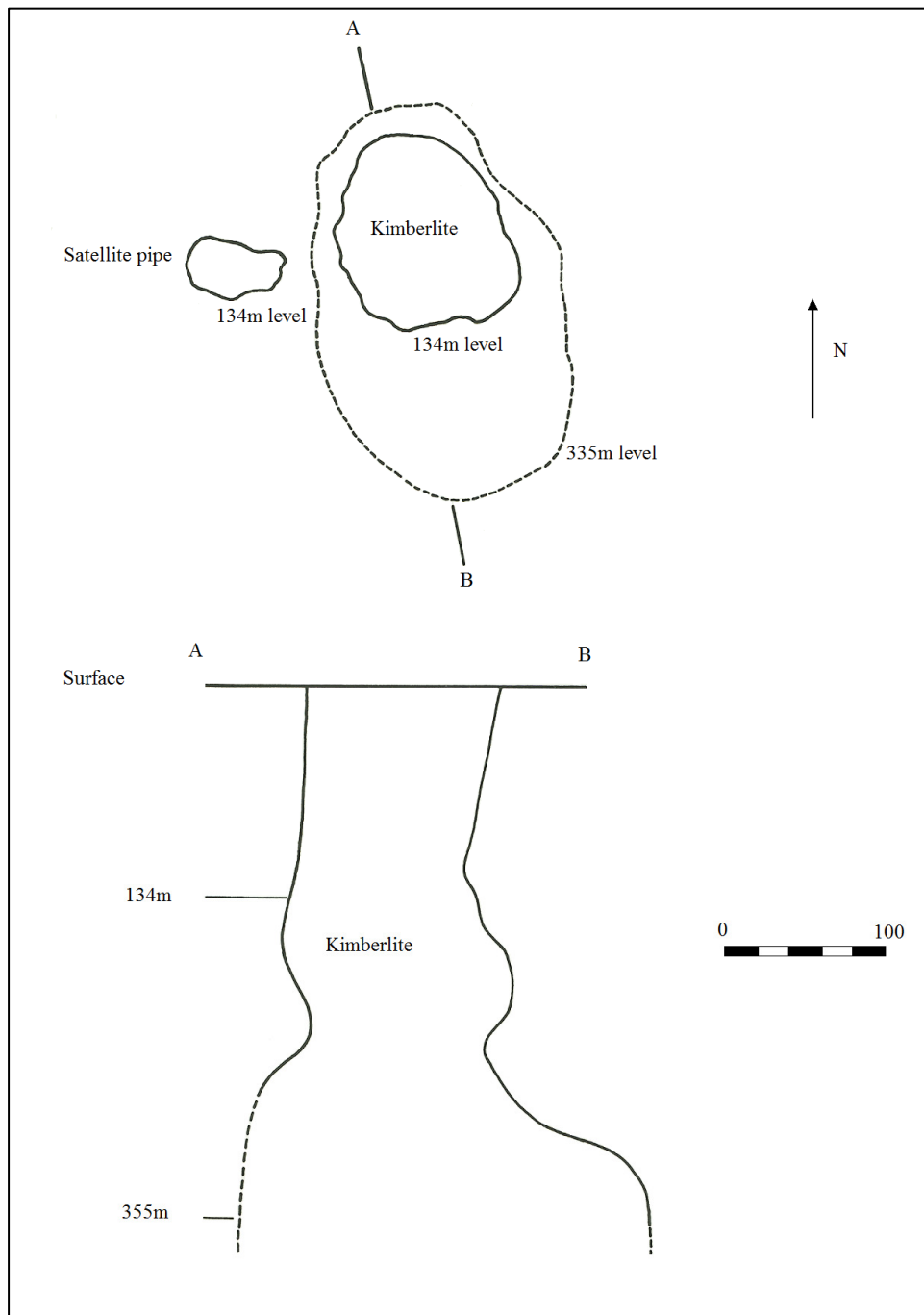


Figure 1.2 Plan view and cross section through the Lace pipe from Clement (1982). The increase in diameter of the pipe with depth is not observed from the current mining plans.

described by Mitchell (1995). No major difference from Wagner (1914) in the mineralogical make up of the Lace pipe has been noted by Mitchell (1995). The only other mineral observed by Mitchell (1995) is opaque hollandite, which occurs in trace amounts. However (Mitchell, 1995) has done a detailed study on the mineral chemistry of Group II kimberlite in general. The diopside and phlogopite from Lace have been analysed. Diopside compositions in particular will be discussed in detail in section 4.1 on mineral chemistry. Wagner (1914)

and Mitchell (1995) did not observe monticellite and melilite at the Lace HK, which have both been observed in this study in relatively high abundance.

1.1.2 Voorspoed Kimberlite

The Voorspoed pipe morphology has been mapped in detail with special interest in the distribution of a large (6 ha surface area) Karoo basalt block, which is present at the surface down to a depth of 300m (Clement, 1982). Wagner (1914) provides the first plan view map of the Voorspoed pipe (figure 1.3), which illustrates the distribution of the basalt block as well as the presence of numerous kimberlite dikes. The basalt block is described in greater detail in section 3 and 5. Roberts (1997) presented geochemical analyses of the basalt and it can be correlated with the Karoo Lesotho Formation. Wagner (1914) interpreted this basalt at the surface as an ancient feeder conduit for the Karoo magmatism. The kimberlite used this zone of weakness to intrude through the crust. This theory no longer stands as the basalt is only present down to 300m and therefore is a large block of basalt, which has been incorporated during the eruption process. The volcanoclastic rocks at Voorspoed have been described by Roberts (1997) and Phillips et al. (1998). The volcanoclastic rocks have all been classified as tuffisitic kimberlites in previous literature. Roberts (1997) notes that microlitic diopside is not pervasive throughout the rock but is rather present in patches. This is an important feature to note as the rocks are not tuffisitic as discussed in section 5. Phillips et al. (1998) has divided the volcanoclastic rocks into three distinct varieties: 1) tuffisitic kimberlite (TK), 2) normal tuffisitic kimberlite breccia (TKB) and 3) basalt-rich tuffisitic kimberlite breccia (TKB). Localized zones of fine grained TK are observed to occur throughout the TKB rocks (Phillips et al. 1998), which indicates some small scale layering within the volcanoclastic rocks. The volcanoclastic rocks are characterized by the differing proportions of country rock xenoliths (CRX) and kimberlite contents. TK contains <30% CRX whereas normal TKB contains 50-60% CRX and basalt-rich TKB contains >80% CRX (Phillips et al. 1998). Corresponding kimberlite contents are low and generally <20% (Phillips et al. 1998). Roberts (1997) gives an average kimberlite magmaclast content of 15% for the volcanoclastic rocks.

The hypabyssal kimberlite (HK) in general is described as diopside phlogopite kimberlite (Roberts, 1997 and Phillips et al. 1998). Phillips et al. (1998) describes seven different varieties of HK. The mineralogical make up of the rocks are very similar and only two

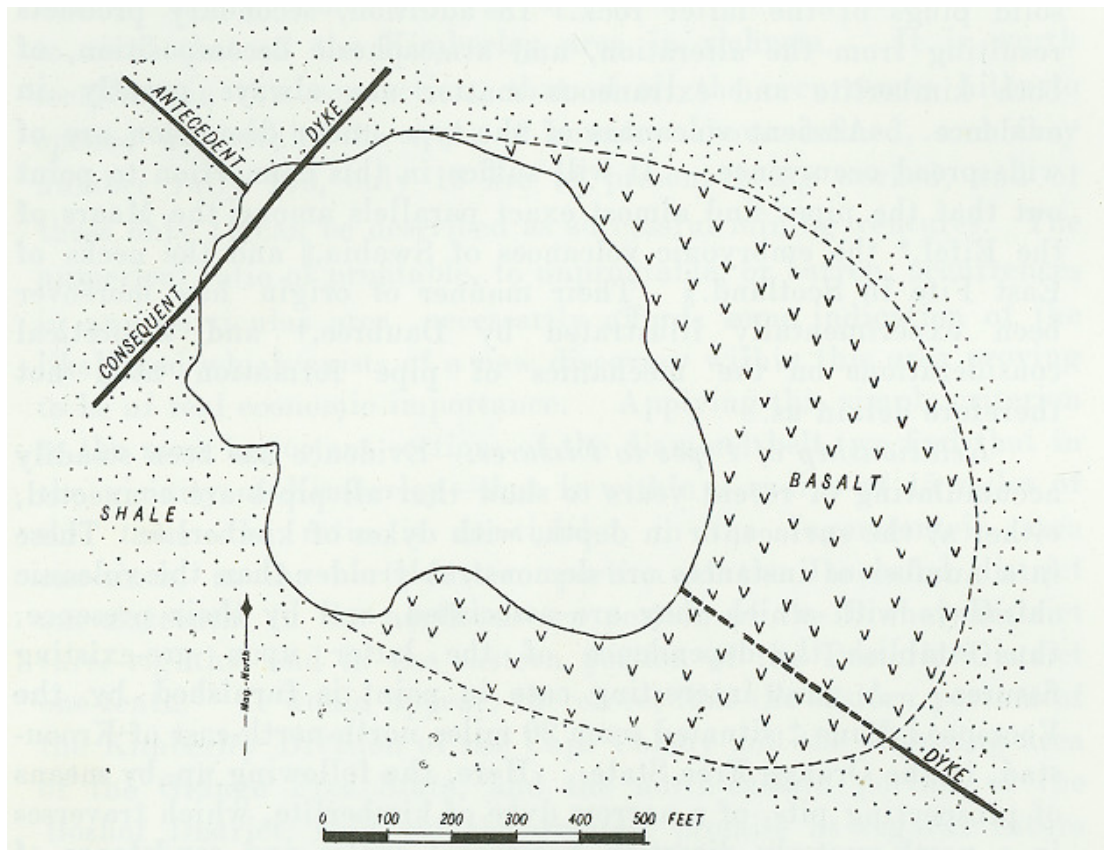


Figure 1.3 Surface (pre-mining) plan view of the Voorspoed pipe showing the distribution of the Karoo basalt and consequent/antecedent dikes. Diagram from Wagner (1914).

mineralogical varieties are described. Diopside phlogopite kimberlite and melilite-bearing kimberlite are present (Phillips et al. 1998). One of the hypabyssal kimberlite (HK) varieties (Type 1A HK) is described as globular segregationary (Phillips et al. 1998). The average proportions of the minerals is: olivine (10%), phlogopite (35%), diopside (20%), melilite (3%) and matrix (32%) (Roberts, 1997). Other minerals present include apatite, monticellite, leucite, amphibole, opaque spinels, perovskite, serpentine and calcite (Roberts, 1997). Monticellite, leucite and amphibole are not observed at the Voorspoed pipe in this study.

1.1.3 Besterskraal North Kimberlite

The Besterskraal North kimberlite is a highly evolved Group II kimberlite, which contains K-richterite, aegirine and sanidine (Mitchell, 1995). Mitchell (1995) is the only published literature available on this kimberlite and is all on the mineral chemistry of primary diopside, K-richterite, sanidine and leucite. No information is available on the volcaniclastic rocks (VK) or the variety of hypabyssal kimberlite (HK) rocks present.

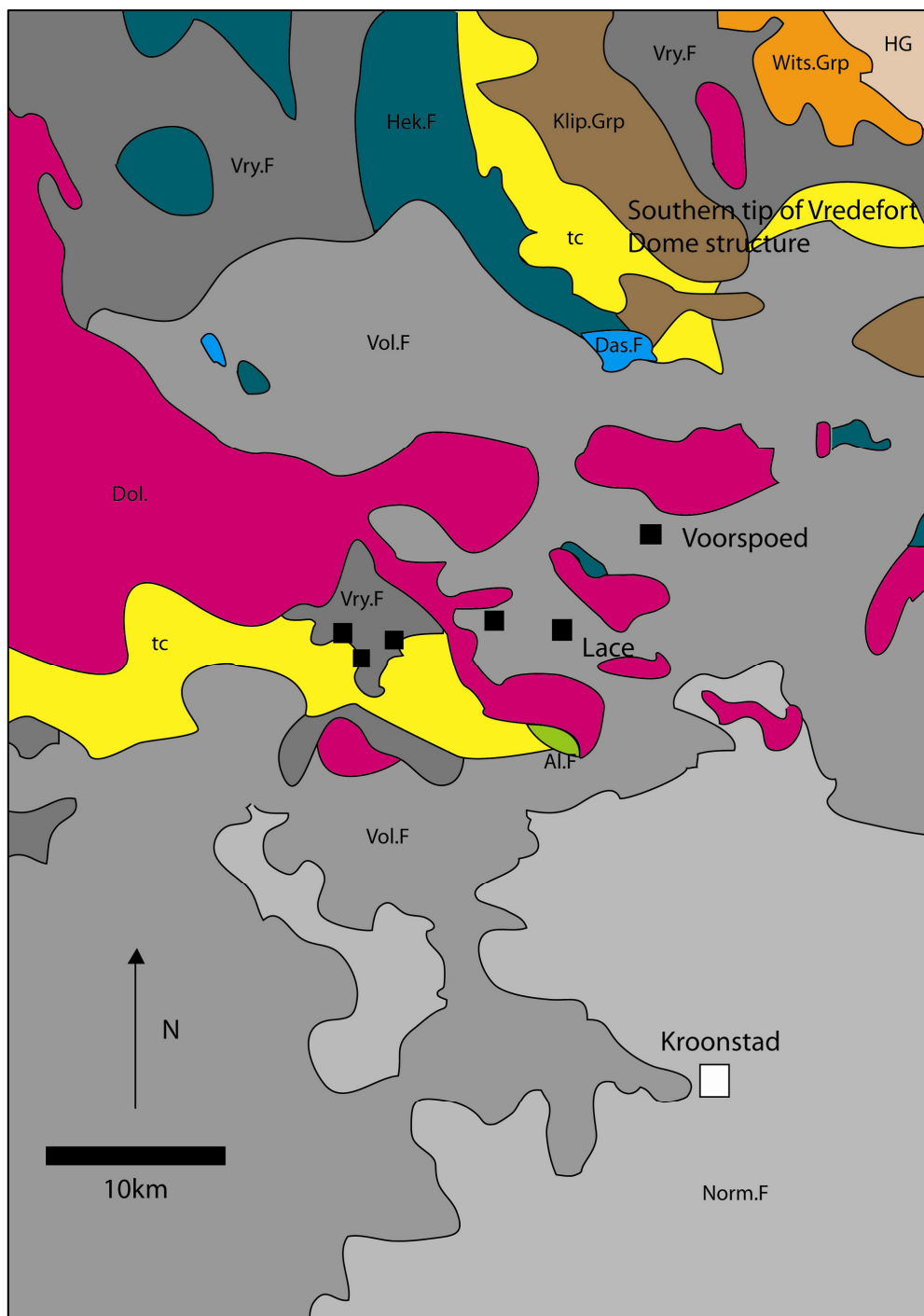


Figure 1.4 Regional geology of the Kroonstad Kimberlite Cluster. HG: Halfway House Granite; Wits. Grp: Witwatersrand Supergroup; Ventersdorp Supergroup (Klip.Grp: Klipriversberg Group; Al.F: Allanridge Formation); Transvaal Supergroup (Hek.F: Hekpoort Formation; Das.F: Daspoort Formation); Karoo Supergroup (Vry.F: Vryheid Formation; Vol.F: Volksrust Formation; Norm.F: Normandien Formation; Dol.: Karoo Dolerite) and tc: tertiary cover. Black squares indicate kimberlite pipes. The Voorspoed and Lace pipes are labelled. See table 1.1 for regional country rock stratigraphy. See figure 1.1 showing the position of the Kroonstad Kimberlite Cluster (KKC) in South Africa.

Table 1.1 Regional country rock stratigraphy for the Kroonstad Cluster area.

Supergroup	Group	Sub-group	Formation	Lithologies
Karoo (300-180Ma)	Drakensberg			Dolerite, basalt
			Clarens	Coarse sandstone
			Elliot	Mudstone, fine sandstone
			Molteno	Coarse sandstone, mudstone
	Beaufort	Tarkastad	Driekoppen	Mudstone
			Verkykerskop	Sandstone
		Adelaide	Normandien	Sandstone, mudstone
	Ecca		Volksrust	Mudstone/shale, siltstone, sandstone
			Vryheid	Sandstone, siltstone, shale
	Dwyka			Diamictite, conglomerate, shale, mudstone
Unconformity				
Transvaal (2650-2050Ma)	Pretoria		Daspoort	Quartzite
			Strubenkop	Shale, tuff
			Hekpoort	Dominant lava, quartzite, shale
			Timeball Hill	Shale, quartzite
	Chuniespoort	Malmani	Monte Cristo	Chert-rich dolomite
			Oaktree	Chert-poor dolomite
			Blackreef	Quartzite, shale, conglomerate
Unconformity				
Ventersdorp (2720-2650Ma)			Allanridge	Mafic lava, tuff
			Bothaville	Conglomerate, quartzite
	Platberg		Rietgat	Mafic lava, quartzite, limestone, chert
			Makwassie	Felsic lava
			Goedgenoeg	Intermediate-mafic lava
			Kameeldoorns	Conglomerate, quartzite, shale
	Klipriviersberg		Edenville	Mafic lava, tuff
			Loraine	Mafic lava, tuff
			Jeanette	Mafic lava, tuff
			Orkney	Mafic lava, tuff
			Alberton	Mafic lava, tuff



Figure 1.5 Present distribution of the Ventersdorp Supergroup. Note the position of the Koonstad Kimberlite Cluster (KKC). Diagram after van der Westhuizen et al. (2006).

1.2 Koonstad Kimberlite Cluster Regional Geology

The Koonstad kimberlite cluster is emplaced into a variety of country rocks including; Karoo Supergroup, Transvaal Supergroup and Ventersdorp Supergroup rocks; the dominant rocks at the current land surface are Karoo Supergroup. Figure 1.4 shows the distribution of the different rock Supergroups. Table 1.1 shows the country rock stratigraphy and lithologies for the Koonstad area. It must be noted here that the blind satellite pipe at Lace does not reach the Karoo Supergroup rocks and the local sidewall lithologies are Transvaal shales.

1.2.1 Ventersdorp Supergroup

The Ventersdorp Supergroup unconformably overlies the Witwatersrand Supergroup and is itself unconformably overlain by the Transvaal Supergroup. The Ventersdorp Supergroup is comprised of two Groups, the Klipriviersberg Group at the base and the Platberg Group immediately above it, which are further subdivided into 11 Formations (Crow and Condie, 1988). The top of the Ventersdorp stratigraphy is comprised of two formations, which do not belong to either of the above-mentioned Groups. The sedimentary Bothaville and volcanic Allanridge Formations form the upper units to the Ventersdorp stratigraphy. The Ventersdorp Supergroup is seen out-cropping at the surface to the south of the cluster as the Allanridge Formation and to the north and northeast as the Klipriviersberg Group. Figure 1.5 shows the distribution of the Ventersdorp Supergroup as a whole and clearly is present at depth beneath the whole kimberlite cluster. Ventersdorp type grey-green xenoliths were observed at the Lace pipe but not at Voorspoed.

The Klipriviersberg Group is essentially a volcanic sequence, which averages between 1500 and 2000m in thickness. The Group is divided into seven Formations including the dominantly sedimentary Venterpost, volcanic komatiitic Westonaria, volcanic Alberton, volcanic Orkney, volcanic Jeannette, volcanic Loraine and volcanic Edenville Formations (Meyers et al. 1990). Therefore volcanic rocks dominate this Group, which range from fine-medium grained phaneritic-aphanitic grey-green amygdaloidal lavas. The Platberg Group is divided into four Formations, which have a wide variety of lithologies as shown in table 1.1. The Platberg Group is essentially absent from the northeastern depository and outcrops inconsistently over the remainder (Van der Westhuizen et al. 2006). Therefore it is most likely not present at depth in the Kroonstad kimberlite cluster (KKC) area. Refer to appendix 7 for a full list of abbreviations used in the text.

The volcanic Allanridge Formation forms the upper unit of the Ventersdorp Supergroup and extruded over large areas covering the underlying rocks. The Allanridge Formation consists of dark-green amygdaloidal lava, light green-grey porphyritic lava and pyroclastic rocks. These lavas are seen as xenoliths at the Lace pipe, although they may be Hekpoort lava xenoliths.

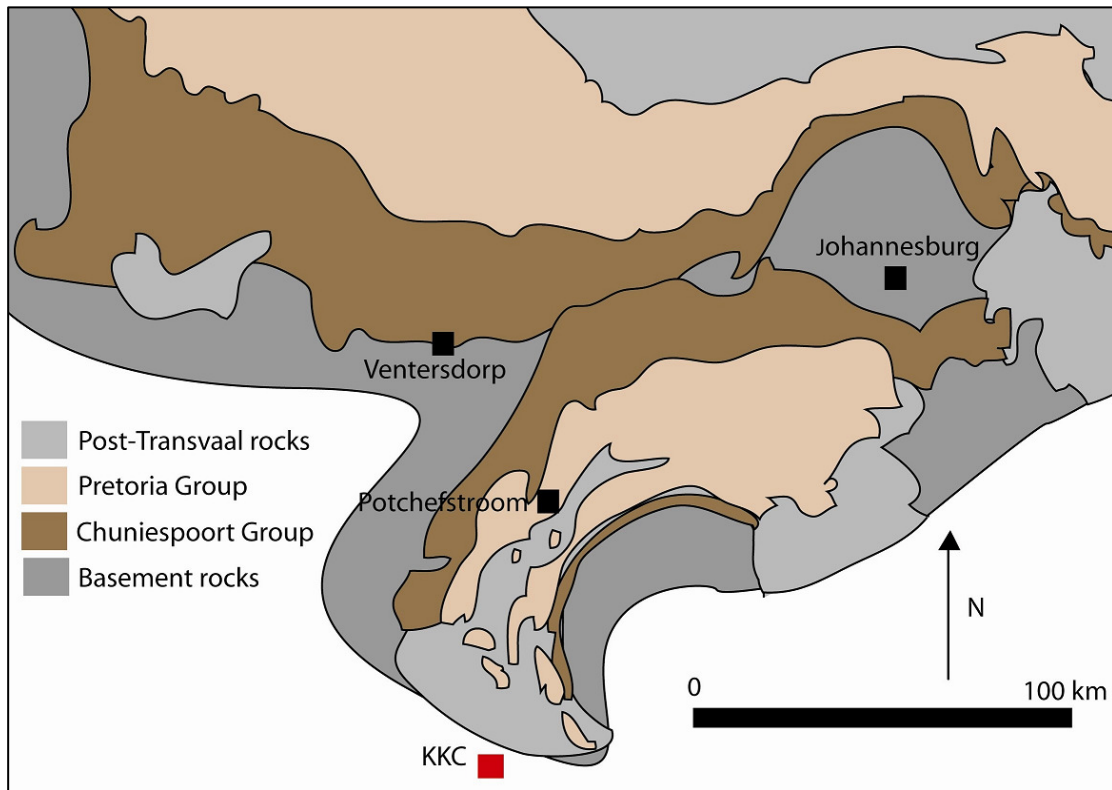


Figure 1.6 Present distribution of the Transvaal Supergroup outcrops. Note the position of the Kroonstad Kimberlite Cluster (KKC). Diagram after Eriksson et al. (2006).

Ventersdorp Supergroup xenoliths are relatively rare within the Kroonstad pipes. However rare occurrences of highly altered green basalt are noted, which are interpreted as Ventersdorp basalts.

1.2.2 Transvaal Supergroup

The Transvaal Supergroup unconformably overlies the Ventersdorp Supergroup and can be divided into three depositional basins in South Africa: 1) Transvaal basin, 2) Prieska sub-basin and 3) Ghaap Plateau sub-basin. The Transvaal Supergroup is divided into the Chuniespoort and Pretoria Groups, which are comprised of numerous lithologies including: quartzite, shale, conglomerate, dolomite and andesitic lava as shown in table 1.1. Two Formations of the Transvaal Supergroup are seen outcropping to the northwest, north, northeast and within the cluster. These are the volcanic Hekpoort Formation and the sedimentary Daspoort Formation both of which are part of the Pretoria Group.

The Pretoria Group is divided into four Formations as shown in table 1.1, all of which are most likely present at depth at the KKC. The sub-aerial volcanism of the Hekpoort Formation

produced green/grey occasionally amygdaloidal basaltic-andesitic lava up to 830m thick (Reczko et al. 1995). Intermittent hiatuses in volcanism produced small lacustrine shale deposits. Local pyroclastic units are also present. The Daspoort Formation is dominated by immature sandstones, pebbly arenites, conglomerates and mudrocks (Eriksson et al. 1993). Both shallow marine and fluvial models are presented for the formation of the rocks.

The lower Chuniespoort Group rocks are seen outcropping further to the North but are covered by Karoo Supergroup sediments nearer the KKC. The Malmani Subgroup is of particular interest as many carbonate xenoliths are found within the Voorspoed pipe massive volcanoclastic kimberlite (MVK). These carbonate xenoliths often contain chert and therefore it is likely that both the Oaktree and Monte Cristo Formations of the Malmani Subgroup are present at depth at the Voorspoed pipe in particular.

1.2.3 Karoo Supergroup

The Karoo Supergroup sedimentary and volcanic rocks are the dominant rock type outcropping in the Kroonstad cluster area. The Ecca, Beaufort and Drakensberg Groups are present. No basalt lava is seen outcropping anywhere near to the cluster, although the dominant country rock xenolith (CRX) at the Voorspoed pipe is basalt (80% of total CRX contents). Numerous intrusive dolerite dikes and sills represent the Drakensberg Group in the Kroonstad area. Dwyka Group rocks are not seen locally but may be present at depth as relatively thin units. The upper Molteno, Elliot and Clarens Formations are not present in this area but have been identified as CRX within both the Voorspoed and Lace pipes (Hanson, 2006 and Howarth, 2007). The distribution of the Karoo Supergroup rocks in the Kroonstad area is illustrated in figure 1.7.

1.2.3.1 Dwyka Group

The Dwyka Group although the least extensive of the Karoo Supergroup rocks is characterised by 7 distinct facies types, which vary from the southern to northern outcrops. These 7 facies include: massive diamictite, stratified diamictite, massive carbonate-rich diamictite, conglomerate, sandstone, mudrock with stones and mudrock (Johnson et al. 2006). The Group is divided into a northern and southern facies. The northern facies is characterised by rapid thickness changes (up to 200m over short distances) and a highly variable lithology. Mudrock facies dominates with lesser massive diamictite.

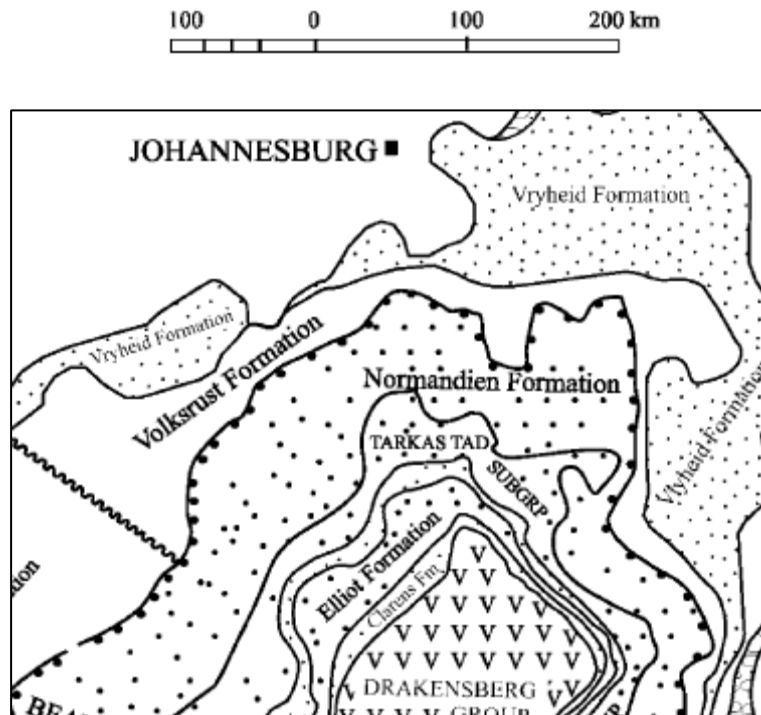


Figure 1.7 Distribution of the Karoo Supergroup in the Kroonstad area. The Kroonstad kimberlite cluster is located approximately 200km to the south west of Johannesburg. Diagram after Catuneanu et al. (2005).

1.2.3.2 Ecca Group

The Ecca Group is the current outcropping geology of the Kroonstad kimberlite cluster (KKC). The Group is divided into 16 Formations (Johnson et al. 2006), two of which are seen outcropping at the KKC, the Vryheid and Volksrust Formations. The Group is characterised by lateral facies changes and can be broadly subdivided into three geographical areas: southern, western/northwestern and northeastern (Johnson et al. 1996). The Vryheid and Volksrust Formations fall into the northeastern area. The only other Formation in the northeastern area is the Pietermaritzburg Formation, which underlies the Vryheid and Volksrust. The Pietermaritzburg formation is present only in the Eastern margin of the basin and therefore it is not present underlying the KKC. Therefore only the Vryheid and Volksrust Formations are present at the KKC.

The Vryheid Formation thins toward the north, east and south from a maximum of 500m in the east (Johnson et al. 2006). In the western area (location of the KKC) the Formation varies greatly in thickness due to the uneven basement topography. The Formation is comprised of upward-coarsening cycles up to 80m thick (Smith et al. 1993). The base of a cycle is characterised by dark muddy siltstone, which coarsens upwards to medium to coarse

sandstones at the top of the cycle. Fining-upward cycles are also present in the east with similar lithologies as described above. Coal swamps formed in the northwestern part of the Formation (Smith et al 1993).

The Volksrust Formation is predominantly argillaceous which interfingers with both the overlying Beaufort Group and the underlying Vryheid Formation (Johnson et al. 2006). The Formation consists of grey/black silty shale with lesser siltstone and sandstone lenses.

1.2.3.3 Beaufort Group

The Beaufort Group can be divided into two subgroups, the lower Adelaide and upper Tarkastad Subgroups both of which are present in the northern part of the Karoo basin (Johnson et al. 1996). The boundary between these subgroups is the only one that can be traced with reasonable certainty throughout the Beaufort Group.

Adelaide Subgroup

In the northeastern basin the Adelaide Subgroup consists of only one formation, the Normandien Formation. This formation has a maximum thickness of 320m (Johnson et al. 2006) and is comprised of alternating mudstones and coarse to very coarse sandstones. Sandstone accounts for 20-30% of the total thickness (Johnson et al. 2006). Generally the Adelaide Subgroup is characterised by upward fining cycles. The lower Normandien Formation however contains upward coarsening cycles. The presence of rhythmites and shale with thin tabular sandstone lenses points to a lacustrine or deltaic setting for deposition (Smith et al. 1993 and Johnson et al. 2006).

Tarkastad Subgroup

The Tarkastad Subgroup is characterised by an increase in sandstone and red mudstone content relative to the Adelaide Subgroup. The Tarkastad Subgroup consists of four Formations, two of which are present in the northeastern basin (Johnson et al. 1996). Groenewald (1989) described two distinct Formations, the Verkykerskop and Driekoppen Formations in the northeastern basin. The lower Verkykerskop Formation is comprised of up to 80m of fine to very coarse sandstone whereas the upper Driekoppen is almost entirely mudstone. The lower coarser unit was interpreted to be the result of braided river deposits whereas the upper formation represents distal meandering river facies (Groenewald, 1989).

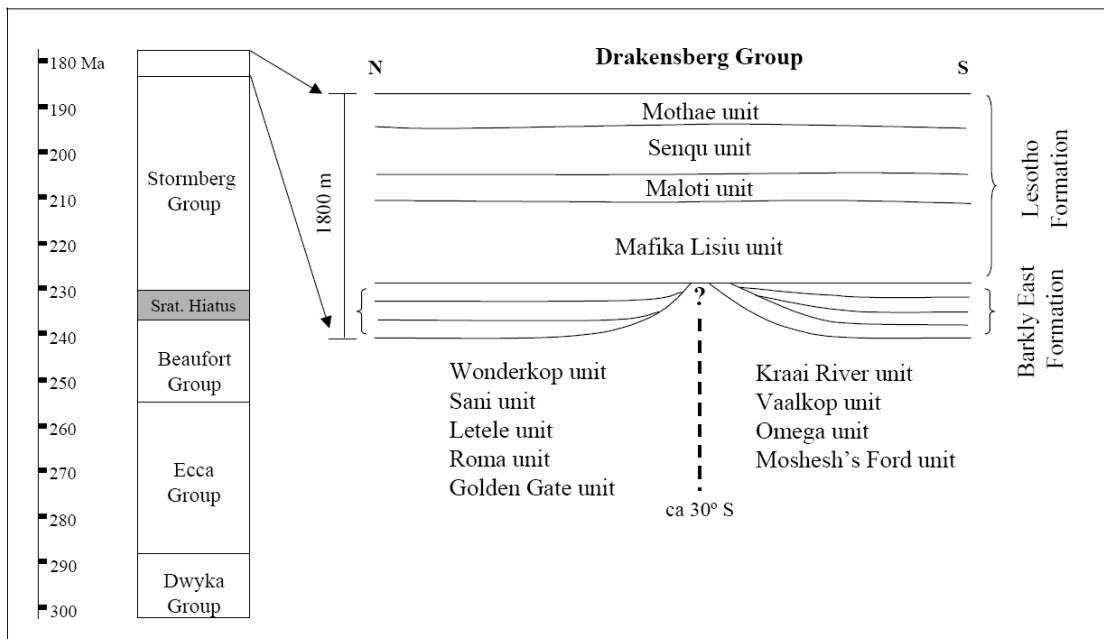


Figure 1.8 Karoo Supergroup (Drakensberg Group) basalt stratigraphy. Diagram from Hanson (2006).

1.2.3.4 Molteno, Elliot and Clarens Formations

The Molteno Formation ranges in thickness from 460m in the south to <10m in the extreme north and can be divided into five members (Smith et al. 1990). The Formation is characterised by alternating medium to coarse-grained sandstones and grey mudstones. The Molteno Formation represents the first of the quartz-rich sandstones at the top of the Karoo sequence. The Elliot and Clarens Formations follow the Molteno, where quartz contents continue to increase.

The Elliot Formation is comprised of alternating mudstone and fine to medium grained sandstone. The Formation reaches a maximum thickness of 500m in the south (Johnson et al. 2006). The Elliot Formation is famous for its vertebrate fossils, which are present in the red and green/grey mudstones. Sandstone contents become more dominant at the top of the Formation as a result of more arid climate with ephemeral rivers.

The Clarens Formation represents the last period of sedimentary deposition within the Karoo basin. The Formation is characterised by fine-grained aeolian sandstone deposits and has an average thickness of 100m (Smith et al. 1990). Minor basaltic layers are present in the upper part of the unit signalling the onset of the flood basalt province (Drakensberg Group).

1.2.3.5 Drakensberg Group

The Drakensberg Group is volcanic comprising of flood basalts and a suite of dolerite intrusions. The Drakensberg Group basalt pile is approximately 1800m thick (Marsh et al. 1997). The basalt pile is subdivided into two Formations as shown in figure 1.8, the lower Barkley East and upper Lesotho Formations. Each Formation is then subdivided into a number of units based on geochemical variations as shown in figure 1.8. Large dolerite outcrops are present at the KKC whereas basalt is not present. A huge basalt block is present within the Voorspoed pipe but this is not part of the local country rock geology.

Karoo basalt xenoliths are particularly abundant in the volcanoclastic kimberlite (VK) at the Kroonstad pipes. In most cases Karoo basalt account for approximately 60-80% of the entire xenolith population, as described in section 3. Karoo type sedimentary xenoliths are relatively rare, especially the sandstones. The distribution of Karoo basalt xenoliths within the KKC pipes is particularly important as discussed in section 5.3.4.1.

Section 2. Methodology

2.1 Terminology

There are numerous classification/terminology schemes available in the literature. The most recent are Cas et al. (2008b) and Scott Smith et al. (2008). Cas et al. (2008b) proposes a new scheme where the terminology is based largely on principles developed in volcanology. This scheme completely changes kimberlite terminology and makes it extremely difficult to use when reading other literature. Therefore this classification/terminology scheme is not used in this study. The schemes developed over the years by Skinner and Clement (1979), Clement and Skinner (1985), Field and Scott Smith (1998) and Scott Smith et al. (2008) have been combined and defined here to give a generally acceptable set of classification terms, which is widely used in the current literature. Refer to appendix 7 for a full list of abbreviations used in the text.

Kimberlite Pipe Classes are described in detail in section 5. It is important to note that three distinct varieties of kimberlite pipes occur: Class 1/tuffisitic kimberlite type; Class 2/Prairies type and Class 3/Lac de Gras type (Field and Scott Smith, 1999; Skinner and Marsh, 2004 and Scott Smith, 2008). Typical South African kimberlites all fall into the Class 1 or tuffisitic kimberlite type pipes. The Kroonstad kimberlites are the first non-Class 1 kimberlites to be documented in South Africa.

Hypabyssal Kimberlite (HK) is used to describe coherent/magmatic kimberlite occurring at depth. Current literature prefers the non-genetic term coherent to describe any magmatic kimberlite (Cas et al. 2008b and Scott Smith et al. 2008). Coherent is a non-genetic term applied to rocks formed by magmatic process, which show no evidence of fragmentation (Scott Smith et al. 2008). Therefore this term would apply to both hypabyssal rocks and lavas.

HK has been traditionally further divided on the basis of proportion of macrocrysts present. These macrocrysts are dominantly olivine and where they exceed 15%; the rock is termed macrocrystic hypabyssal kimberlite. When the rock contains <15% macrocrysts

the rock is termed aphanitic hypabyssal kimberlite. Cas et al. (2008b) has proposed the term inequigranular be used to describe macrocrystic kimberlites, as it is often difficult to distinguish between macrocrysts and phenocrysts. The term inequigranular may be used when the origin of the larger crystals is unknown. Clement and Skinner (1985) have divided HK into two varieties based on the CRX proportions. HK with >15% country rock xenolith (CRX) are called hypabyssal kimberlite breccias (HKB) whereas those with <15% CRX are typical HK. This division is important for this study and therefore it is included in the terminology for this thesis. The presence of high proportions of CRX in hypabyssal rocks can often be misleading and thorough macroscopic and microscopic analyses need to be conducted before interpreting. Rocks containing high proportions of CRX are often classified as volcanoclastic kimberlite (VK) before thorough petrographic investigation has been conducted.

Hypabyssal kimberlite (HK) can be classified mineralogically by the abundances of the major mineral constituents. This scheme was developed by Skinner and Clement (1979). Olivine is ubiquitous and therefore does not form part of the classification scheme. There are four stages of progressive classification. The primary classification is on the most abundant mineral present. A secondary modification can be added where the mineral exceeds 2/3 the modal proportion of the primary mineral. A third stage modification is used for minerals <2/3 the modal proportion of the primary mineral. Third stage modification is indicated by using terms such as –rich or –bearing. The fourth stage modification is based on alteration of the kimberlite.

4 3 2 1

Example: Carbonated, melilite-bearing, diopside, phlogopite kimberlite

Transitional Kimberlite was first described by Skinner and Marsh (2004) and Hetman et al. (2004). These rocks are particularly controversial in the current literature and are often interpreted as agglutinated or welded tuff deposits (e.g. Brown et al. 2009). Transitional kimberlites typically show a gradational change from typical hypabyssal kimberlite to volcanoclastic kimberlite. Hetman et al. (2004) classified transitional kimberlite into two

varieties: 1) hypabyssal/transitional kimberlite (HKt) and 2) transitional tuffisitic kimberlite (TKt). The HKt variety is further subdivided on the basis of country rock xenolith (CRX) content similarly to that described above for the HK sensu stricto. Therefore when an HKt contains >15% CRX it is classified as a hypabyssal transitional kimberlite breccia (HKtB). Refer to appendix 7 for a full list of abbreviations used in the text.

Globular Segregationary is used to describe the texture of hypabyssal kimberlite where the development of globules is observed. This development ranges from incipient to pervasive in typical transitional kimberlites (Skinner and Marsh, 2004). Spherical bodies occurring in the transitional kimberlite are referred to as globular segregations and are the equivalent to nucleated magmaclasts, which have been incorporated into the volcanoclastic kimberlite (VK) infill as discussed in section 5.3.4.2.

Root Zone: Typical kimberlite pipes in South Africa are divided into three distinct zones: root zone, diatreme zone and crater zone (Skinner, 2008). The root zone of a pipe is characterized by numerous hypabyssal intrusions and includes transitional kimberlite. The term root zone is used to describe the base of the kimberlite pipe, which has formed through sub-volcanic hypabyssal processes. Diatreme zone is used when describing Class 1 Tuffisitic kimberlites only.

Volcanoclastic is a non-genetic term applied to rocks containing a substantial proportion of volcanic particles (Scott Smith et al. 2008). This also includes clastic rocks occurring within the pipe. Volcanoclastic deposits include: pyroclastic, resedimented volcanoclastic, epiclastic. Cas et al. (2008b) suggest hydraulic fracture deposits should also fall into this category. Hydraulic fracture deposits are often filled with hypabyssal kimberlite but never by volcanoclastic kimberlite (Skinner, 2008) and therefore can not be classified as volcanoclastic rocks. Volcanoclastic rocks can be similarly divided into two varieties based on the proportion of country rock xenoliths (CRX) present. Volcanoclastic kimberlite (VK) containing >15% CRX are termed breccias whereas those <15% receive

no additional name (Clement and Skinner, 1985). Many of the newer terminology schemes have abandoned the term breccia and simply use CRX-rich.

Magmaclast is a non-genetic term for any kimberlitic clast found within a volcanoclastic deposit. Previously magmaclast has been used to describe fluidal fragments of former kimberlite magma, which does not include brittle fragment (autoliths) of previously lithified kimberlite. However in this study the term magmaclast is applied to any fragment of kimberlite occurring as a clast within the volcanoclastic kimberlite (VK) so as to avoid genetic implications during descriptive sections as the genetic processes forming the magmaclasts can often be complicated.

Autolith and Nucleated Autolith are terms used to describe magmaclasts of kimberlite, which have formed before the eruptive process. Autolith would include older kimberlite formed in intrusive environments, which has been intersected by the vent. Alternatively autoliths may also form by co-magmatic kimberlite solidifying deep within the vent, which is fragmented by later explosive intrusions. These incorporated kimberlite clasts would both fall into the category of an autolith or “garden variety” autolith in section 3. The term nucleated autolith was first introduced by Ferguson (1973) and Danchin et al. (1975) to describe kimberlite magmaclasts from Lesotho and elsewhere in South Africa. This term is not used in any of the current literature but here it may be relevant to the Voorspoed and Lace kimberlites. A nucleated autolith is a co-magmatic kimberlite clast, which forms deep within the vent during the exsolution of volatiles and concurrent nucleation of minerals to form spheroidal structures. Minerals nucleated around the larger components such as xenoliths or xenocrysts. These nucleated spheroids are generally fully crystallized before incorporation into the volcanoclastic deposits. The spherical magmaclasts observed in this study are generally well crystallized and resemble typical hypabyssal kimberlite (HK), which is similar to typical pelletal lapilli in tuffisitic kimberlite. Furthermore the spherical magmaclasts at the Kroonstad kimberlites are interpreted to have formed in a hypabyssal environment in transitional kimberlites. Therefore the term nucleated autolith should be reconsidered in the current literature. The term nucleated magmaclast is used here so as not to imply genetic connotations however

a review of nucleated autolith is required in future terminology developed for kimberlites. Therefore nucleated magmaclasts are globular segregations formed in the transitional kimberlite, which have been later incorporated into the VK infill of the pipes.

Megacryst, Macrocryst, phenocryst and xenocryst are terms, which often become confusing when used all together. Megacrysts and macrocrysts are essentially xenocrysts of mantle material within the magma whereas phenocrysts are primary minerals crystallizing out of the magma. Megacryst, macrocryst and phenocryst are used to describe minerals in the hypabyssal rocks and in magmaclasts within volcanoclastic rocks. The term megacryst is used here on purely a size discrimination basis and no genetic connotations are implied. Megacryst is used to describe anhedral olivine grains >5mm in size. Macrocrysts are generally >0.5mm and anhedral whereas phenocrysts are generally <0.5mm and often have subhedral-euhedral shapes. Furthermore phenocryst can be classified as microphenocrysts when the grains are <0.1mm. The term xenocryst is used only in volcanoclastic rocks to describe single grains in the deposit. Xenocrysts can be either lithic or juvenile in origin and have no restriction on grain sizes.

Inter-Globule Material is used to describe the material between the globular segregations in the transitional kimberlite.

Interclast Material is used to describe the material between the xenoliths and magmaclasts of a volcanoclastic rock. The constituents of the interclast material are juvenile and lithic xenocrysts in a cement of ultra fine grained dark turbid material, which is generally too fine grained to identify.

Primary diopside, microlitic clinopyroxene and basaltic clinopyroxene are all present within the rocks at the various kimberlite pipes. Each variety of pyroxene forms in different environment and therefore it is particularly important not to get them confused. Primary diopside is only used to describe primary kimberlitic diopside, which has crystallized out of the kimberlite magma. Microlitic clinopyroxene, which is also diopside in composition but to avoid confusion is termed clinopyroxene, is

autometasomatic/deuteric in nature and is not a primary crystallization product but rather a late stage gas condensate. The process of formation of the microlitic clinopyroxene will be discussed in greater detail in section 5. Microlitic clinopyroxene generally occurs as laths <0.1mm in size however in rare cases may reach up to 0.2mm. The basaltic clinopyroxene is also diopside in composition and is used here to describe clinopyroxene, which formed in the Karoo Supergroup basalts and has now become incorporated into the volcanoclastic kimberlite as xenocrysts or as a constituent of basalt xenoliths.

2.2 Drill Core Sampling/Logging

Lace

A total of >7 boreholes were drilled at the Lace kimberlite in 1997. One of these boreholes (C6) was logged and sampled to near completion with only the bottom 50m missing from a borehole 869m deep. Borehole logs are presented in appendix 6. The boreholes are drilled from the outside of the pipe within the country rock inward into the pipe (see figure 3.2). Borehole C6 cross-cuts both the main pipe as well as the satellite pipe. This hole provided in situ sampling for petrographic analysis of the kimberlite within the Lace pipe, which has not been done before. A total of 19 samples were taken from the different geological units encountered in borehole C6. Furthermore borehole C7 was partially logged from the contact with the wall rock into the pipe and three samples were taken. Only the top of the borehole was available for logging. These samples were supplemented with 13 hand specimen samples from the surrounding dump sites. Eight samples of hypabyssal kimberlite and a further five samples of volcanoclastic kimberlite.

It must be noted here that the availability of boreholes at the Lace mine was limited and sampling was done on the boreholes available to the best of our ability. The supplementary samples taken from the dumps were taken to bulk up the sample set. Borehole C6 was the only borehole available for detailed sampling and therefore most of the discussion on the Lace kimberlite is based on this borehole intersection as shown in figure 3.2. A full list of samples taken from the Lace pipe is given in appendix 8.

Table 2.1 Depth, bearing and depth of the Voorspoed boreholes logged and sampled in this study.

Borehole #	Depth (m)	Bearing	Dip
2	350.23	Vertical	90
3	339.55	66	77
9	388.65	229	85
10	295.13	Vertical	90

Voorspoed

A total of 10 boreholes were drilled during the 1998 evaluation program at Voorspoed (See figure 3.12 in section 3 for positions of the boreholes at the Voorspoed pipe). All 10 of the original logs produced by De Beers were analysed and four were chosen for detailed sampling and logging. These four boreholes (holes 2, 3, 9 and 10) were chosen on their position within the pipe so as to provide coverage of the geology of the whole pipe as well as on the specific rocks types logged in the original logging. Two of the boreholes (9, 10) are drill near the margins of the pipe and have contacts with the wall rock at the base, the other two (2, 3) are drilled in the centre of the pipe. These four boreholes have been re-logged in this study. Detailed sampling of the individual rocks types within each borehole was also done. 36 samples were taken from the four boreholes for petrographic analysis. These 36 samples are complimented by 26 samples taken by Mike Skinner from the boreholes (see appendix 8 for sample lists) and over 350 samples from the De Beers archives. Borehole logs for the Voorspoed pipe are presented in appendix 4. A full list of samples from the Voorspoed pipe is given in appendix 8.

Besterskraal North

Samples from the Besterskraal North kimberlite were collected from the De Beers archives as the pipe is sub-economic and fresh samples are no longer available from the pipe itself.

2.3 Petrographic Modal Analysis

Modal analyses are conducted on all rock types observed. At the Voorspoed pipe ten varieties of volcanoclastic rocks, a transitional kimberlite and five hypabyssal kimberlite varieties are analysed. 500 point counts are done on each thin section. At least two examples of each rock type were counted and an average was taken. Therefore 1000 counts are done on each rock type. At the Lace kimberlite two varieties of volcanoclastic kimberlite are counted along with the freshest hypabyssal kimberlite sample, as only one hypabyssal kimberlite variety is observed. Furthermore samples approximately every 10m in borehole C6 are also analysed. The main objective of the modal analyses is to determine the abundances of the main constituents within the different rock types. Hypabyssal and transitional kimberlite rocks are analysed for: olivine, phlogopite, primary diopside, melilite, monticellite, spinel, perovskite, apatite, sanidine, K-richterite, leucite, calcite, serpentine, clay minerals, microlitic clinopyroxene and country rock xenoliths. These constituents are not all present in each sample analysed.

Volcanoclastic rocks are analysed for: 1) Xenoliths, which include Karoo basalt, Karoo sedimentary and basement fragments; 2) magmaclasts, 3a) olivine as xenocrysts and 3b) olivine within the magmaclasts, 4) interclast material and 5) xenocrysts, which include lithic and juvenile.

2.4 Geochemistry

Lace

The Lace kimberlite has been sampled from both the in situ core as well as from the surrounding dump sites. All the samples obtained are hypabyssal kimberlites and are dominantly hypabyssal transitional kimberlite (HKt) and hypabyssal transitional kimberlite breccia (HKtB). A total of 21 samples were analysed for major and trace element compositions. Geochemical data is available in appendix 1 and 2. Eight samples are from the surrounding dumps and the remaining 13 were sampled from in situ drill core intersections of the pipe.

Voorspoed

Due to the lack of hypabyssal kimberlite at the Voorspoed kimberlite limited samples were available for sampling. Only one sample of an internal dike was sampled during this study. Further supplementary data has been used from Roberts (1997). Hypabyssal kimberlite (HK) is thought to occur at greater depth.

Geochemical Analysis

21 samples from Lace and one sample from Voorspoed have been analysed for bulk rock geochemistry. Both major elements and trace elements have been analysed by X-ray fluorescence. The major elements were determined using the XRF fusion technique of Norrish and Hutton (1969). Trace elements along with Na were determined using undiluted pressed powder pellets described by Duncan (1984). Loss of ignition and H₂O were determined gravimetrically during the preparation of the XRF fusion discs.

2.5 Mineral Composition

A sample of the Voorspoed hypabyssal kimberlite showing the best development of aegirine has been selected for detailed microprobe analysis. This is sample K1/114 from the De Beers collection, which is a sample from a sill in the surrounding country rock. The sample is analysed using an electron microprobe for aegirine, diopside and phlogopite compositions. Elements analysed include: SiO₂, TiO₂, Al₂O₃, FeO, MgO, CaO, Na₂O and K₂O. The methods used for microprobe analysis for the microlitic clinopyroxene are those outlined by Torab and Lehmann (2007).

2.6 Petrographic Interest Rating

Hypabyssal kimberlite (HK) from all three kimberlites has been rated in terms of economic potential. The rating system relies on petrography to indicate the likelihood of the preservation of diamonds in the magma as well as any possible fractional crystallization evident. Kimberlites are defined as containing 25 vol. % olivine macrocrysts and 25 vol. % olivine phenocrysts (Mitchell, 2008). Therefore during modal analysis of the rock the proportion of olivine is accurately counted. When macrocrystal olivine contents are low it has negative impact on diamond size distribution as the

diamonds will be fractionated out along with the olivine. Therefore the interest rating will decrease with decreasing olivine macrocryst content. The second test is to determine how likely the diamonds are to survive in an oxidizing environment. This is determined by using opaque oxides as an indication. Three grain size categories can be used as an indication of total resorption to no resorption. Grain size of <0.05mm is a good indication that no resorption has occurred. 0.05-0.15mm indicates partial resorption of the diamonds and opaque oxide grain sizes >0.15mm indicates very little survival of the diamonds. This technique has been developed by Mr. Mike Skinner and a brief description is given in Skinner et al. (2004). Furthermore in Group II kimberlite the more evolved magmas resorb the diamonds and therefore interest rating decreases with increasing evolution of the magma. This rating system indicates the possible potential of the diamond deposit and must not be used by itself. The kimberlite can be rated as low, moderate or high in terms of economic potential.

Section 3. Geology of the Kroonstad Kimberlite Cluster

As discussed in section 2 there are three varieties of diopside present within the various kimberlite units at the Kroonstad cluster. Primary diopside is simply called diopside and therefore whenever the term diopside is used it is referring to primary liquidus diopside. Diopside is also present as microlitic diopside in the transitional kimberlite. Therefore this form of diopside is called microlitic clinopyroxene so as not to confuse it with primary diopside. It is important to note that microlitic clinopyroxene is also diopside in composition. Microlitic clinopyroxene varies in habit and size as described below but generally occurs as laths <0.1mm in length. Furthermore clinopyroxene is present as xenocrysts within the volcanoclastic kimberlite (VK) rocks. These augites are the result of the disaggregation of basalt xenoliths and therefore have no link to the kimberlite magma. These augite xenocrysts are called basaltic clinopyroxene xenocrysts in this section. These terms are used throughout this section for Lace, Voorspoed and the Besterskraal North pipes.

Globular segregatory textures are present at both the Lace and Voorspoed kimberlites. The texture is always incipiently developed and never becomes pervasive. However there are varying degrees of development of this incipient globular segregatory texture as outlined in section 2. Therefore to differentiate between rocks with varying degrees of development the incipient globular segregatory textures is divided into three degrees of development: low, moderate and high degrees. A low degree of development is characterised by vague globular structures becoming evident but the outlines of the globules are often difficult to see. The distribution of the globules is very patchy and typically only one or two globules are present within a single thin section. A medium degree of development is characterised by relatively abundant and distinct globules forming in patches, which are beginning to become more dominant than the coherent patches. A high degree of development is characterised by distinct globules with clear outlines, which is becoming the dominant structure of the rock. This high degree of incipiently developed globules is now evident of macroscopic scale whereas the low and medium degrees of development are not visible on a macroscopic scale. These degrees of development of the globular segregatory texture are regularly referred to in the text especially for the Lace pipe

and therefore it is important to note that the texture is always incipient but varying degrees of development are observed.

3.1 Lace (Crown) Kimberlite Pipe

3.1.1 Introduction

The Lace kimberlite consists of two pipes adjacent to one another (figures 3.1 and 3.2). These pipes have not been found to connect at depth. The main pipe is approximately 2ha in size whereas the satellite pipe is <0.5ha in size. Both pipes have been intersected by drilling and a number of rock units have been identified. These include: 1) hypabyssal kimberlite (HK), 2) hypabassal transitional kimberlite and kimberlite breccia (HKt and HKtB) and 3) volcanoclastic kimberlite (VK). The main pipe has been mined out to a depth of 240m with further underground workings extending to approximately 330m as shown in figure 3.2. Due to the limited accessibility to the drill core, parts of two of the core holes have been analysed along with numerous samples from the old dumps. Upon detailed petrographic analysis it is apparent that VK has been completely mined out of the pipe and is not present in any of the drill core observed. The drill core analysed includes holes six and seven, which intersect both the satellite pipe and the main pipe. The satellite pipe is only intersected at 240m below the current surface whereas the main pipe has been intersected from 250m down to approximately 720m below the current surface. From the presence of both VK and HK samples on the old dumps and the presence of HKt at 250m in hole 7 it is interpreted that the VK must have occurred to approximately 240m from the current land surface. Refer to appendix 8 for a full list of samples analysed from the Lace kimberlite pipes.

All HK is classified as macrocrystic phlogopite kimberlite, with varying proportions of altered melilite, altered monticellite and microlitic clinopyroxene in the HKt. Microlitic clinopyroxene is characteristic of HKt and therefore rocks containing microlitic clinopyroxene are classified as HKt/HKtB. HK proper has not been observed in situ within the pipe. The distribution of internal geology of the satellite pipe is mostly based on the original schematic maps from the mine due to the lack of accessibility to core from the satellite pipe and therefore may be inaccurate. The HKtB is the only geology observed and analysed from the core and therefore is the only reliably



Figure 3.1 Photograph of the Lace pit looking west. The competent rock in the wall is the satellite pipe outcropping in the pit. The pit has been open for over a hundred years and yet no caving of the satellite pipe has occurred indicating the highly competent nature.

mapped unit in the satellite pipe. The main pipe on the other hand has been sampled throughout the pipe. An extensive, 380 deep, hypabyssal transitional kimberlite breccia (HKtB) column is evident, which has previously been classified as tuffisitic kimberlite breccia. This HKtB is characterised by two important features: 1) incipient globular segregatory texture and 2) the complete lack of coarse Karoo sandstone and Karoo basalt xenoliths. Karoo basalt xenoliths are particularly abundant in the upper VK units observed from samples collected from the dumps. The differing xenolith population is a very important feature, which has specific genetic connotations (discussed in section 5). HKt is divided into a country rock rich breccia unit (HKtB) and typical HKt with less abundant country rock xenoliths (CRX). Volcaniclastic kimberlite has been divided into two very distinct varieties: 1) basalt-rich volcaniclastic kimberlite (bVK) and 2) quartz-rich volcaniclastic kimberlite (qVK). VK as stated earlier is only present on the dumps and therefore the original internal distribution of these units is unknown. VK has been described

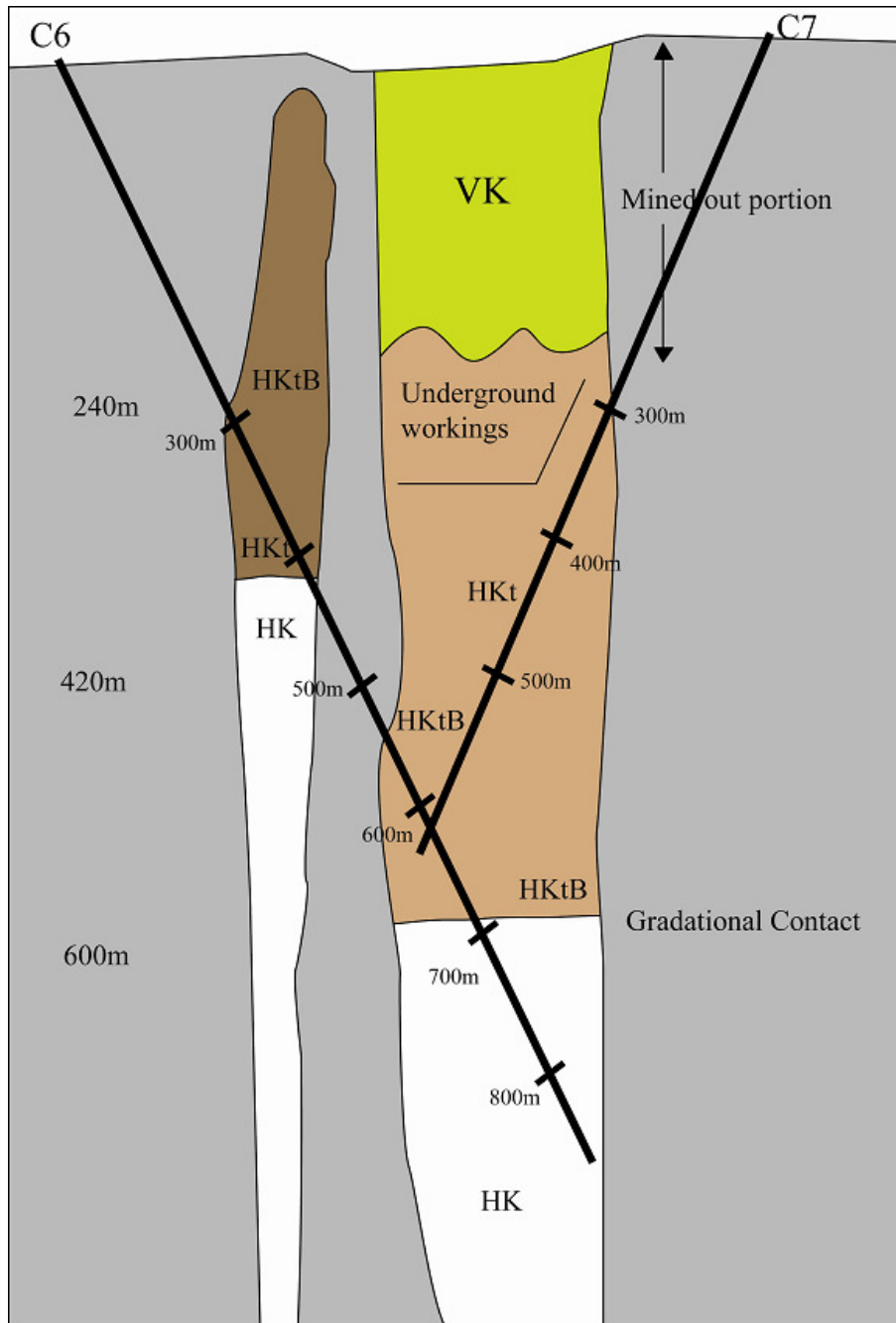


Figure 3.2 Schematic east-west cross-section of the Lace pipe showing the distribution of the internal geology to a depth of 780m from the current land surface. Pipe outlines based on the schematic diagrams at the Lace mine. Boreholes C6 and C7 are illustrated with depth of borehole given every 100m. Depths given on the left are depth below the surface. The main pipe is occupied by variable distribution of HKt/HKtB. Further detailed logging needs to be done to map the distribution of the HKt and HKtB. The satellite pipe is occupied by HKtB only. See appendix 6 for the borehole logs for hole C6 and C7. See appendix 7 for a full list of abbreviations used in the diagram and text. The HKt/HKtB is described in detail in section 3.1.3 and photomicrographs are shown in figure 3.4 – 3.7. See table 3.2 for a full list of samples from the Lace drill core.

in the original schematic models for the pipe but no VK has been intersected by the core samples analysed in this study. Refer to appendix 7 for a full list of all the abbreviations used.

A satellite pipe is present approximately 35m due west of the main pipe and has a diameter of 40m. The satellite pipe has been intersected by boreholes at depth; however it does not join up with the main pipe at the current drilled depth. Furthermore the satellite pipe is overlain by shales at the surface and therefore is a blind pipe, which has not reached the original surface.

Volcaniclastic kimberlite can not be present within the satellite pipe as no explosive breakthrough to the surface has occurred. The satellite pipe has not been previously mined and is clearly evident in the current open pit in the sidewall as shown in figure 3.1. The kimberlite present in the satellite is highly competent indicated by the complete lack of caving etc. in the sidewall of the open pit. The open pit has been open for close to one hundred years and therefore caving would be expected in a less competent rock. The competent nature of the kimberlite at the satellite pit is due to the presence of HKt at this depth and no VK. The satellite pipe has been sampled at 260m below the current land surface in borehole C6. The kimberlite present is HKtB, which is very similar to the kimberlite present at the same depth in the main pipe.

The pipes intrude through the Ventersdorp lavas, Transvaal Supergroup and into the Karoo Supergroup. At the current level of erosion the country rock is Ecca Group sediments. Wagner (1914) notes that the Lace pipe “is remarkable for the enormous quantity of foreign matter which is everywhere.” Wagner (1914) estimated that kimberlite might only constitute 10% of the pipe filling. Merensky (1909) and Clement (1982) describe the VK as crystallinoclastic due to the high quartz content in the rock, which approaches a clastic nature. Wagner (1914) identifies the foreign material as: 1) amygdaloidal purple basalt, 2) white sandstone, 3) pink sandstone, 4) dolerite and 5) granite. The basalt and sandstone have been analysed and correlated with the Karoo Stormberg/Drakensberg Groups of rocks. Erosion has then been estimated using these country rock xenoliths as discussed in section 5.1. All the initial observations made by Merensky (1909), Wagner (1914) and Clement (1982) have been confirmed in this study with the exception of the sandstone breccia noted by Merensky (1909). The estimate of a 10% kimberlite

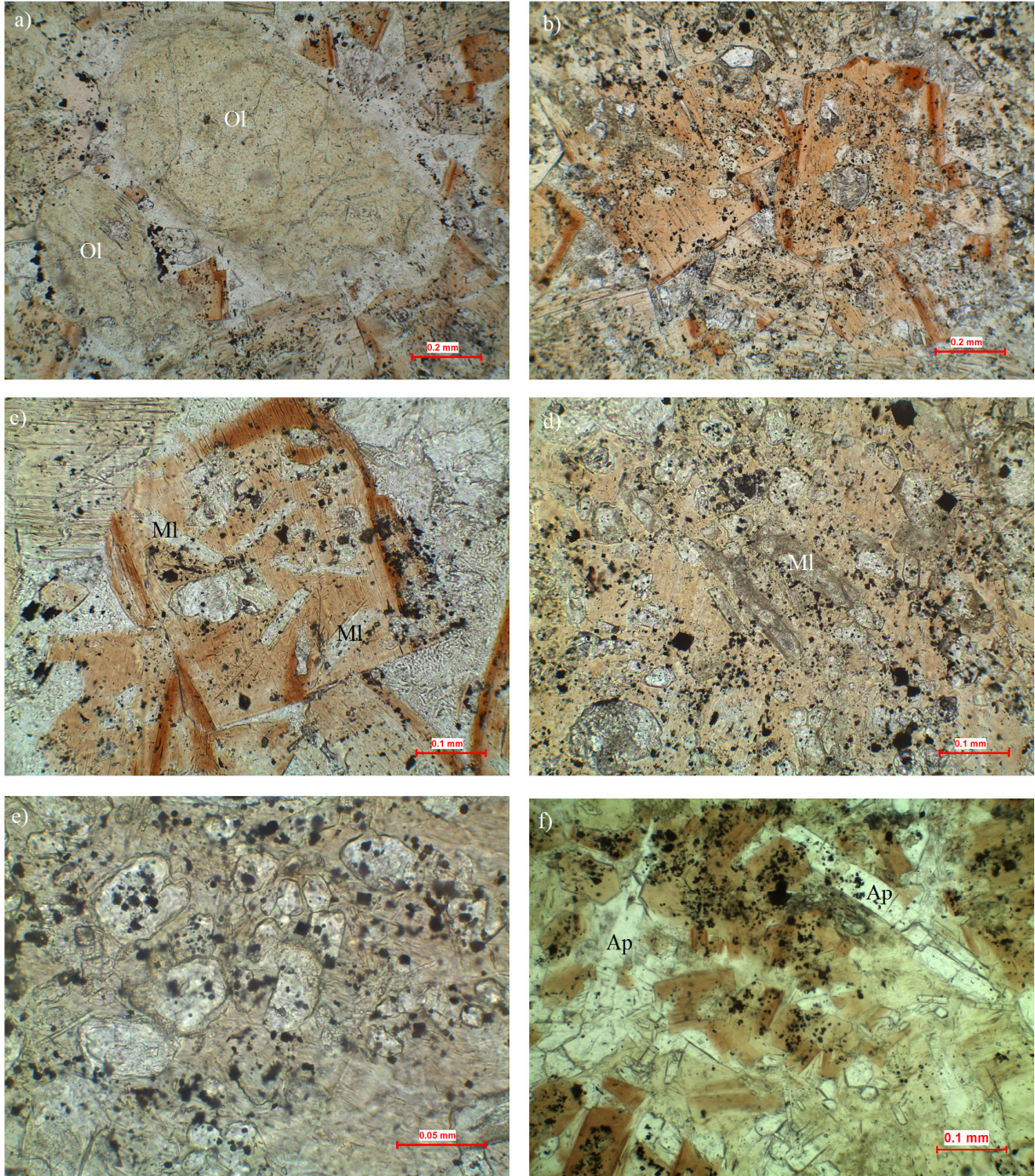


Figure 3.3 See figure caption overleaf.

Figure 3.3 Photomicrographs of the hypabyssal kimberlite sensu stricto at the Lace pipe as described in 3.1.2 (sample K2-1 collected from the dump site). a) Highly altered olivine (Ol). Alteration is to green yellow serpentine and clay minerals and ultra fine opaques. Set in a groundmass of phlogopite rich kimberlite. b) Highly poikilitic interlocking phlogopite plates. Also note the darker red brown tetraferriphlogopite margin on the phlogopite. c) Poikilitic phlogopite plate with numerous inclusions of colourless serpentinised melilite laths (MI). d) Poikilitic phlogopite plate with carbonatised dirty laths of melilite (MI) and abundant fine grained spherical altered monticellite and opaques. e) High power image showing abundant fine grained serpentinised monticellite inclusions, within a phlogopite plate, characterised by inclusions of opaques. f) Apatite (Ap) phenocryst laths in a groundmass of phlogopite rich kimberlite and a base of yellow green clay minerals. Note the abundant inclusions of opaques.

component only applies to the bVK as the qVK contains a slightly greater proportion of kimberlite.

3.1.2 Group II Hypabyssal Kimberlite (HK) Sensu Stricto (Sample K2-1)

The HK is a hypabyssal macrocrystic and megacrystic kimberlite, containing altered olivine (mega/macrocrysts and phenocrysts), phlogopite, monticellite pseudomorphs, melilite pseudomorphs, apatite, perovskite, opaque spinels, and hollandite set in a base of calcite and serpentine. The modal abundances of the respective minerals are given in table 3.1. Sample K2-1 is a rare example of fresh HK, which is characterised by the absence of microlitic clinopyroxene and the presence of abundant monticellite. K2-8 is very similar to this sample except that it contains microlitic clinopyroxene in low abundance. K2-1 can be classified as a macrocrystic melilite- and apatite-bearing, monticellite, phlogopite hypabyssal kimberlite. Figure 3.3 shows photomicrographs to illustrate the characteristics of the mineralogy.

Olivine occurs as three distinct populations: megacrysts, macrocrysts and phenocrysts. All three populations are typically light green/yellow in colour as a result of extensive alteration by serpentine and lesser calcite, clay minerals and fine-grained opaques (figure 3.3 a). Megacrysts (up to 2cm) and macrocrysts (0.5-5mm) are always anhedral whereas phenocrysts (0.15-0.4mm) commonly show subhedral habits. Phenocrysts are often difficult to differentiate from the base of the rock due to the highly altered nature of the olivine.

Phlogopite is highly poikilitic and occurs as interlocking phenocrysts plates (figure 3.3 b), 0.1-0.8mm in length. Phlogopite is pleochroic from light brown to almost colourless and shows zoning to darker red/brown tetraferriphlogopite margins. Mineral inclusions include: monticellite, melilite, opaque spinels, perovskite and olivine phenocrysts.

Monticellite occurs as fine-grained (<0.08mm) pseudomorphs, which have been completely replaced by serpentine and/or calcite. The grains are rounded to irregular in habit and are particularly abundant in this sample. Monticellite is characterised by the presence of fine-grained inclusions of opaque minerals as shown in figure 3.3 (e). Monticellite commonly occurs as inclusions within phlogopite indicating that it crystallised before phlogopite crystallisation.

Melilite was first described in kimberlite by Clement (1982) and later described in detail by Skinner et al. (1999). Melilite is always highly altered and is identified based on the presence of relict median lines which reflect the peg structure often characteristic of melilite in other rocks (Clement, 1982). Melilite in the Lace kimberlite occurs as highly altered laths in the HK, which can not be diopside as there is no diopside present in these rocks. Melilite, similarly to monticellite, occurs as pseudomorphs and is present as highly altered laths, which are <0.2mm in length. Melilite is relatively rare in this sample compared to other samples such as K2-2 where it is particularly abundant. The alteration product is dominantly very fine-grained calcite, which gives the laths a dirty appearance as shown in figure 3.3(c and d). Serpentine is also often seen completely altering melilite and commonly is intergrown with calcite as an alteration product. Melilite typically only survives as inclusions within phlogopite.

Apatite occurs in two distinct varieties: 1) fresh, colourless and high relief laths (figure 3.3 f), which are characterised by a low birefringence and straight extinction. These laths are generally between 0.1-0.3mm in size and commonly have inclusions of fine-grained opaque minerals. 2) Irregular poikilitic groundmass plates. These plates have similar characteristics to the laths described here but contain abundant inclusions of earlier formed opaques and perovskite.

Perovskite and opaque spinels are evenly scattered throughout the base. Both minerals are fine-grained (0.01-0.05mm) microphenocrysts and commonly show euhedral crystal habits.

Table 3.1 Modal abundances of the HK and HKt kimberlites at Lace based on 500 point counts over a single thin section. (Ol: olivine; Phl: phlogopite; Mel: melilite; Mon: monticellite; Ap: apatite; Op: opaque spinel; Per: perovskite; Cal: calcite; Clay: Clay minerals; Ser: serpentine; CRX: country rock xenolith; Mc: microlitic clinopyroxene). See table 3.2 for a summary of the textures for the HKt/HKtB at Lace and appendix 8 for a full list of samples analysed in this study.

	Ol	Phl	Mel	Mon	Ap	Op	Per	Cal	Clay	Ser	CRX	Mc
K2-1	24	34	1	15	1	5	1	11	0	8	0	0
C6- 713	32	34	2	1	1	12	0	6	0	0	1	11
C6- 706	28	37	0	0	0	4	0	7	0	1	7	16
C6- 630	16	31	2	0	0	2	0	6	0	1	20	22

Perovskite is characterised by a typical honey brown colour. Fine-grained stellate clusters of opaque minerals, which have been identified as hollandite, are also observed.

The base of the rock is comprised of calcite and serpentine, which fill the interstitial spaces between the interlocking phlogopite phenocrysts. These minerals are primary phases crystallising as late stage base components of the rock. Serpentine is particularly rare in all the microlitic clinopyroxene bearing hypabyssal kimberlites described for the in situ HKt/HKtB core samples.

3.1.3 Hypabassal Transitional Kimberlite and Kimberlite Breccia (HKt/HKtB)

The sample names used in the descriptions below indicate the borehole (C6 or C7) and the depth of that particular borehole. Note these are not the same as depth from the surface. See figure 3.2 for borehole depths and positioning within the Lace pipe. Refer to appendix 8 for a full list of samples analysed from the Lace kimberlite pipes. See table 3.2 for a summary of the relative development of the HKt/HKtB at the Lace kimberlite.

Borehole C6-Depth 713m

Borehole C6 is shown in figure 3.2 and 713m refers to the depth of the borehole and not depth from the surface. Refer to table 3.1 for modal analysis of the HKt and table 3.2 for relative abundances for all the HKt/HKtB sampled in this study. On first inspection this rock looks remarkably similar to typical fresh coherent hypabyssal kimberlite (HK). Abundant olivine

Table 3.2. Summary table of the relative abundances of: microlitic diopside (Mcpx), globular segregationary (Glob. Seg.) textural development and country rock xenolith (CRX) proportion in the Lace kimberlite hypabyssal transitional kimberlite and kimberlite breccia (HKt/HKtB). Refer to appendix 8 for a full list of all the samples analysed in this study. See section 3.1.3 for detailed descriptions of the samples and table 3.1 for modal analyses for selected samples. Samples labelled C6 are from borehole C6 (C7 from borehole C7) as shown in figure 3.2.

Sample	Depth from Surface	Mcpx abundance and distribution	Glob. Seg. Development	CRX Proportion	Textural Classification	Photomicrographs available in:
C6-713	600m	Low – patchy	None	Low	HKt	Fig 3.4
C6-706	595m	Moderate – patchy	Low	Low	HKt	Fig 3.5 (a+b)
C6-689	582m	Low – associated with altered CRX	Low	Low	HKt	
C6-642	540m	Absent	High	High	HKtB	Fig 3.5 (c+d)
C6-630	534m	High – pervasive	Moderate	Moderate	HKtB	Fig 3.6
C6-626	530m	Moderate – patchy	Low	Low – Moderate	HKtB	
C6-616	520m	Moderate – patchy	Moderate	Low	HKt	
C6-614	519m	Moderate – patchy	Moderate	Low	HKt	
C6-607	515m	Present but abundance unclear due to clay alteration	Moderate	High	HKtB	
C6-599	510m	Present but abundance unclear due to clay alteration	Low	Moderate - high	HKtB	
C6-597	508m	No Kimberlite component. Calcite infills void spaces.			Contact breccia	Fig 3.7 a
C6-552	466m	Present but abundance unclear due to clay alteration	Moderate	Very High	HKtB	Fig 3.7 b
C6-540	457m	Present but abundance unclear due to clay alteration	High	High	HKtB	
C7-372	340m	Absent	High	High	HKtB	
C7-338	302m	Low - patchy	None	Low	HKt	
C6-321 (satellite pipe)	284m	Present but abundance unclear due to clay alteration	High	High	HKtB	Fig 3.7 (c+d)

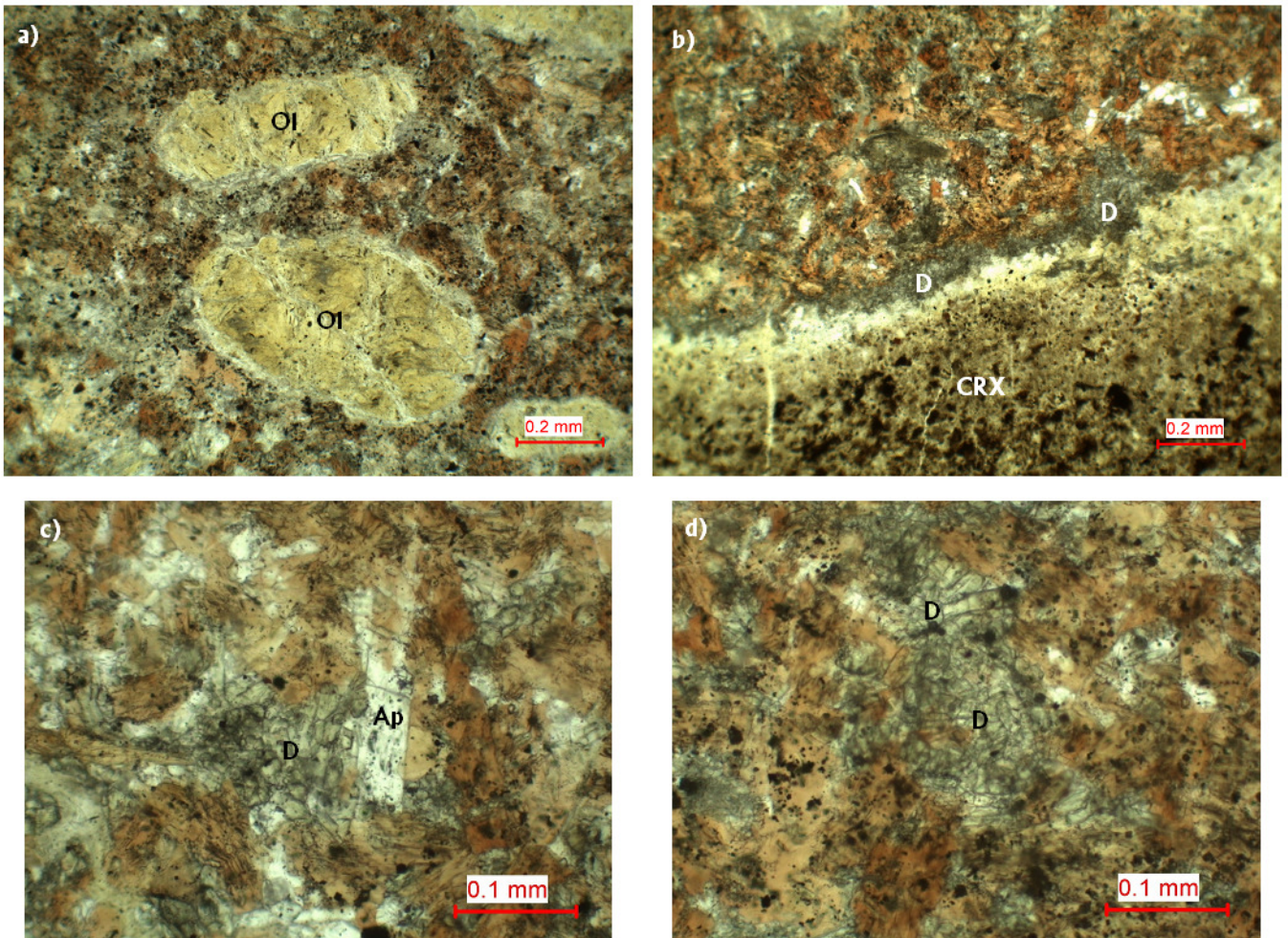


Figure 3.4 Photomicrographs of coherent hypabyssal transitional kimberlite (HKt) from sample C6-713 in borehole C6 as shown in figure 3.2 and described in section 3.1.3. See table 3.1 for a modal analysis of this sample and table 3.2 for relative development of the HKt compared to the rest of the pipe. a) Highly clay mineralised olivine (Ol) phenocrysts in a groundmass of much finer grained phlogopite kimberlite relative to sample K2-1. b) The development of fine grained microlitic clinopyroxene (D) around the margins of country rock xenoliths (CRX). Note the abundance of fine grained microlitic clinopyroxene throughout the groundmass and the presence of colourless apatite in the top right corner. c) Colourless apatite (Ap) lath in relation to pale yellow green fine grained microlitic clinopyroxene (D). d) Abundant fine grained microlitic clinopyroxene (D) in the groundmass of the rock. Note that microlitic clinopyroxene does not occur as inclusions within the phlogopite.

macrocrysts are set in a groundmass of typical phlogopite rich kimberlite. No globular segregatory textures are observed and the rock has a coherent texture. This rock represents the deepest sample obtained from the Lace Kimberlite, although other very fresh HK has been sampled from the surrounding dumps. The major difference is the abundant fine-grained microlitic clinopyroxene and finer grained nature of the kimberlite groundmass as shown in figure 3.4. Olivine occurs as abundant macrocrysts and phenocrysts, which are typically altered by clay minerals and calcite. Serpentine is not observed altering olivine in this case. Phlogopite is finer grained than the HK *sensu stricto* observed from the dumps and typically occurs as <0.1mm laths and rarely reaches 0.2mm in length. The phlogopite is highly poikilitic with abundant opaques and perovskite occurring as inclusions. Some degree of alteration of the phlogopite is observed by the often-dirty appearance, although it is unclear what the alteration product is. Zoning of the phlogopite is not a common feature in this sample. Monticellite is not observed here but is present in the HK *sensu stricto* (K2-1) described from the dumps. Melilite is present as highly carbonated laths (<0.1mm) but generally very rare, relative to K2-2. Apatite occurs as both laths (<0.1mm) and irregular plates in the groundmass and are easily distinguished from microlitic clinopyroxene by two distinct characteristics: apatite has 1) low birefringence and straight extinction and 2) colourless, white whereas microlitic clinopyroxene is a very pale yellow green colour and has inclined extinction. Furthermore the complete lack of microlitic clinopyroxene as inclusions in phlogopite and the fact that microlitic clinopyroxene is observed replacing earlier formed minerals also indicates a distinct textural difference to apatite. Figure 3.4 (c) clearly illustrates the difference between microlitic clinopyroxene and apatite. Microlitic clinopyroxene occurs as stubby lath shaped crystals (<0.1mm) with typical high birefringence and inclined extinction. However microlitic clinopyroxene is often very fine-grained and forms high relief grey masses, which are often associated with altered country rock xenoliths; figure 3.4 (b). These fine-grained masses of microlitic clinopyroxene are identified as such by the presence of identifiable laths within the mass as well as the often-high birefringence. Microlitic clinopyroxene is never observed as inclusions within phlogopite. The base of the rock is dominated by calcite and no serpentine is observed. The modal abundances of the minerals present are given in table 3.1.

Therefore this rock is very similar to HK sensu stricto described earlier apart from the presence of abundant fine-grained autometasomatic microlitic clinopyroxene, the complete lack of serpentine and the relatively finer grained nature of the rock. The autometasomatic nature of the microlitic clinopyroxene is discussed in section 5.3.5.1. The rock is classified as a macrocrystic pyroxenitised spinel-rich, phlogopite hypabyssal transitional kimberlite.

Borehole C6-Depth 706m Borehole C6 is shown in figure 3.2 and photomicrographs of this HKt are given in figure 3.5 (a) and (b). Refer to table 3.1 for a modal analysis of this sample. The rock here shows rare development of globular structures (figure 3.5 (a)) and shows a moderate degree of replacement by calcite relative to sample C6-713. The rock is characterised by a low degree of development of an incipient globular segregatory texture. Olivine occurs similarly to C6-713 but minor serpentine is also present as an alteration product. Phlogopite occurs as inclusion free laths (<0.2mm) in this sample (figure 3.5 (b)), which is very uncharacteristic for the Lace hypabyssal kimberlite (HK) rocks, which are typically highly poikilitic. Only minor opaques are observed as inclusions and perovskite is completely absent from the rock. Phlogopite commonly shows alteration to green chlorite as well as showing common zoning to dark red brown tetraferriphlogopite rims. Highly altered laths are present, which may be melilite but the very highly altered (carbonated) nature of the laths makes it difficult to accurately identify. Apatite is also completely absent from the rock as a result of autometasomatic microlitic clinopyroxene and calcite replacing the early formed groundmass mineralogy. The autometasomatic/deuteric nature of the microlitic clinopyroxene is discussed in section 5.3.5.1. Microlitic clinopyroxene is present in a similar fashion to that described for C6-713. The microlitic clinopyroxene is more abundant and occurs in patches of pure fine-grained grey microlitic clinopyroxene, which is not observed in C6-713. The microlitic clinopyroxene is interpreted to be deuteric and replaces the groundmass of the kimberlite. CRX present in this sample are always highly altered especially around the rims where microlitic clinopyroxene forms. The base again is dominated by calcite with the appearance of lesser serpentine.

The rock is becoming enriched in fine-grained microlitic clinopyroxene with a low degree of an incipient globular segregatory texture developing. Perovskite and apatite are completely

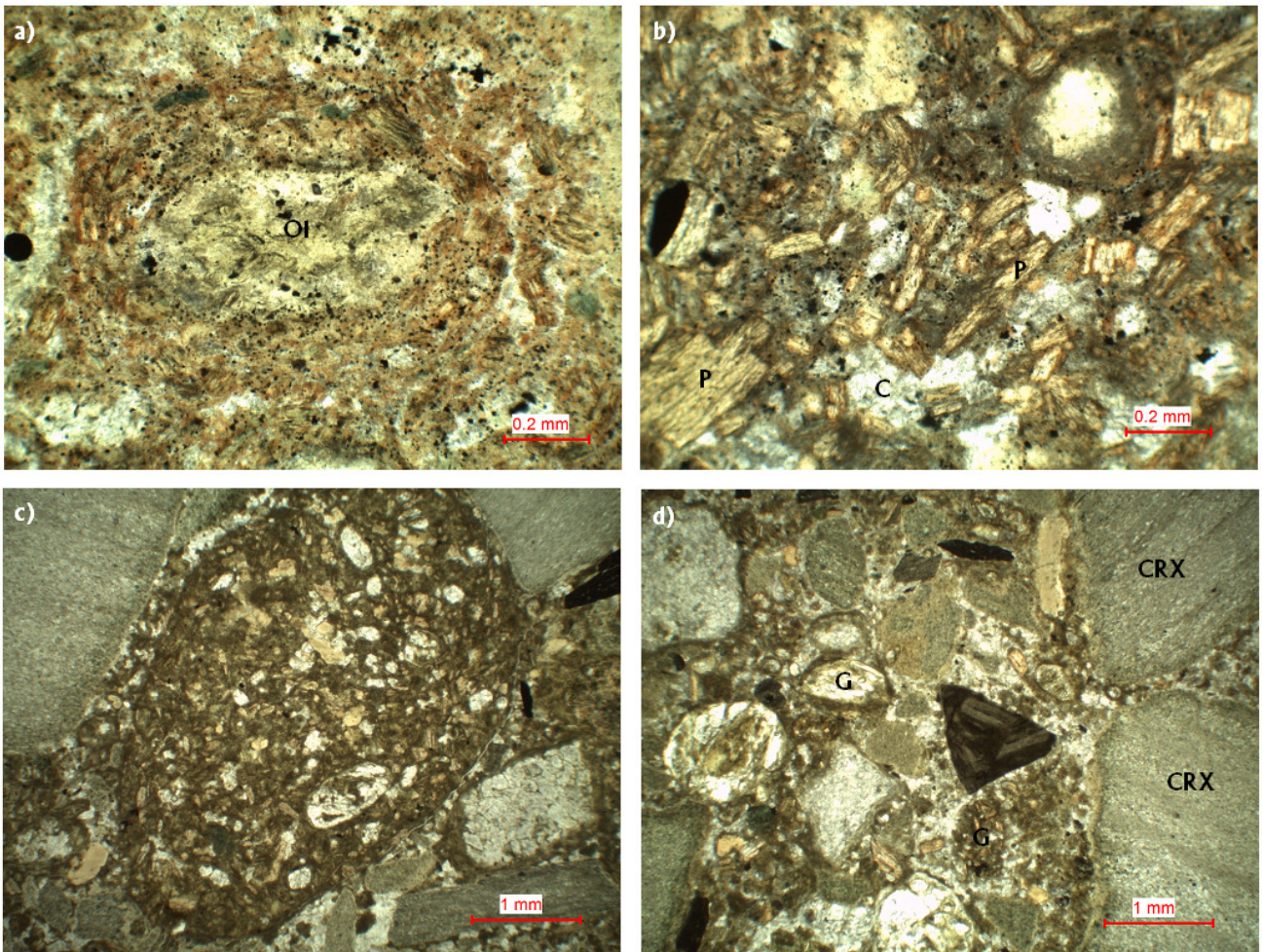


Figure 3.5 Photomicrographs from samples C6-706 (a-b) and C6-642 (c-d) from borehole C6 in figure 3.2. Both these samples are described in detail in section 3.1.3 and a modal analysis is given for C6-706 in table 3.1 and C6-642 in table 3.3. a) Clear development of a nucleated globule with a central kernel of an altered olivine (Ol) phenocryst. b) Non-poikilitic phlogopite (P) laths in a base of colourless calcite (C) and very fine grained grey microlitic clinopyroxene. c) Distinct large globule (4mm) without a central kernel between abundant green shale xenoliths. d) Development of globules (G) in a base of colourless calcite. Note the abundant green shale xenoliths, which are derived locally. See table 3.2 for relative development of the transitional kimberlite compared to the rest of the pipe.

absent and phlogopite is no longer highly poikilitic. The rock is classified as a macrocrystic pyroxenitised phlogopite hypabyssal transitional kimberlite.

Borehole C6-Depth 642m

Borehole C6 is shown in figure 3.2 and photomicrographs of this HKt are given in figure 3.5 (c) and (d). Again depth refers to depth in borehole and not depth from the surface. See table 3.3 for a modal analysis of this sample. Globular structures now become obvious and reach up to 4cm in size and therefore can be classified as a high degree of development of an incipient globular segregatory texture. This rock contains more abundant country rock xenoliths (CRX) (figure 3.5 (c) and (d)) relative to those described above. CRX present include: green shales, black shales, quartzite and peridotite. Globular structures generally contain kernels of either olivine or CRX although globules often do not contain a kernel, as shown in figure 3.5 (c). The kimberlite mantles round these kernels are generally less altered than the other kimberlitic material. Away from the globular structures the kimberlite proportion (olivine, phlogopite) decreases and calcite and clay minerals become more abundant. Therefore there is an inter-globule/CRX material dominated by fine-grained dark brown/green clay minerals and calcite with lesser kimberlitic olivine and phlogopite. The modal abundances for the main components of this rock are given in table 3.3. Olivine occurs as typical macrocrysts and phenocrysts, which are altered by calcite and lesser serpentine. Phlogopite is similar non-poikilitic laths as described for C6-706, although zoning is not as common. Apatite, melilite, monticellite and perovskite are completely absent and opaque minerals are far less abundant. Microlitic clinopyroxene is notably absent from this rock, which is unusual as it is particularly abundant in sample C6-706. The base of the rock is now green brown, very fine-grained clay minerals but calcite is still abundant.

This sample has a high degree of development of a globular segregatory texture where most of the kimberlitic material has clustered in these segregations and calcite and clay minerals fill the inter-globule spaces with lesser phlogopite and olivine phenocrysts. An important feature here is the complete absence of microlitic clinopyroxene, which has been abundant in the previous samples.

This rock (C6-642) is classified as a globular segregatory macrocrystic phlogopite hypabyssal transitional kimberlite breccia (HKtB).

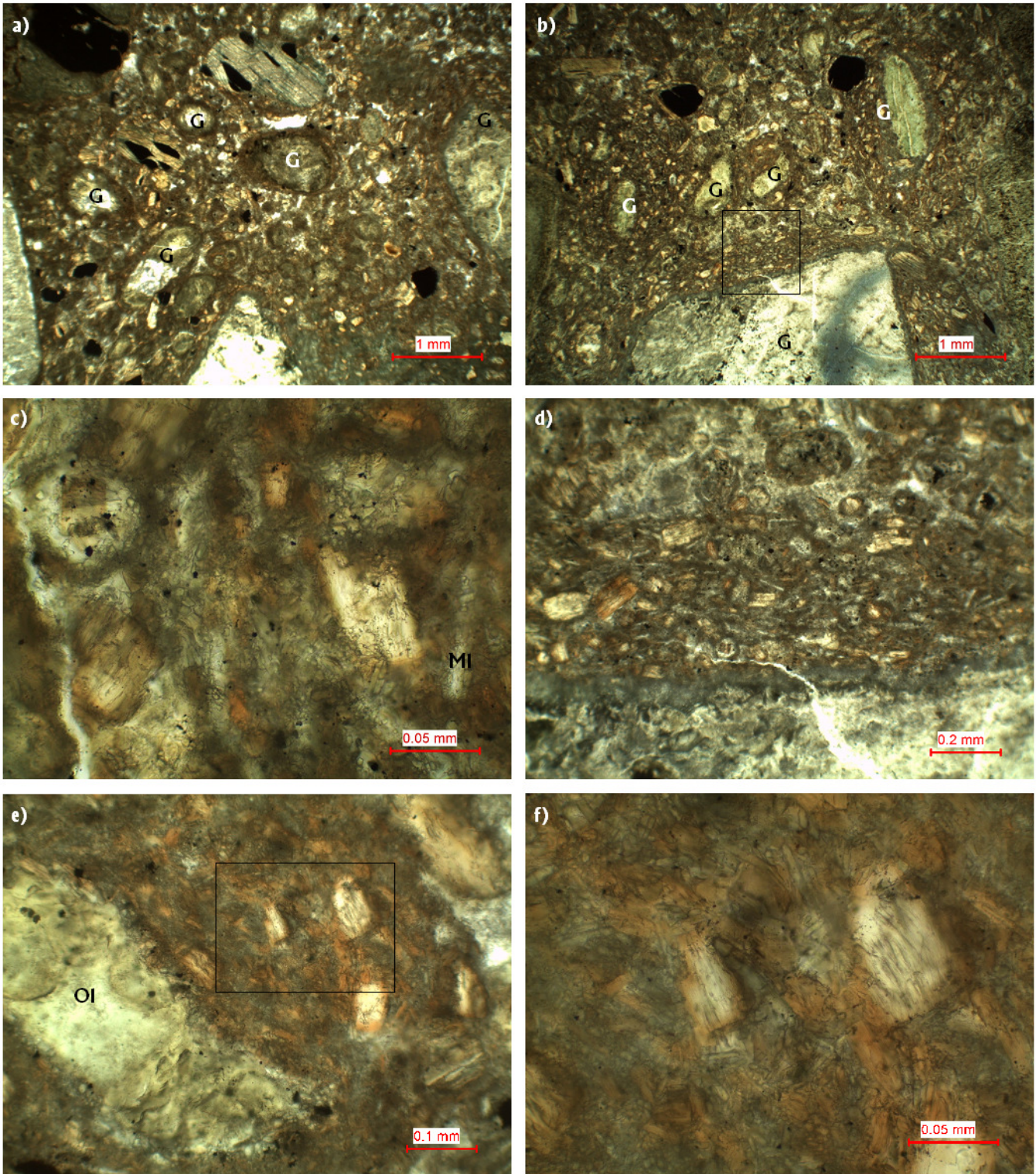


Figure 3.6 See figure caption overleaf

Figure 3.6 Photomicrographs from sample C6-630 from borehole C6 as shown in figure 3.2. Detailed descriptions of this HKt are given in section 3.1.3 and a modal analysis of the sample is given in table 3.1. a) Development of abundant distinct globules (G) with central kernels of altered olivine phenocrysts. b) Similar development of abundant globules (G) with central kernels of either olivine or country rock xenoliths. Note the large globule (3mm) at the bottom of the photo with a carbonate CRX kernel. The region marked by the square is shown in photo d). c) High power image of the groundmass kimberlite within a globule showing abundant microlitic clinopyroxene laths in the matrix. Note the highly altered lath of melilite (MI). d) High power image of the region indicated in b). Note the presence of a rim of fine grained grey microlitic clinopyroxene around the CRX central kernel. The kimberlite mantle around the CRX is composed of abundant phlogopite and minor opaques and highly altered melilite laths in a base of calcite and microlitic clinopyroxene. e) Photo of part of a globule with a central kernel of an altered olivine (Ol) phenocryst. The region indicated by the square is shown in photo f). f) High power image of the region shown in e). Note the abundant pervasive microlitic clinopyroxene, which has replaced the base and the non-poikilitic phlogopite phenocrysts. See table 3.2 for relative development of the transitional kimberlite compared to the rest of the pipe.

Borehole C6-Depth 630m

Borehole C6 is shown in figure 3.2 and photomicrographs of this HKt are given in figure 3.6. Refer to table 3.1 for a modal analysis of the sample. This sample is very similar to C6-706 in terms of the alteration and mineralogy. The main difference is the development of a moderate development of a globular segregatory texture, which is incipient but globules are far more abundant than observed in C6-706. The kimberlite is clustering around the larger components of the rock (olivine and country rock xenoliths (CRX)) to form globules as shown in figure 3.6 (a) and (b). Globules range in size from cm's down to 0.1mm. The larger components form the kernels of the globules. CRX kernels become highly altered by the kimberlite magma and typically have pure microlitic clinopyroxene forming at the contact between the xenolith and the kimberlite as a result of the alteration of the CRX (figure 3.6 (d)). However, deuteric microlitic clinopyroxene is pervasive throughout the groundmass, as shown in figure 3.6 (c), (e) and (f), of the rock and is not only associated with the CRX. Therefore this rock shows a high degree of replacement of primary minerals phases by later deuteric microlitic clinopyroxene. Therefore there is a gradual increase of the degree of replacement by microlitic clinopyroxene from C6-713

Table 3.3 Modal abundances of the components for the hypabyssal transitional kimberlite breccia (HKtB) at Lace based on 500 points counted per single thin section. (Kimb: kimberlite; CRX: country rock xenolith). See table 3.2 for a summary of the textures for the HKt/HKtB at Lace and appendix 8 for a full list of samples analysed in this study. See table 3.2 for relative development of the transitional kimberlite compared to the rest of the pipe.

	Kimb	Matrix	CRX
C6-642	21	17	62
C6-552	28	16	56
C6-321	47	18	35

to C6-630. Modal abundances for this rock are given in table 3.1; note the gradual increase in microlitic clinopyroxene from C6-713 to C6-630. A poorly developed tangential alignment of the phlogopite and melilite grains around the central kernels is commonly present.

The kimberlite is very similar to C6-706 with altered olivine, phlogopite and altered melilite in a base of calcite and deuteritic microlitic clinopyroxene. All the components of the kimberlite are <0.1mm, except for macrocrysts. Olivine phenocrysts are typically highly altered by green clay minerals and calcite. Phlogopite laths are non-poikilitic with minor zoning to tetraferriphlogopite rims observed. Melilite is relatively abundant compared to C6-706 and is always replaced by calcite and microlitic clinopyroxene, as shown in figure 3.6 (c) and (d). Fine-grained opaques (<<0.02mm) are scattered throughout the rock but are far less abundant than in typical HK proper (K2-1). The base of the rock is made up of two components: 1) calcite and 2) microlitic clinopyroxene. The calcite is typical of all the rocks observed at the Lace pipe. The microlitic clinopyroxene is however not common to every sample. Microlitic clinopyroxene forms high relief stubby to lath shaped crystals, which are very fine-grained (<0.05mm). This deuteritic (as discussed in section 5.3.5.1) microlitic clinopyroxene is pervasive throughout the rock.

This rock is unlike C6-642 where the rock has been altered by clay minerals away from the globules. C6-630 is relatively fresh compared to C6-642 and is particularly important as it clearly illustrates the development of globules round central kernels as well as a poorly developed tangential alignment of the grains. Another important feature to note is the development of pervasive microlitic clinopyroxene. The rock is classified as a globular segregatory, macrocrystic pyroxenitised, phlogopite hypabyssal transitional kimberlite breccia.

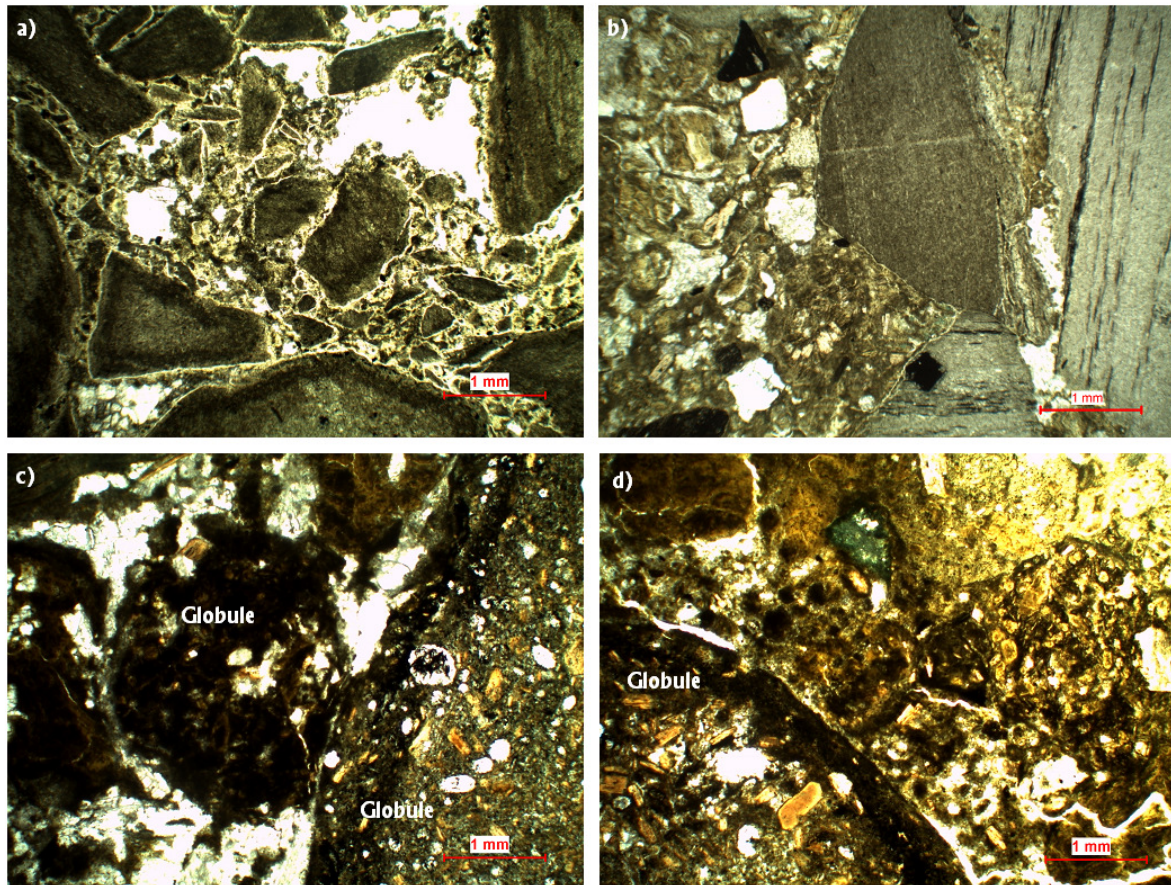


Figure 3.7 Photomicrographs of samples C6-597 (a), C6-552 (b) and C6-321 (c-d) from borehole C6 as shown in figure 3.2. HKt samples are described in detail in section 3.1.3. a) Contact breccia with no kimberlite component. The interclast is colourless calcite. b) CRX rich sample with abundant green and black shales with an interclast material of dominantly clay minerals and lesser kimberlite. c) Distinct globules forming in an interclast material of colourless calcite. d) Distinct large globules with an interclast material of clay minerals and lesser calcite. Note photos c-d is from the satellite pipe. See table 3.2 for relative development of the transitional kimberlite compared to the rest of the pipe.

Borehole C6-Depth 626m

Borehole C6 is shown in figure 3.2. This sample again further illustrates the patchy distribution of fresh kimberlite and microlitic clinopyroxene-rich altered kimberlite. The section shows the presence of fresh kimberlite, similar to that described for C6-706. Minerals such as apatite, melilite and perovskite are present, which have been completely absent since C6-706, but microlitic clinopyroxene is not observed in these fresher patches. Interspersed with this fresh kimberlite are patchy microlitic clinopyroxene-rich zones, which are more similar to that described in C6-630. Globular structures are not well developed in this rock relative to C6-630

and are classified as a low degree of development. Therefore the rock shows a patchy distribution of globular segregatory macrocrystic pyroxenitised phlogopite hypabyssal transitional kimberlite and macrocrystic pyroxenitised phlogopite hypabyssal transitional kimberlite.

Borehole C6-Depth 616m/614m

Borehole C6 is shown in figure 3.2. This rock is very similar to C6-626 and is classified similarly to C6-630. The only difference is the moderate degree of development of the globular segregations. The rock shows a similar patchy distribution of replaced microlitic clinopyroxene-rich zones and original fresh hypabyssal zones. The hypabyssal patches are less abundant than above and therefore the microlitic clinopyroxene-rich zones dominate this sample.

Therefore the rocks between 630-614m show a highly variable and patchy distribution of fresh hypabyssal looking kimberlite and altered more microlitic clinopyroxene-rich kimberlite. The development of a globular segregatory texture is also variable and may be completely absent or moderately developed in different places. The globular segregatory texture is never pervasive, it always develops incipient textures. The rocks can be classified similarly to that in samples C6-626.

Borehole C6-Depth 597m

Borehole C6 is shown in figure 3.2 and a photomicrograph of this sample is given in figure 3.7 (a). The sample shows the presence of a contact breccia devoid of kimberlite (figure 3.7 (a)). The rock has two constituents: 1) abundant green shale xenoliths with an interclast material of calcite and lesser clay minerals. No kimberlite or fine-grained microlitic clinopyroxene is present in this rock unit. The rock is monolithic and with very little mixing of the xenoliths is evident. The fragments are angular and are generally <3cm in size. Some alignment of the long axis of the fragments is evident, which may indicate some flow of the rock. The complete lack of microlitic clinopyroxene must indicate that the microlitic clinopyroxene is not a later secondary feature as it would be expected to alter this rock type as well. The contact breccia is observed in the centre of the pipe and is likely an inclusion of an earlier formed contact breccia. The lack of microlitic

clinopyroxene must indicate that the contact breccia formed prior to the alteration of CRX such as observed in the other HKt samples.

Borehole C6-Depth 552m

Borehole C6 is shown in figure 3.2 and refer to table 3.3 for a modal analysis of this sample. This rock is particularly rich in country rock xenoliths (CRX) (figure 3.7 (b)), which include: black shales, green shales, carbonates, green basalts and quartzite. These are all basement xenoliths and no Karoo lithologies are represented as xenoliths in this rock. The kimberlite is generally highly altered by calcite and minerals such as; apatite and perovskite are absent. Globular segregations are moderately developed here and occur up to 2cm in size. The globules are slightly less altered and typical kimberlite mineralogy of olivine, phlogopite and rare highly altered melilite laths are observed. The base of the globules is typically very fine-grained and consists of calcite and clay minerals. Serpentine is notably absent from this rock. The inter-globule matrix is composed of dominantly calcite and clay minerals with lesser altered olivine and phlogopite. Therefore the kimberlite is crystallising in nucleated segregations. Fine-grained microlitic clinopyroxene is very difficult to see due to the highly clay mineralised nature of the rock but fine stubby crystals are present in this rock. The rock is classified as a globular segregatory macrocystic pyroxenitised melilite-bearing phlogopite hypabyssal transitional kimberlite breccia (HKtB). Modal abundances of the components are shown in table 3.3.

Borehole C7-Depth 372m

Borehole C7 is shown in figure 3.2. Sample C7-372 is very similar to sample C6-552. However a high degree of development of a globular segregatory texture is evident with globules up to 1.2cm in size. The rock is rich in CRX, which include green/black shale, quartzite, dolomite and other highly altered unidentified xenoliths. Again it is important to note that no Karoo Supergroup xenoliths are observed. The kimberlite is highly altered by calcite and clay minerals and the original mineralogy is only readily identified within the globules. Apatite, perovskite and melilite are not observed and the dominant components include highly altered olivine, phlogopite and lesser opaque spinels in a base of calcite. The matrix to the rock (inter-globule/xenolith material) is composed of calcite and clay minerals with lesser phenocrysts of altered olivine and

phlogopite similar to that described for sample C6-552. Microlitic clinopyroxene is absent from this rock. Therefore the rock can be classified as a globular segregationary macrocrystic phlogopite hypabyssal transitional kimberlite breccia.

Borehole C7-Depth 338m

Borehole C7 is shown in figure 3.2. This rock shows similarities to sample C6-713 in that no globular segregationary texture is observed. However microlitic clinopyroxene is rare relative to C6-713. Olivine macrocrysts are common and reach up to 3mm in size. They are always completely replaced by calcite, clay minerals and lesser serpentine with mantles of phlogopite. Olivine phenocrysts are typically anhedral and resorbed with a range in size of 0.2-0.5mm. Phenocrysts are similarly replaced by calcite and clay minerals with distinct mantles of fine grained phlogopite. Phlogopite laths rarely exceed 0.5mm in length and are more typically <0.25mm. There is a distinct zoning from colourless to pale brown cores to darker red brown tetraferriphlogopite margins. Phlogopite is generally non-poikilitic however minor inclusions of opaque spinels are observed. Phlogopite laths are observed as very fine grained groundmass components, which are commonly <0.05mm. This characteristic is not observed in other samples from the pipe but is a common feature at the Voorspoed hypabyssal transitional kimberlite breccia (HKtB). Apatite is present in minor amounts as both phenocryst laths and groundmass anhedral plates, which rarely exceed 0.15mm. Microlitic clinopyroxene is only present in this rock with spatial relation to highly altered country rock xenolith (CRX) and is not pervasive such as in the samples from deeper within the pipe. The base of the rock is dominated by calcite and clay minerals.

This sample further illustrates the patchy distribution of both the globular segregationary texture and the microlitic clinopyroxene. The lack of these characteristic transitional kimberlite features makes this rock difficult to classify. However as it is part of the transitional kimberlite column at the Lace pipe and it is classified as such. Therefore the rock is classified as a macrocrystic carbonated phlogopite hypabyssal transitional kimberlite.

Satellite Pipe-Borehole C6-Depth 321m

Borehole C6 is shown in figure 3.2. Photomicrographs of this sample are given in figure 3.7 and a modal analysis is given in table 3.3. Sample C6-552 was the last sample from within the main pipe but borehole C6 cuts the satellite pipe at 321m and therefore the rock has been sampled at this depth. The rock here is again country rock xenolith (CRX) -rich with a similar CRX assemblage of basement xenoliths. No Karoo type coarse sandstone or amygdaloidal purple basalt is observed. This rock shows the most advanced development of a globular segregatory texture of any observed (figure 3.7 (c) and (d)). Fine-grained microlitic clinopyroxene is again very difficult to see but fine grained stubby crystals are observed. The globules are similar to those described at the main pipe for sample C6-552, where olivine, phlogopite and highly altered melilite are present in a very fine-grained dark brown base of calcite and clays. However a high degree of development is observed with globules reaching 2cm in size. Serpentine is notably absent from this rock similarly to C6-552. Tangential alignment of the phlogopite and melilite grains is observed although this is not well developed. The inter-globule matrix, similar to C6-552 is composed of calcite and green brown clay minerals with lesser individual grains of olivine and phlogopite. The rock here is classified as a globular segregatory macrocrystic pyroxenitised melilite-bearing phlogopite hypabyssal transitional kimberlite breccia.

3.1.4 Volcaniclastic Kimberlite (VK)

The Lace VK is only available on the dumps around the old open pit. Detailed petrographic analysis of samples from the core indicates that no VK is present at depth. Transitional hypabyssal- kimberlite and - kimberlite breccia (HKt and HKtB) are the only rock types intersected by the drill cores. The high country rock contents in these rocks lead previous authors who logged the core to conclude that these rocks were tuffisitic kimberlite breccia (TKB). This is not true as is clearly evident in thin section as described in section 3.1.3.

Two distinct VK types have been identified from samples collected from the old dumps and are described in detail in sections 3.1.4.1 and 3.1.4.2. The discrimination of the two types is based on juvenile kimberlite content, quartz xenocryst content and basalt CRX content. Therefore the two varieties are named basalt-rich volcaniclastic kimberlite (bVK) and quartz-rich volcaniclastic

Table 3.3 Modal abundances of the volcanoclastic kimberlite at the Lace pipe based on 500 points counted per single thin section. (Sed.: sedimentary; Mg.Clast: magmaclasts; Ol. in: olivine inside magmaclasts; Ol. out: olivine as xenocryst; Intercl. Mat.: interclast material; Kim: kimberlitic). See appendix 8 for a full list of samples analysed in this study.

Sample	CRX			Mg.clast	Ol. in	Ol. out	Intercl. Mat.	Xenocrysts	
	Basalt	Sed.	Other					Kim	Lithic
K2-A (qVK)	20	19	3	20	3	6	10	1	18
K2-B (qVK)	14	34	7	10	2	3	14	7	9
K2-9 (bVK)	56	2	3	1	0	1	18	3	16
K2-D (bVK)	57	1	5	7	1	0	16	4	9

kimberlite (qVK). Quartz-rich is applied here as a relative term indicating simply that the latter variety has a greater proportion of quartz xenocrysts. Modal abundances for the VK varieties are given in table 3.3. Merensky (1909) notes a third variety, which has not been found on the dumps in this study. The characteristic feature of the rock is the dominance of sandstone cement. This has been named a sandstone-breccia, which contains a juvenile kimberlite component (Merensky, 1909). Therefore this may represent a resedimented volcanoclastic kimberlite (RVK), as it contains a sedimentary sand matrix.

3.1.4.1 Basalt-rich Volcanoclastic Kimberlite (bVK) (Samples K2-9 and K2-D)

The rock is composed of essentially three components: 1) Magmaclasts, 2) basement/country rock xenoliths and 3) an interclast material consisting of juvenile and lithic xenocrysts in a cement of calcite. The rock is dark grey in colour and is characterised by the presence of large (>15cm) amygdaloidal Karoo Supergroup basalt. Magmaclasts are not seen in hand specimen but are observed in thin section. Modal abundances for the dominant components are show in table 3.3 and photomicrographs are given in figure 3.8 (a) and (b).

The VK is massive with no bedding evident and clasts generally range in size from 1mm to 10cm. However, all the xenocrysts in the interclast material are typically <0.3mm in size. The rock samples analysed contain 5 and 12 vol. % of kimberlitic material. The rock has been classified as a basalt xenolith-rich, massive volcanoclastic kimberlite breccia.

Country Rock Xenoliths (CRX) and Basement Xenoliths

CRX are abundant and can occupy as much as >60% of the rock. Most of the CRX are from the Karoo Supergroup and include basalt, dolerite, white sandstone, pink sandstone and shale. Pink sandstones are thought to come from the Elliott Formation (Stormberg Group) whereas the white sandstones have been identified as coming from either the Beaufort Group or the Clarens formation (Stormberg Group) (Howarth, 2007). CRX have a wide range in size from mm to m. Basalt xenoliths generally dominate the CRX suite and may occupy 57% of the rock and are clearly the dominant CRX type, as shown in figure 3.8 (a) and (b).

Magmaclasts

Magmaclasts are more or less spherical in habit, are generally <1mm in size and occupy <10% of the rock, although rare examples reach up to 5mm in diameter. Therefore Wagner's (1914) estimate of approximately 10% kimberlite material is fairly accurate for this VK. Magmaclasts consist of: Olivine occurs as both macrocrysts and phenocrysts and is always completely altered by calcite and serpentine. Euhedral outlines are evident in the phenocrysts. Phlogopite is most abundant as phenocrysts and microphenocrysts <0.2mm. Microphenocrysts generally are darker coloured indicating an evolution of the composition of the phlogopite to tetraferriphlogopite as observed in the HK proper. Rare phlogopite macrocrysts are also present. Scattered fine-grained (<0.02mm) opaques are seen throughout the magmaclasts as well as abundant microlitic clinopyroxene. The base of the magmaclasts is composed of calcite and serpentine with lesser clay minerals.

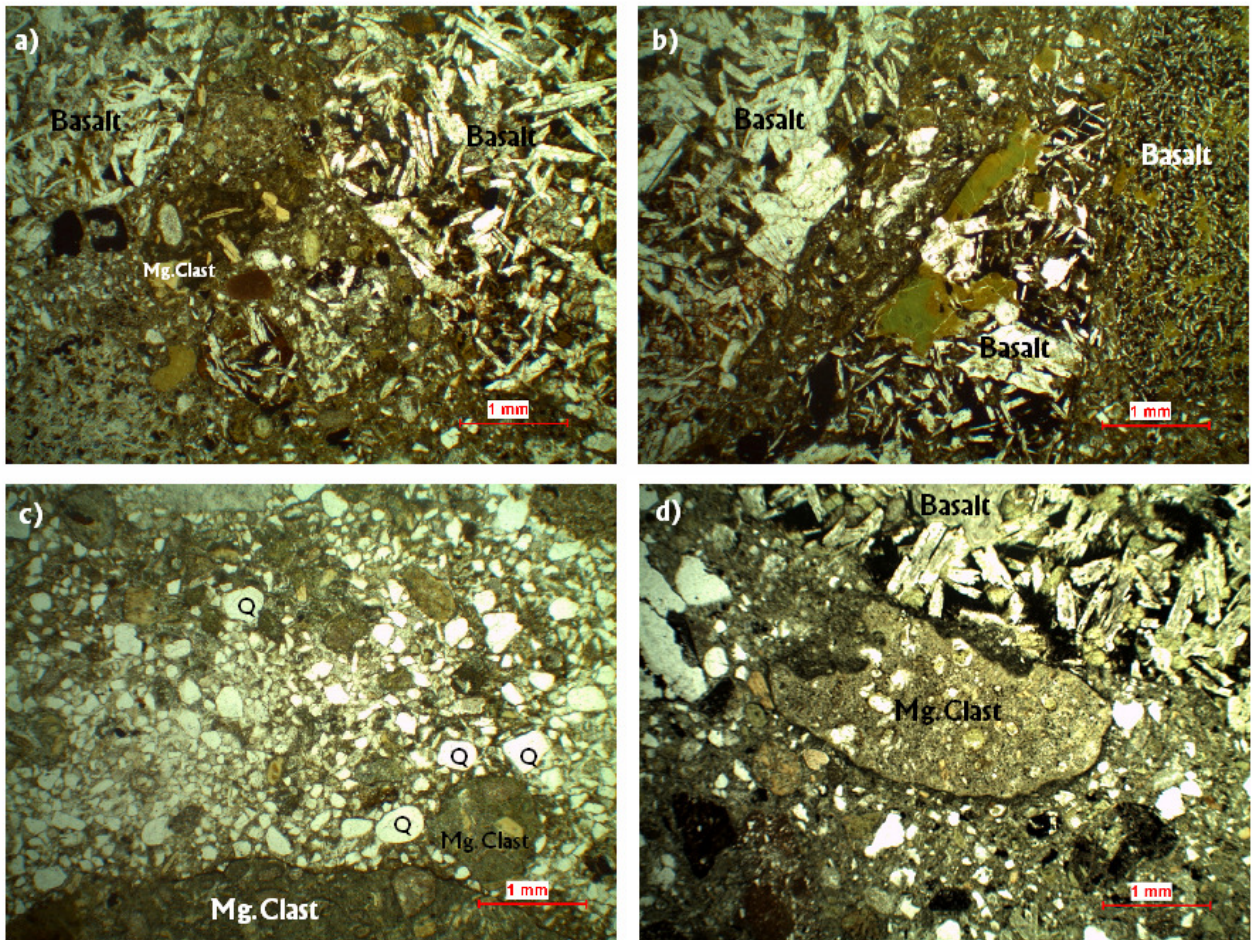


Figure 3.8 Photomicrographs of the volcaniclastic kimberlite at the Lace pipe. a)-b) bVK, as described in section 3.1.4.1, showing abundant basalt xenoliths set in a fragmental interclast material. Note the kimberlite magmaclasts in a). c) qVK, as described in section 3.1.4.2, photo showing abundant quartz xenocrysts in the interclast material and large magmaclasts (Mg.Clast). d) Another example of qVK showing an irregular magmaclast and the presence of basalt xenoliths.

Interclast Material

The interclast material of the rock is made up of three components: kimberlitic xenocrysts, lithic xenocrysts and a cement of calcite. Kimberlitic xenocrysts include olivine and phlogopite macrocrysts. Olivine macrocrysts are highly altered by calcite and difficult to distinguish from the calcite cement. Phlogopite xenocrysts are rare relative to olivine. Lithic xenocrysts are common and can account for >10% of the total rock volume. The xenocrysts are dominantly feldspar and basaltic clinopyroxene, which are from the basalt CRX. Rare quartz is also present but not nearly as abundant as seen in the qVK.

3.1.4.2 Quartz-rich Volcaniclastic Kimberlite (qVK) (Samples K2-A and K2-B)

Samples K2- A and B were collected from the dump sites as no in situ VK is present in the pipes. Photomicrographs are given in figure 3.8 (c) and (d) and modal analyses of both samples are given in table 3.3. The rock is composed of essentially three components: 1) country rock xenoliths (CRX), 2) magmaclasts and 3) interclast material consisting of xenocrysts in a cement of calcite. The rock is light grey/brown in colour and is characterised by 1) the low abundance of basalt relative to the bVK, 2) by the presence of magmaclasts up to 2cm in size, which are abundant in hand specimen relative to the bVK and 3) high abundance of quartz xenocrysts. Pervasive calcite alteration is similar to that of the bVK. The rock is also crystallinoclastic, which is a characteristic feature of the Lace pipe VK. The rock has been classified as a crystallinoclastic, quartz xenocryst-rich, massive volcaniclastic kimberlite.

Country rock and Basement Xenoliths

Country rock xenoliths observed includes basalt, shale and sandstone. These xenoliths are usually altered by calcite as is common with all the components of the rock. CRX are all part of the Karoo Supergroup rocks similarly to those described above for the bVK. Basalt CRX account for <20% of the rock whereas sedimentary CRX can reach as high as 34%. CRX observed from stratigraphic levels below the current level include quartzite and dolomite xenoliths. These dolomite xenoliths may be highly altered olivine macrocrysts and megacrysts as highly carbonated olivine macrocrysts are observed within magmaclasts in the deposit. Therefore it is unclear if carbonate xenoliths are present at Lace. Carbonate xenoliths are abundant at the Voorspoed pipe.

Magmaclasts

The magmaclasts observed in this VK are often characterised by a green colour. The larger magmaclasts often have irregular boundaries (figure 3.8 (d)) whereas the smaller magmaclasts have typical spherical habit. Distinct ultra fine dark rims are seen around many of the magmaclasts, it is important to note that this feature is not observed on the CRX. Olivine grains are always completely altered by serpentine with the outer part altered by calcite with minor clay minerals as well and rimmed by fine-grained opaque minerals. Euhedral olivine phenocrysts are still evident and macrocrysts often form the kernels in smaller magmaclasts. Phlogopite

macrocrysts and phenocrysts are present but do not show any zoning, which is a characteristic feature of the transitional kimberlite. Microlitic clinopyroxene laths are always highly altered by calcite but typically occur as fine (0.04-0.1mm) grains. Melilite may be present but because of the extensive alteration it is difficult to distinguish between melilite and microlitic clinopyroxene. Opaques (<0.02mm) occur scattered throughout the matrix and as inclusions within phlogopite grains. The base of the magmaclasts is dominated by calcite and possibly chlorite as observed by the characteristic green colour of many magmaclasts. The presence of serpentine altering olivine in magmaclasts indicates that serpentine may have originally been present but was later altered out by calcite.

Interclast Material

The interclast material of the rock is particularly important in this rock as it contains abundant xenocrysts of quartz. Other xenocrysts include: feldspar, polycrystalline quartz, olivine, phlogopite and basaltic clinopyroxene. The juvenile xenocrysts (olivine and phlogopite) are less abundant than lithic xenocrysts. Quartz grains occurs as well rounded to angular grains and are extremely poorly sorted with sizes ranging from >1mm to 0.02mm. Figure 3.8 (c) and (d) show the abundance of quartz in this rock. The rock is cemented by calcite, which is often seen filling void spaces, and lesser green clay minerals. Therefore this calcite may be secondary.

3.2 Voorspoed Kimberlite Pipe

The Voorspoed pipe forms the north-eastern limit to the Kroonstad cluster and is situated on a pre-eruption southeast striking kimberlite dike system. The pipe is approximately 12 ha in size and is oval in shape with dimensions of 490 by 350m. The sidewalls of the pipe dip at an angle of 82° (Clement, 1982), which is typical of kimberlite pipes in South Africa (Hawthorne, 1975). The internal geology of the pipe is extremely complex with horizontal layering and bedding present as well as a nested crater (CEZ), as shown in figures 3.12 and 3.14. Approximately half the pipe (6 ha) is occupied by a large block of Karoo basalt, as discussed below and shown in figures 3.9 and 3.10. The original pipe diameter at the surface during eruption can be calculated using the erosion estimate, discussed in section 5, with an average dip of 82° (Clement, 1982) for the pipe walls. The pipe would have been approximately 980m by 700m or 53ha at the original land surface. All the sampling done is from the 1998 drilling programme as the pit is still being developed and therefore fresh samples are not available.

Hypabyssal kimberlite (HK) has all been sampled from internal dikes and/or sills in the surrounding country rock. All the HK analysed are aphanitic and two dominant varieties are observed: diopside phlogopite kimberlite and melilite-bearing phlogopite kimberlite. The HK has an evolved nature, which is indicated by the presence of aegirine overgrowths on primary diopside and sanidine in the base. These minerals are part of an evolved suite of minerals, which are only present in evolved Group II kimberlites (Mitchell, 1995). Microprobe analysis of the primary pyroxenes are presented in section 4.2.2. Numerous volcanoclastic units are observed and include: six Massive volcanoclastic kimberlites (MVKs), at least two bedded volcanoclastic kimberlites (BVKs) as well as crater rim failure deposits. These are discussed in detail in this section. Hypabyssal transitional kimberlite breccia (HKtB) is observed in only one borehole intersection and is characterised by a typical incipient globular segregatory texture, which is common at the Lace pipe.

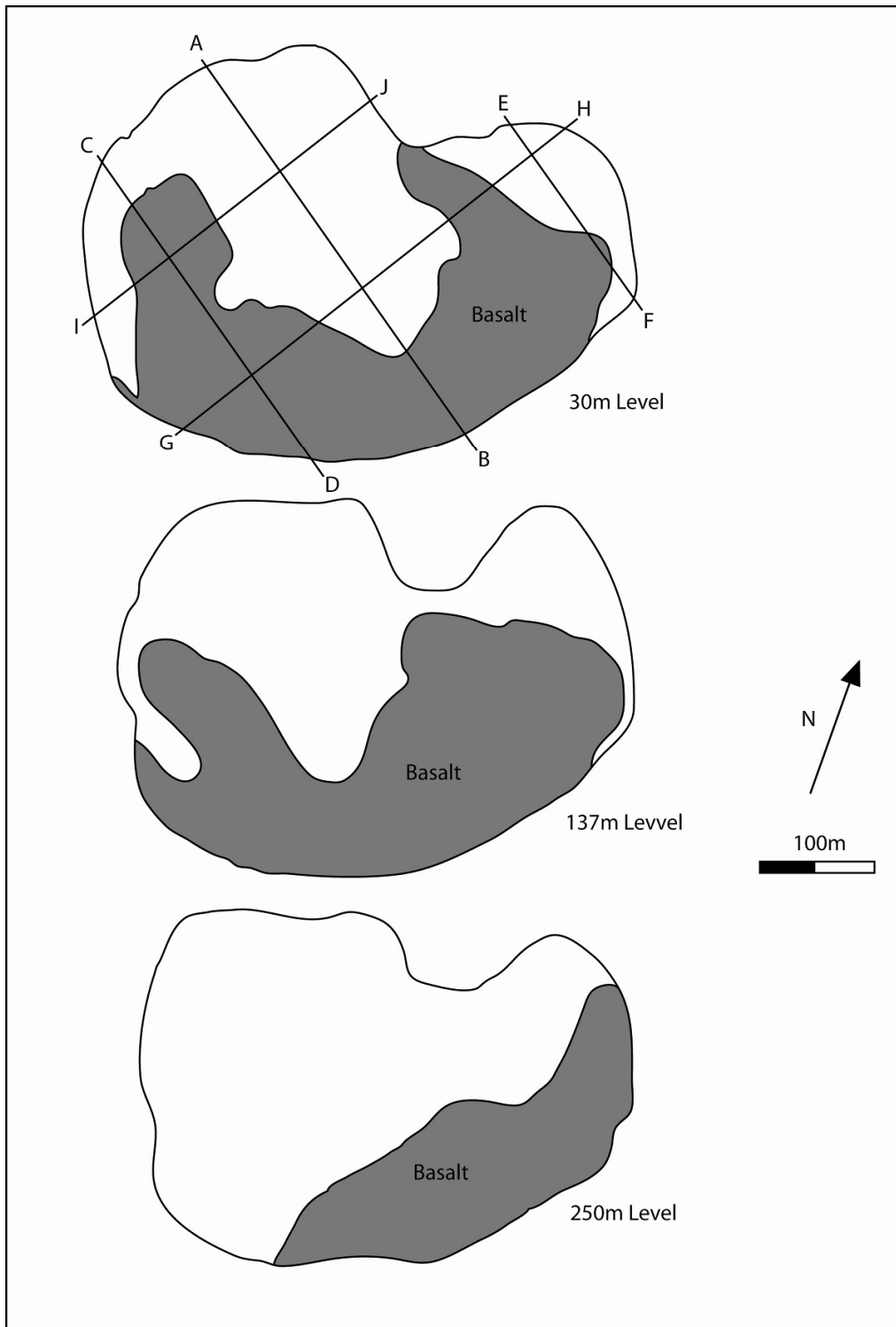


Figure 3.9 Plan view of the Voorspoed pipe showing the distribution of the basalt mega block at the surface, at 137m level and 250m level. Sections lines indicated on the diagram are shown in figure 3.10. Diagram from Clement (1982).

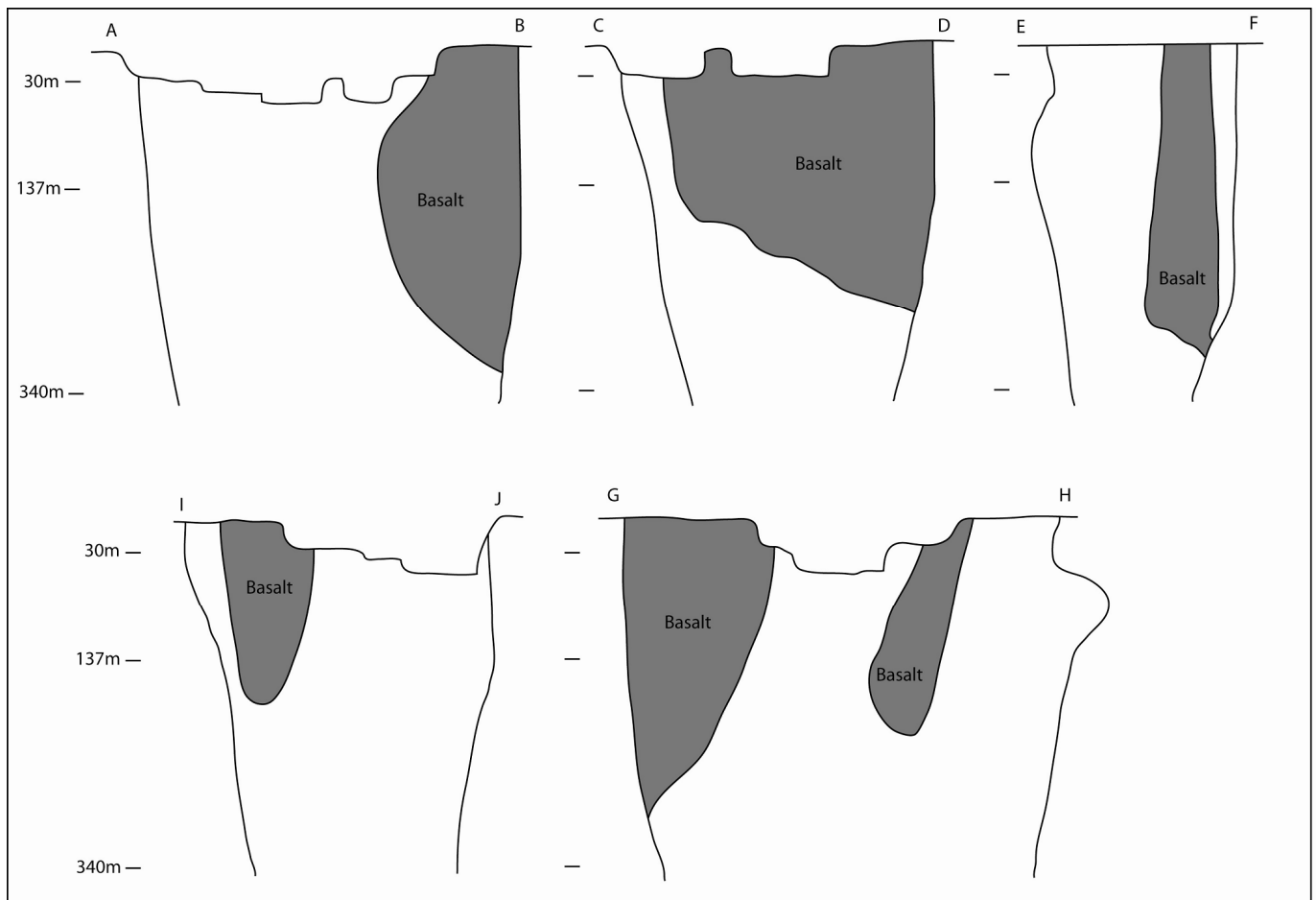


Figure 3.10 Cross-sections through the Voorspoed pipe showing the distribution of the basalt mega block. Section lines are indicated in figure 3.9. Diagram from Clement (1982).

3.2.1 Basalt Megablock

The Voorspoed pipe is characterised by the presence of a huge basalt block, which occupies approximately half the surface area (6 ha). The block sits against the southern wall of the pipe and is not surrounded by MVK as shown in figure 3.10. The basalt, as shown in figure 3.9 and 3.10, has a “C” shape and extends down to 320m at the southern margin. In the north west of the pipe the basalt extends to approximately 130m. Therefore the block occupies a large percentage of the volume of the pipe. This basalt has been analysed geochemically and has been determined to be Karoo in origin but more specifically from the upper Lesotho Formation

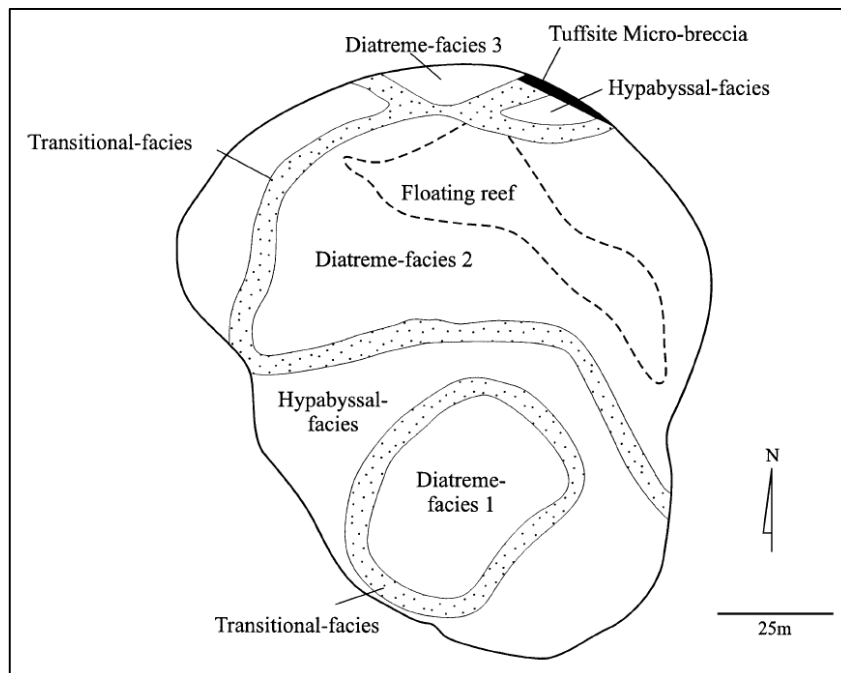


Figure 3.11 Plan view of the Kamfersdam kimberlite pipe showing the distribution of a large floating reef. (Diagram from Skinner and Marsh, 2004).

units (Roberts, 1997). Therefore the top of this basalt block originated approximately 1400m above its current location. The block is highly fragmented around the margins where a basalt breccia zone has developed, which contains low proportions of kimberlite material. At the western extension of the basalt block a large mass 30 m wide has been separated from the main block. These basalt breccia zones are only seen spatially related to the main basalt block and represents an area of major dilution by country rock material. Therefore the basalt block has been partly fragmented during explosive eruptions during the evolution of the pipe infill or alternatively may be separate blocks.

The presence of huge country rock blocks has been noted at various other localities in South Africa such as Kamfersdam, (Skinner and Marsh, 2004) Koffiefontein and Finsch (Clement, 1982). These country rock blocks are usually classified as floating reef as they are typically surrounded by MVK and are therefore suspended or floating. Kamfersdam is a particularly good example, as shown in figure 3.11; the country rock block is completely surrounded by diatreme facies rocks and therefore can be classified as floating reef. The basalt mega block at Voorspoed

is somewhat different in that it is underlain by horizontally layered pyroclastic deposits. The origin of the block is discussed in detail in section 5.4.

3.2.2 Distribution and Macroscopic Description of the Volcaniclastic Kimberlite

The Voorspoed pipe can be divided into two distinct volcaniclastic zones, each of which is characterised by multiple numerous layers of massive volcaniclastic kimberlite (MVK) deposits. These volcaniclastic zones are here called Initial Eruption Zone (IEZ) and the Central Eruption Zone (CEZ), each of which have characteristic defining features. The Initial Eruption Zone (IEZ) was mapped in detail in boreholes 9 and 10 while further correlation of units was seen in boreholes 7 and 8. The CEZ was mapped in detail in boreholes 2 and 3 (appendix 4) while further correlation of distinct MVK types within the zone was noted in boreholes 5 and 6 (De Beers logs; not given in this study). The distribution of the different zones and boreholes is shown in figure 3.12 and. The CEZ is 200m in diameter and is clearly defined by the cored out nature of the basalt block. Both volcaniclastic zones extend to depths in excess of 300m but current drilling has not yet found the bottom contacts with the root zone. A representative selection of boreholes is used to illustrate the distribution of the various geological units within the pipe. These boreholes include 2, 3, 9 and 10 (appendix 4). Further correlation of these units is done using the remaining borehole logs provided by De Beers. The internal distribution of the volcaniclastic zones is shown in figure 3.14. Appendix 5 shows the variation in volcaniclastic kimberlite (VK) terms used over the years by De Beers. Refer to appendix 8 for a full list of samples analysed from the Voorspoed pipe.

3.2.2.1 Initial Eruption Zone (IEZ)

The IEZ is made up of four distinct VK varieties: 1) Type 1a MVK, 2) Soft MVK, 3) atypical MVK and 4) bedded volcaniclastic kimberlite (BVK). Boreholes (logs given in appendix 4) have also intersected the pipe margins at depth, which show the clear development of contact breccias devoid of kimberlite in the wall rock as shown in figure 3.14 and described in section 3.2.4.2. In the northeastern pipe (borehole 10) the contact breccias are filled only with calcite. Furthermore, two distinct massive volcaniclastic kimberlite breccia (MVKB) units almost devoid in kimberlite (<4%) are observed in the northwestern area of the pipe at the surface.

Type 1a Massive Volcaniclastic Kimberlite (T1aMVK)

The T1aMVK is massive with no obvious grading or bedding observed however there are minor grain size variations between individual units. Figure 3.13 (a) shows a photograph of typical T1aMVK in the core and a detailed petrographic description is given in section 3.2.6.1. Xenoliths reach up to 50cm in size but may rarely reach up to 30m in size in close spatial relation to the basalt megablock. The xenoliths are dominated by dark brown to purple amygdaloidal basalt, which has been analysed to have originated from the Karoo Supergroup (Hanson, 2006). Other xenoliths include shale, dolerite, dolomite and other highly altered unidentifiable xenoliths. The xenoliths are typically <10cm, angular and show very little alteration, except for the dolomite and highly altered basement xenoliths. Magmaclasts are present and are spherical in shape and seldom reach larger than 10mm in size. Central kernels are present and are always country rock xenoliths (CRXs); however magmaclasts typically do not contain central kernels. The interclast material is too fine grained to identify at this scale however it is light brown in colour.

T1aMVK occurs as two distinct layers, which have subsequently been cross cut by the CEZ MVKs. The layers are variable in thickness across the pipe. The lower layer occurs at approximately 280m depth and varies in thickness from 52m in hole 9 to 26m in hole 10. The upper T1aMVK layer occurs at approximately 170m in depth and ranges in thickness from 49m in hole 9 to 96m in hole 10. The T1aMVK is also present in boreholes 1, 4, 7 and 8.

Soft Massive Volcaniclastic Kimberlite (sMVK)

The Soft MVK receives its name from the relatively soft nature of the rock, which is indicated by highly weathered nature of the rock in the drill core relative to the other MVK varieties. As a result the soft MVK could not be sampled in this study. Samples of the soft MVK have been obtained from a collection of samples from Mike Skinner and a representative sample is shown in figure 3.13 (b) and a detailed petrographic description is given in section 3.2.6.3. The rock is slightly darker in colour relative to the T1aMVK and on initial inspection seems to contain less basalt xenoliths. However during petrographic analysis it is evident that the basalt contents are very similar. Xenolith size distribution is very similar to the T1aMVK and apart from the soft nature of the rock it is very similar to the T1aMVK. The only difference is the magmaclasts,

which are spherical in shape and commonly contain central kernels of highly altered olivine. Furthermore the magmaclasts are slightly larger in size, reaching up to 15mm.

The soft MVK occurs in two layers, one of which is only observed in hole 10 and therefore is not continuous across the pipe. The lower layer occurs at 233m depth and varies in thickness from 59m in hole 9 to 7m in hole 10. This unit thins substantially across the length of the pipe. The upper discontinuous layer occurs at 127m depth and is 22m thick. This layer pitches out before reaching hole 9, as it is not observed.

Atypical Massive Volcaniclastic Kimberlite (aMVK)

The atypical MVK is very distinct relative to the soft and T1a MVKs. The most distinct features are the much darker colour and presence of abundant large magmaclasts as shown in figure 3.13 (c) and described in detail in section 3.2.6.3. Magmaclast proportions are very similar to the above described MVKs however the average size of the magmaclasts in the atypical MVK is much larger. Typical spherical shapes dominate and central kernels are rare. Xenoliths are dominated by shales rather than basalt. The size distribution and characteristics of the xenoliths are similar to that described above and are typically <10cm in size.

This MVK is only present as a thin layer (5m thick) at 290m depth in hole 9. The MVK overlies the first occurrence of hypabyssal kimberlite (HK), which is transitional hypabyssal kimberlite (HKt). This MVK represents the first MVK unit deposited at the Voorspoed pipe.

Bedded Volcaniclastic Kimberlite (BVK)

Three distinct graded/bedded sequences are observed in the IEZ. Firstly, in borehole 10 between 105 and 87m. The zone is characterised by numerous graded units up to 3m in thickness. Secondly a similar bedded unit is observed in borehole 9 between 125 and 120m. This unit is comprised of three graded beds with a maximum thickness of 2m. A third graded sequence is observed in borehole 9 only at depth and directly overlies the aMVK. Detailed petrographic descriptions of the BVK are given in section 3.2.6.8 The origin of these graded sequences is discussed in detail in section 5.4.

The graded sequence in borehole 10 is characterised by a much lower proportion of basalt xenoliths relative to the other two sequences in borehole 9. Xenoliths range in size from 6cm at the base of a graded unit to <3mm at the top. Xenoliths include shale, basalt and dolomite, the latter is generally altered. Magmaclasts are clearly evident at the base however the constituents are difficult to identify at the top of the unit due to the fine grained nature. Magmaclasts are <10mm in size and central kernels are rare. The unit at 125m in borehole 9 is characterised by a large proportion of basalt xenoliths (see section 3.2.9 for accurate point count proportions) relative to the bedded VK in hole 10. Xenoliths range in size from 5cm at the base to <1cm at the top of individual graded beds. Other xenoliths present include altered dolomite and highly altered unidentifiable xenoliths. Shale xenoliths are only observed at the top of the sequence and are rare relative to BVK in hole 10.

Massive Volcaniclastic Basalt Breccia (MVBB)

As the name implies this MVK is very rich in basalt and no shale xenoliths are observed within this unit. Basalt xenoliths range in size from mm scale up to metres in size. The MVBB is described in detail in the petrography section 3.2.6.10. Kimberlite content is very low and no magmaclasts are observed in the core, however rare magmaclasts are observed microscopically.

MVBB occurs in both holes 9 and 10 (see logs in appendix 4). In hole 9 basalt breccia underlies the major basalt block as a 28m thick unit whereas in hole 10 the MVBB is adjacent to the major basalt block and is 45m thick. The basalt breccia is restricted to holes 9 and 10 and is not present in holes 2 and 3, which were drilled away from the major basalt block. Therefore the MVBB is only present around the outer margins of the pipe and not in the centre. The MVKs in the Central Eruption Zone (CEZ) of the pipe are basalt rich but the MVBB is very distinct in thin section and only occur in the Initial Eruption Zone (IEZ).

Massive Volcaniclastic Sandstone Breccia (MVSB)

The MVSB is very similar to the MVBB however this unit contains significant amounts of sandstone xenoliths. Sandstone xenoliths are particularly rare at the Voorspoed pipe and therefore this unit is unique in this characteristic. Basalt xenolith content varies within the MVSB and basalt xenoliths may be completely absent in some samples. Kimberlite content is

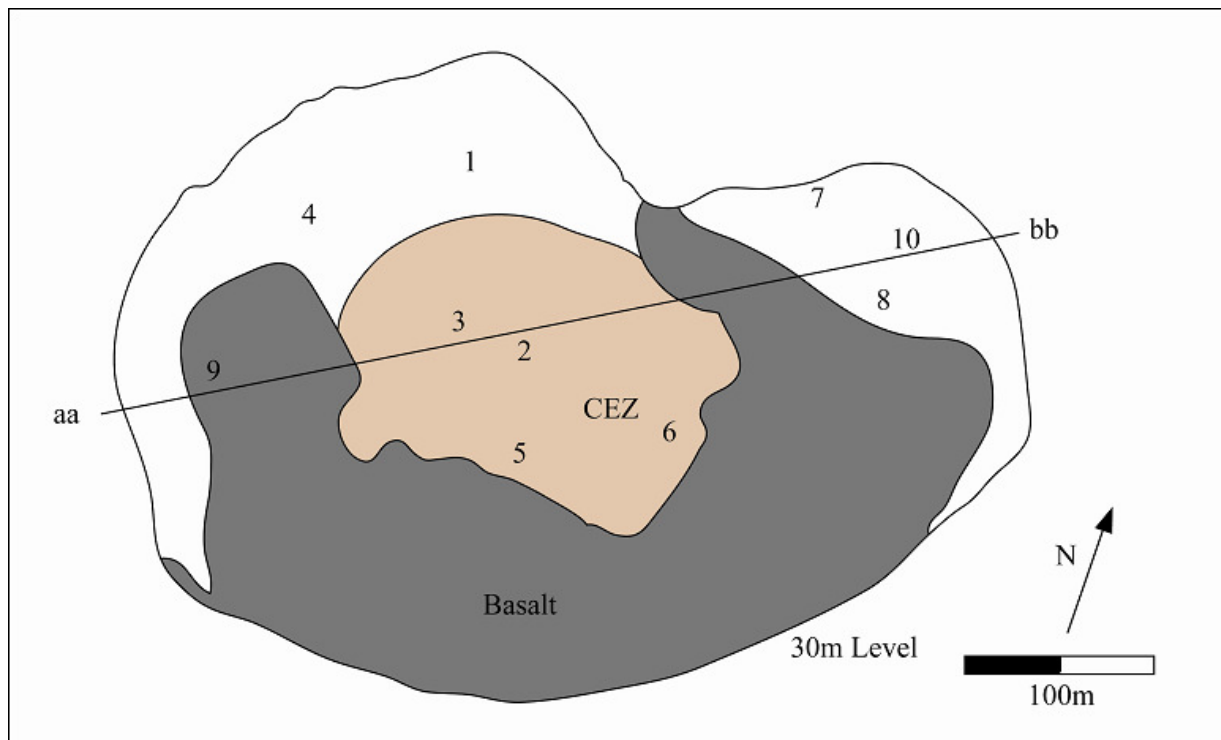


Figure 3.12 Plan view of the Voorspoed pipe showing the positions of boreholes and the distribution of the Central Eruption Zone (CEZ) (pale brown). The Initial Eruption Zone (IEZ) is the white area and underlies the basalt (grey). The section line aa-bb is shown in figure 3.14. Borehole logs created in this study for holes 2, 3, 9 and 10 are given in appendix 4. The rest of the logs are not given but De Beers logs were used to compare with the logs created in this study. Diagram modified after (Clement, 1982).

again very low and no magmaclasts are observed in the core samples. Shale xenoliths are present in this unit, which are absent in the MVBB. Xenoliths are typically <15cm in size. Sandstone breccia occurs as a discrete unit in the northwestern area of the pipe and has been logged in hole 10, 7 and 8. In hole 10 the unit is 42m thick and is present at the surface. This is a very localised unit but it is important in terms of eruption mechanisms, as discussed later.

Contact Breccias

Contact breccia is observed only in borehole 10. The contact breccia in hole 10 occurs at 256m from the surface and extends to the bottom of the hole at 295m where very little rotation and mixing of the fragments occur. The contact breccia zone is comprised of two distinct lithological varieties. Firstly, a dolerite contact breccia is observed at 256m depth, which is 8m in thickness

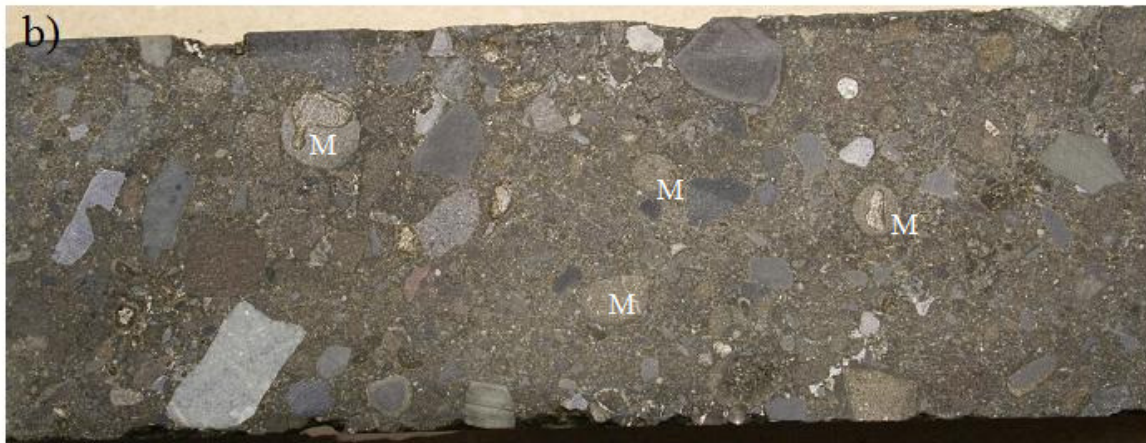


Figure 3.13 Photographs of representative samples from the IEZ MVKs. a) T1aMVK: Note the typical amygdaloidal basalt xenolith (B). b) Soft MVK: Note the spherical magmaclasts (M) and pitted edges of the core. c) Atypical MVK: Note the spherical and angular magmaclasts (M). Detailed petrographic descriptions of these rock units are given in section 3.2.6.

and shows very little rotation of the fragments. Fragments are typically >1cm in size and void spaces infilled by calcite commonly reach up to 5cm in size. A second lithological variety underlies the dolerite contact breccia and extends down to 295m. This unit is comprised of shale fragments only, which are more highly fragmented and show some degree of rotation. Individual fragments may reach up to 4cm however may be as small as 2mm. This shale contact breccia shows a gradational change with increasing depth. At greater depth the degree of rotation of the fragments becomes much less and eventually only fractures are present with no rotation of fragments. The fractures and voids in both the dolerite and shale contact breccias are infilled by calcite only.

3.2.2.2 Central Eruption Zone (CEZ)

The CEZ contains three distinct MVK varieties: 1) Type 1b, 2) Type 2 and 3) Intermediate as shown in logs in appendix 4. Detailed petrographic descriptions of these units from representative samples are given in section 3.2.6. This zone is characterised by a higher kimberlite proportion as well as higher basalt CRX content than the Initial Eruption Zone (IEZ). The most dominant variety of MVK is the T1b whereas in terms of economics the T2 MVK has the highest kimberlite content of all the MVKs and therefore the diamond grade would be expected to be the highest. The CEZ was logged in detail in boreholes 2 and 3 as shown in appendix 4 and compared with De Beers borehole logs from hole 5. Figure 3.12 shows the distribution of the boreholes and figure 3.14 shows a cross section created from boreholes 2, 3, 9 and 10 in appendix 4.

Type 1 b Massive Volcaniclastic Kimberlite (T1bMVK)

T1bMVK is similar to the T1aMVK in holes 9 and 10, although T1b has slightly higher kimberlite content. The only major difference is the higher proportion of basalt xenoliths, which is not obvious at macroscopic scale but is evident through microscopic modal analysis (see table 3.5 in section 3.2.6 for modal analyses of the MVK units). The largest xenolith present is 3m in size however this is extremely rare and the xenoliths are typically <8cm with rare occurrences up to 15cm in size. The larger xenoliths are typically brown to purple amygdaloidal basalt, which is Karoo in origin. Magmaclasts are difficult to distinguish on this scale and are never observed >10mm in size. The rock is very similar in colour to the T1aMVK.

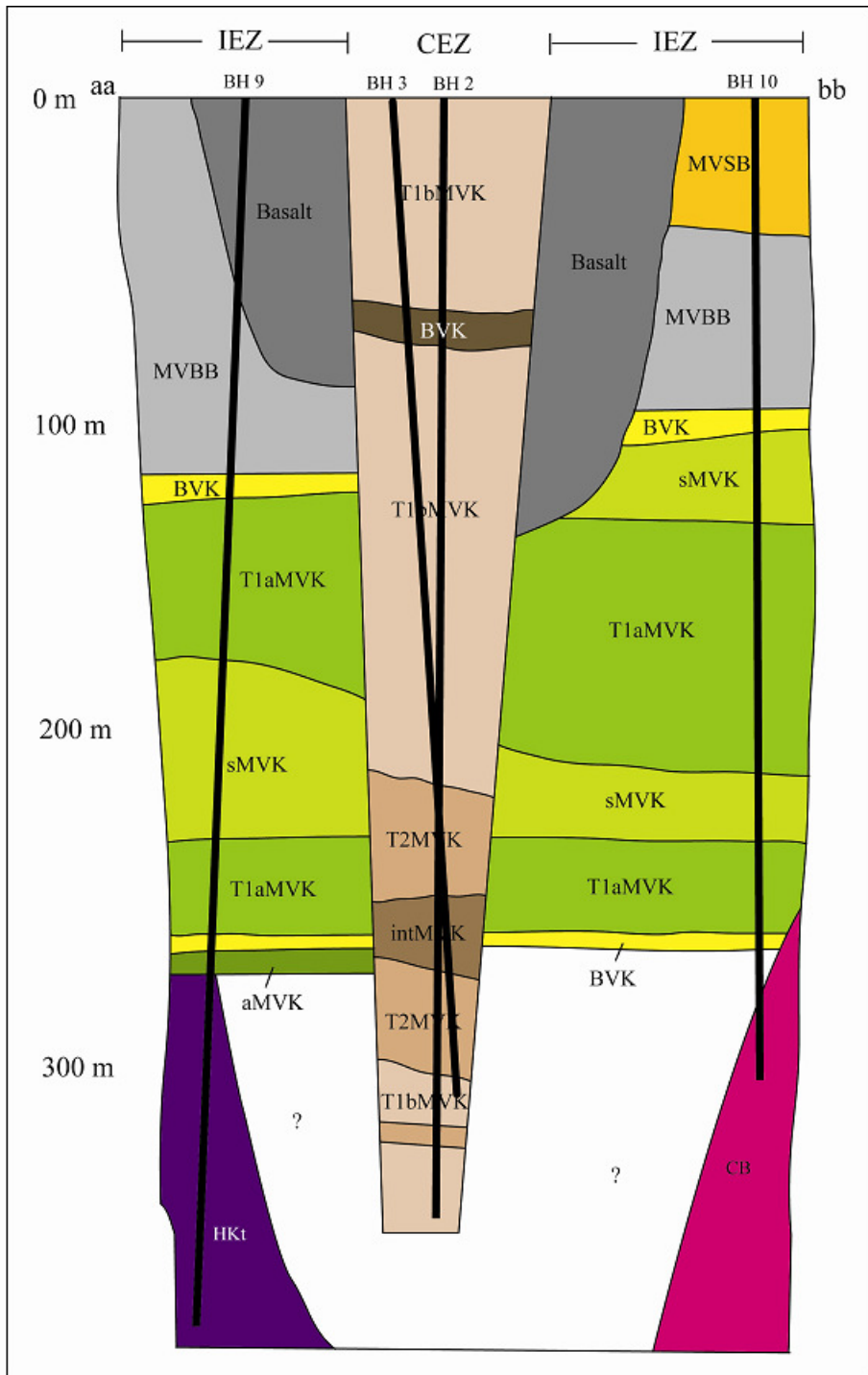


Figure 3.14 Schematic cross-section aa-bb; (as indicated on figure 3.12) showing the interpreted distribution of internal geology at the Voorspoed pipe. The section is based on the geology logged in boreholes 2, 3, 9 and 10 as shown on the diagram and in appendix 4. Note the distribution of the central and initial eruption zones as indicated at the top of the section. The latter CEZ cross cuts the earlier formed IEZ. (HKt: transitional kimberlite; CB: contact breccia). See appendix 7 for a full list of abbreviations used in the diagram and text. Pipe outline modified after Clement (1982).

T1b dominates the CEZ and occurs in two zones. Firstly, a relatively thin unit of 28m thickness occurs at 310m depth. This layer is not continuous to hole 2. The main T1b layer occurs at 215m depth in hole 2 and 210m depth in hole 3. This layer is present from this depth to the surface and therefore is over 200m thick. The layer is broken at 70m from the surface by a 10m thick normally graded sequence and therefore this T1bMVK unit can be divided into two separate deposition processes, which has produced an MVK of similar characteristics. Figure 3.15 (a) shows a representative sample photographed from the core.

Type 2 Massive Volcaniclastic Kimberlite (T2MVK)

T2MVK is very distinct and is characterised by abundant coarse grained (up to 15cm) magmaclasts. The rock is also much lighter in colour relative to the Type 1 and soft MVK varieties as shown in figure 3.15 (c). Magmaclasts are spherical to ellipsoidal in shape and are characterised by the common occurrence of altered olivine macrocryst central kernels (figure 3.15c), which are uncommon in all other MVK varieties. The xenolith population is dominated by basalt, which is common to all the MVK varieties. However this MVK contains a much greater proportion of kimberlite and therefore country rock xenolith (CRX) contents are lower. Dolomite xenoliths are highly altered in this MVK relative to the other MVK varieties.

This MVK occurs as three layers below 210m depth. The deepest of which occurs in hole 2 at 328m and is just 6m thick. This layer is not observed in hole 3 as hole 3 does not extend to this depth. The second T2 layer occurs at 282m depth in hole 2 and 295m in hole 3. The layer varies in thickness from 12m in hole 2 to 27m in hole 3. The final layer occurs at 248m in hole 2 and 250m in hole 3. The layer varies in thickness from 33m in hole 2 to 40m in hole 3. It must be noted here that the upper hole 3 T2MVK unit is interbedded with intermediate MVK over the upper 30m. These interbedded layers range from 1m to 5m in thickness and are not present in hole 2. Furthermore confirmation of the horizontal distribution is obtained by examination of the logs given by De Beers for boreholes 5 and 6 where both holes have the distinct T2MVK at 220m in hole 5 and 210m in hole 6. These are both near vertical and detailed logs are not presented in thesis but are given in Stiefenhofer (int. report).

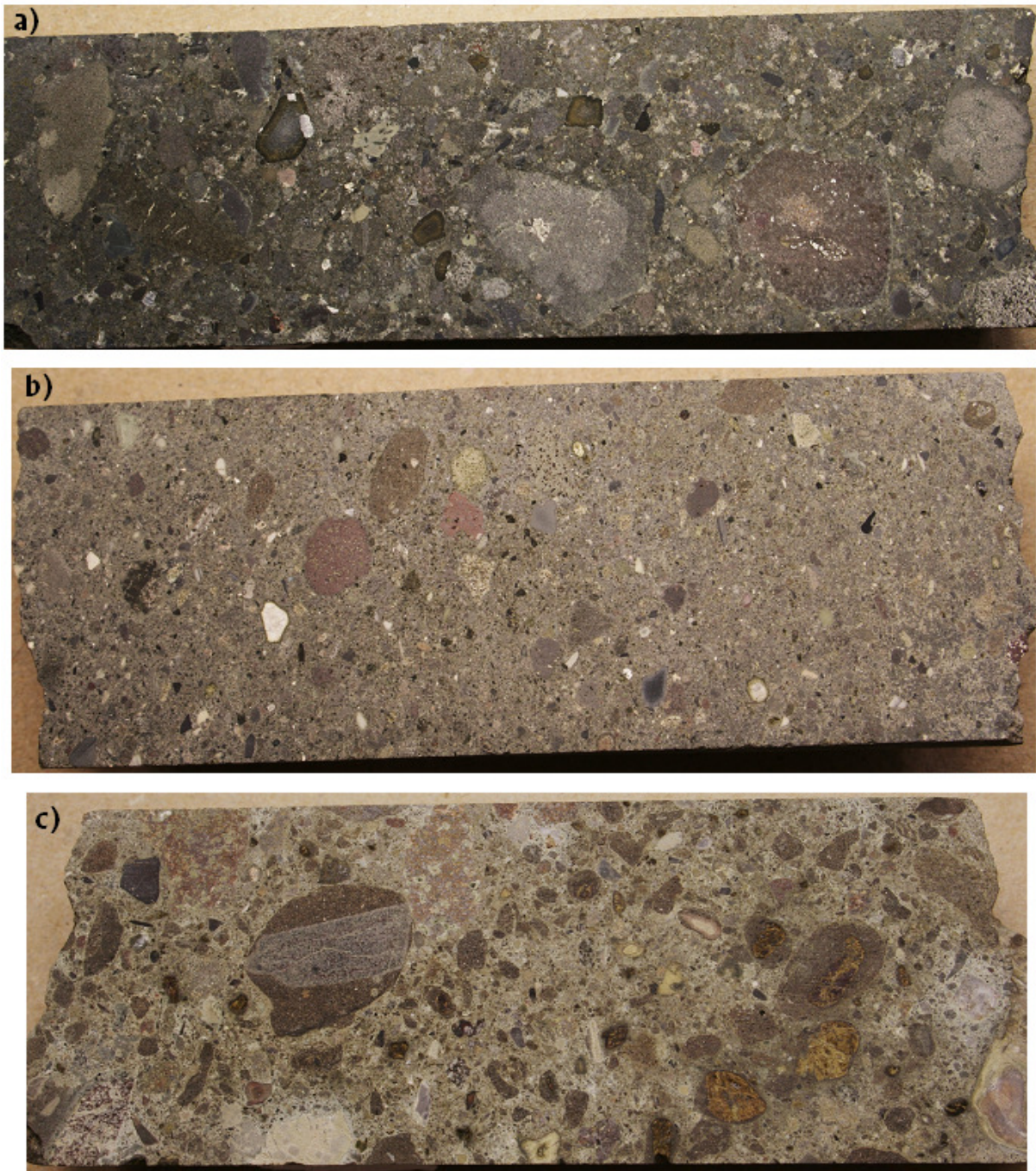


Figure 3.15 Photographs of the CEZ MVK samples. a) Type 1 b MVK. b) Intermediate MVK. c) Type 2 MVK. Note the colour variation between the T1bMVK and the intMVK and T2MVK. The latter varieties are clearly lighter in colour. The T2MVK contains abundant spherical magmaclasts with central kernels of either altered green olivine macrocrysts or country rock xenoliths.

Intermediate Massive Volcaniclastic Kimberlite (intMVK)

The intMVK as the name implies contains proportions of the major constituents of the MVKs, which are intermediate between the T2MVK and the T1bMVK. Basalt xenoliths are still the dominant component of the rock however magmaclast content is high relative to the T1bMVK. This MVK is finer grained than the T2MVK and minor grading is evident on small scales where the components grades from cm scale to mm scale, although it is dominantly massive in texture. The MVK is very similar in colour to the T2MVK.

This MVK is only observed in hole 3 and a thin layer in hole 5. Therefore this MVK occurs only in the central region of the CEZ over a horizontal distance of approximately 60m. Two distinct layers occur with a third unit interlayered with T2MVK as described above. Hole 3 ends in the lower unit, which occurs at 310m depth and is 15m thick. The upper layer occurs at 265m depth and is also 15m thick. Figure 3.15 (b) shows the finer grained nature relative to the T2MVK.

Bedded Volcaniclastic Kimberlite (BVK)

This sequence is very similar to that described for borehole 9 at 125m in the IEZ. Normally graded beds are again observed with a maximum thickness of 1.5m. The sequence here varies from 12m to 10m thickness between holes 2 and 3 respectively and at a depth of 79 in hole 2 and 75m in hole 3. Xenoliths range in size from 4cm at the base of a bed to mm scale at the top. Basalt xenoliths dominate as is typical of the entire VK deposit. Detailed petrographic descriptions of the BVK are given in section 3.2.6.

Fine-grained VK Bands

Numerous fine-grained bands are present throughout the CEZ only. These bands are typically <6cm in thickness and therefore are not modelled with the rest of the rock units as they are volumetrically insignificant. However these layers are particularly important from a genetic perspective and will be discussed in greater detail later. Detailed petrographic descriptions of these fine grained layers are given in section 3.2.6.

Table 3.4 Modal abundances for the hypabyssal and transitional hypabyssal (9/2) kimberlite at the Voorspoed pipe. (Ol.: olivine; Phlog: phlogopite; Diop: diopside; Serp: serpentine; Clay: clay minerals; Sani: sanidine; Mel: melilite).

	Ol.	Phlog.	Diop.	Spinel	Calcite	Serp.	Clay	Sani.	Mel.	Other
4/1 (int. Dike)	8	40	25	1	12	8	4	1	0	0
K1/111 (sill)	4	43	28	0	7	5	11	2	0	0
K1/151 (unknown)	30	3	57	3	0	3	0	0	0	4
K1/135 (unknown)	10	35	9	8	21	6	8	0	9	0
9/2 HKtB	13	32	9	1	17	0	8	0	0	20

3.2.3 Hypabyssal Kimberlite (HK)

Hypabyssal kimberlite sensu stricto has not been intersected in a distinct root zone within the Voorspoed pipe, although HKtB is intersected and believed to represent the top of the root zone preserved in the pipe. A number of post-eruptive internal hypabyssal dikes are observed and described below. A hypabyssal sill in the country rock adjacent to the Voorspoed pipe, which shows very similar mineralogy to the internal dikes, has also been described below. Furthermore analysis of the magmaclasts within the MVK infilling the pipe shows at least two distinct varieties of hypabyssal kimberlite (HK) could be present in the root zone. The dominant magmaclast mineralogy is diopside phlogopite kimberlite but rarer melilite-bearing phlogopite kimberlite is also observed. Melilite-bearing phlogopite HK thin sections are present in the De Beers collection but unfortunately no information on the location of this sample is available.

3.2.3.1 Hypabyssal Sill (K1/111)

The sill is aphanitic containing rare macrocrysts of olivine and phlogopite. Figure 3.16 shows photomicrographs from this sample and a modal analysis of the rock is given in table 3.4. The rock is composed of dominant phlogopite (43 vol. %) and diopside (28 vol. %) set in a base of

clay minerals, calcite, serpentine and lesser sanidine. Rare opaque minerals are also observed as inclusions in phlogopite and throughout the base. The rock can be classified as hypabyssal aphanitic clay mineralised, sanidine and aegirine-bearing, diopside, phlogopite kimberlite.

Olivine occurs as rare macrocrysts (>0.5mm) and phenocrysts (0.1-0.4mm). These grains are always highly altered by a combination of two minerals. The more dominant of the two is colourless with a dirty appearance due to numerous inclusions of fine-grained opaque needles and has a low birefringence. This mineral is serpentine. The second less abundant mineral is very fine-grained, light brown green and has a high birefringence; these are clay minerals. Clay minerals are present in very minor proportions relative to the serpentine. Olivine phenocrysts seldom show subhedral habits and are typically rounded due to resorption.

Phlogopite occurs as three distinct forms: 1) rare macrocrysts (>0.5mm), 2) phenocrysts (average 0.2-0.4mm) and microphenocrysts (+/- 0.05mm). Macrocrysts are characterised by deformation features such as undulose extinction or kink banding. Phenocrysts are weakly pleochroic with shades of pale brown and show fine mantles of darker red/brown tetraferriphlogopite. Minor inclusions of opaque minerals are also observed with lesser red translucent grains. Microphenocrysts are characterised by a distinct darker brown tetraferriphlogopite, which is similar to the mantles of the phenocrysts.

Diopside occurs in one generation as both phenocrysts (>0.1mm) and microphenocrysts (<0.1mm) although they are very similar; the only difference is the size of the grains. Therefore these occurrences are described together. Diopside occurs as grains with a range of size <0.05-0.35mm with rare grains up to 1.2mm. The diopside is of particular interest as they show the development of green mantles at the terminations of the grains. These mantles have been described at more evolved kimberlites as titanian aegirine but have not previously been identified at Voorspoed. The cores of the grains are typical colourless, high birefringence laths with inclined extinction whereas the green mantles show almost straight extinction. The characteristic feature of aegirine over other pyroxenes is the 0-10° extinction angles and therefore the development of a green mantle at the terminations of diopside is most likely aegirine. The

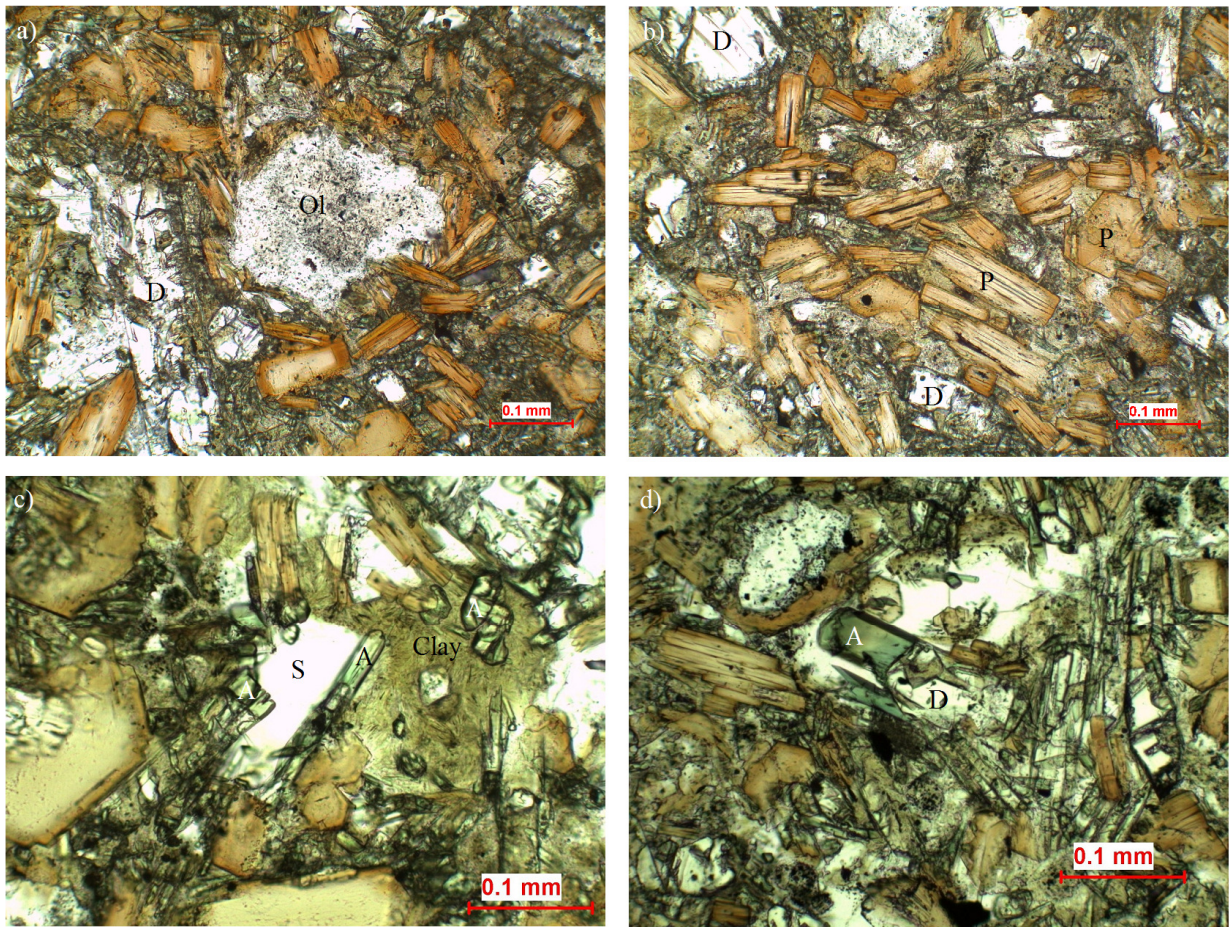


Figure 3.16 Photomicrographs of the hypabyssal sill (K1/111, De Beers collection, appendix 8) as described in section 3.2.3.1. Modal analysis for this sample is given in table 3.4 a) Highly serpentinised olivine (Ol) phenocryst surrounded by non-poikilitic phlogopite. Also note the large diopside phenocryst (D). b) Non-poikilitic phlogopite laths showing minor evolution to red/brown tetraferriphlogopite margins. c) Clear colourless sanidine (S) segregation with inward protruding pyroxene. The sanidine is being altered by brown yellow clay minerals (Clay). Two pyroxenes are present: typical colourless diopside and light green overgrowths on the diopside of aegirine (A). d) Clear development of aegirine (A) overgrowth on a diopside (D) lath. In this case the clear segregation is calcite.

composition of these mantles is further described in section 4 by microprobe analysis. Diopside may be partially altered by calcite.

The base of the rock is dominated by calcite and clay minerals. The calcite is typically colourless with a dirty appearance. Clay minerals are observed as fine grained light brown green turbid

material with high birefringence. Serpentine is observed as an alteration product of olivine and typically is colourless with a dirty appearance, low birefringence and commonly shows undulose extinction. The presence of colourless, low birefringence and very clear segregations in the base indicate the presence of sanidine. The segregations commonly have inward protruding diopside laths, which show green overgrowths within the sanidine segregations. These clear colourless and low birefringence segregations are commonly altering to clay minerals and calcite along the margins. Alteration to clay minerals is particular indicative of feldspars. Therefore these segregations may represent late stage evolved liquids, which crystallise more evolved minerals such as sanidine and aegirine.

The characteristic features of this rock are: 1) dominantly serpentine altered olivine with rims of microphenocryst phlogopite, 2) green overgrowths on diopside terminations and 3) weakly evolved phlogopite. The presence of green mantles on diopside as well as sanidine in the base indicates the evolved nature of the kimberlite. This rock is very similar to other evolved kimberlites as described by Mitchell (1995)

3.2.3.2 Hypabyssal Dikes

Two internal hypabyssal dikes were sampled from the core available. These dikes were both approximately 30cm thick and cross cut the MVK within the pipe. Sample 4/1 (Skinner collection; appendix 8) comes from hole 4 at 230m and contains abundant coarse country rock xenolith (CRX). Sample 3/112 comes from hole 3 at 112m (collected in this study). The dikes are both typical sanidine and aegirine-bearing diopside phlogopite kimberlite, although some variation is noted with respect to the alteration. The mineralogy of the dikes is discussed together below and shown in figure 3.17.

Olivine occurs as typical highly altered phenocrysts (average 0.1-0.3mm) and macrocrysts are rare. Olivine in sample 4/1 is altered by two distinct minerals. The more dominant is typically

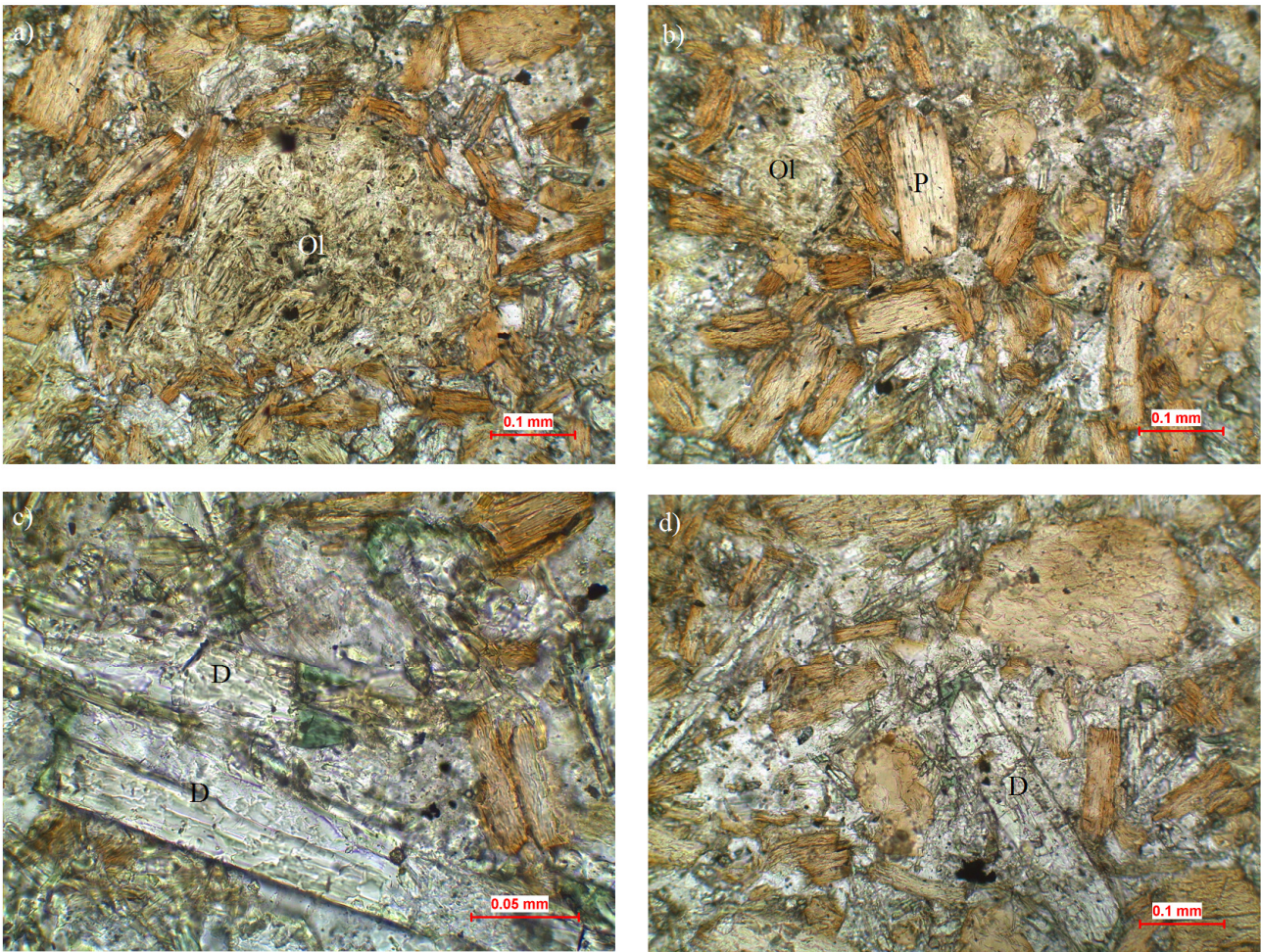


Figure 3.17 Photomicrographs from an internal hypabyssal dike (section 3.2.3.2) at the Voorspoed pipe (sample 4/1; Skinner collection, appendix 8). Modal analysis of the rock is given in table 3.4 a) Altered clay mineralised olivine (Ol) phenocryst surrounded by phlogopite. b) Non-poikilitic phlogopite phenocrysts showing some evolution to tetraferriphlogopite. c) High power image showing green aegirine overgrowths on colourless diopside (D) laths. d) Development of fine green aegirine overgrowths on a diopside (D) lath.

light green brown, high birefringence and very fine-grained with a fibrous texture; identified as a clay mineral. The second mineral occurs around the rims of the clay-altered core of the olivine, which is identified as calcite. Microphenocrysts of phlogopite are always seen rimming the alteration assemblage of the olivine. The presence of these phlogopite rims greatly aids in the

identification of the relict olivine grains. Most olivine is resorbed with lesser subhedral grains, although rare euhedral olivine is present.

Phlogopite occurs as three typical forms: 1) rare macrocrysts, 2) phenocrysts and 3) microphenocrysts. Macrocryst phlogopite is rare and occurs up to 1.2mm and have similar characteristics to the phenocrysts. Phenocryst phlogopite are characterised by their weak zoning relative to the phlogopite observed at the Lace hypabyssal kimberlite (HK). The phenocrysts are weakly pleochroic pale brown with thin mantles of darker red/brown tetraferriphlogopite. These grains are generally not poikilitic although minor inclusions of opaque spinels and rare translucent red minerals are observed. Microphenocrysts (<0.1mm) are characterised by the darker red/brown colour, which is a result of the more evolved composition of the mica. These grains have characteristics similar to the thin tetraferriphlogopite mantles of the phenocrysts. Therefore the phlogopite is very similar to that described of the hypabyssal sill K1/111.

Diopside occurs as typical phenocrysts and microphenocrysts similar to that described for the hypabyssal sill sampled. There is no difference between phenocrysts and microphenocrysts besides the arbitrary size limits and therefore they are described together. Sample 4/1 contains fresh diopside, which is very similar to the diopside described for the sill sample K1/111. Similar green aegirine overgrowths are present, which have been analysed and discussed in section 4. Therefore diopside will not be discussed again here. Microphenocrysts commonly show complete evolution to green aegirine, which are not observed in sample K1/111.

Opaque minerals are generally rare in the dike samples. Scattered microphenocrysts on average 0.01mm in size are seen throughout the rock.

The base of the rock is similar to that described above for the hypabyssal sill K1/111 although the rock is slightly more altered by calcite. Similar low birefringence clear colourless sanidine segregations are observed but in general are altered out by calcite. The base here is dominantly a very fine grained light brown turbid material with varying birefringence with lesser dirty colourless calcite. The turbid material is a mixture of intergrown serpentine and clay minerals.

Therefore the important characteristics of these rocks are very similar to those of the hypabyssal sill described above and include: 1) highly altered olivine rimmed by microphenocryst phlogopite, although serpentine is not observed altering olivine in the dike samples 2) relatively unevolved phlogopite and 3) evolved green mantles on diopside. A similar conclusion of the evolved nature of the kimberlite can be made from the presence of sanidine and titanian aegirine mantles.

3.2.3.3 Other Hypabyssal Varieties

The De Beers collection contains over 70 thin sections of hypabyssal kimberlite (HK) but unfortunately no information on the location of the samples is available. Most of these samples are typical diopside phlogopite kimberlite but two distinct varieties not observed elsewhere have been identified. Olivine diopside kimberlite and melilite-bearing kimberlite are both observed in a number of thin sections. Melilite-bearing phlogopite kimberlite has been observed as magmaclasts within MVK but no hypabyssal equivalent has been sampled in this study. The only hypabyssal equivalents available are the samples in the De Beers collection. These two distinct varieties are briefly described below and shown in figure 3.18.

Diopside kimberlite (samples K1/154; De Beers collection) is characterised by the dominance of fine-grained diopside (figure 3.18 a) and modal analysis shown in table 3.4. Olivine occurs as rare macrocrysts and more common phenocrysts, which are always completely altered by serpentine and clay minerals. Euhedral to subhedral habits are common. Phlogopite is not abundant in this rock but rare pleochroic, poikilitic grains are observed which do not show any zoning. Diopside rarely exceeds 0.1mm and most commonly is 0.02mm in size. The larger grains form distinct colourless laths whereas the finer grains are typically resorbed. Diopside does not show any evolution to green mantles as observed elsewhere. Opaque spinels are relatively abundant relative to other HK varieties and occur up to 0.06mm with common resorption features. The base of the rock is comprised of dominantly serpentine with lesser clay minerals. Calcite is characteristically absent from this rock. This rock can be classified as a poorly macrocrystic diopside kimberlite.

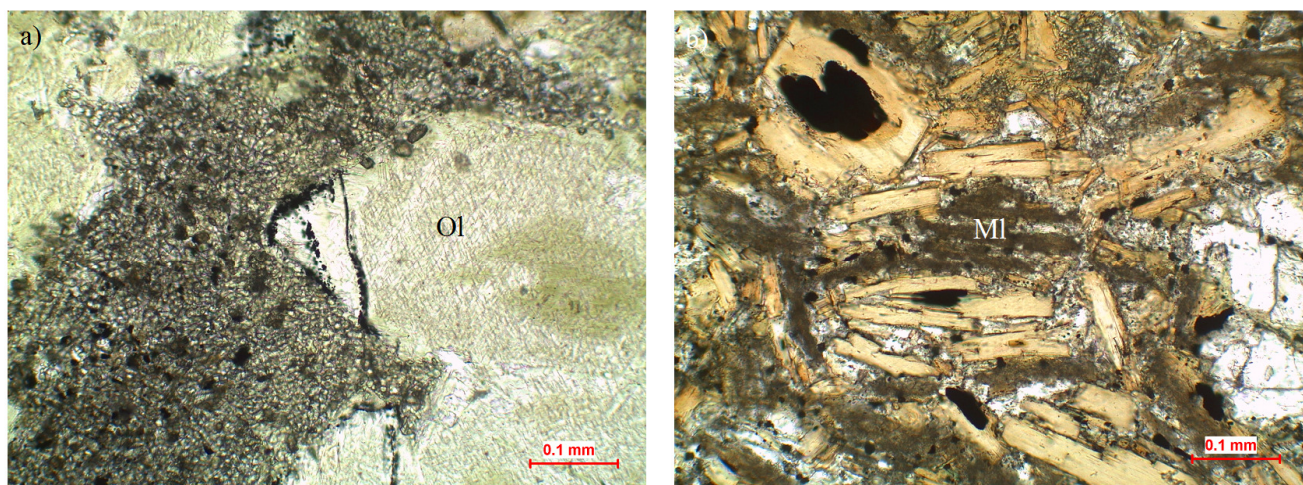


Figure 3.18 Photomicrographs from two rare hypabyssal varieties at the Voorspoed pipe (samples K1/154 and K1/135 respectively; De Beers collection). a) Diopside kimberlite containing abundant fine grained diopside and euhedral olivine (Ol) phenocrysts. b) Melilite-bearing kimberlite. Note the presence of abundant highly altered dirty looking carbonatised melilite (Ml) laths.

Melilite-bearing phlogopite kimberlite (sample K1/135; De Beers collection) is characterised by much lower diopside content than other HK varieties as shown in table 3.4 and by the presence of altered melilite (figure 3.18 b). Olivine is difficult to distinguish as it is highly altered by calcite in most cases. Olivine phenocrysts typically occur as 0.2-0.35mm grains, which are often rimmed by phlogopite microphenocrysts. Phlogopite occurs similarly to most other HK described. Zoning of the phlogopite is more evident here with common mantles of darker red/brown tetraferriphlogopite and reverse zoning is evident in some microphenocrysts. Typical light brown and weakly pleochroic phenocrysts dominate, which show minor alteration to chlorite. Diopside is less abundant relative to most other HKs and is commonly completely altered by calcite. No green aegirine overgrowths on diopside are observed in this rock. Melilite is the characteristic mineral of this rock and occurs as phenocrysts (0.1-0.2mm) and is always completely altered. The melilite has a typical lath habit and a dirty grey colour. The grains are near isotropic due to the very fine-grained nature of the alteration products, where visible they have a high birefringence and are tentatively identified as clay minerals and calcite. Opaques occur scattered throughout the rock and occur up to 0.04mm but more commonly <0.02mm. The base

of the rock is dominated by calcite with lesser clay minerals and serpentine. This rock is classified as an aphanitic melilite-bearing phlogopite kimberlite.

3.2.4 Hypabyssal Transitional Kimberlite Breccia (HKtB) and Contact Breccias

3.2.4.1 Hypabyssal Transitional Kimberlite Breccia (HKtB) (Sample 9/2)

Transitional kimberlite is particularly important in the understanding of the processes operating during the formation of the pipe. Figures 3.19 and 3.20 show the HKtB in both core and microphotographs. Modal analysis of sample 9/2 is given in table 3.4, this is a relatively xenolith poor sample. The rock underlies the MVK units within the pipe in hole 9 (appendix 4) only and is characterised by an incipient globular segregatory texture (figure 3.20) similar to that observed at the Lace kimberlite. The rock contains on average approximately 20 vol. % xenoliths, which are all locally derived shales and dolerite from the sidewall with rarer carbonate basement xenoliths also present. Xenolith content varies and can reach values up to 70 vol. % (figure 3.19). It is particularly important to note that no Karoo type basalt or Karoo sedimentary xenoliths are observed in the transitional kimberlite zone. Dolerite is present but it is clearly identified as dolerite and not basalt due to the coarse grained nature. The most likely source of the dolerite is observed at the bottom of hole 10 as an intrusive dike/sill, which has been highly fractured during the formation of the pipe. Calcite in the form of segregations occupies approximately 20 vol. % of the rock as well as pervasively altering the globules. Globules often do not contain central kernels and when kernels are present they are typically highly altered xenoliths of shale or carbonate. The globules have vague indefinite spherical shapes up to 2cm in size.

Olivine occurs as typical highly altered (clay mineralised) phenocrysts, which rarely exceed 0.25mm. The phenocrysts range in habit from anhedral to subhedral habits where crystal outlines are still present. Macrocrysts are particularly rare and only one is observed in this sample. All olivine observed is totally altered by clay minerals and lesser calcite. Serpentine is notably absent from the rock. Phlogopite occurs as non-poikilitic laths up to 0.5mm in length. The phlogopite is light brown in colour with minor zoning to darker red brown tetraferriphlogopite at the margins. Diopside is relatively fine-grained and generally <0.1mm in length but more

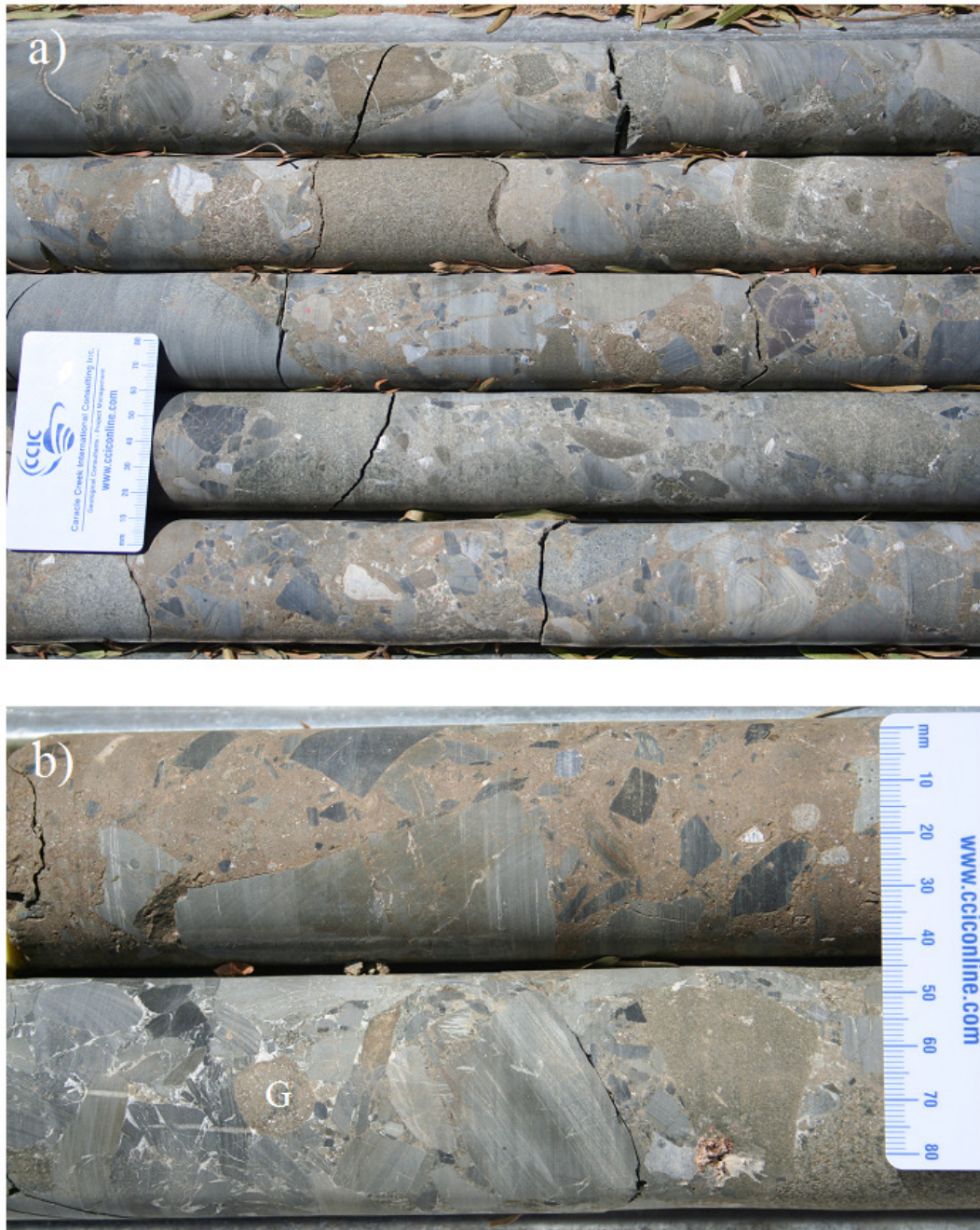


Figure 3.19 Core photos of the hypabyssal transitional kimberlite breccia (HKtB) at the Voorspoed pipe from borehole 9 at approximately 320m depth in the borehole. Note the abundant xenolith content in (a) and the presence of a large globule in (b). Also note the variation in xenolith content between the upper and lower cores in photo (b). Photomicrographs of the HKtB are given in figure 3.20 and modal analysis of a relatively xenolith poor sample (9/2) is given in table 3.4.

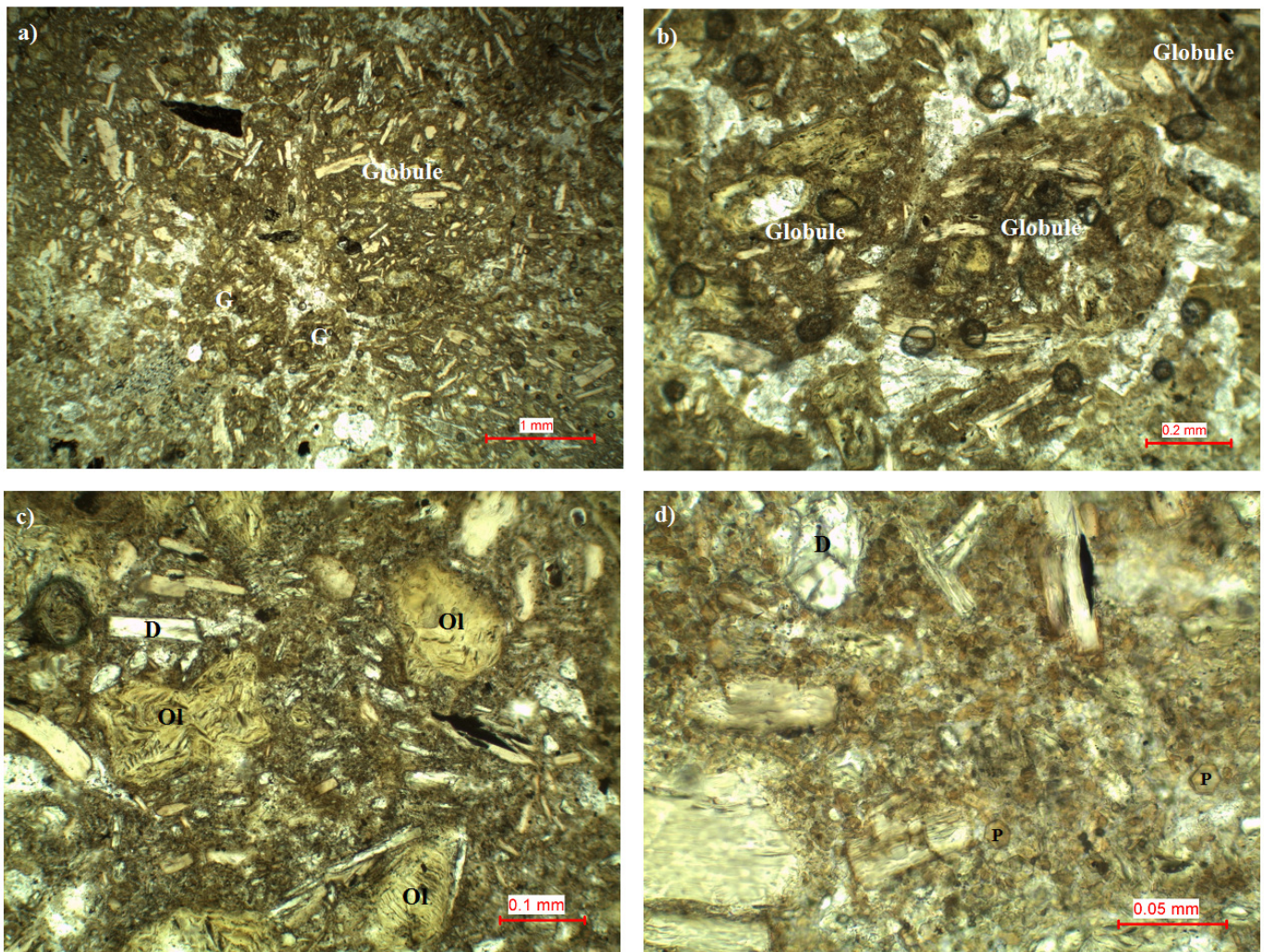


Figure 3.20 Photomicrographs of the hypabyssal transitional kimberlite breccia (HKtB) sample 9/2 (Skinner collection) from borehole 9 at 292m depth at the Voorspoed kimberlite. Refer to appendix 8 for a full list of the samples analysed in this study. Photos from the core are show in figure 3.19 and modal analysis for this sample (9/2) is given in table 3.4. a) Low power image showing incipient development of globules (G) in base of colourless calcite. b) Clear development of globules, which do not contain central kernels, in a base of colourless calcite. c) Higher powered image of the kimberlite groundmass showing highly clay mineralised olivine (Ol) phenocrysts, diopside (D) phenocrysts and phlogopite phenocrysts in a base of calcite and ultra fine grained phlogopite. d) High power image showing the ultra fine grained phlogopite base material. Note the hexagonal basal phlogopite sections marked with a P. Diopside (D) is also show.

commonly 0.02mm. Therefore the diopside occurs only as microphenocrysts, which may be autometasomatic and not primary.

Diopside is unlike that observed at the Lace hypabyssal transitional kimberlite (HKt) in that it occurs as distinct laths and not stubby crystals in the base of the rock. No green aegirine overgrowths are observed on the diopside. Melilite may occur as <0.1mm highly altered laths but due to the highly altered nature of the laths they are very difficult to identify. Opaques occur in relatively minor proportions and never exceed 0.03mm. They are not observed as inclusions within phlogopite such as at the Lace kimberlite.

The most interesting characteristic of the hypabyssal transitional kimberlite breccia (HKtB) at Voorspoed is the base of the rock. The base is comprised of three components: 1) calcite, 2) clay minerals and 3) ultra-fine grained phlogopite (figure 3.20d). The calcite forms distinct segregations as part of the globular segregationary texture as well as the base to the rest of the rock. Clay minerals are not as abundant as the other two constituents of the base but never the less are present as typical green brown clays similar to those altering the olivine. It is often difficult to distinguish altered olivine from the base and therefore olivine proportions may be slightly undercounted. Phlogopite occurs as ultra fine rounded to oval habit grains, which rarely exceed 0.01mm in size (figure 3.20 d). This characteristic has not been observed anywhere else in the Kroonstad cluster. It is possible to identify these ultra fine grains as phlogopite by: 1) become fine grained brown laths where coarse enough and 2) hexagonal brown basal sections. In general this fine-grained phlogopite is darker brown in colour than the phenocryst population, indicating some degree of evolution of the magma. Phlogopite is the dominant component of the base material except in the areas of pure calcite segregations. Therefore the globules are incipient with an inter globular matrix of calcite and minor clay and an intra globular matrix of ultra fine phlogopite.

3.2.4.2 Contact Breccias

Contact breccias occupy a position below the MVK in hole 10 in the sidewall of the pipe at depth (250m) in borehole 10. Two distinct varieties are identified on the country rock present in each as shown in figure 3.21. A dolerite contact breccia and a shale contact breccia are both present in

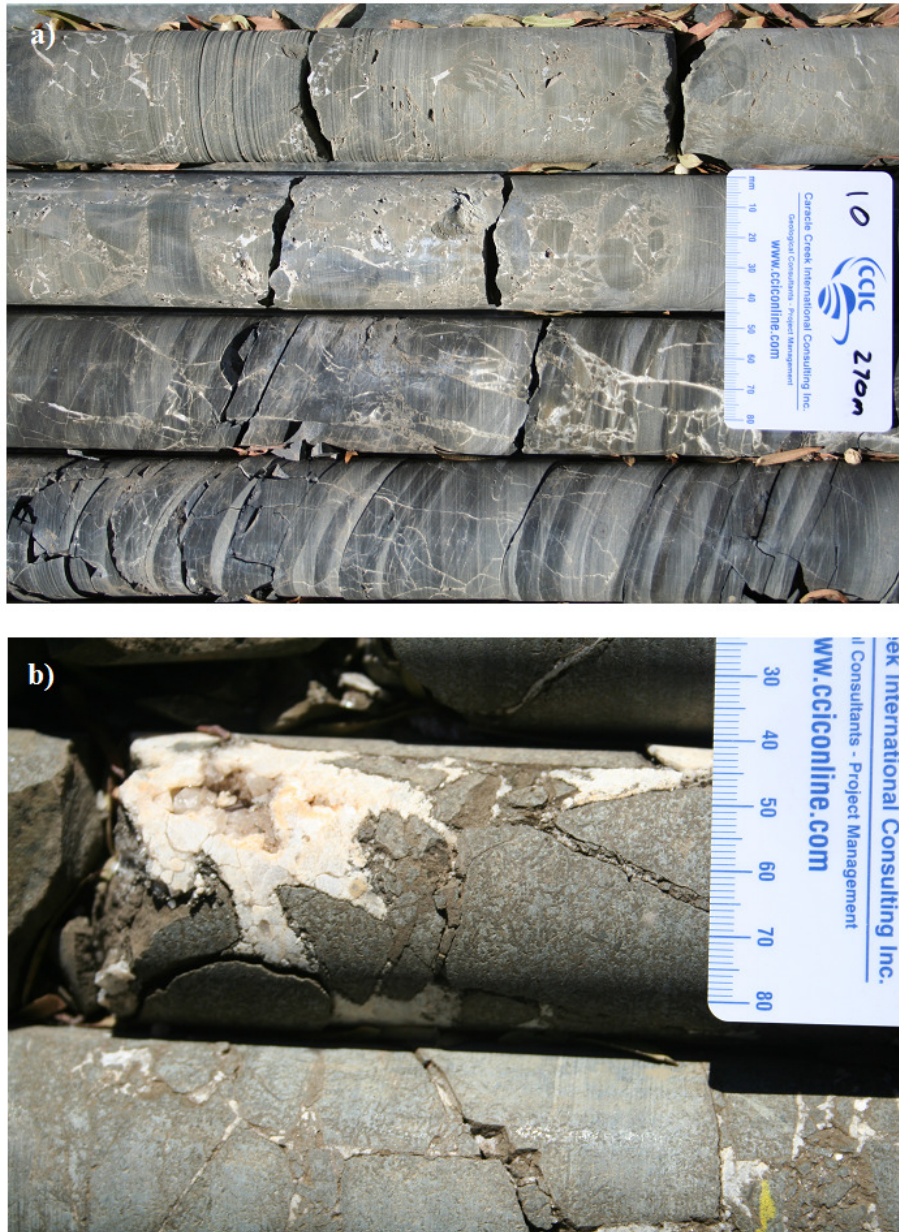


Figure 3.21 Photographs of contact breccias observed in the borehole 10 at 260m and 270m depth at the Voorspoed pipe. a) Contact breccia is the sidewall shales at 270m in borehole 10. The bottom of the core is at the bottom of the photo. Note the progressively decreasing intensity of fracturing. Calcite is infilling the fractures and no kimberlite is present. b) Narrow contact breccia zone at 260m depth directly overlying the contact breccia in a). The contact breccia has formed in a dolerite sill, which pre-dates the kimberlite intrusion. Note the calcite infilling a large void.

borehole 10. The contact breccia varieties simply indicate changing lithology in the country rock with increased depth. Contact breccias consist of in situ, angular fragments of country rock, which are kimberlite free. The fragments may be partially rotated where fragmentation has been extensive. In general the breccias are monolithic and clast supported with a matrix of calcite. The degree of fragmentation and rotation of fragments decreases gradually with depth and eventually only fine calcite filled fractures are present. Cavities may reach up to 15cm in diameter in the dolerite contact breccia whereas in the shale breccia cavities are seldom >2-3cm. The shale is typically more highly fractured, which is most likely due to the less competent nature of the rock relative to the dolerite. The cavities are always filled with calcite, which may indicate the presence of CO₂ as a gaseous phase present during the formation of the breccias.

3.2.5 Volcaniclastic Kimberlite

Dominant Components

The dominant constituents of the Voorspoed MVK include 1) country rock xenoliths (CRX), 2) magmaclasts, 3) basement xenoliths and 4) interclast material. Figure 3.22 shows modal analyses of the dominant components indicated on the cross section of the Voorspoed pipe. CRX are generally the dominant constituent occupying 40-60 vol.% of the rocks. Magmaclasts rarely exceed 50 vol.% of the rock and for most of the MVK occupy approximately 25 vol.%. Basement xenoliths occur in much lesser proportions relative to the CRX and magmaclasts and typically only represent <5% of any given MVK. The interclast material proportion varies slightly between MVK types but generally is 10-14 vol.%, although it may reach up to 25%. Modal analyses for the different MVK units are given in table 3.5. CRX xenoliths are dominated by Karoo basalt with lesser sandstone, shale and dolerite. Dolerite however is very similar to basalt and may be present in greater proportions than counted. Magmaclasts typically form two distinct morphological varieties as well as two mineralogical varieties as discussed below. The interclast material of the rock is not typical of South African Class 1 kimberlites and is highly fragmental containing comminuted juvenile and lithic fragments set in an ultra fine base. Refer to appendix 7 for a full list of abbreviations used in the text. The distribution of the VK units was discussed in section 3.2.2 and shown in figures 3.12 and 3.14.

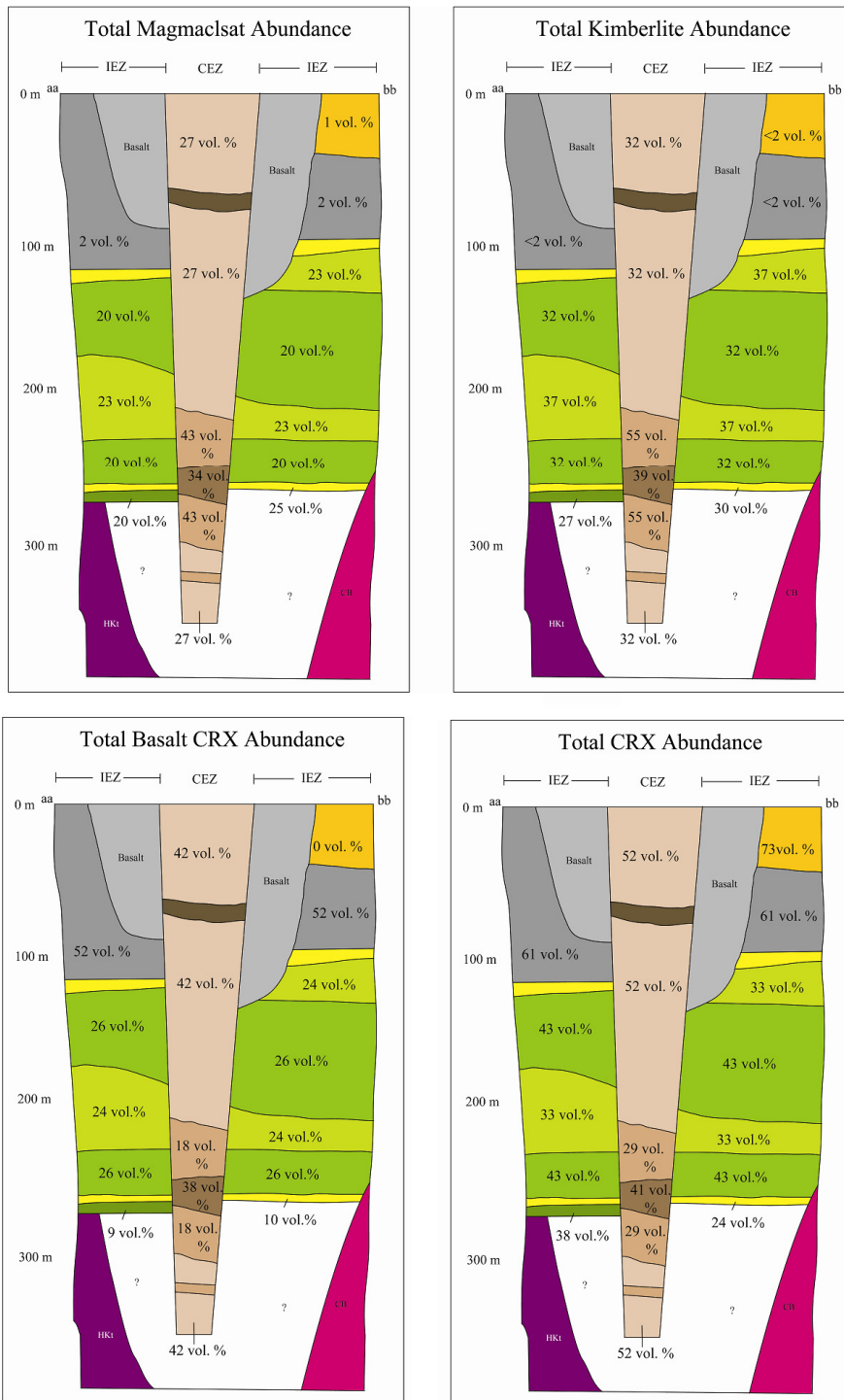


Figure 3.22 Cross-section aa-bb; (as indicated on figure 3.12) showing the interpreted distribution of internal geology at the Voorspoed pipe. Sections show the distribution of the dominant components of the MVK as discussed in section 3.2.5 and given in table 3.5 and 3.6. These sections are based on the geology logged in boreholes 2, 3, 9 and 10 as shown in appendix 4.

3.2.5.1 Upper-crustal Country Rock Xenoliths

Upper-crustal xenoliths are the dominant component of the pipe infill and generally account for 40-60% of the MVKs. These xenoliths include basalt, sandstone, shale and dolerite from the Karoo Supergroup stratigraphy. Therefore these xenoliths have come downward from their original position in the stratigraphy and were incorporated during explosive eruption of the kimberlite. The CRX are always fresh and angular, rounding and milling effects are not observed. Altered Karoo type basalt xenoliths are only observed where they form the central kernels to magmaclasts. Sandstones and shales are very rare as central kernels in magmaclasts.

Basalt

Basalt represents the upper most formation of the Karoo Supergroup and has come from approximately 1-2km above the current locality (Hansen, 2006). Basalt is comprised of varying proportions of plagioclase, clinopyroxene, glass and vesicles (figure 3.23). The grain size varies widely in a single MVK unit and throughout the entire MVK deposit. The glass and vesicles are not always present in individual CRX. This makes the identification of basalt over dolerite difficult, as they can be petrologically indistinguishable when no glass or vesicles are present. The occurrence of glass and vesicles are characteristic features of basalt and in general the fine-grained varieties are also believed to be basalt. Figure 3.23 shows examples of typical basalt xenoliths occurring in the MVK at Voorspoed. Therefore only the very coarse grained xenoliths are believed to be dolerite. Basalt occupies between 20-80vol. % of the MVK units although basalt most commonly is approximately 50vol. % of the MVKs. Basalt contents have been accurately point counted and make up 60-80% of the total xenolith population observed in any MVK unit. Therefore basalt is by far the most dominant xenolith within the Voorspoed pipe. Vesicular basalt blocks are observed up to 3m in diameter in the drill core and are by far the largest components of the volcaniclastic rocks.

Basalt country rock xenoliths (CRX) are commonly observed as central kernels within magmaclasts (figure 3.25 b) and in these cases the plagioclase is often partly or totally altered by serpentine and clay minerals. The presence of these xenoliths as kernels indicates they were

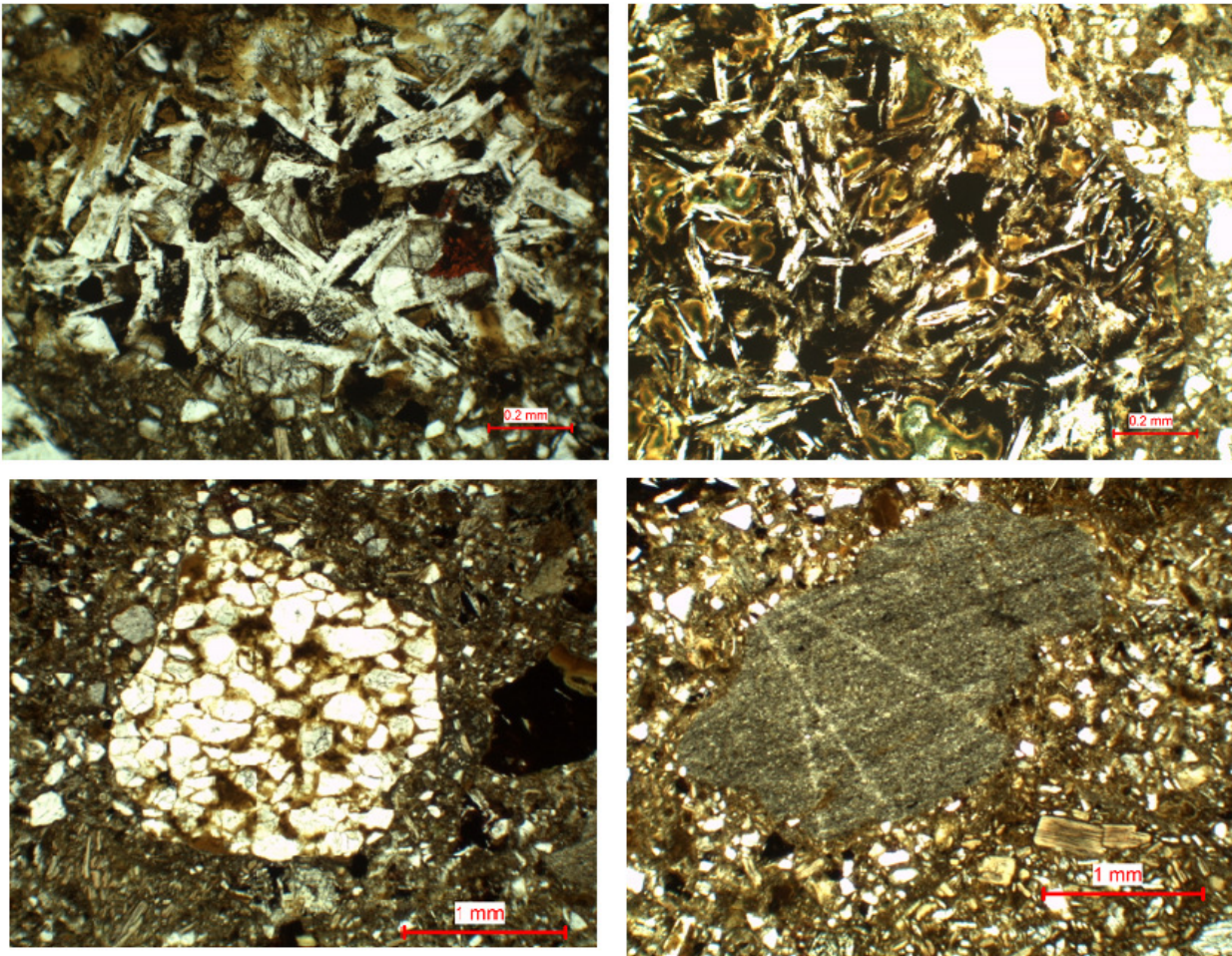


Figure 3.23 Photomicrographs of the dominant country rock xenoliths present within the volcaniclastic kimberlite. The top two are typical Karoo basalt xenoliths. Bottom left: a rare sandstone xenolith and bottom right: typical shale xenolith.

present in the magma prior to eruption and is discussed in detail in section 5. Basalt xenoliths commonly show minor alteration of the plagioclase to clay minerals or calcite. This is however not always the case and pristine basalt is observed in certain rock types as discussed later.

Basalt xenoliths have been analysed geochemically and correlated to the Mafika Lisiu and the Maloti-Senqu-Mothae units of the Lesotho formation (Hansen, 2006). Therefore they represent a complete sequence of Lesotho formation lavas, which have been thoroughly mixed through fluidisation during incorporation.

Sandstone

Sandstone xenoliths are particularly rare relative to the other Karoo Supergroup lithologies. Sandstones are absent from the bulk of the MVK and are only present in the north west of the pipe in a kimberlite poor volcanoclastic rock. This rock contains abundant sandstone xenoliths and quartz xenocrysts. Sandstone xenoliths are typically fresh (figure 3.23) as is the case with all CRX. The sandstone xenoliths have been correlated to upper Beaufort Group (Tarkastad Subgroup) and the Stormberg sandstones (Hanson, 2006).

Shale

Shales are the dominant sedimentary xenolith observed in the volcanoclastic deposits at Voorspoed (figure 3.23). Shales are generally grey to black in colour and rarely exceed 10cm in the core samples. These xenoliths are always angular indicating they were explosively fractured during the eruption process. Similar to all the other CRX the shales are always fresh and generally do not show any alteration. Shales are believed to have originated from the Eccca Group and lower Beaufort Group sequences. This is based on hand specimen analysis only and thorough analysis of these xenoliths has not been done.

Dolerite

Dolerite as discussed earlier is very similar to basalt in mineralogy and therefore it is often difficult to distinguish between the two. Dolerite however does occur in relatively high proportions in a distinct zone 40m thick in hole 9 between 205-245m. Dolerite occurs as intrusive dikes and sills throughout the Karoo Supergroup. Therefore it is possible to locally incorporate dolerite when these intrusive rocks are intersected by an eruptive phase. The dolerite here is very course grained relative to the typical basalt xenoliths. Dolerite however is not an abundant constituent of the volcanoclastic deposits.

3.2.5.2 Basement Xenoliths

Basement xenoliths are those xenoliths, which have been carried upward from their original position in hot kimberlite magma. These xenoliths are not common in the volcanoclastic rocks and generally only occupy <5 vol.% of any given MVK. Unlike typical CRX, basement

xenoliths are always highly altered and typically show some degree of rounding due to resorption of the rock into the hot kimberlite magma. Highly altered basement xenoliths are seen as central kernels in magmaclasts within the MVK deposits. The more common basement xenoliths include carbonates, non-Karoo basalt and quartzites with lesser more exotic xenoliths, which are difficult to identify as they are highly altered. Figure 3.24 shows photomicrographs of the dominant basement xenolith types.

Carbonates

Carbonate xenoliths are the most common basement component in the MVK deposits. They may be either chert-rich or chert-poor (figure 3.24 a; chert-rich variety), which is an indication of their original lithologies. These xenoliths rarely exceed 10cm in diameter. Generally they are highly altered during their ascent in the hot kimberlite magma. This is particularly evident in certain MVK deposits relative to others, which may indicate that the xenoliths were held in the kimberlite magma at high temperatures for longer in certain MVKs relative to other carbonate xenoliths. Carbonate xenoliths are believed to have originated from the Malmani Subgroup of the Transvaal Supergroup. Chert-rich and chert-poor varieties may even be divided into the Monte Cristo and Oaktree formation within the Malmani Subgroup.

Basalt

Basalt also occurs in the basement rocks at the Voorspoed pipe. These rocks are easily distinguished from typical Karoo basalt by the highly altered nature (figure 3.24 d), which gives them a distinct green colour. In hand specimen the distinct green colour as well as the highly rounded nature of the rock makes it easily identified as a basement xenolith. The exact origin of the xenolith is debatable as no geochemical studies have been undertaken at the Voorspoed pipe. Basalt/andesitic basalt are present in both the Ventersdorp Supergroup and the Hekpoort formation (Transvaal Supergroup) in the basement rocks at Voorspoed. These green basalt xenoliths have been analysed geochemically at other kimberlites and they have been identified as Ventersdorp in origin (Hanson, 2006). Therefore it seems likely that this is the same case at the Voorspoed pipe and the basement basalt xenoliths are Ventersdorp in origin.

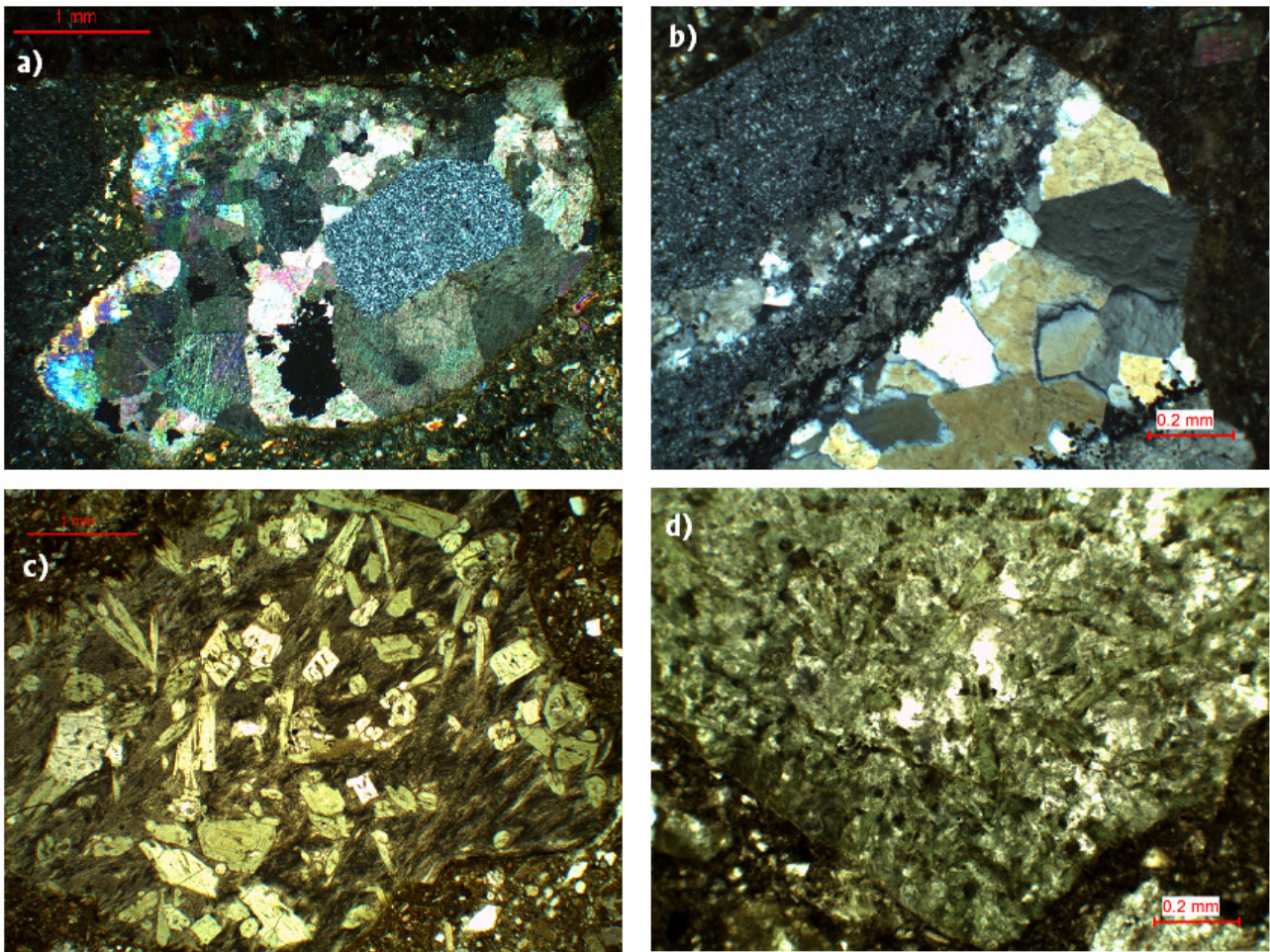


Figure 3.24 Photomicrographs of the typical basement xenoliths observed in the volcanoclastic infill. a) Chert-rich carbonate xenolith most likely from the Monte Cristo Formation of the Malmani Subgroup, Transvaal Supergroup. b) Quartzite xenolith. c) Exotic unidentified xenolith containing clinozoisite phenocrysts in a base of feldspar. d) Altered basement basalt xenolith from the Ventersdorp Supergroup. Note the distinct green colour relative to the basalt in figure 3.21.

Quartzite

Quartzite xenoliths are particularly difficult to identify in hand specimen as they are relatively uncommon. They are however easily identified in thin section (figure 3.24 b) and are never seen >2cm in size although larger xenoliths may be present. Quartzite occurs in both the Transvaal and Ventersdorp Supergroups and therefore it is difficult to pinpoint the origin of these xenoliths,

although it seems more likely they are from the Transvaal Supergroup as quartzite is more abundant.

3.2.5.3 Magmaclasts

Magmaclasts occur as two morphological varieties as well as two mineralogical varieties and range in size from 0.1mm to 12cm in size. Magmaclast proportions vary greatly through the MVK deposits from 20 vol. % up to 55 vol. %. Diopside phlogopite kimberlite is the most common variety observed with lesser melilite-bearing phlogopite kimberlite also observed. Magmaclasts also occur as two distinct morphological types, 1) spherical to ellipsoidal and 2) irregular/angular. Figure 3.25 shows photomicrographs of typical magmaclasts.

Mineralogy of the Magmaclasts

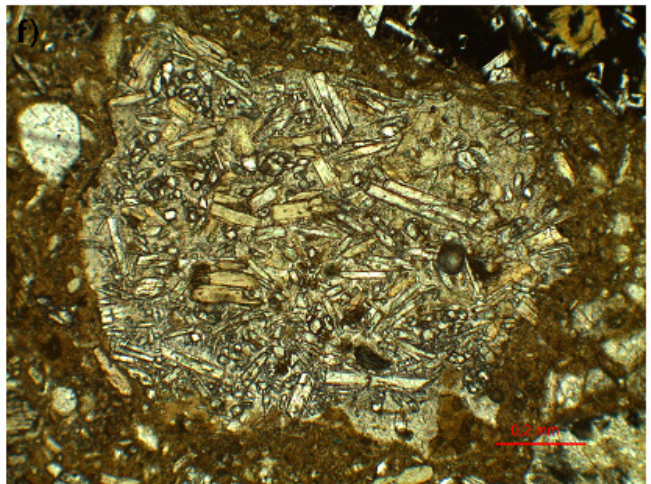
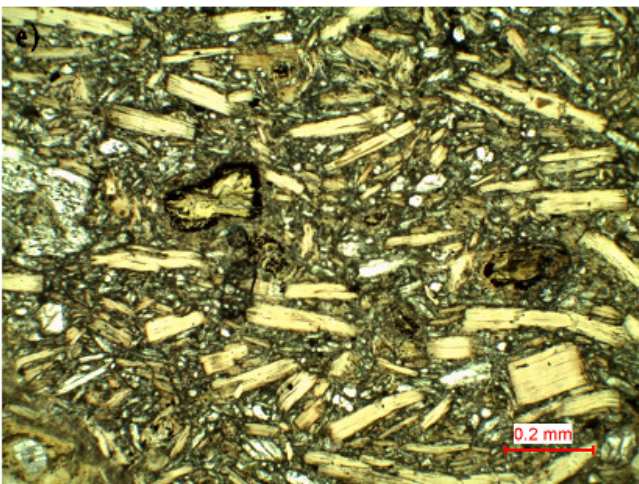
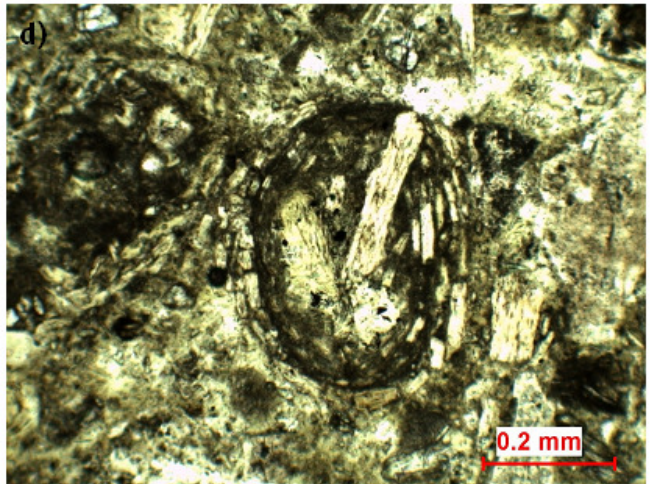
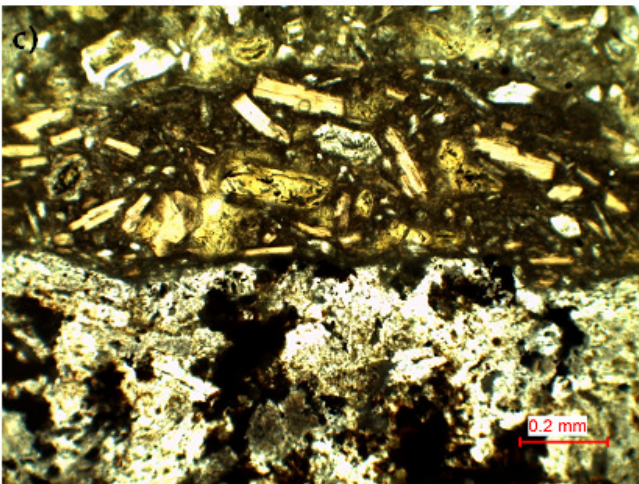
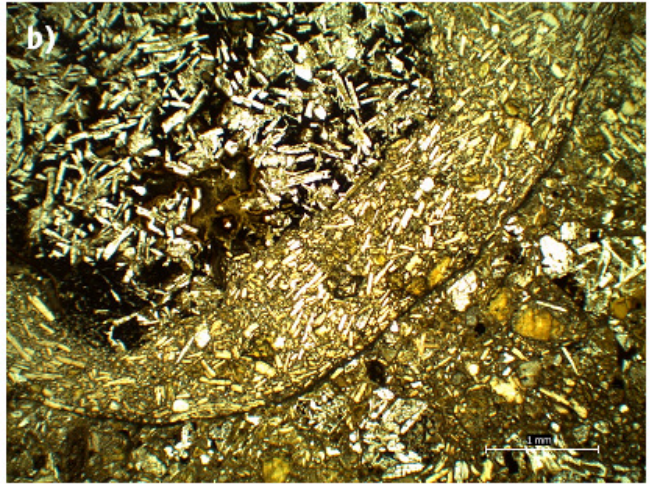
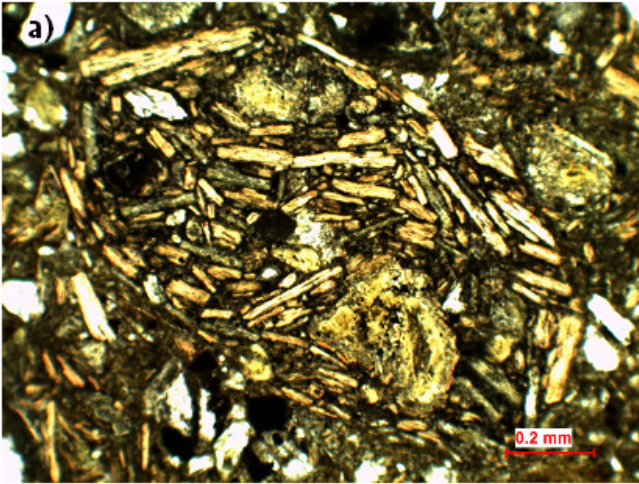
Diopside phlogopite kimberlite is the most abundant mineralogical variety and occurs throughout all the MVK types whereas melilite-bearing kimberlite (figure 3.25 a) magmaclasts are restricted to certain MVK types as discussed later. Phlogopite typically occurs as non-poikilitic light brown laths up to 0.5mm. Diopside occurs as colourless laths, which rarely exceed 0.2mm and are more commonly 0.1mm in length. Diopside contents vary from approximately 10 vol.% up to 70 vol.% within magmaclasts. Melilite is always highly altered by dominantly calcite with lesser serpentine and clay minerals also observed. Melilite occurs as typical laths up to 0.2mm in length and are clearly distinguished from diopside by the highly altered dirty appearance. Olivine is not always present within magmaclasts but where present they are always highly altered by clay minerals and calcite. Olivine generally is only present as phenocrysts, which rarely exceed 0.3mm and subhedral to euhedral habits are common. Olivine macrocrysts are rare but are present in the T2MVK only (as described in section 3.2.6.6). Olivine macrocrysts are similarly altered to the phenocrysts. Opaque minerals are rare throughout all the magmaclasts. The base of the magmaclasts is typically a mix of calcite and clay minerals with lesser serpentine also present. The base may be ultra fine grained and cryptocrystalline. In these cases it is difficult to identify the mineralogy of the base. Green aegirine is present within magmaclasts in extremely rare examples in a similar occurrence to that described for the hypabyssal sill/dike samples described in section 3.2.3.

Irregular/Angular Magmaclasts (Autolith sensu stricto)

Irregular type magmaclasts are abundant in all MVK varieties although less common than the spherical type magmaclast. Irregular type magmaclasts are typical angular and have shapes similar to CRX. They are very rarely altered, which is typical of CRX as well. Central kernels, which are common in the spherical variety, are never present in irregular type magmaclasts. Tangential alignment of grains is similarly never present. Melilite-bearing kimberlite has not been observed, as irregular magmaclasts and only diopside phlogopite kimberlite are present. The kimberlite typically is well crystallised and never has a cryptocrystalline base. The base is always easily identifiable as calcite and/or serpentine with lesser clay minerals also present. These magmaclasts look like typical hypabyssal kimberlite (HK) sensu stricto. These are typical autoliths sensu stricto. These magmaclasts are shown in figure 3.25 e and f.

Spherical Magmaclasts (Nucleated Magmaclast)

Spherical magmaclasts (figure 3.25 a-d) often contain central kernels of the larger components present in the magma prior to crystallisation, these include: country rock xenoliths (CRX) (basalt, shale), olivine macrocrysts and phenocrysts, phlogopite macrocrysts and phenocrysts, basement xenoliths, other mantle xenocrysts/xenoliths and in rare cases the irregular type magmaclasts form central kernels. These central kernels are typically altered and therefore must have been incorporated into the magma during the formation of the magmaclasts at high temperature. CRX such as basalt and shales are only seen altered within the magmaclasts and are not altered outside of magmaclasts, therefore they must be incorporated when the magma is still hot enough to alter them. Central kernels are not always present and in these cases tangential alignment of the grains is not observed whereas tangential alignment of the elongate grains is common where central kernels are present. This variety of magmaclast is commonly altered by calcite whereas the irregular variety is not altered. Both mineralogical types are observed as spherical magmaclasts. The base of this variety of magmaclasts varies from the irregular type in that it is often cryptocrystalline and dark brown ultra fine grained. This is particularly evident in the smaller (<0.5mm) clasts whereas the larger magmaclasts may look like typical hypabyssal kimberlite (HK). Spherical magmaclasts often shows features indicating that they crystallised in



See figure 3.25 caption overleaf

Figure 3.25 Photomicrographs of typical magmaclasts in the volcanoclastic infill. a) Oval shaped clast containing no central kernel. The kimberlite is composed of two highly clay mineralised olivine phenocrysts, one clear colourless diopside phenocryst, abundant phlogopite laths and highly altered melilite laths in a base of calcite and clay minerals. b) Large spherical autoliths with a Karoo basalt central kernel. Note the ultra fine grained dark rim around the autoliths. c) Medium power image showing a relatively altered central kernel of basalt with a mantle of kimberlite containing olivine, diopside and phlogopite set in a fine grained dark base. Note the fine grained nature of the base relative to photographs e) and f). d) Fine grained autolith showing clear tangential alignment of phlogopite grains around a central kernel of olivine and phlogopite phenocrysts. e) Medium power image of an autolith *sensu stricto* showing clear flow alignment of the phlogopite grains. Note the coarse grained nature of the base relative to photo c). f) Typical irregular shaped autolith *sensu stricto* with a well crystallised base component. The autolith is comprised of abundant clear diopside and phlogopite laths in a base of calcite and serpentine. Note the lack of olivine.

the same environment as HK. The presence of late stage aegirine and sanidine segregations indicates that the magmaclast must have crystallised at temperature similar to that of typical HK.

It is important to note some of the characteristic features described here, as these will be discussed later: Variation in morphology, Karoo basalt CRX as kernels in magmaclasts, the often highly altered nature of spherical magmaclasts but not the irregular type, often cryptocrystalline base of spherical magmaclasts compared to typical hypabyssal look to the irregular type and presence of aegirine and sanidine in late stage segregations

3.2.5.4 Interclast Material

The interclast material is highly fragmental with abundant xenocrysts of both lithic and juvenile origin. In most cases the base/cement of the rock is an ultra fine grained and turbid, although calcite and clay minerals are often coarse enough to identify. Microlitic clinopyroxene is very rare and is not pervasive such as in typical Class 1 kimberlites.

Xenocrysts

Xenocrysts originate from both lithic and juvenile sources. Lithic xenocrysts include basaltic clinopyroxene, plagioclase and quartz whereas juvenile xenocrysts include phlogopite, diopside and olivine. Garnet and other mantle derived xenocrysts are also present in rare cases. All

xenocrysts are <2mm in size and therefore can be classified as ash particles. Pyroxene originates from both basalt CRX and from the kimberlite. These are easily distinguished from one another on crystal habit. Basaltic clinopyroxene is generally blocky whereas kimberlitic diopside occurs as colourless laths. Basaltic clinopyroxene is far more abundant than juvenile diopside as xenocrysts. Plagioclase also comes from the disaggregation of basalt whereas quartz is slightly more difficult to pinpoint an origin. Two possibilities occur for quartz: 1) disaggregation of sandstone xenoliths or 2) the incorporation of sands from the surface. The complete lack of sandstone xenoliths within most of the MVK suggests the latter is more likely. Quartz xenocrysts in general are not as abundant as the other lithic xenocrysts, although they are particularly abundant in the bedded volcanoclastic kimberlite (BVK) sequences. Phlogopite is the most abundant juvenile xenocryst and never occurs >0.5mm. Olivine is always totally replaced by clay minerals with lesser calcite and is often difficult to distinguish from the base material.

Base/Cement

The base of the rock is often very difficult to identify as it is very fine grained. In general the base is dark brown and ultra fine grained. It is sometimes possible to identify calcite and clay minerals as the base components. This is again uncommon in typical South African diatreme facies Class 1 kimberlites as generally the base/interclast material is serpentine and microlitic clinopyroxene (Skinner, 2008). Ultra fine-grained grey patches are also present in rare examples. These may be microlitic clinopyroxene but this is very uncommon.

3.2.6 Petrographic Descriptions of representative samples of the Massive Volcanoclastic Kimberlite (MVK) varieties

The MVK at the Voorspoed pipe can be subdivided into at least nine characteristic varieties. Volumetrically the Type 1 MVKs are the most abundant. The MVKs can also be subdivided based on the distribution within the pipe. T1a, Soft and atypical MVKs are present only in the outer regions of the pipe whereas the T1b, T2 and intermediate MVKs are present only within the central region of the pipe. The distribution of the MVK units has been discussed in detail earlier. In this section the distinct MVK varieties are discussed. T1a, Soft and atypical MVKs are

described first followed by the MVKs present in the central region (T1b, T2 and intermediate). In terms of a mining perspective it is very important to note the variations in the MVK deposits, in particularly the kimberlite content within each MVK variety. Figure 3.26 shows photomicrographs of the individual MVK units. The distribution of these units is discussed in section 3.2.2 and borehole logs for the boreholes logged in this study are given in appendix 4. A cross section illustrating the distribution of the MVK units is given in figure 3.14. Refer to appendix 8 for a full list of the samples analysed. Modal analyses for the varies units are given in table 3.5.

3.2.6.1 Type 1 (a) Massive Volcaniclastic Kimberlite (T1aMVK) (Sample 9-145)

T1aMVK is volumetrically the most abundant MVK type within the Voorspoed pipe. The magmaclast content is slightly lower than the rest of the MVK varieties but the juvenile xenocryst population is substantially higher relative to the other MVK varieties. Therefore the rock still contains a relatively high proportion of kimberlite material. Basalt CRX content is high but low relative the T1bMVK. A photo of the T1a MVK is given in figure 3.13 (a). Modal analysis of a representative sample is given in table 3.5 below.

Country Rock Xenoliths (CRX)

Karoo type purple amygdaloidal basalt is the most abundant CRX present in this MVK (26% vol.%), which is the case in almost all the MVK varieties. Basement xenoliths (13 vol.%) and sedimentary Karoo xenoliths (5 vol. %) make up the rest of the xenolith population. Therefore 60% of the xenolith population is Karoo basalt; this is also a common characteristic throughout the Voorspoed pipe. Basalt xenoliths typically show some degree of alteration of the plagioclase to clay minerals. Plagioclase laths within different basalt CRX vary widely in grain size from 0.08-0.5mm in length, indicating that numerous basalt flows have be sampled during eruption. Sedimentary Karoo xenoliths include shales only and no sandstone CRX are observed. Basement xenoliths include carbonate, green shales and other highly altered exotic xenoliths, which could not be identified due to alteration. Xenoliths are typically <5cm in size but may occur up to 15-20cm.

Magmaclasts

The magmaclast content of this MVK is the lowest of all the MVK varieties at approximately 20 vol. %. Both mineralogical as well as both morphological varieties of magmaclasts are observed. Magmaclasts are generally fine-grained relative to other MVK varieties and are always <3mm. The dominant magmaclasts variety here is the spherical type, with lesser irregular type magmaclasts. Central kernels within the spherical magmaclasts are rare and where present are highly altered country rock or basement xenoliths. Phlogopite and melilite grains show tangential alignment around these central kernels when present. Olivine is very rarely seen as a central kernel and only phenocrysts are present. Flow alignment of the phlogopite grains is observed in the irregular type magmaclasts, which suggests that these magmaclasts are autoliths of sills or dikes. Another important feature to note, which is rare, is the presence of irregular type magmaclasts as kernels within the spherical magmaclasts, which further suggests that the irregular magmaclasts were formed before the spherical type.

Diopside phlogopite kimberlite is by far more abundant than melilite-bearing phlogopite kimberlite and consists of the typical phlogopite laths (<0.5mm), diopside laths (<0.2mm) and highly clay mineralised olivine phenocrysts (<0.2mm) set in a base, which differs between spherical and irregular type magmaclasts. Spherical magmaclasts typically have an ultra fine dark brown base, which is very difficult to identify due to the fine-grained nature. The irregular magmaclasts have a much coarser grained base, which is readily identified, as calcite with lesser clay minerals. Serpentine is not common. These irregular magmaclasts have a fresh, clean look whereas the spherical magmaclasts are altered by calcite and have a dirty appearance due to the ultra fine-grained nature of the base material. Melilite-bearing magmaclasts are particularly rare and only one example is present in this sample. The melilite grains are highly altered by clays and calcite and showed tangential alignment around a central kernel of a spherical type magmaclast. Melilite-bearing phlogopite kimberlite is not observed as irregular type magmaclasts.

Interclast Material

The interclast material is highly fragmental, which is characteristic of all the MVK varieties at the Voorspoed pipe. Abundant juvenile and lithic fragments are set in a base of ultra fine-grained

Table 3.5 Modal abundances of the major constituents for the MVK varieties at the Voorspoed pipe. (Sed: sedimentary; Mg.Clast: magmaclast; Ol. in: olivine within magmaclasts; Ol. out: olivine as xenocrysts; Kim: kimberlitic). Sample numbers for the modal analysis are given in the descriptions of the units in the text.

Sample	CRX			Mg.clast	Ol. in	Ol. out	Base	Xenocrysts	
	Basalt	Sed.	Other					Kim	Lithic
Type 1 (a)	26	5	12	20	1	5	17	6	8
Soft	24	3	6	23	4	4	20	6	10
Atyp.	9	19	10	20	0	1	27	6	8
Type 1 (b)	42	4	6	27	2	2	11	1	5
Interm	38	2	1	34	3	2	16	0	4
Type 2	18	7	4	43	8	3	13	1	3

dark brown material, which is dominantly clay minerals and calcite with lesser serpentine also present. Xenocrysts are particularly abundant in this MVK variety (19 vol.%). Lithic xenocrysts (8 vol. %) include basaltic clinopyroxene, plagioclase and very minor quartz. Juvenile xenocrysts (11 vol.%) include highly altered olivine xenocrysts (5 vol. %) and phlogopite xenocrysts (6 vol.%). Therefore although the magmaclast content is slightly lower than other MVK types, the juvenile xenocryst population is much higher and boosts the overall kimberlite content to 31 vol.%. Ultra fine grey patches are observed, which may be microlitic clinopyroxene but no distinct laths are present for accurate identification.

3.2.6.2 Soft Massive Volcaniclastic Kimberlite (sMVK) (Sample 7/1; Skinner collection)

The soft MVK is very similar to the T1a MVK in all respects except for the characteristic feature, which gives it the name “Soft”. This MVK appears to be more readily altered and therefore becomes soft. The core samples are crumbling and pitted. Apart from this distinct difference the general constituents of the rock are similar to T1aMVK. Basalt CRX content is 24 vol.%, magmaclast content is 23 vol. % and again the juvenile xenocrysts population is high (15

vol. %) relative to the other MVK types. Modal analysis for a representative sample is given on table 3.5. Olivine is particularly abundant as xenocrysts (9 vol. %). Therefore this unit is not described in great detail as the only difference compared to T1MVK is the soft nature of the rock. The exact reason for this is not well understood but may have something to do with the matrix of the rock, as it is very difficult to identify the base material due to the very fine-grained nature. Patches of ultra fine microlitic clinopyroxene are coarse enough to accurately identify but are incipient and very rare.

3.2.6.3 Atypical Massive Volcaniclastic Kimberlite (aMVK) (Sample 9-288)

As the name implies this MVK is not a typical MVK as described for the T1MVKs. The major difference is the interclast material, lower basalt CRX content and the large magmaclasts. The latter are much larger than typical T1MVK. The interclast material here is extremely fine grained and the base has not been identified due to the fine-grained nature. This MVK is only intersected in hole 9 as a small 7m thick unit at 280m depth, although it may extend deeper as the hole is inclined. This rock is much darker in hand specimen relative to the other MVKs. A core photo is given in figure 3.13 (c); microphotograph in figure 3.26 and modal analysis is given in table 3.5.

Country Rock and Basement Xenoliths (CRX)

The CRX population here is somewhat different to the bulk of the MVK in the Voorspoed pipe. Karoo basalt xenolith content is very low at 9 vol. %. Basalt xenoliths are however altered relative to the other MVKs. Xenoliths tend to be more local in origin. Karoo shales and basement xenoliths are the most abundant at 19 and 10 vol. % respectively. Therefore total xenolith content is 38 vol.%. The basement xenoliths all tend to be altered by carbonate to some degree. Basement xenoliths present include quartzite, basalt and carbonate with lesser highly altered more exotic xenoliths. In general all xenoliths are <1.5cm although they can reach up to 5cm in size.

Magmaclasts

Magmaclasts reach up to 1.4cm in size and are only represented by the spherical type; no irregular autoliths sensu stricto are present. The spherical magmaclasts sometimes have rough edges. Tangential alignment of the phlogopite grains is common in the smaller <1mm

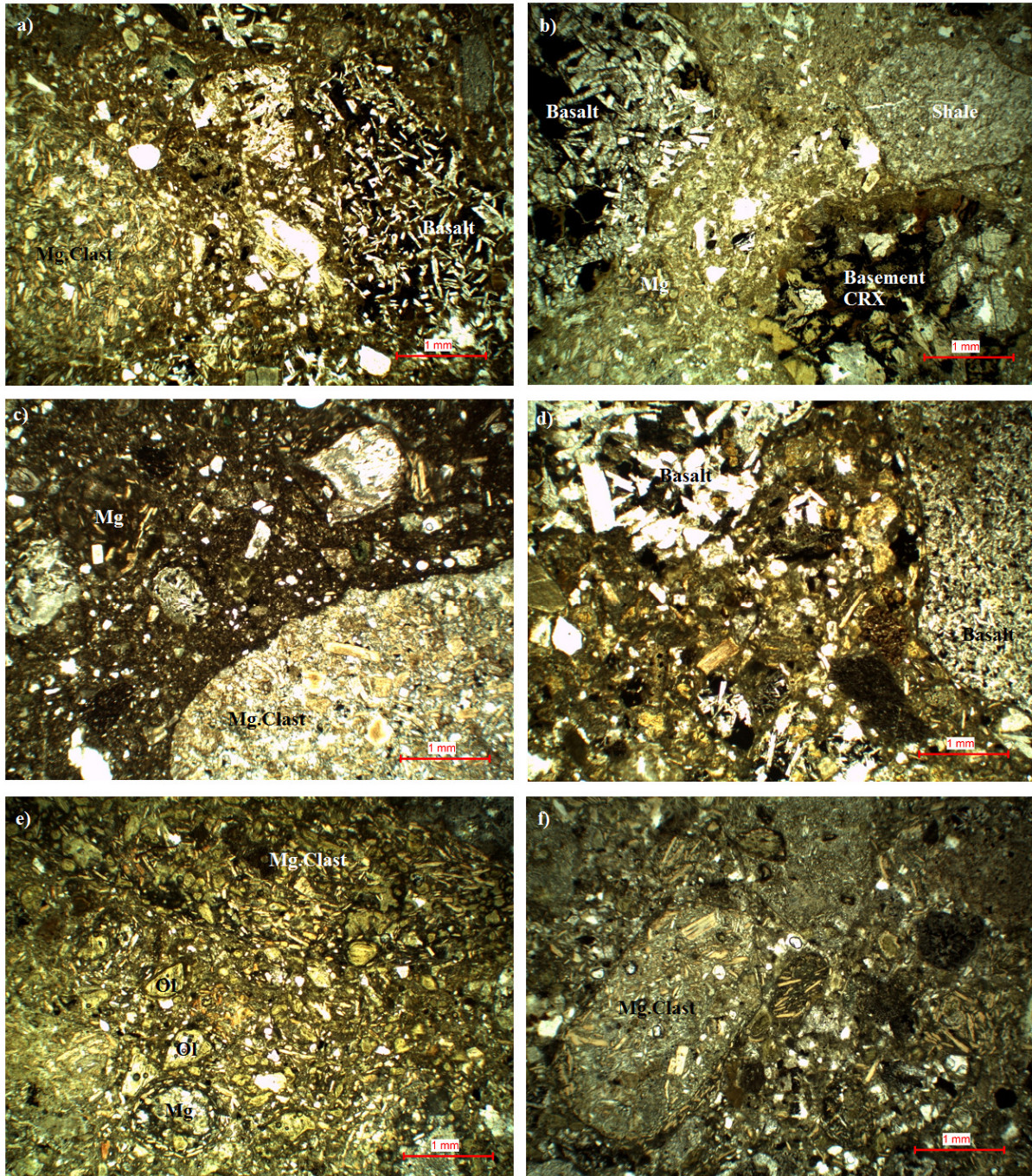


Figure 3.26 Photomicrographs of representative samples of each of the MVK varieties. a) Type 1a MVK. b) Soft MVK. c) Atypical MVK. d) Type 1b MVK. e) Type 2 MVK. f) Intermediate MVK. Note the higher kimberlite proportion in e) and f). Also note the slightly higher basalt CRX proportion in photo d) and the lack of basalt CRX in photo c).

magmaclasts, which contain central kernels. The central kernels are typically highly altered fragments, which could be olivine or basement xenoliths. Magmaclasts occupy 20 vol.% of the rock, which is typical for the T1A and Soft MVKs of the outer region at the Voorspoed pipe.

The magmaclasts are all diopside phlogopite kimberlite and no melilite-bearing equivalents are present. They are all highly carbonated. Phlogopite occurs as typical non-poikilitic laths up to 0.5mm in length. Diopside is commonly partially replaced by calcite and rarely exceeds 0.2mm. Fine-grained (<0.05mm) opaques are scattered evenly through the magmaclast. Olivine phenocrysts are rare and always totally replaced by calcite and clay minerals. The base of the magmaclasts is dominated by calcite and no serpentine is observed, very minor sanidine is tentatively identified but the highly altered nature of the rock makes it difficult to accurately identify the base mineralogy.

Interclast material

The interclast material of this rock is much darker in colour relative to the rest of the MVKs sampled. It is typically highly fragmental with abundant lithic and juvenile xenocrysts set in an ultra fine dark brown base. The juvenile xenocrysts are dominantly phlogopite and are <0.4mm in length. Olivine xenocrysts are rare and often difficult to identify as they are highly altered. The lithic xenocrysts are generally highly carbonated fragments of basement xenoliths with rare feldspars also present. The base of the rock is ultra fine grained. None of the usual constituents (calcite, clays, serpentine) could be identified due to the fine grained nature. The base however accounts for 27 vol. % of the rock, which is the highest for any of the MVK varieties.

3.2.6.4 Type 1 b Massive Volcaniclastic Kimberlite (T1bMVK) (Sample 3/1; Skinner collection)

This MVK unit is characterised by a very high proportion of Karoo basalt xenoliths relative to the initial eruption zone MVKs. The components of the rock are typical of the deposit in general.

Country Rock Xenoliths (CRX) and Basement Xenoliths

Basalt xenoliths are particularly abundant in this MVK variety (46 volume %) and accounts for 82% of the CRX population present in the MVK. The basalt CRX typically ranges in size from

5cm-0.2mm and commonly occurs as kernels to magmaclasts. Basalt blocks are observed up to 3m in the core. Other CRX observed in this sample include: quartzite, shale and other highly altered unidentified exotic basement xenoliths. CRX are generally unaltered except when occurring as kernels within magmaclasts where they are usually altered to a certain degree. Again it is important to note here that no sandstone xenoliths are observed in the rock.

Magmaclasts

Magmaclasts are not evident in hand specimen and are not seen larger than 5mm in thin section. Magmaclasts are generally 0.2-4mm in size. Olivine macrocrysts are absent and only rare magmaclasts contain olivine phenocryst kernels. Magmaclasts commonly do not contain a kernel but still have a typical spherical morphology. Ultra fine-grained dark isotropic rims are relatively common, which may represent a late stage gas condensate coating. Magmaclasts, while spherical in shape, commonly have slightly irregular margins. The ultra fine dark rims however have constant thickness regardless of any irregularities. Melilite-bearing phlogopite kimberlite magmaclasts are not observed in this sample and only diopside phlogopite kimberlite magmaclasts are present.

Olivine phenocrysts are common in the larger magmaclasts but macrocrysts are absent. CRX, in particular basalt CRX, form the kernels to the larger magmaclasts and tangential alignment of kimberlitic grains around the central kernel is common. Olivine phenocrysts rarely form the kernels in the finer magmaclasts. Olivine is always completely altered by clay minerals and lesser serpentine and opaques. Phlogopite occurs as typical phenocrysts (<0.4mm), which commonly show alignment around kernels. Diopside occurs as high birefringence and colourless laths, which occur in large proportions in relation to altered CRX kernels. Diopside shows the presence of green aegirine overgrowths, in rare cases. These evolved primary green pyroxenes occur in a similar setting to that described for the hypabyssal kimberlite (HK). Aegirine is observed protruding inward into colourless segregations, which is identified as sanidine in the fresher HK but here the sanidine is altered out by calcite and clay minerals. Euhedral opaques are scattered evenly throughout the magmaclasts. The base of the magmaclasts consists of very fine-

grained turbid brown calcite and lesser serpentine. Clay minerals may be present in the base but it is often difficult to distinguish them from altered olivine phenocrysts.

Interclast material

The interclast material of the MVK is fragmental and is comprised of comminuted lithic and juvenile xenocrysts (4 vol.%), which rarely exceed 0.4mm. Juvenile fragments include phlogopite and rare altered olivine. Lithic fragments include basaltic clinopyroxene, plagioclase and polycrystalline quartz. Free quartz grains are absent in this sample. The base of the MVK is ultra fine grained near isotropic turbid material. It is not possible to identify this material due to the fine-grained nature.

3.2.6.5 Intermediate Massive Volcaniclastic Kimberlite (intMVK) (Sample 3/3; Skinner collection)

As the name implies this MVK unit is intermediate in terms of the content of the dominant components between T1bMVK and T2MVK. The constituents of the MVK are similar to the T1bMVK and therefore will not be discussed in great detail again. Magmaclast (34 vol. %) and basalt CRX (38 vol. %) content is still relatively high compared to the T1a and soft MVKs and is therefore more similar to the T2MVK. Volumetrically this unit is not abundant and is always associated with the T2MVK. Intermediate MVK is very distinct in hand specimen as the colour is very similar to typical T2MVK but it does not contain the large magmaclasts and macrocrysts of olivine, which are the characteristic features of the T2MVK as discussed below. The intermediate MVK is finer grained than the T2MVK and generally the constituents are <2cm in size.

3.2.6.6 Type 2 Massive Volcaniclastic Kimberlite (T2MVK) (Sample 2/4; Skinner collection)

Type 2 MVK (T2MVK) contains the typical components observed in the MVKs as described above. These components include: CRX, basement xenoliths, magmaclasts and an interclast material. The interclast material can be further divided into xenocrysts and a cement component. The characteristic feature of this rock type is the abundant magmaclast content, which is



Figure 3.27 Core photo of the Type 2 MVK showing abundant highly altered carbonate xenoliths.

generally between 40-50 vol. % of the rock. Photographs from the core are given in figure 3.15 and modal analysis is given in table 3.5.

Country Rock Xenoliths (CRX) and Basement Xenoliths

CRX include abundant basalt and lesser shales, sandstone xenoliths are not observed. Basalt CRX account for 20 vol. % of the rock and 66% of the total CRX and basement xenolith population. The xenolith content in this MVK variety (30 volume %) is substantially lower than typical T1bMVK (50-60%). Basalt is comprised of varying proportions of blocky basaltic clinopyroxene, plagioclase laths and may or may not contain opaque glass and vesicles.

Plagioclase is commonly partly altered to clay minerals whereas basaltic clinopyroxene is fresh. Glass is commonly present but vesicles are not always present. Grain size varies between basalt xenoliths from 0.1mm to 0.5mm.

Basement xenoliths are always highly altered, which often makes identification impossible. The most abundant basement xenolith is carbonate. These carbonate xenoliths are typically highly altered in this MVK variety relative to other MVKs (figure 3.27). Therefore the temperature during deposition of this MVK may have been higher than other MVKs or the xenoliths were exposed to the hot magma prior to eruption in a hypabyssal environment for greater periods of time relative to the other MVKs.

Magmaclasts

Magmaclasts are typically spherical but may be elliptical when the central kernel is elongated. They typically vary between 0.1mm to 12cm in size. Almost all the magmaclasts observed are cored by olivine macrocrysts or phenocrysts. Olivine macrocrysts are relatively abundant in this MVK compared to other MVK varieties where olivine macrocrysts are absent. The finer magmaclasts (<1mm) typically have cryptocrystalline rims of ultra fine isotropic dark material with phlogopite laths aligned around a central olivine phenocryst kernel. The boundaries of the finer magmaclasts are very distinct relative the larger clasts, which do not contain a dark rim. The larger magmaclasts typically contain an olivine macrocryst kernel with lesser CRX and basement xenoliths also occurring as kernels. The mantles are crystalline with poorly developed tangential alignment and are very similar to typical HK. Magmaclasts typically occupy >40 vol. % in the T2MVK. Two mineralogical varieties of magmaclasts are observed in this MVK type, which includes diopside phlogopite kimberlite and melilite bearing kimberlite.

Melilite-bearing phlogopite kimberlite typically occurs as spherical magmaclasts, which rarely exceed 0.5mm. The magmaclasts typically contain a highly altered olivine phenocryst as a kernel. Olivine is always completely altered by light brown green clay minerals. Phlogopite and melilite are tangentially aligned around the central kernels. Melilite is always highly altered by an ultra fine, near isotropic material with low birefringence, which is identified as serpentine. Altered melilite laths occur up to 0.2mm in size but generally are approximately 0.1mm. Phlogopite occurs as light brown pleochroic and unzoned laths (up to 0.5mm), which are similarly aligned to the altered melilite. The base of the magmaclasts is ultra fine dark brown material, which is difficult to identify due to the fine-grained nature.

Diopside phlogopite kimberlite magmaclasts are far more abundant and occur up to 23mm in size, in this sample. Olivine macrocrysts or phenocrysts form kernels with lesser CRX and basement xenoliths also present as kernels. The magmaclasts containing olivine macrocryst kernels also contain abundant olivine phenocrysts in the surrounding kimberlitic mantle. Olivine macrocrysts are typically altered by calcite in the core of the macrocrysts and typical clay minerals around the calcite. The phenocrysts are completely altered by clay minerals with rare examples showing calcite cores. Diopside may be abundant to almost absent but is particularly abundant in magmaclasts with lithic xenolith kernels possibly as a result of the alteration of the xenolith and release of silica. Diopside is commonly altered by calcite and this may be the reason for low proportions in many magmaclasts. Phlogopite is present similarly to that described above for the melilite bearing magmaclasts. Tangential alignment of the phlogopite is well developed in the finer magmaclasts and poorly developed in the coarser grained magmaclasts. The base here is typically dominated by dirty colourless calcite and light brown green clay minerals

Interclast material

The interclast material has a fragmental texture with abundant juvenile and lithic xenocrysts set in an ultra fine brown base. Xenocrysts of both juvenile and lithic components are present (4 vol. %) and rarely exceed 0.2mm in size. Lithic xenocrysts include: quartz, blocky basaltic clinopyroxene and plagioclase. Juvenile xenocrysts include: altered olivine and phlogopite. The blocky basaltic clinopyroxene and plagioclase xenocrysts are a result of the disaggregation of basalt xenoliths whereas the origin of the quartz is somewhat more intriguing as there are no sandstone xenoliths observed in this rock. The base of the MVK is ultra fine dark brown turbid material. This material, where it can be identified, is an intergrowth of calcite and clay minerals.

Resedimented Volcaniclastic Kimberlite (RVK)

3.2.6.7 Fine-grained Bands (Sample 2-280)

These fine-grained bands occur as thin (<6cm) light brown–tan coloured horizontal to slightly inclined layers, which occur in the Central Eruption Zone (CEZ) only. The bands are characterised by a subtle normal grading. Very fine-grained beds are observed at both the top and

bottom of these bands and are generally <0.15mm thick with constituents <0.02mm in size. These bands are insignificant in terms of mining but are particularly important in understanding the genetic processes involved during the formation of the Voorspoed pipe. Photomicrographs of this unit are shown in figure 3.28 (a) and modal analysis is given in table 3.6.

Constituents

Country rock assemblages here are typical of the entire pipe with abundant basalt and shale with lesser basement carbonates also present. All constituents are <1mm in size. Magmaclasts are all the spherical variety and have the typical characteristics associated with this type of magmaclast. The interclast material is dominated by abundant juvenile xenocrysts of olivine and phlogopite. Lithic xenocrysts present include; plagioclase, microcline, basaltic clinopyroxene, quartz and carbonate. These xenocrysts are set in a base dominated by green brown clay minerals and lesser calcite.

3.2.6.8 Initial Eruption Zone (IEZ) Bedded Volcaniclastic Kimberlite (BVK) (Samples 10-90)

Country rock Xenoliths (CRX) and Basement Xenoliths

Numerous xenoliths are present, which include: basalt, shale, sandstone, carbonate and other more altered basement xenoliths. Xenoliths vary in size from <5cm at the base of the sequence to <2mm at the top of the graded sequence. Basement xenoliths are only present as kernels within magmaclasts and not as free xenoliths. Basalt xenoliths are very fresh indicated by the always unaltered plagioclase. Photomicrographs shown in figure 3.28 (c) and (d). Modal analysis of this sample is given in table 3.6.

Magmaclasts

Magmaclasts are relatively abundant and reach 1cm in size. Magmaclasts are typical spherical type, which often show a more elongated oval shape. Tangential alignment around central kernels is common where kernels are present. Central kernels are generally xenoliths in the larger magmaclasts and olivine or phlogopite phenocrysts in the smaller magmaclasts. The magmaclasts vary in size from <1cm at the base to <0.5mm at the top of the sequence.

Mineralogically they are typical diopside phlogopite kimberlite, melilite-bearing kimberlite is not observed. Irregular type magmaclasts are also present but not as common as the spherical variety.

Interclast Material

The interclast material contains abundant quartz xenocrysts, which may reach up to 1mm in size but are generally <0.25mm. Other xenocrysts include rare juvenile components of altered olivine and phlogopite and the more common lithic basaltic clinopyroxene and feldspar. The xenocrysts are set in a green brown base of clay minerals and lesser calcite.

3.2.6.9 Central Eruption Zone (CEZ) Bedded Volcaniclastic Kimberlite (BVK) (Sample 3-67)

Country Rock Xenoliths (CRX)

The dominant xenolith is typical basalt and lesser grey to black shales are also present. Rare dolomite and green basalt xenoliths are also observed. Xenoliths range in size from a maximum of 6cm at the base to mm scale at the top of the normally graded beds. Basalt xenoliths show alteration of the plagioclase grains and clinopyroxene is always fresh.

Magmaclasts

Magmaclasts are typically spherical to ellipsoidal but often have irregular margins. Mineralogically only diopside phlogopite kimberlite is observed. Olivine is always highly altered by clay minerals and lesser calcite. The base of the magmaclasts is typical calcite dominated with lesser clay minerals and rare serpentine. Central kernels are generally not present in the magmaclasts however rare cases are observed with highly altered xenoliths as kernels. Ultra fine dark grey rims are often present, which are also observed on the CRX. This may be microlitic clinopyroxene however it is too fine grained to identify. Magmaclasts are typically <4mm in size.

Interclast Material

The interclast material is slightly different from the IEZ BVK as no quartz xenocrysts are observed in this sample. Xenocrysts include olivine, phlogopite and lithic basaltic clinopyroxene,

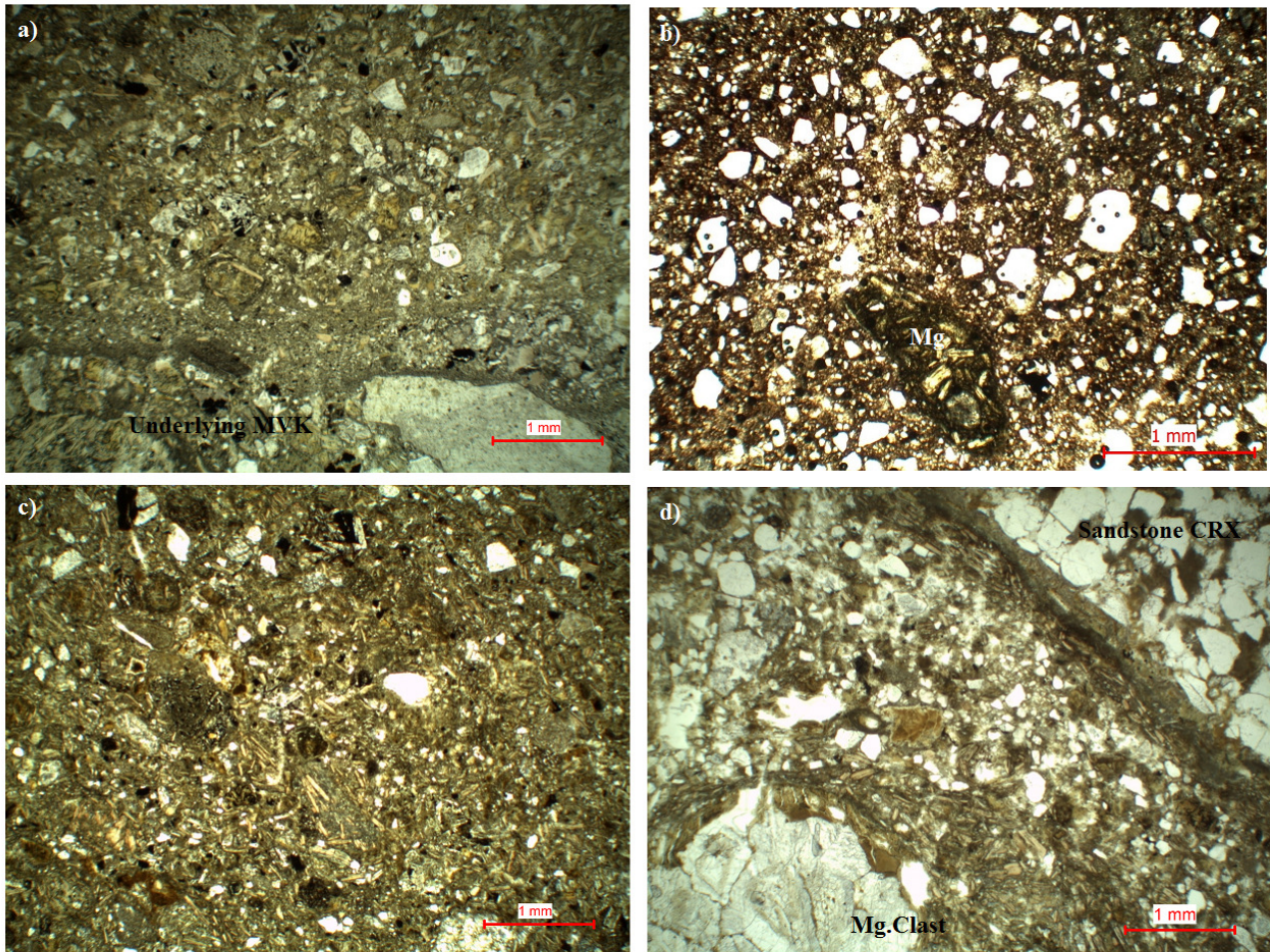


Figure 3.28 Photomicrographs of the resedimented volcaniclastic kimberlite infill. a) Low power image of the contact between typical MVK (bottom) and a fine grained RVK band (top) (Sample 2-280). b) RVK sample from the De Beers collection. Note the abundant quartz grains and rare kimberlite magmaclast (Sample location unknown). c) Fine grained top of a graded bed (Sample 10-90). d) Coarse grained equivalent to photo c) (Sample 10-90).

plagioclase. All xenocrysts are <0.2mm in size and rarely up to 0.3mm. The matrix of the rock is composed of ultra fine grained brown material made up of clay minerals and calcite.

3.2.6.10 Massive Volcaniclastic Basalt Breccia (MVBB) (Sample 10-36)

Country Rock Xenoliths (CRX) and Basement Xenoliths

As the name implies, this rock is dominated by basalt xenoliths (52 vol. %), although in other samples basalt may occur up to 70 vol.%. The basalt is very fresh and alteration is never observed (figure 3.29a-b), unlike the typical MVKs where plagioclase is often partly or wholly replaced by clay minerals or calcite. This variation in alteration is an important characteristic to note and will be discussed in greater detail later. Therefore these are typical Karoo type basalt xenoliths. Sedimentary xenoliths are also present in varying proportions (0-8 vol.%). Shales dominate the sedimentary xenoliths and rare sandstones are also observed. All xenoliths are typically <5cm in size, although rare examples are observed >1m. Basement xenoliths are not observed in any samples from the basalt breccia zones. Modal analysis of the sample is given in table 3.6.

Magmaclasts

Kimberlite contents are particularly low in this rock, always <4 vol.%. The magmaclasts observed are <3mm in size are the spherical variety, although they often show very irregular margins. The classification as a spherical type magmaclast is done on the presence of central kernels and tangential alignment, which is never present in typical irregular type magmaclasts. Only diopside phlogopite kimberlite is observed as magmaclasts.

Interclast Material

The interclast material consists of abundant lithic xenocrysts set in a base dominated by clay minerals. Juvenile xenocrysts are rare and always <1 vol.%. Lithic xenocrysts however are abundant (8 vol.%) and include: basaltic clinopyroxene, feldspars and quartz. Xenocrysts are <0.5mm in size. The basaltic clinopyroxene and plagioclase feldspar originate from the basalt whereas the quartz and other feldspars are more difficult to place as sandstone xenoliths are particularly rare in this rock type. Therefore it is more likely that a cover of sand was present at the surface during the incorporation on this rock, this will be discussed in greater detail later. In general the interclast material has a clastic look with abundant quartz xenocrysts.

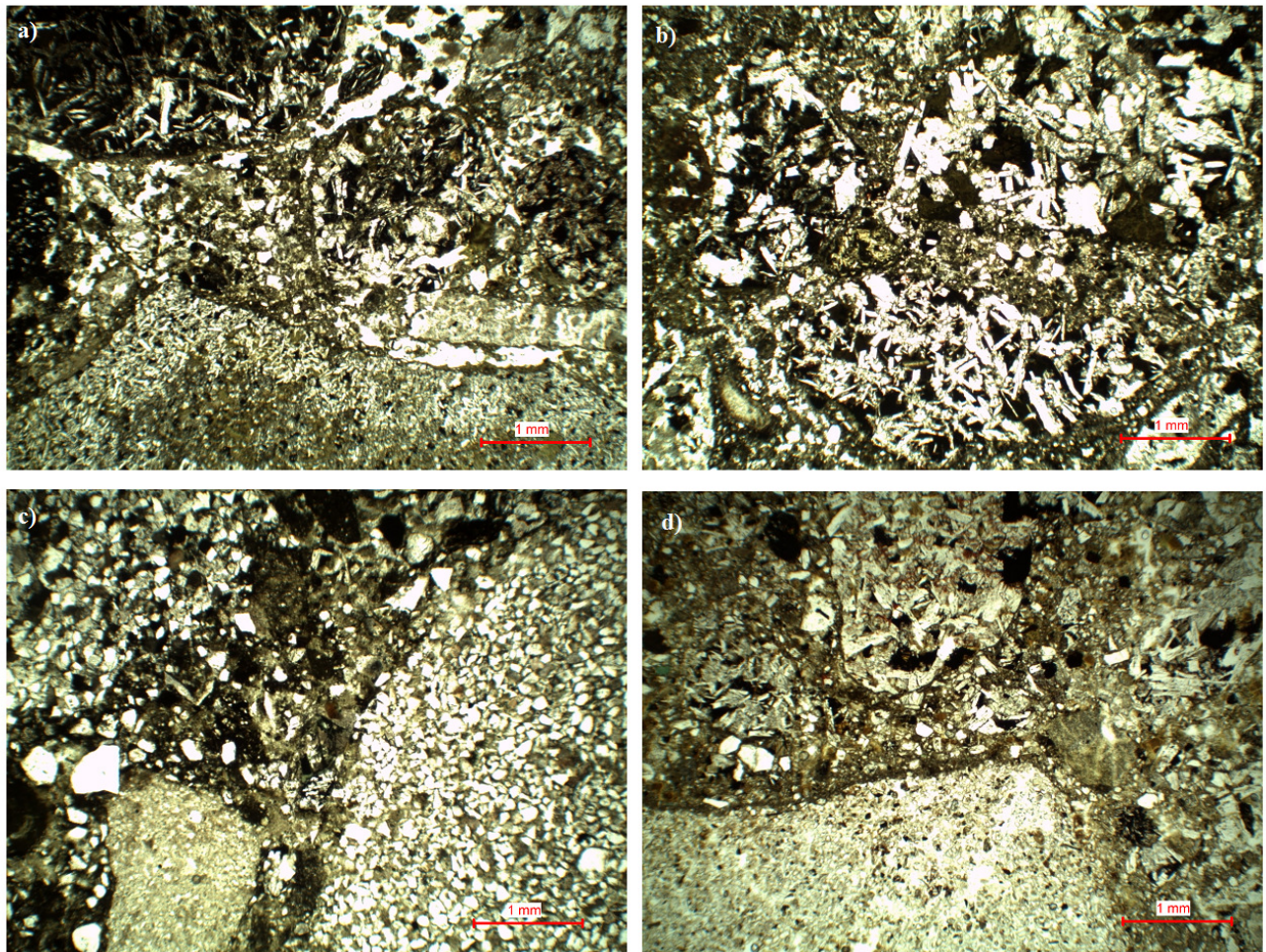


Figure 3.29 Photomicrographs of the massive volcaniclastic basalt and sandstone breccias. a) and b) show the basalt breccia (Sample 10-36). c) and d) show the sandstone breccia (Sample 8/1; Skinner collection). Note the still relatively abundant basalt xenoliths within the sandstone breccia.

3.2.6.11 Massive Volcaniclastic Sandstone Breccia (MVSb) (Sample 8/1)

Country Rock Xenoliths (CRX) and Basement Xenoliths

This rock is characterised by the relatively high abundance of sandstone xenoliths (figure 3.29c-d), which are very rare constituents at the Voorspoed pipe. This particular sample is very rich in sandstone xenoliths (73 vol. %) but this is not always the case. Sandstone contents range

Table 3.6 Modal abundances for the resedimented VK and the MVBB/MVSB kimberlites. (See table 3.5 for definition of acronyms)

Sample	CRX			Mg.clast	Ol. in	Ol. out	Matrix	Xenocrysts	
	Basalt	Sed.	Other					Kim	Lithic
MVBB	52	9	0	2	0	0	29	0	8
MVSB	0	73	0	0	0	0	19	0	8
Grade. (f)	14	13	1	14	1	13	18	9	17
Seq. (c)	7	14	3	34	5	0	19	3	15
(RVK)									
F.g. Band	15	10	1	12	0	17	15	11	19
(RVK)									

between 40-75 vol. %. Basalt xenoliths may also become relatively abundant (up to 30 vol. %) but may also be entirely absent as is the case in this sample. Sandstone and basalt xenoliths are never altered, similar to the basalt breccia. Basement xenoliths are again absent from this rock type. Modal analysis of this sample is given in table 3.6.

Magmaclasts

The kimberlite content again is very low (<3 vol.%) in this rock type. The magmaclasts show features similar to those described above for the basalt breccia and therefore will not be discussed again.

Interclast Material

The interclast material is also very similar to the basalt breccia and therefore will not be described again. It is particularly important to recognise these rocks during mining as they should likely be treated as waste.

3.3 Besterskraal North Kimberlite pipe

3.3.1 Introduction

The Besterskraal North kimberlite has previously been classified as a highly evolved sanidine and K-richterite bearing Group II kimberlite (Mitchell, 1995). Mitchell (1995) describes the mineralogy of the kimberlite in great detail. The findings are confirmed here with the further identification of three distinct HK varieties. No other literature on this kimberlite is available. K-richterite occurs up to 15% in type 1 and 2 whereas it is absent from the country rock xenolith (CRX) -rich type hypabyssal kimberlite (HK). Sanidine is present in all the HK types but occurs only in trace amounts in type 2 HK. All the HK types are characterised by a high proportion of diopside, which is characteristic of evolved Group II kimberlites (Mitchell, 1995). It is important to note that calcite is not as abundant here as seen at the Lace kimberlite. Volcaniclastic kimberlite is also present and is typical of the cluster as a whole. All samples analysed come from the De Beers archives.

3.3.2 Hypabyssal Kimberlite (HK)

The HK rocks here can be classified into three distinct types. These observations are made on a limited number of thin sections available and therefore further sampling is required to determine whether there are more than three types of HK. These types are 1) Aphanitic Type 1; 2) Aphanitic Type 2 and 3) CRX-rich. These distinct types are described below.

Type 1 Hypabyssal Kimberlite (HK) (Sample K5/34) (figure 3.30) is characterised by a high phlogopite content, low olivine content and fairly equal proportions of diopside, K-richterite and sanidine as shown in table 3.8. Olivine occurs only as phenocrysts (0.15-0.4mm) and is always highly altered. This makes the identification of olivine in Type 1 HK very difficult. The olivine is altered to serpentine and/or clay minerals and is resorbed not euhedral. The characteristic feature, which helps in identification of the olivine, is the rim of phlogopite microphenocrysts, which replaces the olivine. This is a common characteristic of the more evolved Group II kimberlites (Mitchell, 1995). This feature aids in identification but the olivine content may still be under counted due to the highly altered nature.

Table 3.8. Modal analysis results for the characteristic Besterskraal North HK types. Results given as percentage abundance of total rock volume. Samples are from the De Beers collection and locations within the pipe are unknown.

	Type 1		CRX-rich			Type 2
	34	35	30	32c	31	9
Olivine	4.6	3.8	12.6	13.6	13.2	25.2
Phlogopite	38.8	40.8	22.6	22.8	20.8	20.4
Diopside	14.2	17.6	14	19.2	22	25.2
K-Richterite	15.2	15	0	0	0	11.4
Sanidine	14	15.2	1.6	1.2	1.2	10
Melilite	0	0	0	0	0	0.8
Spinel	0	0	0.2	0.4	0.4	1.2
Perovskite	0	0	0	0	0	0.8
Leucite	0	0	3.2	0	0	0
Calcite	0	0	0.4	1.2	1.2	3.4
Serpentine	3.6	2	7.6	8	13.2	2
Clay min.	6.8	3.6	0	0	0	0
CRX	0	0	36.6	33.6	26.4	0

Phlogopite proportions as seen in table 3.8 are high relative to the other HK types. Phlogopite occurs as both phenocrysts (0.3-1mm) and microphenocrysts (<0.1mm). Phenocrysts show a characteristic zoning with clear to pale brown cores and dark red/brown tetraferriphlogopite rims. The phlogopite is unlike the highly poikilitic phlogopite at Lace. The Besterskraal North type 1 HK phlogopite is not poikilitic. This may be as a result of the lower opaque mineral content as well as the lack of melilite and monticellite crystallising as earlier mineral phases. Microphenocrysts are characterised by the lack of zoning, blocky crystals and dark red/brown colour. They are interpreted to represent similar tetraferriphlogopite compositions to the rims on the phenocryst population.

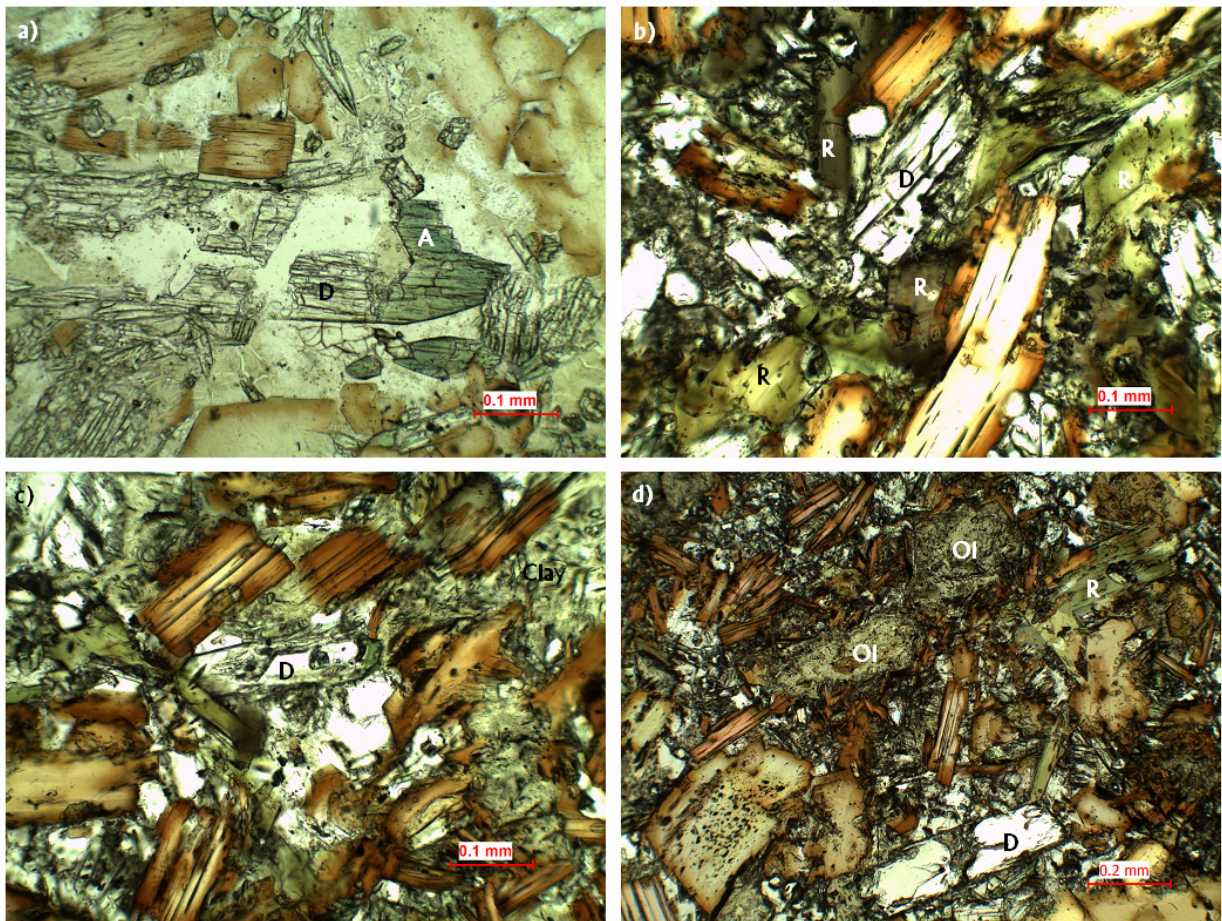


Figure 3.30 Photomicrographs of the Type 1 hypabyssal kimberlite from samples K5/34 and K5/35. a) Coarse diopside (D) with distinct green overgrowth of aegirine (A). b) Medium power image showing diopside (D) and K-richterite (R). Note the distinct pleochroism of the K-richterite from brown to green. c) Photo showing finer grained diopside with a green overgrowth of aegirine in a base of clay minerals (Clay). Note the non-poikilitic phlogopite laths, which show evolution to tetraferriphlogopite. d) Highly clay mineralised olivine (Ol) phenocrysts surrounded by fine grained phlogopite laths. Note also the K-richterite (R) and diopside (D).

Diopside is particularly abundant in all the HK facies rocks. Diopside occurs, in Type 1, as both phenocrysts (0.1-0.5mm) and microphenocrysts (<0.1mm) as colourless, high relief, high birefringence laths with inclined extinction. These laths commonly show the development of pale green rims, which have extinction angles closer to 0. These green rims are much brighter in colour and show no pleochroism. They are therefore interpreted to be aegirine similarly to Voorspoed. The evolution of diopside to Na, Fe rich mantles of aegirine is common in evolved

kimberlites (Mitchell, 1995). Figure 3.30 (a and c) shows the bright green rim around a colourless diopside lath.

K-richterite occurs as phenocryst (0.2mm) laths and anhedral plates. K-richterite is characterised by the distinct brown/green pleochroism and two cleavages ($60^{\circ}/120^{\circ}$). The cleavage is not common but evident in rare examples. This mineral is extremely rare in any kimberlites but here represents up to 15% of the rock. This mineral indicates a much more evolved type of Group II kimberlite with a lamproitic nature.

Sanidine is the dominant base component occurring as anhedral plates and is also a very rare mineral in kimberlites, which indicates a more potassium-rich evolved kimberlite. Other base components include serpentine and clay minerals. There is a distinct lack of calcite relative to the Lace kimberlite. Clay minerals are believed to form as a result of the alteration of sanidine in the base. Very rare perovskite microphenocrysts are also observed.

This rock is classified as a hypabassal, aphanitic, sanidine-bearing, K-richterite, diopside, phlogopite kimberlite.

Type 2 Hypabyssal Kimberlite (HK) (Sample K5/9) (figure 3.31) is characterised by increased olivine, the lack of phlogopite phenocrysts and calcite is the dominant base component. Olivine occurs as fresh euhedral phenocrysts up to 2mm in size. Generally the grains are <0.6mm. The larger grains are interpreted as phenocrysts as they are euhedral. Minor alteration to serpentine occurs along the rims of the larger grains while the smaller grains (0.1-0.2mm) show higher degrees of alteration with fresh cores. Olivine often is rimmed by microphenocryst phlogopite, which is common in this kimberlite.

Phlogopite occurs as microphenocrysts (0.01mm) and groundmass poikilitic plates (2mm). Phlogopite plates are yellow/red/brown in colour and show distinct zoning to dark red/brown mantles. This indicates a highly evolved tetraferriphlogopite mantle, which is consistent with this kimberlite. Microphenocrysts occur as fine blocky crystals often surrounding the olivine grains. Microphenocrysts are dark red/brown in colour similar to the mantles of the phlogopite plates.

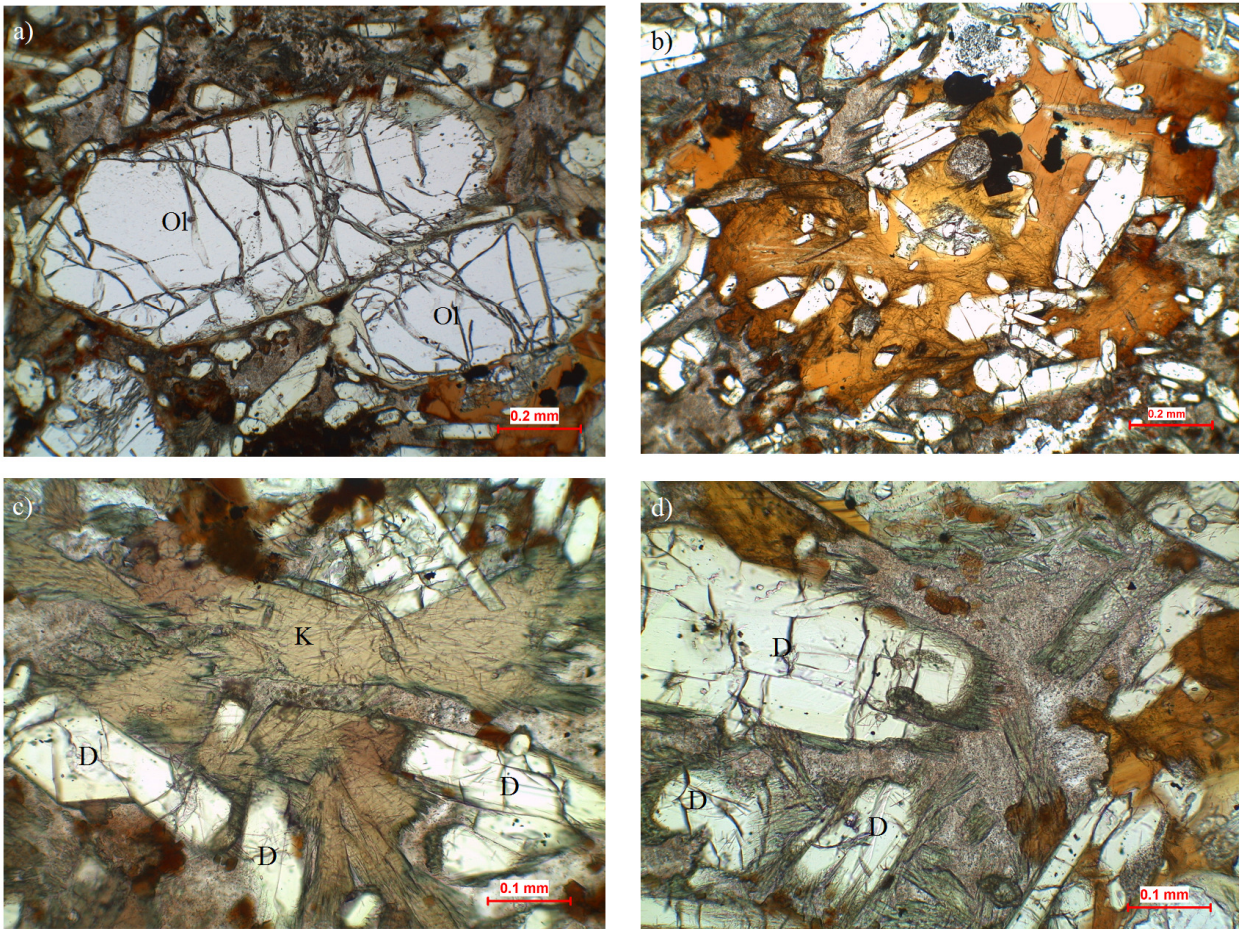


Figure 3.31 Photomicrographs of the Type 2 hypabyssal kimberlite from sample K5/9. a) Very fresh olivine (Ol) phenocrysts. b) Dark red brown highly poikilitic phlogopite plate. c) Light green brown K-richterite (K) with colourless diopside (D). Note the feathery green margins. d) Diopside (D) phenocrysts with feathery overgrowths, which look more similar to the margins on the K-richterite in photo (c).

Diopside is very abundant (25%) in the rock. The grains are typical colourless laths and range in size from 0.07-1mm, therefore are classified as both phenocrysts and microphenocrysts. Diopside often shows resorption features such as embayment structures. Green/brown pleochroic rims are evident around most diopside. In this case the rims look more like the K-richterite in the rock and not like the bright green rims described above for type 1 HK. Detailed microprobe work needs to be done to identify this mineral although it seems more likely that the mineral is aegirine as it is common in the other HK varieties.

K-richterite occurs in a different fashion to that described in type 1 HK. The grains are anhedral green/brown pleochroic plates (<0.5mm). K-richterite is also seen surrounding olivine grains similarly to microphenocryst phlogopite and shows some zoning with yellow/brown/green cores with slightly darker green mantle. The mantles have very irregular feathery boundaries. Detailed microprobe analyses of these grains needs to be done in order to determine the variation of core to mantle compositions. The proportion of diopside to K-richterite is much greater in the type 2 HK. Therefore the magma may have been at a higher temperature (diopside crystallisation) for a greater period of time. This is also evident from the generally coarser grained nature of the rock.

Opaque spinels occur in smaller amounts and often as inclusions within diopside. These grains are anhedral and 0.06mm in size. Hollandite is also present as fine radiating clusters of acicular opaque minerals. Perovskite is present as groundmass anhedral grains (+/- 0.2mm). Melilite occurs only in the type 2 HK as highly altered laths, which are preserved as inclusions in phlogopite plates, which are always altered by calcite.

The base of the rock is dominated by calcite with lesser proportions of serpentine and sanidine. Calcite is rare in the type 1 and CRX-rich HK. The lack of serpentine in the base is consistent with the fresh nature of the olivine and indicates that free H₂O was not abundant in the magma. Sanidine occurs in smaller proportions relative to type 1 HK. This may be as a result of alteration of the sanidine by calcite in the base. From the abundance of diopside, tetraferriphlogopite, sanidine and K-richterite this rock can be classified as a highly evolved Group II hypabassal, aphanitic, K-richterite-bearing, phlogopite, diopside kimberlite.

Country Rock Xenolith (CRX) -rich Hypabyssal Kimberlite (HK) (Samples K5/30-32) (figure 3.32) is characterised by the high proportion of CRX. CRX contents range from 26% to 36% and are all highly kimberlitised. Dolerite is the only identifiable CRX while possible sandstone and shale are tentatively identified as they are highly altered. This rock is also

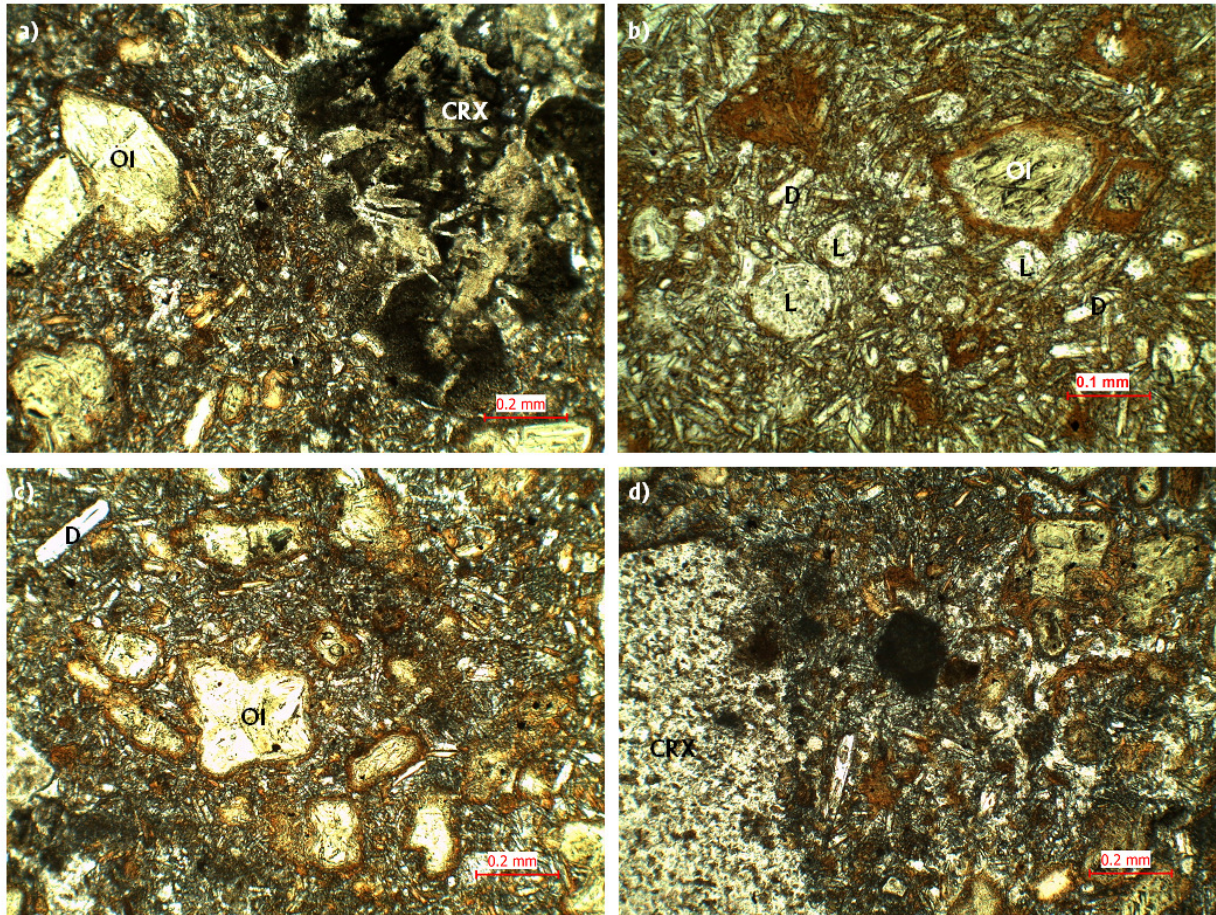


Figure 3.32 Photomicrographs of the CRX-rich hypabyssal kimberlite from sample K5/30-32. a) Large CRX surrounded by kimberlite with euhedral clay mineralised olivine (Ol) phenocrysts with abundant fine grained diopside. b) Photo showing clay mineralised olivine (Ol) phenocryst with distinct rim of fine grained phlogopite and distinct colourless rounded and highly altered leucite (L) phenocrysts. Note the leucite does not have rims of phlogopite. Fine grained diopside (D) is also particularly abundant. c) Typical example of the CRX-rich variety with abundant clay mineralised olivine (Ol) with rims of fine grained phlogopite and abundant fine grained diopside laths. d) Typical example with a large CRX present.

characterised by the absence of K-richterite and the presence of leucite. Olivine is highly altered by serpentine and occurs as euhedral relict phenocrysts (0.1-0.5mm) and microphenocrysts (<0.1mm). Olivine is also characterised by a rim of microphenocryst phlogopite, which aids in the identification of olivine.

Phlogopite occurs only as microphenocrysts (<0.1mm) and is seen rarely as 0.15mm grains. Phlogopite is dark red/brown in colour and represents evolved tetraferriphlogopite. The larger grains show some zonation with colourless cores and dark red/brown rims.

Diopside occurs as phenocrysts (0.1-0.25mm) and microphenocrysts (<0.1mm). Diopside is abundant (up to 22%) and occurs in high concentrations in spatial relation to altered CRX. No green aegirine overgrowths are observed in this rock type. The diopside may be autometasomatic, which would form in a similar way to that at the Lace transitional zone. However there is a lack of sufficient samples and no locations within the pipe of the samples are known. Therefore it is difficult to classify this rock as it could be either hypabyssal with primary diopside or transitional with autometasomatic diopside.

Leucite occurs as microphenocrysts (0.08-0.1mm) rounded and partially altered grains. This mineral is particularly distinct in sample K5-30a in the De Beers collection, as shown in figure 3.32 (b) and further demonstrates the highly evolved nature of the Besterskraal kimberlite. Leucite is easily identified from olivine as they do not contain a rim of phlogopite whereas the olivine is characterised by a rim of fine-grained phlogopite.

Opaque minerals are scattered throughout but are rare relative to the Lace kimberlite. The base consists of sanidine, serpentine and clay minerals. Clay minerals are thought to be the product of the alteration of sanidine. The base occupies far less proportions of the rock due to the high abundance of fine-grained diopside throughout the rock.

Apart from the olivine this rock is fine grained relative to type 1 and type 2 HK and is characterised by a high abundance of CRX. Therefore this rock possibly occurs toward the edge of the intrusions where CRX may be incorporated as well as cooling quicker producing the fine-grained matrix. This rock is classified as a hypabyssal, aphanitic, CRX-rich, diopside, phlogopite kimberlite.

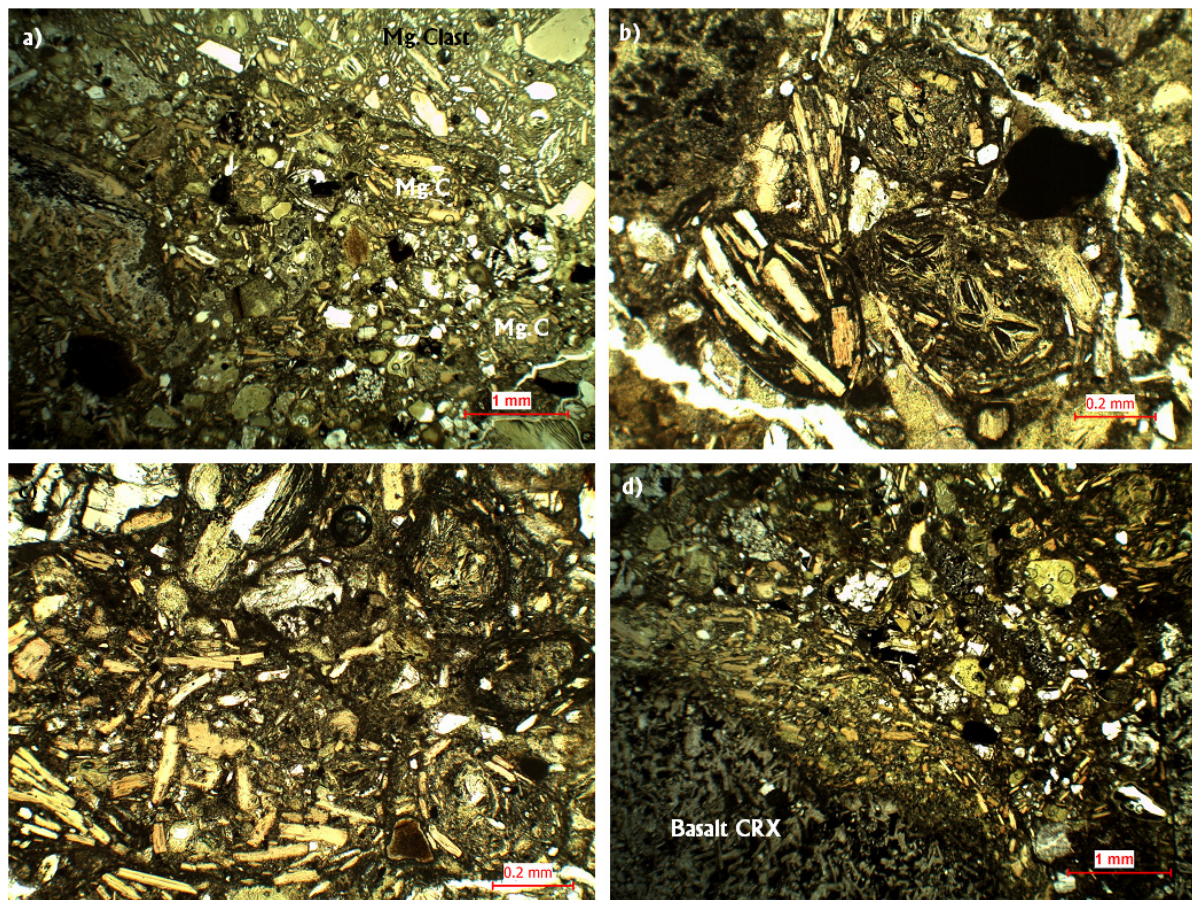


Figure 3.33 Photomicrographs of the volcaniclastic kimberlite at the Besterskraal kimberlite. a) Low power image showing the fragmental nature of the interclast material. Note the presence of two magmaclasts (mg.clast). b) Typical spherical magmaclasts. c) Typical magmaclasts. d) Basalt CRX as a central kernel in a relatively large magmaclasts.

3.3.3 Massive Volcaniclastic Kimberlite (MVK)

Only one sample of MVK from the Besterskraal North MVK was available (figure 3.33) and therefore the following is a description of this thin section. The rock consists of four components: 1) magmaclasts, 2) basalt CRX, 3) sedimentary CRX and 4) interclast material.

The magmaclasts range from 10mm to 0.2mm in size and are characterised by a thin rim of grey optically irresolvable material, which may be microlitic diopside. This rim is not well developed and is absent in many cases. They most commonly form typical spherical shapes similar to those described at the Voorspoed pipe, although irregular autoliths *sensu stricto* are also present. The

magmaclasts contain phenocrysts of olivine, phlogopite, diopside, with scattered opaques in a base of serpentine.

Magmaclasts comprise 40% of the rock. On rare occasions magmaclasts are seen within magmaclasts as central kernels. Basalt CRX are observed as kernels within magmaclasts, which is a common feature at the Voorspoed pipe and therefore the MVK at Besterskraal may have formed in a similar process.

Basalt CRX (29%) are more abundant than the sedimentary CRX (5%), which includes sandstone and fine-grained shale. The matrix is composed of commuted lithic and kimberlitic fragments in a base of serpentine, clay minerals and calcite. Xenocrysts of kimberlitic material are common whereas quartz xenocrysts are rare. The bulk of the lithic xenocrysts are derived from the abundant basalt CRX.

The interclast material of the rock is similar to that described for Lace. It is comprised of comminuted juvenile and lithic fragments set in an ultra fine base of clay minerals. This matrix is typical of the MVKs for the whole cluster and is atypical for South African kimberlites. This rock is classified as CRX-rich MVK and is very similar to the Type 2 magmaclast-rich MVK described from Voorspoed.

4. Mineral Composition and Bulk Rock Geochemistry of Selected Voorspoed and Lace Hypabyssal Kimberlite Samples

4.1 Introduction

The following chapter contains two sections: 1) mineral composition and 2) bulk rock geochemistry. The original analytical work was done to describe the evolution between the Voorspoed and Lace kimberlites, which is clearly evident petrographically. Due to the lack of hypabyssal kimberlite available for bulk rock analysis at Voorspoed, mineral composition was done to highlight the evolution of the magma. This work at Voorspoed is concentrated on the evolution of the pyroxene compositions from the primary diopside to late stage aegirine. Primary diopside composition does not vary indicating that there is no change in magma composition during early crystallisation of the magma. A clear trend of increasing Na₂O and FeO is observed with subsequent depletion in MgO and CaO in the residual fluid is indicated by the changing aegirine compositions. Aegirine is an indicator of evolved Group II kimberlites (Mitchell, 1995) and confirms initial petrographic analysis. However the Voorspoed pipe does not contain K-richterite, which is an indicator of the highly evolved end member. Therefore the Voorspoed pipe magma is intermediate in terms of its evolution. The compositions of the primary diopside and aegirine are compared with compositional data for microlitic clinopyroxene from Skinner and Scott (1979), Mitchell et al. (2009) and from Lace, this study. Microlitic clinopyroxene compositions are found to be very similar to typical primary diopside at the Voorspoed pipe.

Bulk rock geochemistry is done on the Lace kimberlite due to the availability of samples. The trends observed indicate crustal contamination has affected many of the samples. Fractional crystallisation is also observed from trends showing a decrease in Ni and MgO, which is likely a result of the fractionation of olivine from the magma. The most important trend observed is in the uncontaminated samples. These samples show very subtle trends, which have been petrographically linked to the occurrence and abundance of microlitic clinopyroxene in the samples. Geochemical trends from the Lace hypabyssal transitional kimberlite (HKt) have been compared with data from Clement (1982) for the Wesselton and Dutoitspan kimberlites, which indicates that CO₂ degassing plays a major role in the evolution of the magma.

This chapter has evolved from originally simply describing the evolution of the kimberlite magma to linking certain geochemical variations and possibly mineral compositional data to microlitic clinopyroxene paragenesis and composition. The complete absence of microlitic clinopyroxene at the Voorspoed pipe may be linked to the composition of the late stage residual fluids, which is indicated by the presence of aegirine and sanidine crystallising late in the evolution of the magma. The occurrence of microlitic clinopyroxene at the Lace HKt is discussed in detail and comparison of the geochemical data from Clement (1982) an interpretation is given as to the formation of the microlitic clinopyroxene. However most of this chapter is dedicated to describing mineral compositions and paragenesis at the Voorspoed pipe and outlining geochemical trends at the Lace pipe to show the variation in the evolution of the magma.

4.1.1 Evolution of Group II Kimberlite Magma

Group II kimberlites are unique to South Africa and show a relatively broad range in mineralogy and geochemistry. Two end members are identified: 1) unevolved and 2) evolved types (Mitchell, 1995) with a gradational variation between the end members. The majority of the diamondiferous Group II kimberlites are the unevolved types and therefore most of the analytical work has been concentrated on these kimberlites. As a consequence relatively little work has been done on evolved Group II kimberlites and the only substantial available analytical work is from Mitchell (1995). The nature of the evolution of the magma can be identified petrographically as well as by bulk rock analysis. Petrographically the unevolved end member is similar to typical Group I kimberlite mineralogy but contains high proportions of phlogopite whereas the evolved Group II mineralogy is distinctly different. Minerals indicating an evolved Group II kimberlite include: K-richterite, aegirine, sanidine, leucite and high abundances of primary diopside (Mitchell, 1995). Primary diopside is the first indication of evolution of the magma as it indicates an increase in silica content of the magma. Furthermore phlogopite compositions vary but detailed microprobe analysis is required to identify these variations. The geochemistry of evolved Group II kimberlite is also very distinct. Unevolved Group II kimberlites are essentially mixtures of olivine, phlogopite, carbonate and apatite (Mitchell, 1995). The majority of olivine are mantle-derived xenocrysts and therefore are contaminants in the kimberlite magma. The bulk rock chemistry will correspond with mixing lines from forsteritic olivine and primary groundmass minerals

(Mitchell, 1995). Unevolved kimberlites have relatively low SiO_2 , Al_2O_3 and Na_2O and high MgO and P_2O_5 contents. Evolved Group II kimberlites are characterised by the highest SiO_2 of any kimberlite type as well as high Al_2O_3 and Na_2O contents. Mitchell (1995) ascribes this elevated SiO_2 to the presence of sanidine and richterite whereas high Na_2O contents are ascribed to the alteration of leucite and sanidine to Na-zeolites. The former may not be entirely correct as data from the Voorspoed kimberlite indicate an evolved magma while petrographic analysis indicates a lack of richterite and only minor sanidine although titanian aegirine is present as mantles to diopside cores. Therefore high silica contents may not simply be the result of sanidine and richterite. Diopside contents are much higher in the more evolved types and therefore the high silica must be related in part to diopside as well as the above-mentioned evolved Group II kimberlite minerals. High Na_2O contents are likely related to sanidine and aegirine at the Voorspoed kimberlite.

4.2 Mineral Composition

The Voorspoed kimberlite shows some degree of evolution relative to the Lace kimberlite. This evolution is indicated by the presence of more evolved minerals such as aegirine and sanidine. However, optically phlogopite at Voorspoed does not show extensive evolution to red/brown tetraferriphlogopite (as described in section 3.2.3), which would be expected in evolved Group II kimberlites. Therefore the diopside, aegirine and phlogopite at the Voorspoed kimberlite are analysed to investigate the extent of the evolution of the magma. Sanidine could not be analysed due to the often highly altered nature. Numerous evolved aegirine-bearing kimberlites have been analysed by Mitchell (1995), which provides a data set for comparison with the Voorspoed occurrence. Furthermore aegirine overgrowths have also been observed at the Besterskraal North kimberlite, which has previously not been documented. Aegirine and sanidine are the last minerals to crystallise apart from calcite. Therefore the composition of the minerals gives an indication to the composition of the late stage residual fluids, which are very different to typical late stage fluids described by Mitchell et al. (2009). Furthermore the lack of microlitic clinopyroxene at the Voorspoed hypabyssal transitional kimberlite (HKt), as described in section 3.2.4, may be the consequence of the different composition of the residual fluid.

Microclitic clinopyroxene from the Lace HKt and hypabyssal transitional kimberlite breccia (HKtB) has been analysed and compared with the primary diopside and aegirine compositions from the Voorspoed pipe. The microclitic clinopyroxene is the controlling factor on the slight geochemical variation observed in the HKt and therefore the composition of the microclitic clinopyroxene is compared with geochemical trends in section 4.3.

4.2.1 Paragenesis of Diopside, Aegirine and Phlogopite at the Kroonstad Cluster

The paragenesis of diopside, aegirine and phlogopite has been described in section 3 and will not be discussed in great detail again. The important characteristics are summarised below. Detailed petrographic descriptions of the HK at Voorspoed and Lace respectively are given in section 3.2.3 and 3.1.2.

Primary diopside accounts for approximately 27 vol. % of the bulk of the hypabyssal kimberlite (HK) analysed with rare examples reaching as high as 57 vol. % as described in section 3.2.3. Diopside is characterized by a high relief, inclined extinction, high birefringence and colourless nature, which typically occurs as laths ranging in size from 0.05-0.35mm and rare examples up to 1.2mm in length. Euhedral six sided grains are also observed but are not common. Diopside is commonly partially or wholly altered by calcite and does not show any resorption features.

Aegirine typically occurs as fine (<0.1mm) overgrowths at the terminations on diopside laths, overgrowths round the entire diopside crystal are rare, and is characterized by the green colour and nearly straight extinction, which is clearly different from the diopside laths as described in section 3.2.3. Aegirine is never altered by calcite and modes are typically <2 vol. %. Aegirine is typically observed as crystals protruding into sanidine segregations and is only rarely observed as complete crystals (not overgrowths), which are restricted to within the late stage sanidine segregations. Aegirine is observed as fine grained (<0.05mm) laths within magmaclasts, which are associated with sanidine plates in the base.

Table 4.1 Representative compositions of diopside and aegirine from Voorspoed Sample K1/114 and microlitic clinopyroxene (Mcpx) from the HKt (Sample K2-5) and HKtB (C7-713) from Lace. See appendix 3 for full tables of the compositions of the pyroxenes.

Wt%	Diop. (195)	Diop. (205)	Aeg. (194)	Aeg. (208)	Mcpx HKt	Mcpx HKtB
SiO₂	55.41	54.49	53.64	52.7	51.51	52.83
TiO₂	0.45	0.67	4.05	3.9	2.92	1.02
Al₂O₃	0.22	0.24	0.01	0.28	0.08	0.29
FeO	4.52	3.12	4.92	5.46	5.9	5.21
Fe₂O₃	-	-	17.45	19.36	-	-
MgO	15.72	16.94	4.51	2.8	14.10	14.90
CaO	23.56	24.33	6.5	3.54	23.75	24.48
Na₂O	0.43	0.13	9.92	11.53	0.99	0.61
Cr₂O₃	-	-	-	-	0.1	0.07
MnO	-	-	-	-	0.16	0.11
Total	100.33	100.04	101.00	99.57	99.53	99.51

Table 4.2 Structural formula for the Voorspoed pyroxenes on the basis of four cations and six oxygens

	Diop.(195)	Diop.(205)	Aeg.(194)	Aeg.(208)
Si	2.02	1.99	2.01	2.02
Ti	0.01	0.02	0.11	0.11
Al	0.01	0.01	0.01	0.01
Fe³⁺	-	-	0.44	0.50
Fe²⁺	0.14	0.10	0.21	0.24
Mg	0.85	0.92	0.25	0.16
Ca	0.92	0.95	0.26	0.15
Na	0.03	0.01	0.72	0.86

Table 4.3 Representative compositions of phlogopite phenocrysts from Voorspoed sample K1/114. See appendix 3 for full tables of the compositions.

Wt%	Phlog.(217)	Phlog.(228)	Phlog.(209)
SiO₂	40.96	42.11	42.02
TiO₂	2.26	3.15	2.97
Al₂O₃	11.82	11.91	11.30
FeO_T	5.60	5.67	5.58
MgO	23.41	21.08	21.84
CaO	0.06	0.07	0.05
Na₂O	0.16	0.21	0.32
K₂O	10.01	9.84	9.82
Total	94.28	94.05	93.91

Table 4.4 Structural formula based on 22 oxygens

	Phlog.(217)	Phlog.(228)	Phlog.(209)
Si	5.91	6.06	6.07
Ti	0.24	0.34	0.32
Al	2.01	2.02	1.92
Fe	0.68	0.68	0.67
Mg	5.04	4.52	4.70
Ca	0.01	0.01	0.01
Na	0.05	0.06	0.09
K	1.85	1.81	1.81

Phlogopite occurs as three generations including macrocrysts, phenocrysts and microphenocrysts. Phlogopite ranges in size from 0.05- >0.5mm. Macrocrysts are easily distinguished by common deformation textures such as kink banding and undulose extinction. Macrocrysts are xenocrysts and therefore are of no use in determining the evolved nature of the kimberlite magma. Phenocrysts and microphenocrysts are analysed to determine the relative evolution of the magma. These generations have similar characteristics and therefore are described together. Phlogopite at the Voorspoed kimberlite occurs as non-poikilitic and generally only weakly pleochroic from light to slightly darker brown laths. Minor zoning is observed with darker red/brown mantles, which were too fine to analyse. Therefore some evolution of the phlogopite is observed.

Microlitic clinopyroxene at the Lace pipe occurs as <0.1mm high relief, colourless laths as described in section 3.2.3. These laths never occur as inclusions within phlogopite, which indicates a later stage crystallisation. Microlitic clinopyroxene is observed replacing earlier formed minerals such as monticellite and apatite.

4.2.2 Composition

4.2.2.1 Primary Diopside

Diopside typically forms a solid solution with hedenbergite between $\text{CaMgSi}_2\text{O}_6$ and $\text{CaFeSi}_2\text{O}_6$ (Deer et al. 1992). At the Voorspoed pipe the diopside is Fe-poor (3-5 wt%) and show little solid solution toward hedenbergite. The diopside analysed are poor in TiO_2 (0.4-0.8 wt%), Al_2O_3 (0.1-0.5 wt%) and Na_2O (0.2-0.8 wt%). There is very little variation in diopside compositions within the dike sample analysed, as shown in figure 4.1. The slightly higher Na content than Al indicates an aegirine component rather than a jadeite component, similar to that described by Mitchell (1995). Representative composition data is given in table 4.1 and 4.2. See appendix 3 for a full data table of the analyses done in this study.

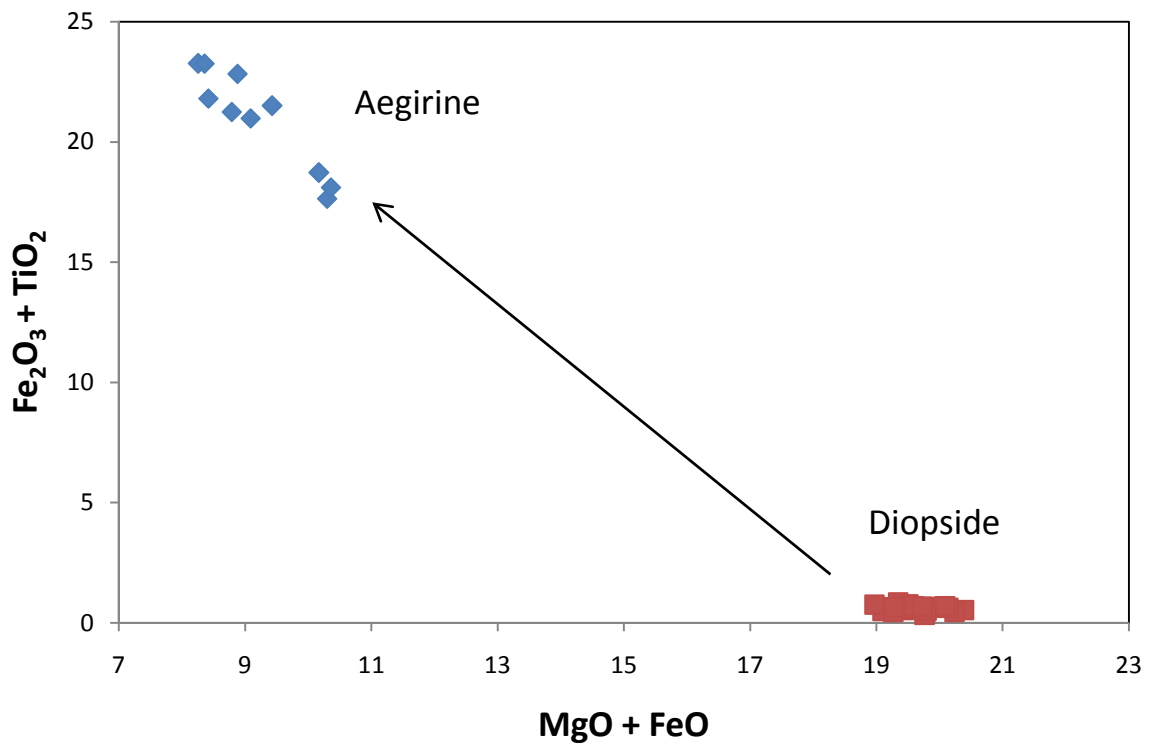
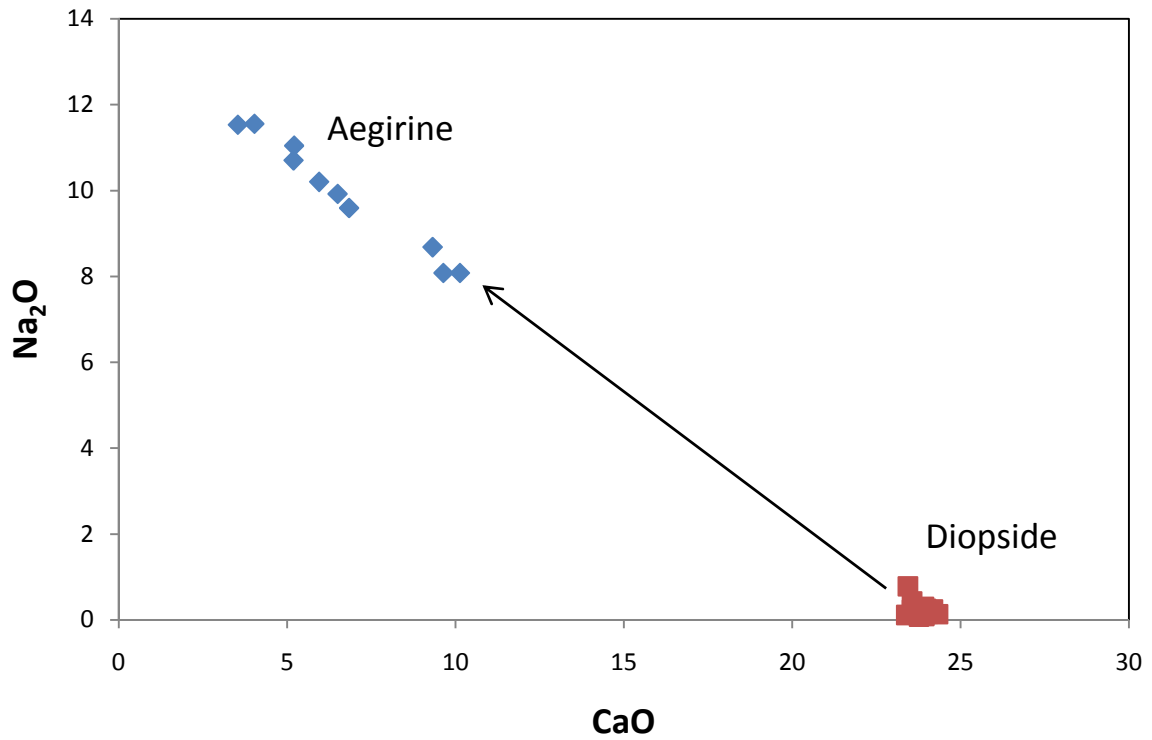


Figure 4.1 Compositional variation of pyroxene at the Voorspoed kimberlite sample K1/114. Note the clear gap in compositions indicating that there is no gradational change from diopside (brown points) to aegirine (blue points).

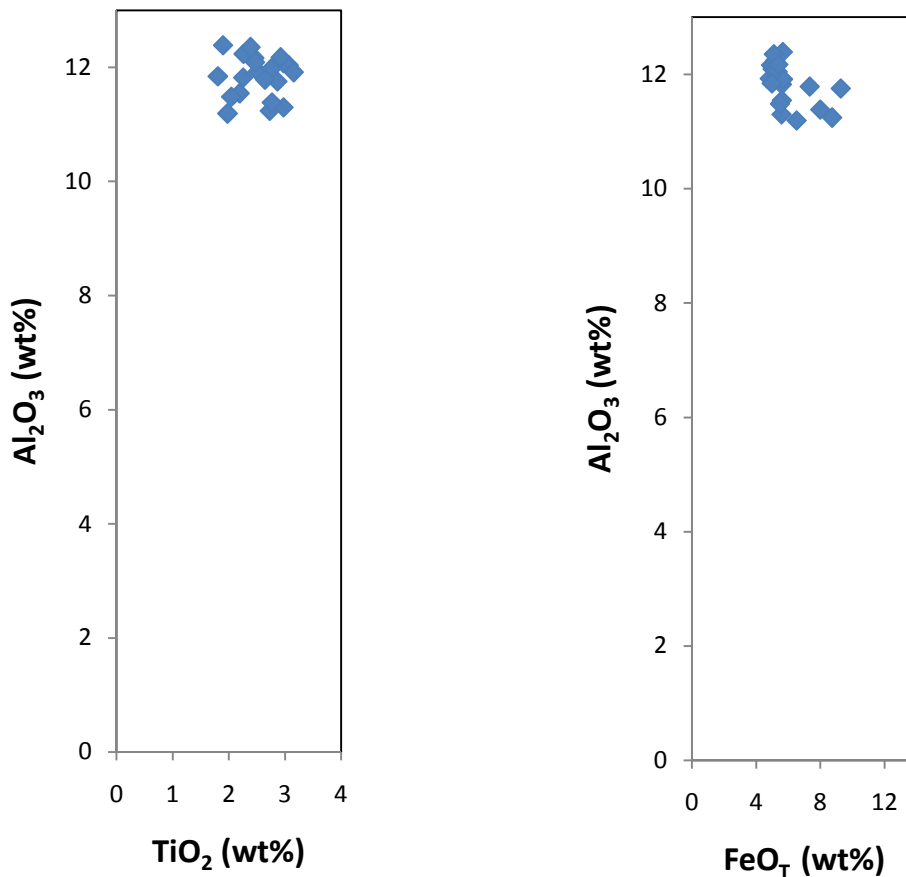


Figure 4.2 Composition of phlogopite at Voorspoed sample K1/114. Note the complete lack of evolution to tetraferriphlogopite.

4.2.2.2 Aegirine

As described above aegirine is observed as green overgrowths on the primary diopside laths. The composition of the green pyroxene is richer in Na and Fe. This trend reflects aegirine enrichment with some solid solution to augite. Aegirine-augite, $(\text{Na}, \text{Ca})(\text{Fe}^{3+}, \text{Fe}^{2+}, \text{Mg})(\text{Si}_2\text{O}_6)$, forms the solid solution where NaFe^{3+} replaces $\text{Ca}(\text{MgFe}^{2+})$. Aegirine at the Voorspoed pipe contains high Na_2O (8-11 wt%), Fe_2O_3 (22-25 wt%) and TiO_2 (2-6 wt%) but still contain low yet significant contents of Ca (3-10 wt%) and Mg (3-6 wt%). Therefore an average structural formula for the aegirine molecule shows some solid solution to hedenbergite as follows: $(\text{Na}_{0.8}, \text{Ca}_{0.2})(\text{Ti}_{0.1}, \text{Fe}^{3+}_{0.7}, \text{Mg}_{0.2}) \text{Si}_2\text{O}_6$. Figure 4.1 clearly shows the substitution between Na/Ca and Fe/Mg. Na and Fe content clearly become enriched at the expense of Ca and Mg respectively. Therefore solid solution is approaching the aegirine end

member, although a component of augite is present. Representative composition data is given in table 4.1 and 4.2. See appendix 3 for a full data table of the analyses done in this study.

4.2.2.3 Phlogopite

Group II kimberlite phlogopite show similar compositional variation of Al, Fe, Ti and Mg and therefore compositional variation is best illustrated by plots of Al_2O_3 , TiO_2 and FeO_T (Mitchell, 1995) as shown in figure 4.2. The phlogopite analysed in this study show compositions consistent with the moderate Al-depletion trend described by Mitchell (1995). Al_2O_3 (11-12 wt%), FeO_T (5-9 wt%) and TiO_2 (2-3 wt%) contents all show very little variation. Therefore the compositions of the phlogopite analysed show no evolution to higher Fe and Ti tetraferriphlogopite, which was expected after initial petrographic analysis as very little zonation of the phlogopite laths was observed. Representative composition data is given in table 4.3 and 4.4. See appendix 3 for a full data table of the analyses done in this study.

4.2.2.4 Microlitic Clinopyroxene at Lace Hypabyssal Transitional Kimberlite (HKt) and Hypabyssal Transitional Kimberlite Breccia (HKtB)

Microlitic clinopyroxene compositions from the Lace HKt and HKtB are very similar to the primary diopside compositions from the Voorspoed kimberlite. The microlitic clinopyroxene is poor (<1wt.%) in Al_2O_3 , Na_2O and Cr_2O_3 . TiO_2 content range from 1-3 wt.% and FeO 4-6 wt.%. The TiO_2 contents are significantly higher than those of the primary diopside from Voorspoed and are more similar to the aegirine compositions. The composition of the microlitic clinopyroxene does not show any variation between the HKt and HKtB and compositions are similar to the primary diopside from Voorspoed apart from the elevated TiO_2 and slightly higher Na_2O . Representative composition data for the microlitic clinopyroxene is given in tables 4.1 and 4.2. See appendix 3 for a full data table of the analyses done in this study.

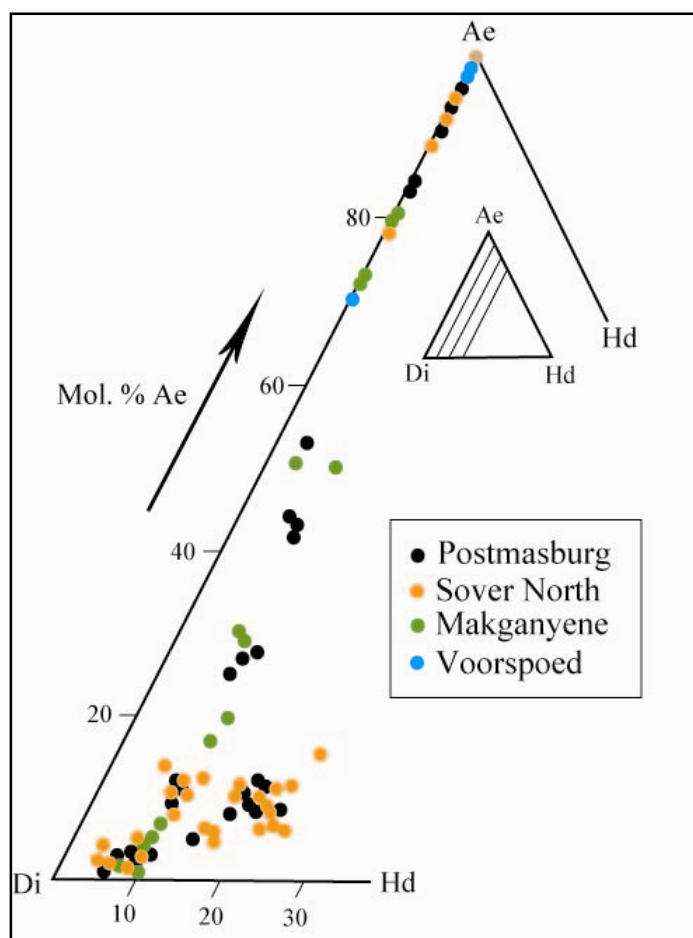


Figure 4.3 Compositions of evolved aegirine-rich clinopyroxene from Postmasburg, Sover North, Makganyene and Voorspoed plotted in the ternary system diopside (Di)- hedenbergite (Hd)- aegirine (Ae). Diagram from Mitchell (1995).

4.2.3 Primary Diopside-Titanian Aegirine at other Localities

Primary diopside is a common component of Group II kimberlites and becomes particularly abundant in the more evolved Group II type (Skinner and Scott, 1979; Mitchell and Meyer, 1989 and Mitchell, 1995). However, aegirine has only been documented at five kimberlite occurrences (figure 4.3), namely the Postmasburg, Makganyene, Sover North, Voorspoed and Pniel hypabyssal kimberlites (Mitchell, 1995). Mitchell (1995) is the only literature available, which presents compositional data on aegirine in kimberlites. TiO_2 contents generally range from 0.3 to 6.6 wt% and those containing higher TiO_2 contents may be regarded as titanian aegirine (Mitchell, 1995). Mitchell (1995) suggests that pyroxene is part of an unusual quaternary solid solution between $\text{Na}(\text{Fe}^{2+}_{0.5}, \text{Ti}_{0.5})\text{Si}_2\text{O}_6$, $\text{Na}(\text{Mg}_{0.5}, \text{Ti}_{0.5})\text{Si}_2\text{O}_6$, diopside, and aegirine. Compositional data for aegirine obtained in this study show some variation to that reported by Mitchell (1995) for the Voorspoed kimberlite.

4.2.4 Primary Diopside Composition at Voorspoed

Typical primary kimberlitic diopside is Fe-poor and show little solid solution toward hedenbergite (Mitchell, 1995). Diopside is also typically poor in TiO_2 (0.1-2.0 wt %), Al_2O_3 (0.02-1.3 wt%) and Cr_2O_3 (0-1.0 wt%) with very little variation observed within the same intrusion (Mitchell, 1995). The diopside analysed in this study (table 4.1 and appendix 3) at Voorspoed are typical of the above characteristics, they are Fe-poor although some solid solution to hedenbergite is present. The structural formula for primary diopside at Voorspoed is $\text{Ca}(\text{Mg}_{0.9}, \text{Fe}_{0.1})\text{Si}_2\text{O}_6$, which indicates minor solid solution to hedenbergite. Figure 4.3 shows the minor hedenbergite solid solution in some pyroxenes analysed by Mitchell (1995), which reaches up to 30 mol. %.

4.2.5 Aegirine at Besterskraal North Hypabyssal Kimberlite (HK)

Aegirine at the Besterskraal kimberlite occurs in a similar paragenesis to the Voorspoed kimberlite and is observed as distinct green overgrowths on colourless primary diopside laths. The overgrowths are in general larger in size and reach up to 0.2mm in length. Overgrowths are observed in both the Type 1 and Type 2 HK, although they are distinctly different. The aegirine in the Type 1 HK is identical to that described at the Voorspoed kimberlite but the overgrowth in the Type 2 HK is not similar to that described at Voorspoed. Diopside is particularly abundant in the Type 2 HK variety along with K-richterite, which occurs as light brown to pale green irregular plates. The edges of the K-richterite are slightly darker green in colour and have a feathery appearance. Green mantles on colourless diopside laths in the Type 2 HK are very similar to the green margins of the K-richterite. Therefore the overgrowths on the diopside at the Type 2 HK at Besterskraal North is distinctly different from the aegirine at Voorspoed and the Type 1 HK at Besterskraal North, which are interpreted to be aegirine overgrowths. No compositional data are available for the Besterskraal North kimberlite aegirine and therefore the overgrowths in the Type 2 HK can not be accurately identified. Further work needs to be done to understand the evolution of both the K-richterite and diopside in this distinct HK (Type 2) variety.

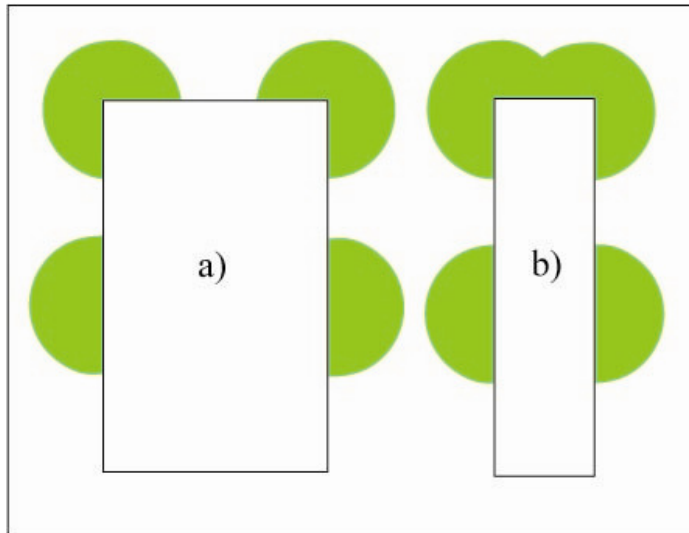


Figure 4.4 Diagram illustrating epitaxis where in a) the volume of the liquid available to an edge or corner of the crystal is greater than at the side and b) volume of liquid available for a narrow crystal is even greater. Diagram after Winter (2001).

4.2.6 Epitaxial growth of Aegirine

The aegirine overgrowths on diopside laths are interpreted to be a late stage epitaxial growth. Epitaxis is defined as: the preferred nucleation of one mineral on another pre-existing mineral, thereby avoiding problems associated with slow nucleation, figure 4.4 (Winter, 2001). A similarity of the crystal structure is a prerequisite for this kind of growth and therefore the atomic constituents of the new mineral find favourable nucleation sites to accumulate (Winter, 2001). This interpretation is based on the significant gap in mineral compositions observed in figure 4.1 where the composition of diopside and aegirine do not show any evolution. This trend is also observed at Sover North although there is a gradational evolution from diopside to aegirine at Makganyene and Postmasburg kimberlites (Mitchell, 1995). Detailed description of the textural relationship of aegirine and diopside is given in section 3.2.3.

Therefore at Voorspoed and Sover North the diopside laths form early in the evolution of the magma near surface and provide suitable nucleation sites for epitaxial growth of aegirine at a later stage during the evolution of the magma. This is also supported optically as distinct boundaries are observed between the diopside and aegirine minerals. Furthermore epitaxial

Table 4.5 Comparison of composition of aegirine from Mitchell (1995) (1,2) and this study (Aeg. 187 and 239)

Wt%	1	2	Aeg. (187)	Aeg. (239)
SiO₂	51.94	50.24	52.90	52.96
TiO₂	1.55	2.42	6.32	3.20
Al₂O₃	-	0.17	0.08	0.17
FeO_T	-	-	-	-
Fe₂O₃	29.55	29.55	22.87	23.27
MgO	1.85	1.24	3.48	4.24
CaO	2.08	2.46	3.22	6.47
Na₂O	12.68	12.48	11.07	9.45
MnO	0.09	0.24	-	-
Total	99.74	98.80	99.97	99.75

Table 4.6 Structural formula on the basis of four cations and six oxygens for table 4.5.

	1	2	Aeg.(187)	Aeg.(239)
Si	1.986	1.965	2.09	2.10
Ti	0.045	0.071	0.19	0.10
Al	-	0.008	0	0.01
Fe³⁺	0.879	0.866	0.68	0.70
Fe²⁺	-	-	-	-
Mg	0.105	0.072	0.2	0.25
Ca	0.085	0.103	0.14	0.28
Na	0.940	0.947	0.85	0.73

growth is favoured at the terminations of crystals, which is typical of the aegirine at Voorspoed as the volume of liquid available at the corner of a crystal is greater than at the side (Winter, 2001), as shown in figure 4.4. Therefore slender crystals are expected to crystallise longer overgrowths.

4.2.7 Comparison with Mitchell (1995) and Voorspoed Aegirine data

Mitchell (1995) provides the only other data available on the composition of aegirine at the Voorspoed kimberlite but only three analyses are given as shown in figure 4.3. There are marked differences in the data compared to that obtained in this study as shown by representative compositions in table 4.5. The data presented by Mitchell (1995) show that Fe_2O_3 (29.55 wt%) is much higher while the Na_2O (12.50 wt%) contents are slightly higher. However the TiO_2 (1.5-2.5 wt%), MgO (1.2-1.8 wt%) and CaO (2.0-2.4 wt%) contents are lower. The data obtained in this study suggested that the aegirine shows some solid solution with augite, which ranges between $(\text{Na}_{0.6}, \text{Ca}_{0.4})(\text{Ti}_{0.1}, \text{Fe}^{3+}_{0.6}, \text{Mg}_{0.3})\text{Si}_2\text{O}_6$ and $(\text{Na}_{0.9}, \text{Ca}_{0.1})(\text{Ti}_{0.1}, \text{Fe}^{3+}_{0.8}, \text{Mg}_{0.1})\text{Si}_2\text{O}_6$.

4.2.8 Evolution of Phlogopite in Group II Kimberlite

Phlogopite composition can vary from core to margin/groundmass in both evolved and unevolved Group II kimberlites. Phenocryst cores usually contain 9-13.5 wt. % Al_2O_3 , 1-3 wt. % TiO_2 and 2-6 wt % FeO_T (Mitchell, 1995). Intra and inter intrusion variation is insignificant for phlogopite composition (Skinner and Scott, 1979 and Mitchell, 1995). The mantles of phenocrysts as well as groundmass phlogopite become enriched in FeO_T at constant or decreasing TiO_2 content at the expense of Al_2O_3 in unevolved kimberlites. However in evolved kimberlites the phlogopite is strongly enriched in FeO_T with moderate depletion of Al_2O_3 as well as MgO , which is not depleted in typical unevolved kimberlites. Along with the strongly enriched FeO_T (up to 15 wt%). Most importantly in evolved types there is also an enrichment in TiO_2 (up to 7 wt%), which is not present in unevolved types. The enrichment in both evolved and unevolved varieties is observed optically by an increase in intensity of red pleochroism. The evolution of phlogopite is gradational and intermediate kimberlites such as Postmasburg show a trend of increasing TiO_2 with decreasing Al_2O_3 toward compositions of the evolved type kimberlites such as Sover North. Figure 4.5 show

these trends for the Kroonstad Cluster, which contains unevolved, intermediate and evolved phlogopite compositions.

4.2.9 Evolution of Phlogopite at the Kroonstad Kimberlite Cluster

The Kroonstad Kimberlite Cluster provides a unique opportunity to observe a gradational evolution in kimberlite magma from the unevolved Lace kimberlite to the moderately evolved Voorspoed kimberlite and finally the highly evolved Besterskraal North kimberlite. This trend is made obvious by a number of mineralogical and geochemical characteristics. Phlogopite shows a gradational evolution from Lace-Voorspoed-Besterskraal North. The evolution observed at this cluster results in an increase in TiO_2 and FeO_T wt % with a subsequent decrease in Al_2O_3 content in the phlogopite as shown in figure 4.5. The phlogopite compositions discussed below are from Mitchell (1995). The unevolved Lace kimberlite optically shows distinct zoning of the phlogopite to tetraferriphlogopite mantles. The composition of these tetraferriphlogopite rims show an increase in FeO_T content with subsequent decrease in Al_2O_3 but the TiO_2 content remains relatively unchanged. A similar trend is observed at Voorspoed although the zoning is somewhat less extensive. The major difference at the Voorspoed kimberlite is the increase in TiO_2 along with FeO_T . The Besterskraal North Kimberlite continues on this trend of Al_2O_3 depletion and TiO_2 and FeO_T enrichment. Figure 4.5 clearly shows this evolution of the phlogopite within the Kroonstad Cluster.

The phlogopite analysed in this study show no evolution relative to the phlogopite described above for the evolved Group II kimberlite. Mitchell (1995) analysed phlogopite from two samples K1/110 and K1/111. These samples are from kimberlite sills in the surrounding country rock and therefore pre-date the explosive emplacement of the Voorspoed pipe. Sample K1/110 (figure 4.5) shows no evolution of the phlogopite and is very similar to the phlogopite analysed in this study. Sample K1/111 however does show evolution of the phlogopite to a more TiO_2 rich and Al_2O_3 poor phlogopite such as those described above. Figure 4.5 shows the trend toward the evolved Besterskraal North phlogopite compositions. Therefore the phlogopite at Voorspoed does show some evolution but are not nearly as evolved as the Besterskraal North kimberlite. Mitchell (1995) suggests that evolved micas

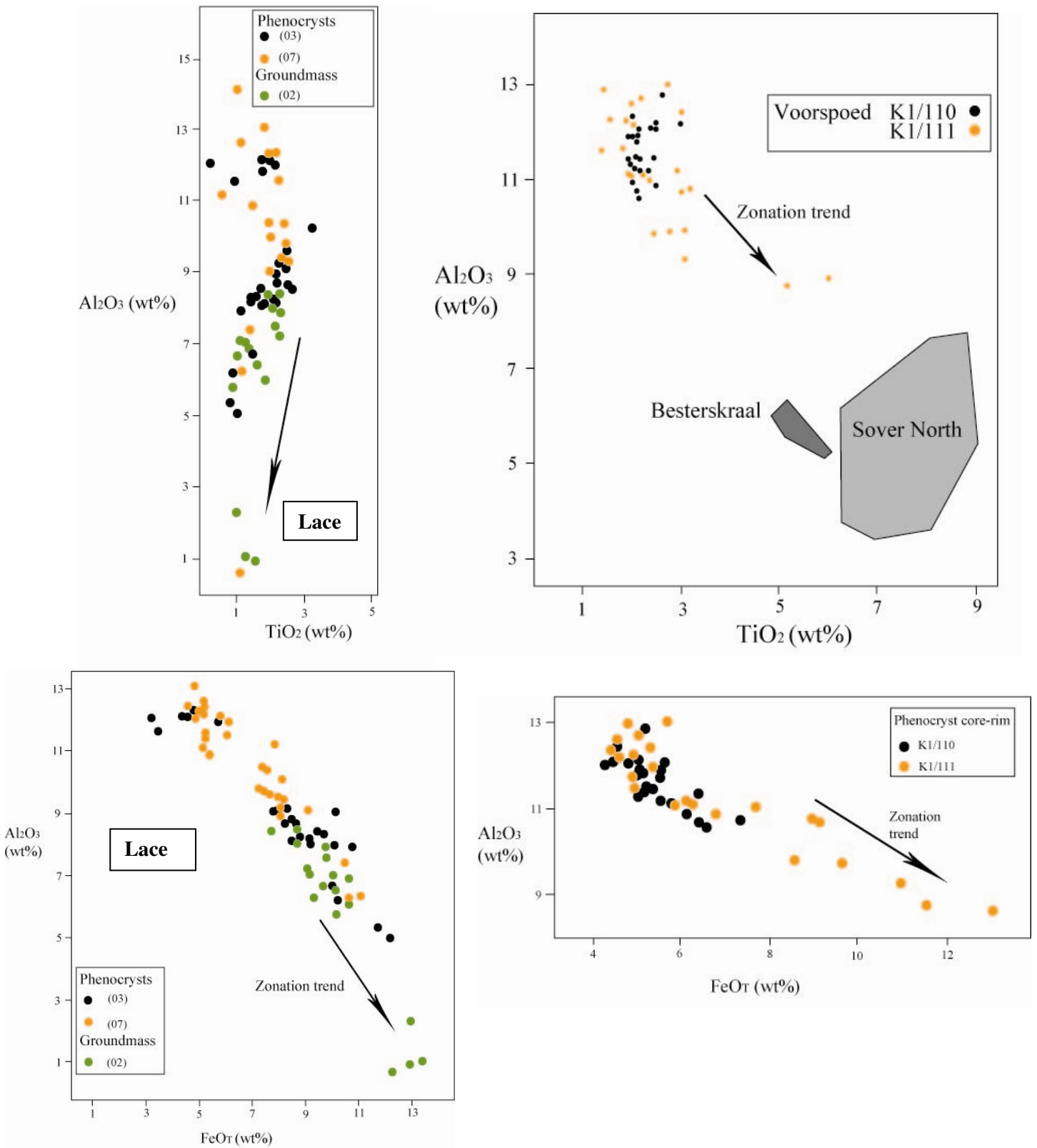


Figure 4.5 Composition of phlogopite at the Voorspoed and Lace HK. Top and bottom left are compositions from Lace. Top and bottom right are from Voorspoed. Note the clear zonation trend of the phlogopite from Voorspoed in sample K1/111 but not in sample K1/110. The phlogopite analysed in this study (sample K1/114) is very similar to that of sample K1/110. Also note the trend of the phlogopite at Voorspoed to the highly evolved Besterskraal and Sover North phlogopite compositions. The composition of the phlogopite at Lace does not increase in TiO₂, which is characteristic of unevolved Group II kimberlites. Diagrams from Mitchell (1995).

such as those at Besterskraal North originate from extensive fractional crystallisation of Voorspoed-type precursor magmas. It must be noted that while phlogopite shows very little evolution between varies samples; aegirine does not occur in all the samples analysed and therefore there is some variation in the evolution of the different HK samples.

4.2.10 Mineralogical evidence for the Evolution of the Voorspoed Kimberlite

The Voorspoed hypabyssal kimberlite (HK) is clearly evolved in nature but not highly evolved such as the Besterskraal North and Sover North kimberlites. The presence of aegirine, sanidine and Ti-rich phlogopite indicates this evolution. Both sanidine and aegirine are in low abundances and therefore indicating only intermediate evolution. The most important mineralogical characteristic indicating intermediate evolution is the phlogopite as shown in figure 4.5. Phlogopite analysed in this study did not show any evolution and neither did sample K1/110 analysed by Mitchell (1995). Therefore not all the hypabyssal intrusions associated with the Voorspoed pipe show evolution of the phlogopite. Sample K1/111 however does show evolution of the phlogopite with increased TiO_2 content in the mantles, which is characteristic of evolved Group II kimberlites. The TiO_2 contents are intermediate between unevolved and evolved kimberlite but the trend is toward compositions analysed in evolved kimberlites. Therefore based on the mineralogy the Voorspoed kimberlite is an intermediate evolved Group II kimberlite, which shows mineralogical characteristics intermediate between the Lace and Besterskraal North kimberlites.

4.2.11 Comparison of Primary Diopside at Voorspoed with Microlitic Clinopyroxene Composition

Compositional data for microlitic clinopyroxene is limited to Skinner and Scott (1979), Mitchell et al. (2009) and this study. In general there is limited variation in the data however minor trends are observed in the relatively small data set available. Most of the microlitic clinopyroxene are low-Al and low-Ti (<1wt % respectively) diopsides (Mitchell et al. 2009) however the clinopyroxene from this study has higher TiO_2 (1-3wt%) (table 4.1 and appendix 3). A subtle trend is noted in two samples where increased Na_2O is accompanied by an increase in Al_2O_3 . However in general the compositions are relatively consistent with minor variation in MgO, CaO and FeO as shown in figure 4.6. Microlitic clinopyroxene is

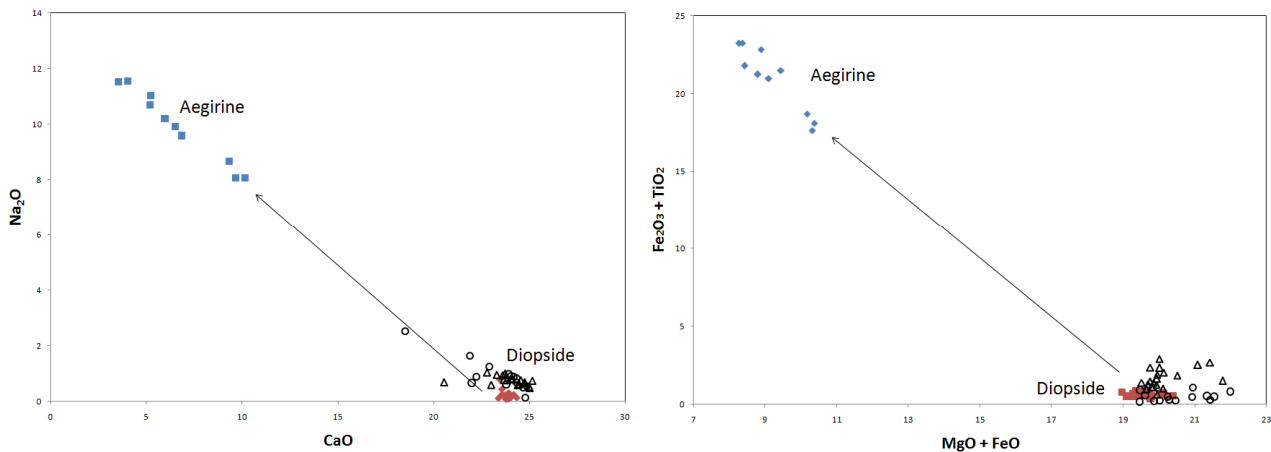


Figure 4.6 Comparison of diopside and aegirine from Voorspoed (this study) with microlitic clinopyroxene data from Skinner and Scott (1979), Mitchell et al. (2009) and Lace (this study). Microlitic clinopyroxene plotted as open circles are from Skinner and Scott (1979) and Mitchell et al. (2009). Microlitic clinopyroxene from the Lace HKt/HKtB are plotted as the open triangles.

interpreted to have formed through two possible mechanisms or both: 1) crustal contamination or 2) CO₂ degassing (Mitchell et al. 2009). However alternate interpretations have been given by numerous authors such as Stripp et al. (2006) who suggest a secondary post-emplacement formation process, although this seems unlikely to be the case at the Lace pipe (as discussed in section 5.3). Microlitic clinopyroxene data shows compositions very similar to typical primary diopside from the Voorspoed hypabyssal kimberlite (HK) (figure 4.6). It seems unlikely that a later secondary process would produce microlitic clinopyroxene (diopside) compositions so similar to the primary phases. Therefore it is likely that the formation of microlitic clinopyroxene is related to the kimberlite rather than a later secondary post emplacement process.

Crustal contamination of a magma chamber is generally indicated by an increase in SiO₂, Na₂O and Al₂O₃ contents (Clement, 1982; le Roex et al. 2003 and Becker and le Roex, 2006).

A significant increase is noted in Na₂O for the aegirine forming at a late stage at the Voorspoed kimberlite (figure 4.6), which is accompanied by late stage sanidine containing high proportions of SiO₂ and Al₂O₃ (Mitchell, 1995). However the HK is petrographically

analysed and no xenolithic material is observed, which indicates that no crustal contamination has occurred near surface. Furthermore the aegirine is FeO rich, which indicates that late stage magma fluids must have been SiO₂, Na₂O, Al₂O₃ and FeO rich and depleted in MgO and CaO. Microlitic clinopyroxene is not observed at the Voorspoed pipe HKt (as discussed in section 3) and is likely a function of the composition of the late stage magma fluid. Typically kimberlite magma fluid evolves to a H₂O, K₂O, CaO and MgO –rich residual fluid, which contains SiO₂ and is CO₂ poor (Mitchell et al. 2009). Therefore the late stage residual fluid at the Voorspoed pipe is not conducive for the formation of microlitic clinopyroxene. The residual fluid composition at Voorspoed is Na₂O rich, which favours the crystallisation of aegirine over diopside. Furthermore typical Class 1 kimberlites do not contain primary diopside and microlitic clinopyroxene crystallise as microlites or replaces pre-existing minerals (Skinner, 2008). In the case of the Voorspoed pipe primary diopside crystallising at an early stage provides sites for nucleation of the later aegirine. Sanidine then crystallises at a later stage in a similar process to serpentine in typical Class 1 kimberlites. Most of the sanidine is replaced by calcite, which is the final mineral phases crystallising from CO₂ degassing.

4.3 Bulk Rock Geochemistry of the Voorspoed and Lace Kimberlites

4.3.1 Introduction

Group II kimberlites are unique to South Africa and are often ignored when interpreting average kimberlite geochemistry. Group II kimberlites show a clear variation in geochemistry from an unevolved end member to an evolved end member Mitchell (1995). Data on Group II kimberlites are relatively scarce in the literature, especially the evolved Group II end member. The available data is limited to Smith et al. (1985), Skinner (1989), Fraser and Hawkesworth (1992), Mitchell (1995), Becker and le Roex (2006) and Coe et al. (2008). Mitchell (1995) are the only sources, which deals with the evolution of Group II kimberlites. This evolution has not been dealt with by Becker and le Roex (2006) for the comparison of Group I and II kimberlites. Smith et al. (1985) first showed the characteristic isotopic variation between Group I and II kimberlites, which also have significant distinctions in major and trace element variations. Group II kimberlites generally contain higher proportions of SiO₂ and K₂O with lower TiO₂. Unevolved Group II kimberlites have very similar major element variation to Group I kimberlites and Smith et al. (1985) showed that the only K₂O and TiO₂ provide adequate discrimination when both elements exceed 1 wt%. Evolved Group II kimberlites are clearly discriminated by their high SiO₂ and Na₂O contents.

The geochemical work presented below is based mostly on samples obtained from the Lace kimberlite. The Voorspoed pipe is currently dominated by volcanoclastic kimberlite (VK) infill and no distinct hypabyssal kimberlite (HK) in the root zone has been intersected. The Lace pipe has been sampled from both core and from the surrounding dumps. In situ core samples show low to high degrees of crustal contamination whereas the dump samples show little to no crustal contamination. Therefore the dump samples are discussed in detail below as subtle geochemical trends are noted, which have been petrographically linked to the occurrence and abundance of microlitic clinopyroxene. The term microlitic clinopyroxene is used for any diopside occurring in the kimberlite, which is not primary but rather deuteric as interpreted by (Skinner and Marsh 2004; Skinner, 2008 and Mitchell et al. 2009). The majority of this clinopyroxene has a microlitic texture but does become slightly coarser grained and blocky at depth within the Lace pipe, similar to that described by Mitchell et al. (2009) for the Wesselton kimberlite. Primary diopside is only observed at the Voorspoed and

Besterskraal kimberlites and not at Lace. Microlitic clinopyroxene is only observed at the Lace pipe. The geochemical trends at the Lace pipe are interpreted to be controlled by the abundance of microlitic clinopyroxene as discussed below. Microlitic clinopyroxene compositions are briefly discussed in terms of their variation and possible link to paragenesis. Crustal contamination is evident for most of the in situ core samples analysed and is discussed below. Furthermore evidence for fractional crystallisation is also presented for both the Voorspoed and Lace kimberlites, which has been petrographically linked to the abundance of olivine of the HK.

4.3.2 Major Element Geochemistry relative to Group I kimberlite

Group II kimberlites are characterised by higher SiO_2 contents relative to Group I contents, as shown in table 4.7 (Skinner, 1989), although SiO_2 is still low relative to other mafic rocks such as basalts (45-52 wt % SiO_2). SiO_2 rarely exceed 40 wt % in Group II, although some cases such as Finsch have an average SiO_2 of approximately 40 wt % (Skinner, 1989 and Fraser and Hawkesworth, 1992), which is much higher than the average for Group II kimberlites on a whole. SiO_2 for Group II kimberlite can vary from as low as 29 wt % to >40 wt % with an average of 33 wt % (Becker and le Roex, 2006). Group II kimberlite with silica contents >40 wt % are usually the more evolved type Group II kimberlites, as discussed below.

MgO variations are large (17-36 wt %) and no correlation with SiO_2 is evident in Group II kimberlites (Becker and le Roex, 2006), although increased SiO_2 is often accompanied by the loss of MgO in evolved Group II kimberlites (Mitchell, 1995 and Roberts, 1997). The characteristic feature of Group II kimberlite is the lower TiO_2 but higher K_2O relative to Group I (Smith et al. 1985). Fe_2O_3 contents are lower in Group II whereas MnO and MgO contents are similar in both Group I and Group II. Table 4.7 shows a comparison of geochemistry between Group I and II kimberlites. Mitchell (1995) notes a mineralogical control on Group II kimberlite geochemistry variation and has divided Group II geochemistry into evolved and unevolved types as discussed for the mineralogy of Group II kimberlites.

4.3.3 Unevolved and Evolved Group II Geochemistry

The following discussion is on the evolution of Group II kimberlites based on the bulk rock geochemistry. Available data on evolved Group II kimberlites is limited to Mitchell (1995) and therefore the following discussion is based mostly on the observations made by Mitchell (1995).

Unevolved Group II kimberlites are essentially mixtures of olivine, phlogopite, carbonate and apatite (Mitchell, 1995). The majority of olivine are mantle-derived xenocrysts and therefore are contaminants in the kimberlite magma. The bulk rock chemistry corresponds with mixing lines from forsteritic olivine and primary groundmass minerals (Mitchell, 1995). Unevolved kimberlites have relatively low SiO_2 , Al_2O_3 and Na_2O and high MgO and P_2O_5 contents as shown in table 4.7.

Evolved Group II kimberlites are characterised by the highest SiO_2 of any hypabyssal kimberlite type. Mitchell (1995) ascribes this elevated SiO_2 to the presence of sanidine and richterite whereas high Na_2O contents are ascribed to the alteration of leucite and sanidine to Na-zeolites. The former may not be entirely correct as data from the Voorspoed kimberlite indicate an evolved magma while petrographic analysis indicates a lack of richterite and only minor sanidine although aegirine and primary diopside are abundant mineral phases present. The high silica contents may not simply be the result of sanidine and richterite. Primary diopside contents are much higher in the more evolved types and therefore the high silica must be related in part to diopside as well as the above-mentioned minerals. Table 4.7 gives a full comparison of major element chemistry for the different Group II kimberlite types.

The average chemistry for Group II kimberlite provided by Becker and le Roex (2006) may be incorrect as sampling of unevolved kimberlites only would produce lower average silica values as well as the accompanied geochemical differences associated with unevolved kimberlites.

Table 4.7 Comparison of geochemistry of Average Group I and Group II kimberlite (Becker and le Roex, 2006); Unevolved Group II kimberlite (Mitchell, 1995) and Evolved Group II kimberlite (Mitchell, 1995).

Wt%	Grp. I (Average)	Grp. II (Average)	Unevolved	Evolved
SiO₂	26.15	33.89	35.52	43.68
TiO₂	2.58	1.77	1.06	1.5
Al₂O₃	2.76	3.76	2.88	5.98
Fe₂O₃	10.72	8.76	7.92	7.84
MnO	0.19	0.18	0.16	0.13
MgO	25.20	23.15	27.46	20.48
CaO	13.26	9.96	7	6.48
Na₂O	0.16	0.25	0.18	0.72
K₂O	0.83	3.63	3.12	4.15
P₂O₅	2.04	1.85	1.01	0.81
SO₃	0.17	0.21	-	-
NiO	0.11	0.14	-	-
Cr₂O₃	0.18	0.23	-	-
LOI	14.71	10.75	11.27	5.15
H₂O⁻	0.66	1.34	-	-
Total	99.71	99.41	97.6	97.4
H₂O⁺	6.67	7.33	-	-
CO₂	8.19	4.21	-	-

Only one of the eleven Group II kimberlite sampled by Becker and le Roex (2006) has a silica content >40 wt % and therefore the average values produced for Group II kimberlites will be biased toward unevolved type Group II kimberlite chemistry. This is shown in table 4.7 where the average Group II silica content from Becker and le Roex (2006) is much lower than the silica in the three typical Group II kimberlites. Therefore the average values given by Smith et al. (1985) may give a more accurate representation of Group II kimberlite chemistry.

4.3.4 Contamination Index (C.I.)

The assessment of the crustal contamination is a primary concern when analysing bulk rock geochemistry of kimberlites. Clement (1982) formulated a contamination index (C.I.), which is based mainly on Group I kimberlites. This C.I. has also been used in more recent studies by Mitchell (1995), Becker and le Roex (2006) and Coe et al. (2008). The application of the formula to petrographically uncontaminated hypabyssal kimberlite gives a value near unity (1), although minor variation is observed (Clement, 1982). Generally crustal contamination is indicated by increase in SiO_2 , Al_2O_3 and Na_2O , which is also the case with near surface weathering of the kimberlite. Therefore detailed petrographic analysis of the rocks should be done along with C.I. calculations, so as to differentiate between the two possible sources of a high C.I. The highest C.I.'s are usually from phlogopite and/or diopside –rich rocks (Group II kimberlites) and reach up to 1.5. Mitchell (1995) states that it is likely they reach far greater values especially for the more evolved Group II end members. Becker and le Roex (2006) and Coe et al. (2008) show that the C.I. for the numerous Group II kimberlites analysed generally have C.I.'s <1.5 , which is interpreted to represent uncontaminated HK. Kjarsgaard et al. (2009a) uses bivariate plots of Yb vs Al_2O_3 and $\ln \text{Mg/Yb}$ vs $\ln \text{Si/Al}$ to further constrain the effects of crustal contamination. A combination of the Clement C.I. and the method used by Kjarsgaard et al. (2009a) provides a useful technique to identify crustal contamination. However the application of the above discussed contamination assessments are based on Group I kimberlites only, which in general contain low SiO_2 , Al_2O_3 and Na_2O . Uncontaminated unevolved Group II kimberlites generally have C.I.'s of 1.5 (Clement, 1982) whereas the evolved type Group II kimberlite can have significantly higher values (Mitchell, 1995). Therefore a Clement C.I. of 1.5 is used to indicate uncontaminated samples from the Lace kimberlite. Kjarsgaard et al. (2009a) shows that uncontaminated Group I type kimberlite

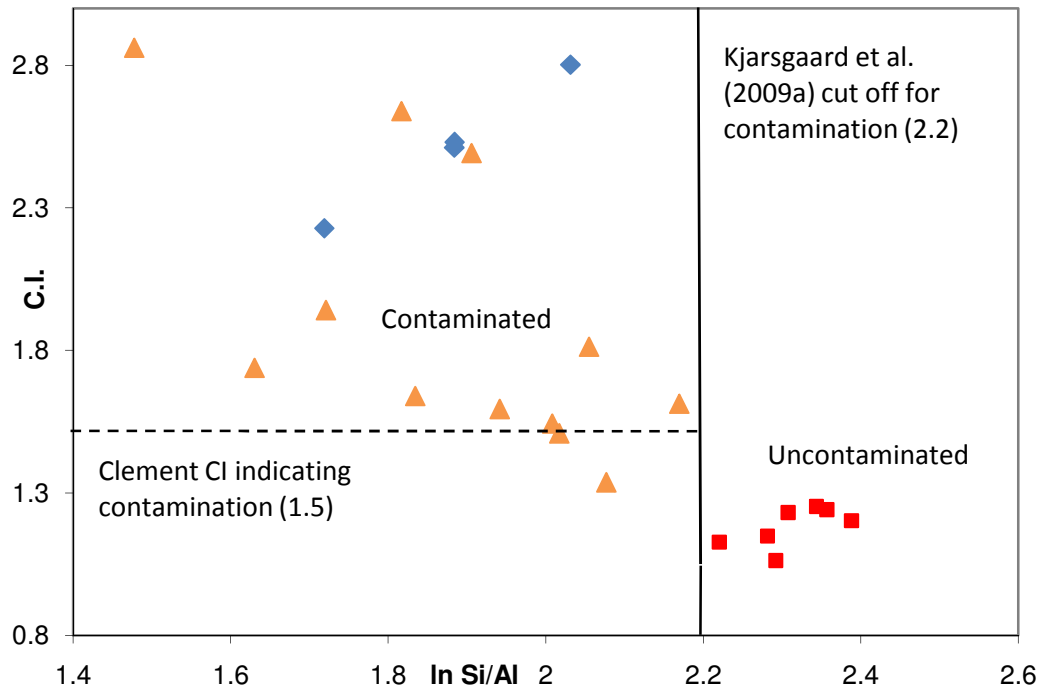


Figure 4.7 Combination of Clement (1982) C.I. and the contamination technique used by Kjarsgaard et al. (2009a) to indicate the degree of crustal contamination for the samples analysed at the Kroonstad cluster. Red squares: Lace dump samples (HKt); Orange triangles: Lace core samples (HKtB) and Blue diamonds: Voorspoed HK data from Roberts (1997) and this study.

contains $\ln \text{Si/Al}$ values >2.2 and Clement C.I. values between 0.8 and 1.38. The application of these contamination assessments needs to be applied in conjunction with petrographic work for Group II kimberlites as the methods may not always apply, particularly for evolved Group II kimberlite.

4.3.5 Contamination of the Voorspoed and Lace Kimberlites: Indicated by the Geochemistry

4.3.5.1 Voorspoed Kimberlite

The Voorspoed pipe samples all show a high degree of crustal contamination from both the Clement C.I. and the Kjarsgaard et al. (2009a) method, as shown in figure 4.7. However Voorspoed is an evolved type Group II kimberlite and the high contamination index is expected due to the characteristic high SiO_2 , Al_2O_3 and Na_2O . The evolved nature of the Voorspoed kimberlite is discussed further below.

4.3.5.2 Lace Kimberlite

The Lace kimberlite dump samples have Clement C.I.'s of 1.1-1.25, which is indicative of an uncontaminated Group II kimberlite. The $\ln \text{Si/Al}$ values calculated are all > 2.2 , which is also indicative of an uncontaminated kimberlite (Kjarsgaard et al. 2009a). The latter function has never been applied to Group II kimberlite, however the two assessment criteria compliment each other and most likely indicate very little or no contamination of the dump samples. The core samples show some degree of contamination shown by the Clement C.I., which vary between 1.5-3.6, although some of the samples still fall into the uncontaminated Group II kimberlite field of <1.5 C.I. However the $\ln \text{Si/Al}$ values are always < 2 , which indicates some degree of contamination of the rocks. All the core samples contain significant proportions of crustal material, which is clearly evident from the geochemical analysis. Only three samples show petrographic and geochemical trends indicating an uncontaminated nature, although they still contain $\ln \text{Si/Al}$ values of <2 , as shown in figure 4.7 with Clement C.I of approximately 1.5 for the orange triangles.

4.3.6 Geochemistry of the Voorspoed and Lace Kimberlites

4.3.6.1 Voorspoed Kimberlite

The Voorspoed pipe infill is dominated by VK as discussed in section 3 and the available HK for sampling was limited to one sample from an intrusive dike. However Roberts (1997) has given data for HK samples for the Voorspoed pipe, which are discussed here. The most evident major element variation is the high proportion of SiO_2 and Na_2O and low MgO . There is also a slight increase in Al_2O_3 . The kimberlite clearly plots within the Group II kimberlite fields as shown in figure 4.8. Sample VSPD-9 shows very low SiO_2 with elevated CaO contents. This is similar to samples C6- 607, -552, -540 and C7-375 from the Lace kimberlite, which are interpreted petrographically to be as a result of crustal contamination by carbonate xenoliths and is discussed later for Lace. The major element variation observed at the Voorspoed pipe is consistent with the more evolved Group II kimberlite as discussed above and shown in figure 4.8. The decrease in MgO is coupled with a decrease in Ni ppm, as shown in figure 4.9.

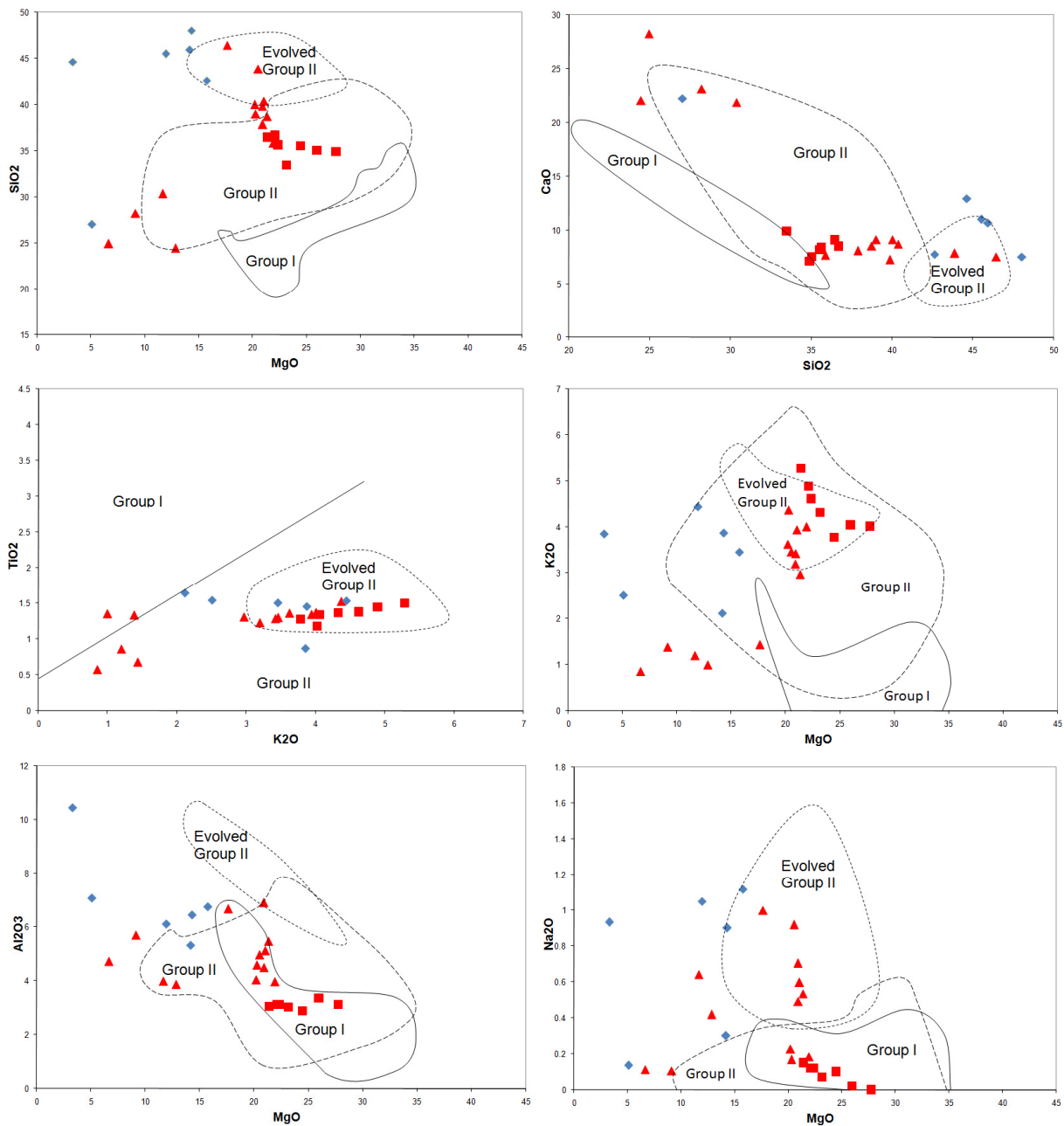


Figure 4.8 Geochemical variation of the Lace and Voorspoed kimberlites. Lace Dump represents the HKt; Lace Core represents the HKtB. Group I and Group II kimberlite field from data presented by Fraser and Hawkesworth (1992), Mitchell (1995), le Roex et al. (2003), Becker and Le Roex (2006), Coe et al. (2008). Chemistry given as wt%. Blue diamonds: Voorspoed. Red Squares: Lace HKt. Red triangles: Lace HKtB.

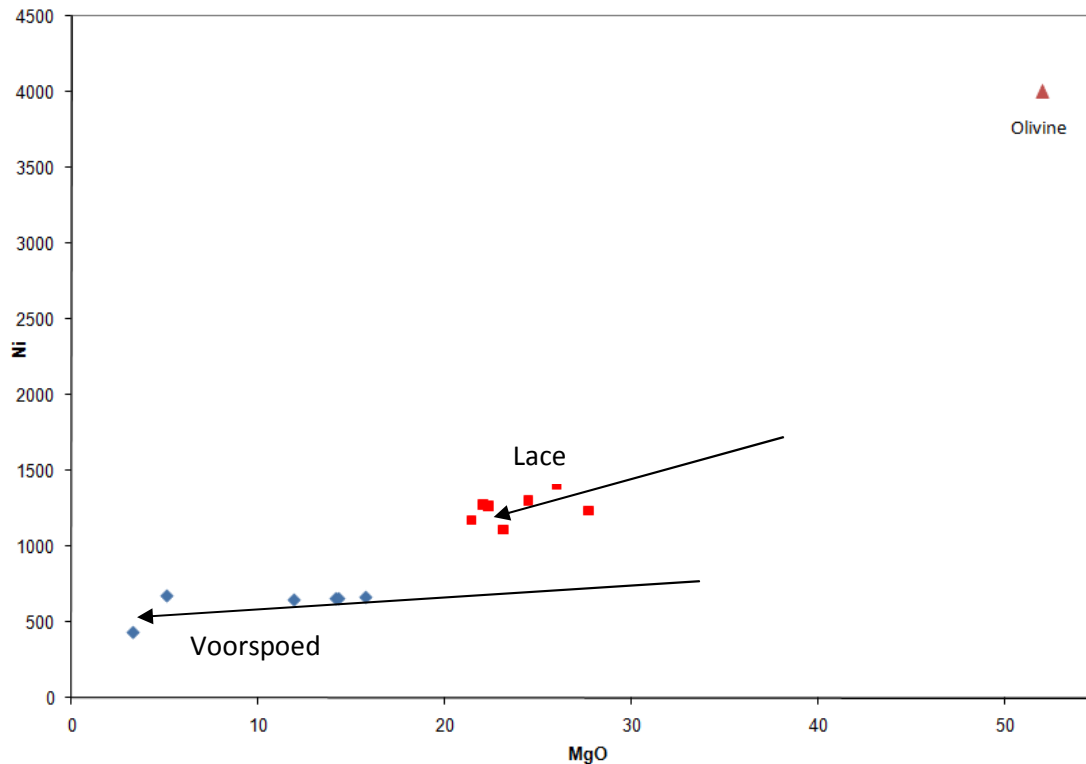


Figure 4.9 Variation diagram showing Ni vs. MgO, evidence for fractional crystallisation of olivine at Lace and Voorspoed. Note the trends away from olivine composition, although it seems likely that olivine is not the only phase fractionating as the trend is not directly away from olivine. MgO given as wt% and Ni as parts per million.

4.3.6.2 Lace Kimberlite

The Lace kimberlite is infilled with hypabyssal transitional kimberlite (HKt), which shows some petrographic variation with depth. This variation is to kimberlite texturally and mineralogically more similar to typical HK, although it still contains characteristics of HKt as discussed in section 3. No HK *sensu stricto* has been observed in situ within the pipe. A number of samples have been collected from the surrounding dump sites, which show characteristics of HK proper. These samples have also been analysed here, as it is expected that at depth in the pipe the kimberlite will likely grade into kimberlite very similar to the dump samples. It is unclear where the dump samples originated and they may be from either a late stage intrusion within the pipe or from a sill in the country rock, although no sills have been documented at the mine. Therefore it is more likely that the samples are from a later stage intrusion, which reached nearer the surface than the HKt observed.

The Lace kimberlite HKt clearly shows a positive relationship between SiO₂ and Na₂O with decreasing Al₂O₃ as shown in figure 4.8; 4.11 and 4.12. The samples from the in situ HKtB from the core show progressive increase in SiO₂, Na₂O and Al₂O₃. This progressive increase is also accompanied by an increase in country rock xenolith (CRX) content as well as microlitic clinopyroxene. Niobium contents clearly decrease with increasing SiO₂ and Al₂O₃ whereas other incompatible elements such as TiO₂ and V contents remain constant. Four of the core samples analysed show very low SiO₂ relative to Group II kimberlites in general, which is accompanied by a very high CaO content and very high loss of ignition (LOI).

Major element variation for the dump samples show geochemistry similar to typical unevolved Group II kimberlites (figure 4.8). The samples of HK/HKt collected from the dump contain very little xenolith material and three of the samples analysed from the core (C7-713, -607, -338) consistently plot within the dump sample trends. These core samples are included in this discussion. The samples show a slight increase (3 wt. %) in SiO₂ and a very minor increase in Na₂O (0.22 wt. %) relative to a decrease in MgO content of approximately 8 wt. % and a minor decrease in Al₂O₃. There is no relationship with the Nb although two of the samples contain very low Nb, which is more similar to the Nb contents observed in the core samples at high SiO₂. The major element relationship of SiO₂ and Na₂O is similar to that observed in the core samples but not nearly as pronounced as shown in figures 4.11 and 4.12. Furthermore Al₂O₃ contents decrease with increasing Na₂O, which is the opposite too the HKtB core samples. Ni ppm shows progressive decrease in relation to MgO as shown in figure 4.9.

4.3.7 Evolution of the Magma at the Kroonstad Cluster

The Kroonstad kimberlite cluster shows progressive evolution of the magma from the unevolved Lace kimberlite to the intermediate Voorspoed kimberlite to the highly evolved Besterskraal kimberlite. This is clearly observed in the geochemistry and the mineralogy of the former. No geochemical data is available for the Besterskraal kimberlite, however the mineralogy clearly indicates the highly evolved nature. The Lace kimberlite dump samples (uncontaminated samples) show major element variation, which all plot within the unevolved Group II kimberlite field as shown in figure 4.8. Increases in SiO₂ and Na₂O are noted with

decreasing MgO at Lace. The Voorspoed kimberlite consistently plots within the evolved Group II fields in figure 4.8 and is characterised by high SiO₂ and Na₂O and low MgO relative to typical Group II kimberlites.

4.3.8 Geochemical Evidence for Fractional Crystallisation

Crystal fractionation has been proposed by numerous authors based on detailed geochemical studies on kimberlites (Fraser and Hawkesworth, 1992; le Roex et al. 2003; Harris et al. 2004; Becker and le Roex, 2006 and Coe et al. 2008). Fractional crystallisation processes generally lead to depletion in MgO and Ni as a result of the loss of olivine from the magma (le Roex, 2003). Fractional crystallisation has clearly occurred at the Lace and Voorspoed kimberlites, which show similar geochemical trends as show in figure 4.10. Coe et al. (2008) show that along with MgO, SiO₂ is also depleted with Al₂O₃ and K₂O remaining constant at the Star and Swartruggens dikes. The trend at the Lace kimberlite is to slightly enriched SiO₂ and FeO_T, slight depletion in Al₂O₃ and enriched K₂O. The trend of increasing SiO₂ is anomalous for crystal fractionation but can be explained by other processes, such as CO₂ degassing as discussed below. The trends discussed above are consistent with the fractionation of olivine and possibly minor phlogopite, which is similar to trends discussed by Harris et al. (2004). The dramatic enrichment in K₂O can only be explained by the concentration of K₂O in phlogopite crystallising in the residual magma. Coe et al. (2008) interpret the constant K₂O and Al₂O₃ trend to indicate a certain proportion of phlogopite fractionation. However the K₂O and Al₂O₃ trends observed for the Lace kimberlite are opposite. The slight decrease in Al₂O₃ may indicate some phlogopite fractionation (Harris et al. 2004), although calculating the proportion is not possible as the sample set is not large enough to produce a consistent linear trend. Furthermore an increase in FeO_T is likely a result of fractionation of a Fe-free groundmass phase, which le Roex (2003) interpret to be calcite. Further detailed geochemical work needs to be done on the Kroonstad Cluster to constrain the fractional crystallisation processes as a detailed analysis of the fractionation processes occurring is outside the scope of this study.

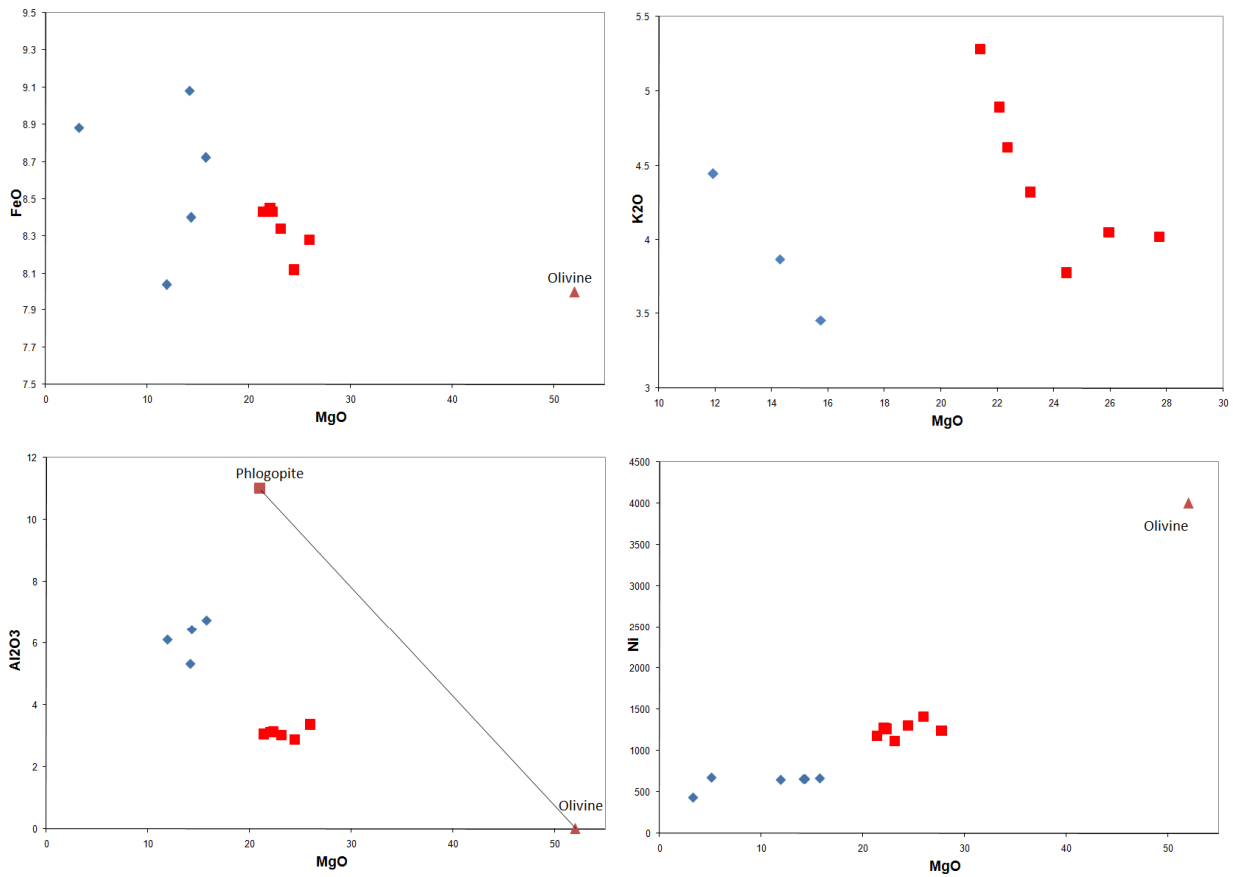


Figure 4.10 Geochemical variation diagrams showing trends interpreted to result from fractional crystallisation of olivine and possibly minor phlogopite. Red squares: Lacey HKt. Blue Diamonds: Voorspoed.

It must be highlighted here that the above discussed trends are for the uncontaminated samples, as discussed in section 4.3.5.2. The contaminated Lacey core samples trends are based on a small set of data but the fractional crystallisation processes has also been identified petrographically by the low proportions of olivine in the HK, as discussed in section 3.

4.3.9 Geochemical Variation at the Lacey Kimberlite

Geochemical variation observed for the Lacey kimberlite indicates two distinct trends. Figures 4.11 and 4.12 clearly show the two trends: 1) firstly a trend showing dramatic increase in SiO₂, Na₂O and Al₂O₃ and 2) a trend showing a slight increase in SiO₂ and Na₂O at decreasing Al₂O₃. The MgO variation is controlled by fractional crystallisation of olivine as

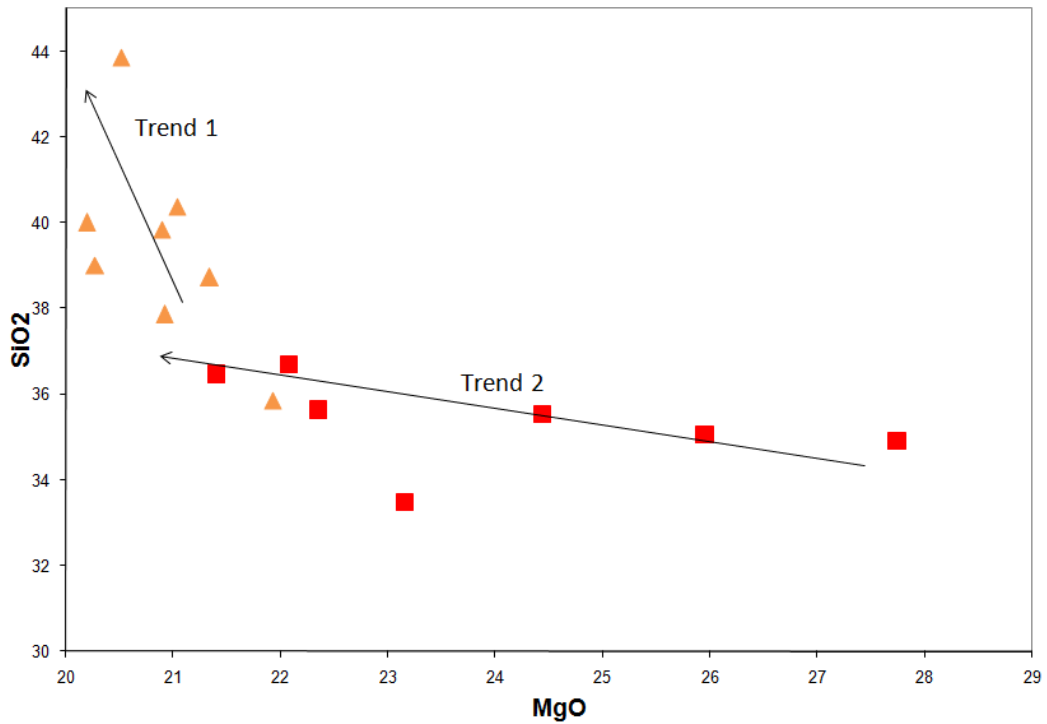
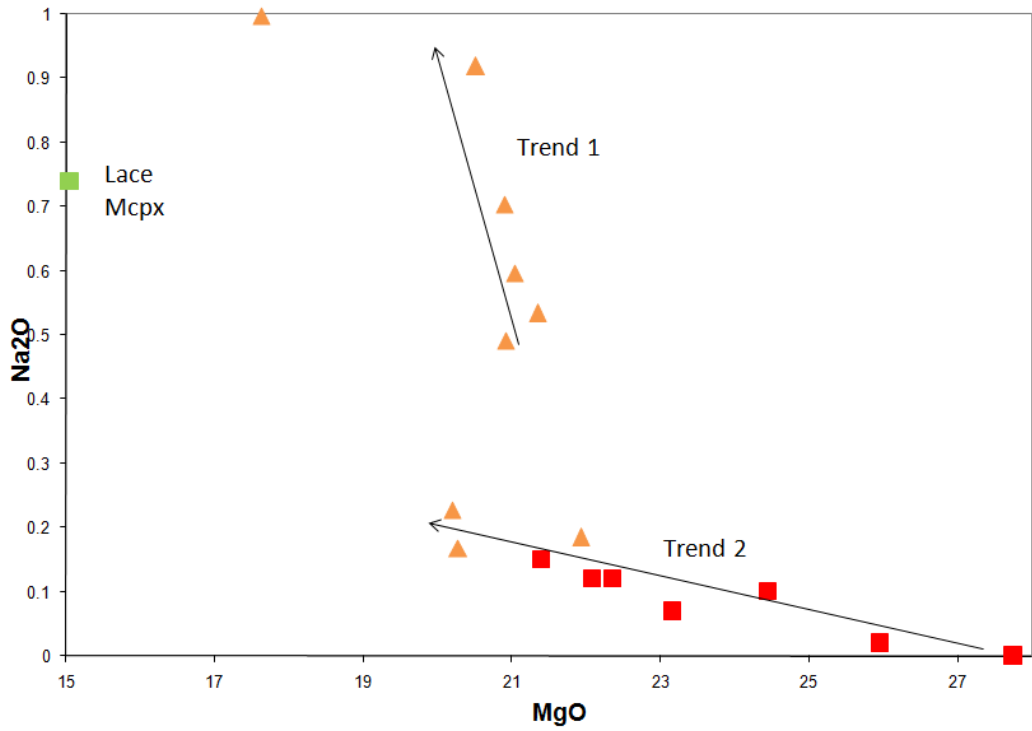


Figure 4.11 Geochemical variation diagrams for the Lace kimberlite HKt (red squares) and Lace kimberlite HKtB (orange triangles). Note the composition of microlitic clinopyroxene plotted on the diagram. This is an average composition from all the Lace HKt microlitic clinopyroxene data. Trend 1 indicates crustal contamination. Trend 2 is interpreted to indicate CO₂ degassing.

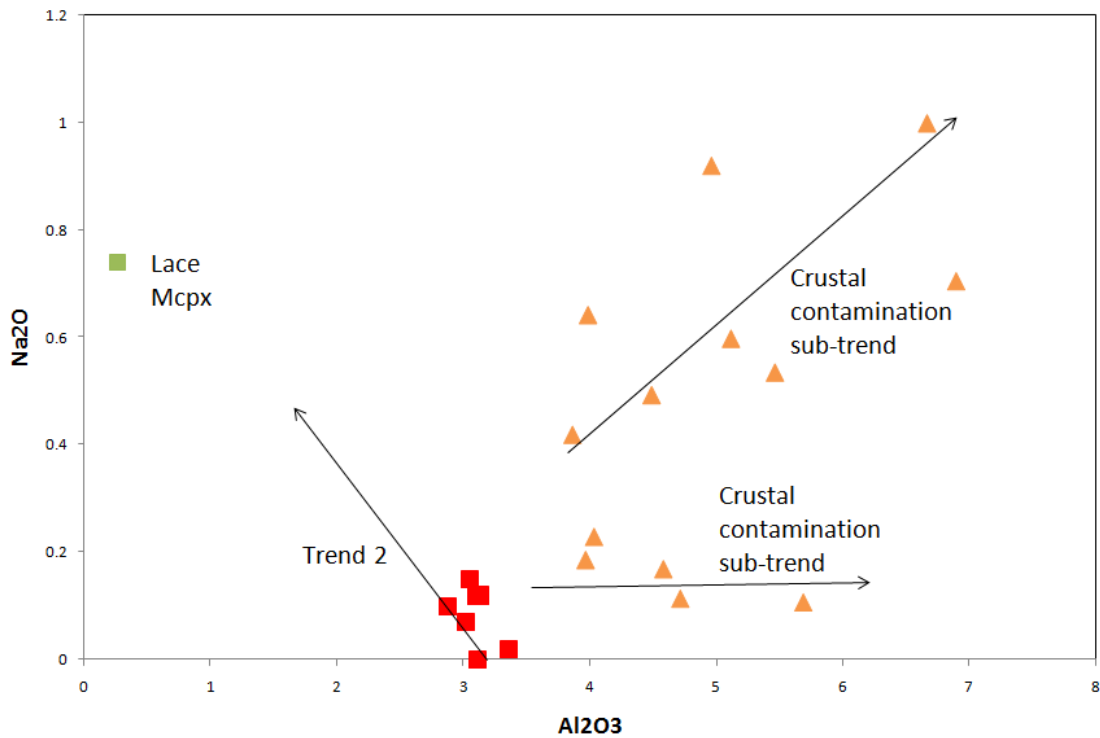
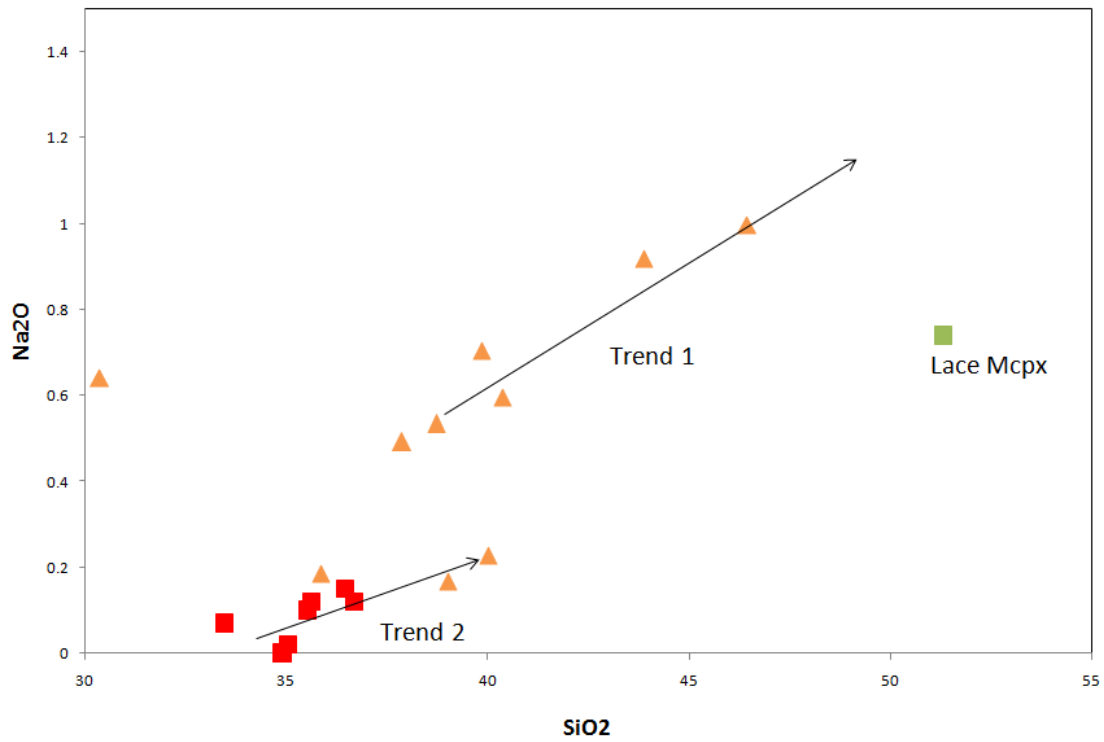


Figure 4.12 Geochemical variation diagrams for the Lace kimberlite HKt (red squares) and Lace kimberlite HKtB (orange triangles). Note the composition of microlitic clinopyroxene plotted on the diagram. This is an average composition from all the Lace HKt microlitic clinopyroxene data. Trend 1 indicates crystal contamination. Trend 2 is interpreted to indicate CO₂ degassing. Note the sub-trends of crustal contamination in the bottom diagram.

discussed above. The first trend is observed for the HKtB, which contain high proportions of country rock material. This trend is simply interpreted to result from crustal contamination. The second trend for the HKt can not be explained similarly to trend 1 as the HK/HKt contains insignificant proportions of crustal material, however the trend is linked petrographically to the increase in microlitic clinopyroxene abundance. Furthermore microlitic clinopyroxene compositions are plotted on the variation diagrams, which indicate some control on the geochemistry by the clinopyroxene. Mitchell et al. (2009) states that microlitic clinopyroxene can crystallise as a result of either 1) crustal contamination or 2) CO₂ degassing. Skinner and Marsh (2004) show that; degassing of CO₂ can induce the crystallisation of microlitic clinopyroxene in tuffisitic kimberlites. It seems likely that both these mechanisms for clinopyroxene crystallisation have occurred at the Lace kimberlite as discussed below.

4.3.9.1 Geochemical Variation of Hypabyssal Transitional Kimberlite Breccia (HKtB): Crustal Contamination (Samples: C6-713 – C6 338)

Figures 4.11 and 4.12 clearly show trend 1, which is characterised by dramatic increase in SiO₂, Na₂O and Al₂O₃. Typical contamination by crustal material is characterised by an increase in these three components (Clement, 1982; le Roex et al. 2003 and Becker and le Roex, 2006). In the case of the Lace HKtB it is clear that trend 1 is a result of crustal contamination. Furthermore figure 4.12 show that trend 1 can be sub-divided into two sub-trends based on the Al₂O₃ and Na₂O variation, which is likely the result of a variation in the geochemistry of the country rock incorporated into the magma. A similar trend and conclusion is given by Nowicki et al. (2008) for VK kimberlite containing high proportions of xenolithic material at Lace de Gras. Furthermore four samples show a clear contamination by carbonate xenoliths, which has resulted in low SiO₂ (approximately 25%) and high CaO (approximately 22%). Therefore the crystallisation of microlitic clinopyroxene in these rocks is likely related to crustal contamination. CO₂ degassing may play a role as well however the abundant crustal xenolith material suggests contamination is the dominant factor in these rocks.

4.3.9.2 Geochemical Variation of Hypabyssal Transitional Kimberlite (HKt): CO₂ Degassing (Samples: K2-1 – K2-10 and K2-C)

The HKt does not contain significant proportions of xenolithic material and therefore a similar crustal contamination is not occurring. Microlitic clinopyroxene is observed petrographically and is found to correlate with the geochemistry of individual samples (e.g. samples with higher SiO₂ contain higher proportions of clinopyroxene). Furthermore extrapolation of trend 2 is toward the average microlitic clinopyroxene composition as shown in figures 4.11 and 4.12. Therefore it seems likely that this trend is controlled by the crystallisation of microlitic clinopyroxene. Microlitic clinopyroxene can crystallise through two mechanisms: 1) crustal contamination or 2) CO₂ degassing (Mitchell et al. 2009). However there is an insignificant amount of xenolithic material in these rocks. Therefore the crystallisation of clinopyroxene in the HKt is likely the result of CO₂ degassing. Unfortunately CO₂ analysis could not be done on the Lace samples. Trend 2 does not show an increase in Al₂O₃, which further suggests that crustal contamination is not the control on the geochemistry as one would expect the Al₂O₃ content to increase with increasing SiO₂ and Na₂O. The increased SiO₂ and Na₂O contents indicate that these components are being added to the magma. This is not through crustal contamination as there are insignificant proportions of xenolith material in these rocks. A possible hypothesis, based on stable isotope work by Sheppard and Dawson (1975), is the influx of an aqueous fluid at depth during the formation of the embryonic pipe. This hypothesis is discussed in section 5.3 and 6.1 for the formation of initial embryonic pipes at the Kroonstad cluster.

4.3.10 Comparison with Wesselton and Dutoitspan Kimberlites

Comparison of the geochemical trends obtained above with geochemistry of the Wesselton and Dutoitspan kimberlites from Clement (1982) show very similar trends. The Wesselton and Dutoitspan kimberlites are Group I kimberlites but are compared with the Kroonstad cluster due to the availability of CO₂ data. Figure 4.13 show the geochemical variation observed for the Wesselton and Dutoitspan kimberlites. Two trends are identified again: 1) a trend very similar to trend 1 at Lace with an increase in SiO₂, Al₂O₃ and Na₂O and 2) a trend of increasing SiO₂ with subsequent decrease in Al₂O₃ and TiO₂. The former trend is observed for samples of TKB and HKB (high CRX proportion) whereas the latter trend is observed for

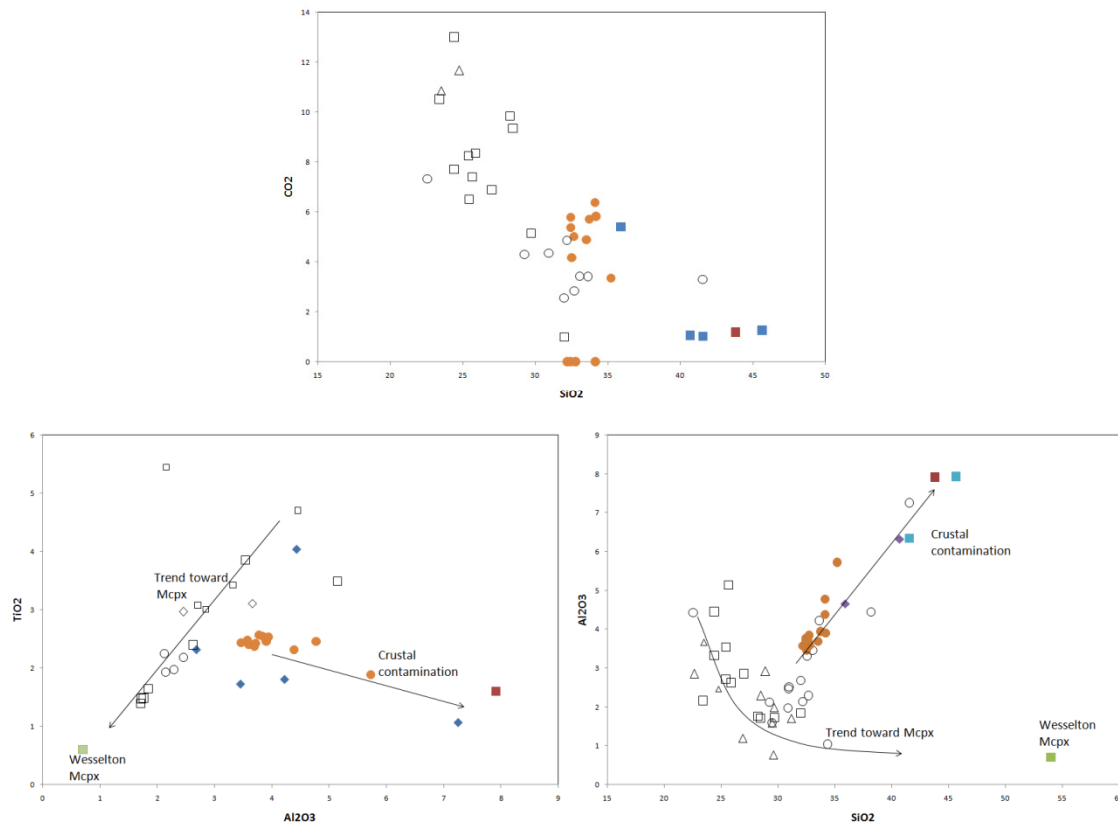


Figure 4.13 Geochemical variation diagrams for the Wesselton and Dutoitspan kimberlites. Open symbols represent intrusive dike/sills (Clement, 1982) and root zone hypabyssal kimberlite (Clement, 1982). Closed symbols represent TKB (Clement, 1982) and Nucleated Autoliths, closed circles, (Danchin et al. 1975). Note the composition of microlitic clinopyroxene plotted on the diagrams. Microlitic clinopyroxene data from Mitchell et al. (2009) for the Wesselton kimberlite.

HK and intrusive dike/sill samples (low CRX proportion). Therefore the first trend is similar to trend 1 at Lace and is controlled by crustal contamination. The latter trend for the Wesselton and Dutoitspan kimberlites is again extrapolated and microlitic clinopyroxene compositions for the Wesselton kimberlite (Mitchell et al. 2009) plot on these extrapolated trends as shown in figure 4.13. Therefore similar to trend 2 at Lace this latter trend for Wesselton and Dutoitspan is likely controlled by microlitic clinopyroxene. Microlitic clinopyroxene is likely formed during CO₂ degassing as the crustal xenolith proportion is very low in these rocks (Clement, 1982). CO₂ clearly is decreasing from the sill/dike samples to the pipe root zone hypabyssal samples, which indicates that CO₂ has degassed from the pipe root zone samples as shown in figure 4.13. CO₂ clearly correlates with increasing SiO₂,

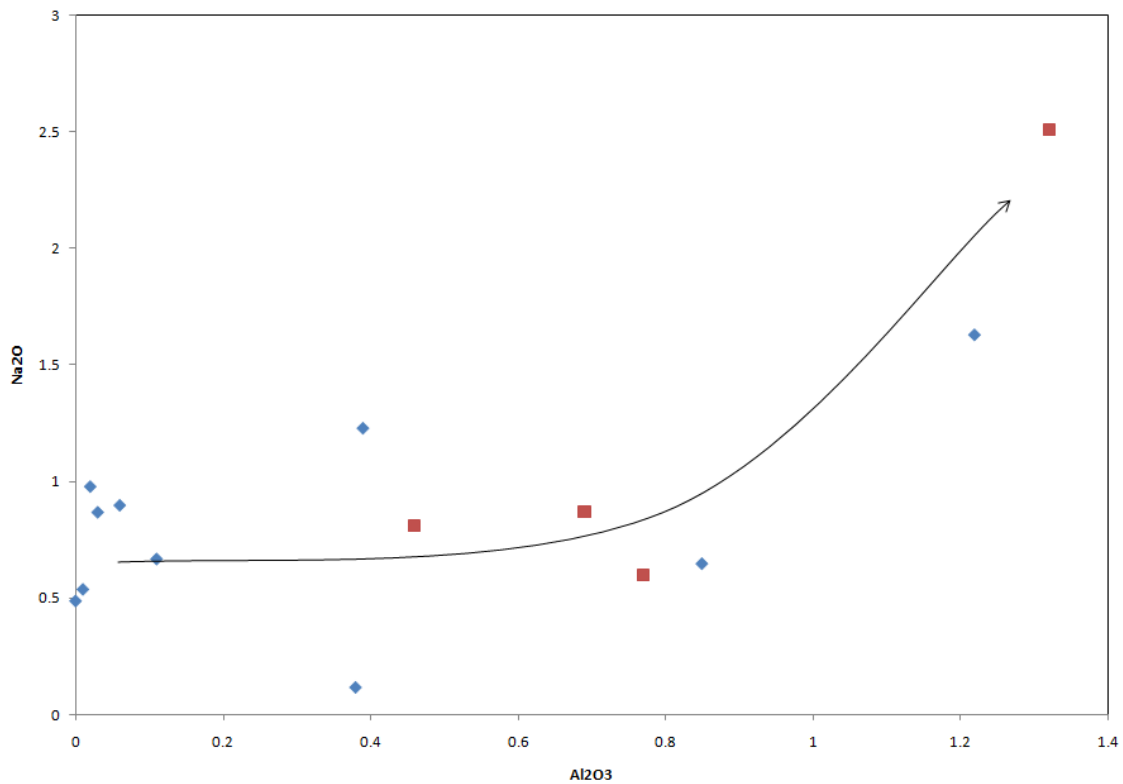


Figure 4.14 Compositional variation of microlitic clinopyroxene. Data from Skinner and Scott (1979) and Mitchell et al. (2009). Note the possible trend of increasing Na₂O and Al₂O₃.

as shown in figure 4.13. Therefore it can be concluded here that the geochemical trends are clearly controlled by crustal contamination for the xenolith-rich TKB and HKB whereas the geochemical trend observed for the xenolith-poor HK is controlled by microlitic clinopyroxene crystallising as a result of CO₂ degassing.

It seems highly likely that a similar conclusion of CO₂ degassing can be made for the Lace trend 2 based on the trends observed for the Wesselton and Dutoitspan kimberlites, the correlation of microlitic clinopyroxene with the geochemical variation at Lace and the lack of Al₂O₃ enrichment at Lace.

4.3.11 Implications on Microlitic Clinopyroxene Compositions

Microlitic clinopyroxene shows some subtle variation in composition as discussed in section 4.2. However conclusions on this variation have not been interpreted in any current literature. As discussed above Mitchell et al. (2009) state that microlitic clinopyroxene can crystallise by two mechanisms: 1) crustal contamination and 2) CO₂ degassing. Analysis of the compositional data for microlitic clinopyroxene from Skinner and Scott (1979), Mitchell et al. (2009) and this study may indicate a possible link between clinopyroxene data and their mechanism of formation. Figure 4.14 shows the variation in Na₂O and Al₂O₃ contents of microlitic clinopyroxene. SiO₂ content does not show significant variation. Mitchell et al. (2009) states that; CO₂ degassing would result in a late stage magma fluid with composition H₂O, K₂O, CaO and MgO rich as well as being SiO₂-bearing. Therefore the possible correlation of increasing Al₂O₃ and Na₂O contents of the microlitic clinopyroxene may be attributed to formation by crustal contamination of the magma, which would introduce Na₂O and Al₂O₃ into the system. This is only the case for the microlitic clinopyroxene compositions containing high Al₂O₃ and Na₂O. The majority of the compositional data presented by Skinner and Scott (1979) and Mitchell et al. (2009) do not show high Na₂O and Al₂O₃, which indicates that CO₂ degassing may be the dominant mechanism for their formation. These conclusions are again speculative and further detailed petrographic and mineral chemistry analysis is required.

4.4 Summary

4.4.1 Evolution of the Magma

Mineral composition and bulk rock analysis of selected samples from the Kroonstad kimberlite cluster clearly indicate an evolution of the magma from the unevolved Lace kimberlite to the intermediately evolved Voorspoed pipe to the highly evolved Besterskraal kimberlite. The Lace kimberlite is characterised by geochemistry, which is typical of unevolved Group II kimberlites. SiO₂ and Na₂O contents are low relative to the Voorspoed pipe. Furthermore the Lace pipe HK is classified as a macrocrystic melilite- and apatite-bearing, monticellite, phlogopite hypabyssal kimberlite, which does not contain any of the evolved type minerals. None of the evolved kimberlite indicator minerals are present at Lace, which compliments the geochemistry. In contrast the Voorspoed kimberlite is characterised

by the presence of aegirine, sanidine and abundant primary diopside, which indicates some evolution of the magma relative to the Lace HK. This is confirmed by analysis of the geochemistry, which clearly shows an increase in SiO_2 and Na_2O . However the Voorspoed pipe is not a typical highly evolved type end member of the evolution. The lack of the highly evolved type minerals such as K-richterite and leucite indicate that the Voorspoed magma had an intermediate evolution, which is also indicated by intermediate phlogopite compositions. The Besterskraal North HK is clearly a highly evolved end member of Group II magma evolution. The HK is characterised by abundant primary diopside, sanidine, aegirine, K-richterite and leucite. Geochemistry data is not available but it is expected that SiO_2 in particular would increase relative to the Voorspoed pipe HK due to the high abundances of the above mentioned minerals.

Fractional crystallisation has clearly affected all the HK varieties to some degree. Fractional crystallisation is identified geochemically as well as petrographically. The Lace HK shows minor fractional crystallisation of olivine has occurred as the HK is still macrocrystic but contains approximately 35 vol. % olivine, which indicates a loss of approximately 15 vol. % of olivine as described by Mitchell (2008). The Voorspoed and Besterskraal HK are both aphanitic indicating that fractional crystallisation of the olivine may have been relatively extensive. The petrogenesis of the magma at the Kroonstad cluster is outside the scope of this study but the evidence for fractional crystallisation may indicate some differentiation of the magma has occurred at depth during the ascent of the magma. Mitchell (1995) suggests that evolved Group II magmas are differentiates of unevolved type magmas due to the absence of diamonds, paucity of macrocrystic olivine, assemblage of primary minerals and their evolutionary trends. Therefore the Kroonstad cluster kimberlites may show varying degrees of differentiation of a Group II magma.

4.4.2 Microlitic Clinopyroxene

Microlitic clinopyroxene has been found to be the controlling factor for the geochemistry of the HKt (uncontaminated dump samples) at the Lace kimberlite. Refer to table 4.1 for microlitic clinopyroxene compositions and figure 4.12 for geochemical variations. Subtle trends for increasing SiO_2 , Na_2O and decreasing Al_2O_3 clearly indicate that crustal

contamination by the assimilation of xenolithic material is not responsible for the geochemical variation of the HKt. This is further confirmed by the low Clement C.I. and by comparing the chemistry with the contamination technique of Kjarsgaard et al. (2009). Skinner and Marsh (2004) and Mitchell et al. (2009) show that microlitic clinopyroxene may form as a result of CO₂ degassing of the magma. Therefore the geochemical trends observed, which are linked to microlitic clinopyroxene, must result from CO₂ degassing. This is confirmed by comparison of the Lace data to data from Wesselton and Dutoitspan, which clearly show CO₂ degassing trends. Furthermore some initial observations may indicate that microlitic clinopyroxene compositions may vary depending on the mechanism of formation. Microlitic clinopyroxene forming due to CO₂ degassing is likely to have low Na₂O and Al₂O₃ as no new material is added to the magma whereas microlitic clinopyroxene forming as a result of crustal contamination may have elevated Na₂O and Al₂O₃ due to the addition of crustal material.

Section 5. Discussion

5.1 Erosion Estimate for the Kroonstad Kimberlite Cluster

Post-emplacment erosion at the Kroonstad cluster is based on the xenolith population within the pipe. The Karoo Supergroup basalts and sandstone are used, which can be correlated with the in situ stratigraphy in South Africa. Two methods of erosion estimation have been developed by Hanson (2006) along with a third method using denudation rates will be used here to estimate post-emplacment erosion at the Kroonstad cluster. Geochemical data for the basalt xenoliths at the Kroonstad cluster are presented by Roberts (1997), Hanson (2006) and Howarth (2007) and sandstone data from Hanson (2006) and Howarth (2007). These xenoliths analysed represent the now eroded part of the Karoo stratigraphy and are used to re-create the stratigraphy at the Kroonstad cluster during emplacements of the pipes. See table 1.1 for a summary of the country rock stratigraphy in the Kroonstad area.

5.1.1 Methodologies for Estimating Erosion

Method 1: The thickness of the original stratigraphy represented by the xenoliths can be calculated by using documented thicknesses and thinning rates for the specific Karoo Supergroup units. This allows for the re-creation of the original stratigraphy and the extent of post-emplacment erosion is calculated in the process.

Method 2: This method is slightly less complex and simply takes into account the current elevation above sea level of the cluster and the current elevation of the youngest unit represented by the xenoliths analysed. This method provides a reasonable estimate for a minimum erosion estimate as it is likely that the Lesotho Formation has undergone some extent of erosion since the emplacements of the Kroonstad cluster, as discussed below for basalt xenolith correlation.

Method 3: This is a simple method based on the denudation rates calculated by Hanson (2006) for scarp retreatment between 140Ma and present. The denudation rate varies slightly with original rates of 16m/Ma between 140-85 Ma and 10m/Ma from 85 Ma to present. The Kroonstad kimberlite pipes are 133Ma (Phillips et al. 1998) and a simple calculation can be done to give an estimate of the post-emplacment erosion.

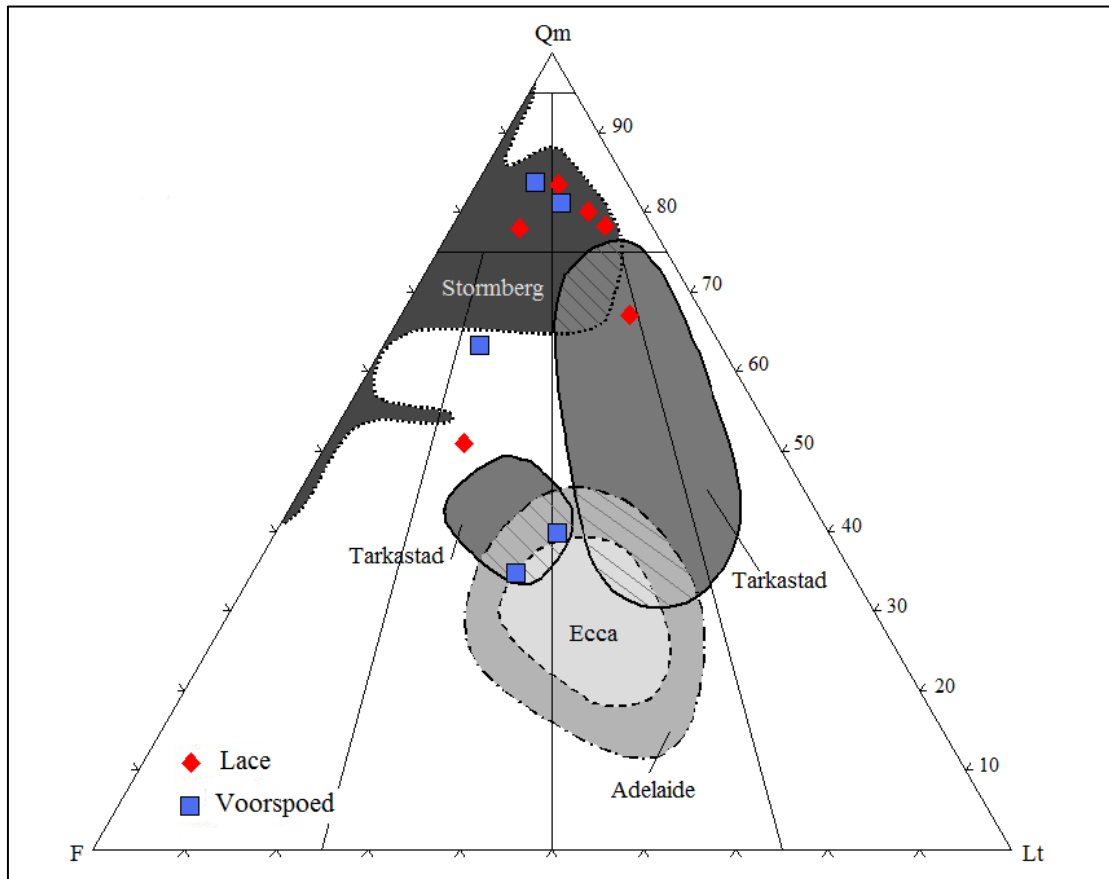


Figure 5.1 Ternary diagram showing point count results and Karoo Supergroup correlation for sandstone xenoliths from the Voorspoed and Lace pipe VK. Qm: Monocrystalline quartz; F: Feldspar and Lt: Lithic fragments. Diagram after Hanson (2006) and Howarth (2007).

5.1.2 Karoo Supergroup Xenolith Correlation

5.1.2.1 Sandstone Xenoliths

Sandstone xenoliths from the Voorspoed and Lace pipes have been analysed by Hanson (2006) and Howarth (2007) respectively and similar results are observed. Figure 5.1 shows the combined data from Hanson (2006) and Howarth (2007). The xenoliths analysed represent a full sequence of Karoo sedimentary rocks from the Eccca/lower Beaufort, upper Beaufort and Stormberg Groups. A full sequence of Karoo sedimentary rocks needs to be considered during the estimation of erosion. The Clarens Formation sandstone xenoliths generally contain very little to no lithic fragments. The xenoliths analysed with greater lithic fragment abundances in the Stormberg field are most likely Molteno or Elliott in origin.

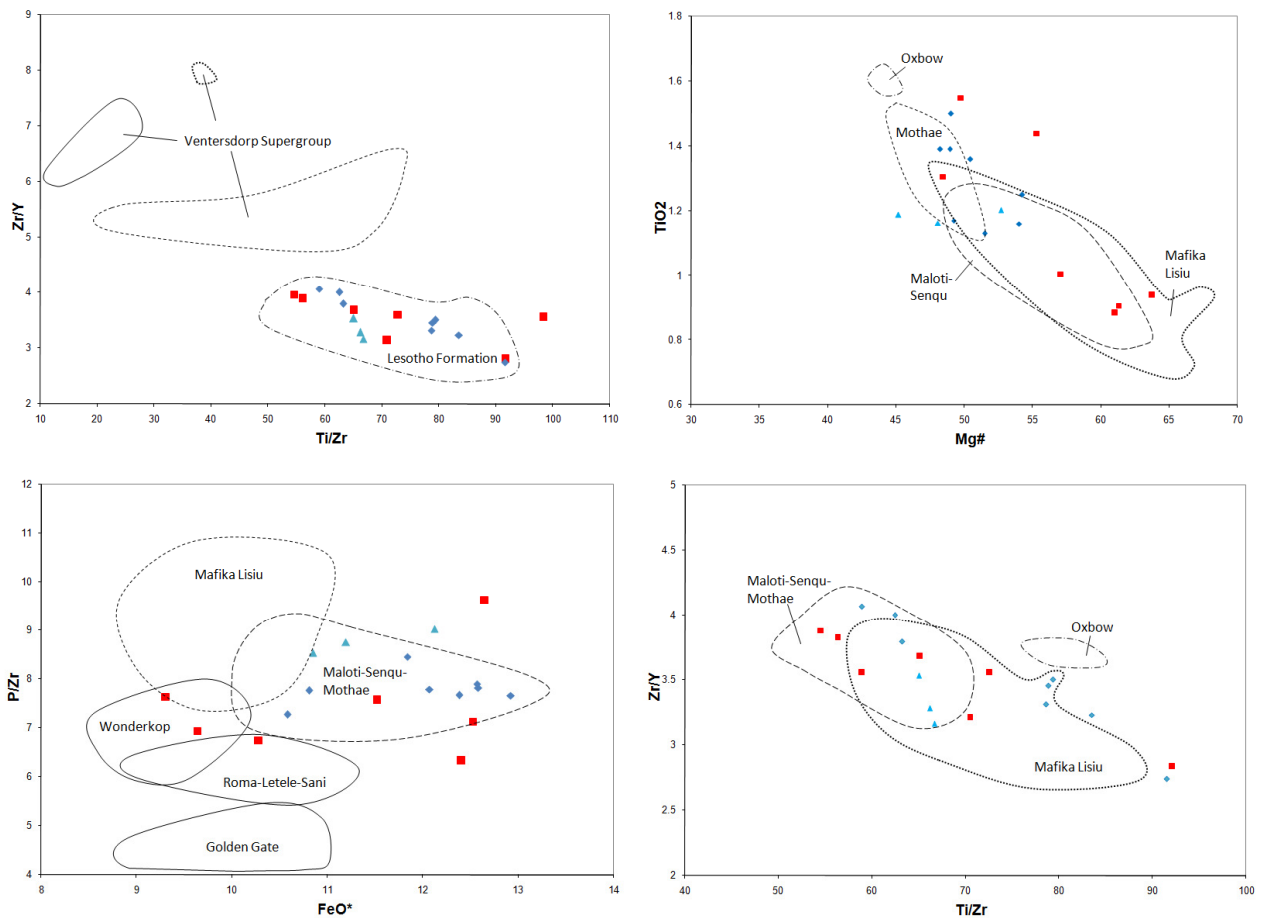


Figure 5.2 Geochemistry variation diagrams showing the geochemistry and Karoo Supergroup correlation of the basalt xenoliths from the Lace and Voorspoed VK. Lesotho Formation fields from Marsh et al. (1997) and Marsh (1998). Venterdorp fields from Crow and Condie (1988). Lace: Red squares (data from Howarth, 2007). Voorspoed: Blue triangles (data from Roberts, 1997) and Blue diamonds (data from Hanson, 2006).

5.1.2.2 Basalt Xenoliths

Basalt xenoliths present within kimberlite pipes in South Africa have two origins, firstly from the Venterdorp Supergroup and secondly the Karoo Supergroup. The Venterdorp Supergroup xenoliths have distinct geochemistry, which is easily distinguished from the Karoo basalt. Venterdorp basalt is typically easily identified in hand specimen by the green nature whereas Karoo basalt is generally amygdaloidal purple to red/brown.

Re-evaluation of the geochemical data present by Roberts (1997), Hanson (2006) and Howarth (2007) indicate a dominance of the upper Lesotho Formation basalts of the Maloti,

Senqu and Mothae units. Two of the xenoliths have less evolved geochemistry and are more similar to the lower Lesotho Formation and Barkley East Formation chemistry. One of these xenoliths is correlated with the lower Lesotho Formation Mafika Lisiu unit and the other with the upper Barkley East Formation (Wonderkop unit). Furthermore several xenoliths show geochemical trends, which are more similar to the oxbow series of dikes, which show compositions more evolved than the documented basalts. These xenoliths may represent basalt units, which have been completely eroded from the stratigraphy since the emplacement of the Karoo basalt. Hence the use of Method 2 for a minimum erosion estimate only, as it is likely the basalt would have been more extensive at the time of emplacement and therefore the elevation would have been lowered post-emplacement.

5.1.3 Erosion Estimation

5.1.3.1 Method 1: Palaeo-stratigraphy of the Karoo Supergroup

Karoo Supergroup Sedimentary Sequences

The sedimentary sequences present at the time of emplacement of the Kroonstad kimberlite pipes include the Volksrust Formation (Ecca), Normandien Formation (lower Beaufort), Tarkastad Subgroup (upper Beaufort), and Molteno/Elliott/Clarens Formations (Stormberg), as indicated by the xenoliths present within the pipe infill. Thinning rates for each of the units can be calculated by comparing the thickness in the south and north. Table 5.1 gives the calculated thinning rates and estimated thicknesses of each unit extrapolated to the Kroonstad cluster. The thinning rates are calculated as thinning into the north, which is clearly evident from all the units within the Karoo Supergroup. The Kroonstad cluster lies just to the west of the extreme north of the Karoo basin. Thinning rates are calculated for the extreme north of the Karoo basin and thinning rates to the west (i.e. to the Kroonstad cluster) are assumed to be insignificant.

The local geology at surface at the Kroonstad cluster varies from east to west. In the east the pipes are exposed in the Volksrust Formation whereas in the west they are exposed in the Vryheid Formation. The estimated thickness of the Ecca Group at the time of emplacement is taken as the thickness of the Volksrust Formation in the area as the cluster is situated on the

Table 5.1 Calculation of Karoo Supergroup sedimentary unit thinning rates and projected thicknesses used in erosion estimate method 1. (See text for references of thicknesses of the units). See table 1.1 for the full country rock stratigraphy in the Kroonstad area and figure 1.4 for their distribution.

	Maximum	Minimum (north basin)	Thinning Rate	Distance to KCC	Projected Thickness at KCC
Stormberg Group					
Clarens Formation	300m	100m	0.7m/km	140km	5m
Elliott Formation Upper Lower	150m 300m	50m 50m	0.3m/km 0.8m/km	125km 125km	10m 0m
Molteno Formation	600m	10m	1.6m/km	100km	0m
Beaufort Group					
Tarkastad Subgroup	800m (central basin)	150m	2.2m/km	60km	20m
Adelaide Subgroup	800m (central basin)	200m	2m/km	0km	200m
Ecca Group					
Volksrust Formation		100m		0km	100m

contact between the Vryheid and Volksrust Formations. This thickness is approximately 100m (Tavenor-Smith, 1988 and Johnson et al. 2006). The overlying, lower Beaufort, Normandien Formation has a maximum thickness of 320m in the type area (Groenewald, 1989 and Johnson et al. 2006) but is approximately 200m in the proximity of the Kroonstad cluster (Johnson et al. 2006). The Kroonstad cluster lies directly to the west of the current outcrop and it is assumed that the thickness of the current outcrop would have been similar to the thickness at the time of emplacement. An estimate of 200m is used for the Adelaide (Normandien Formation) Subgroup. The Tarkastad Subgroup has a maximum thickness in the south of 2000m and thins to 800m in the centre of the basin and thins further to 150m in the north (Johnson et al. 1996 and Johnson et al. 2006). A thinning rate of approximately 2.2m/km is calculated using these values, which when extrapolated to the Kroonstad cluster indicates a thickness of only 20m at the time of emplacement. The Molteno Formation thins from 600m in the south to 10m in the north (Johnson et al. 2006) and easily pinches out before reaching the Kroonstad cluster. The Elliott Formation thins from approximately 400m in the south to 100m in the north. Bordy et al. (2004) showed that there is a decrease in the

thinning rate between the upper (UEF) and lower (LEF) Elliott Formation from the LEF 0.8m/km (300m in south to 50m in north) to the UEF 0.3m/km (150m in south to 50m in north). Therefore the Elliott Formation is likely to be present at the Kroonstad but would be relatively thin. Only the UEF would be present and approximately 10m thick. The Clarens Formation has a maximum thickness of 300m in the south and thins to 100m in the north (Johnson et al. 2006). Calculating thinning rates indicates that the Clarens Formation would just reach the Kroonstad cluster at approximately 5m thickness.

The approximate thickness of the sedimentary sequence at the Kroonstad cluster would be a combination of the above discussed thicknesses. This gives an approximate value of 335m. This estimate may explain the scarcity of sedimentary xenoliths present within the volcanoclastic kimberlite (VK) infill at the Voorspoed pipe. However the dominance of Stormberg Group xenoliths from the sample set collected at the Kroonstad cluster may indicate that the Stormberg Group was thicker than estimated above. Although, this may be a function of sampling units rich in Stormberg Group sandstones.

Karoo Supergroup Volcanic Sequences

The Karoo Supergroup volcanics are subdivided into two distinct Formations: 1) Barkley East Formation and 2) Lesotho Formation. The basalt has an average thickness of 1800m, although it is dominated by the upper Lesotho Formation (1400m) (Marsh et al. 1997). As discussed above, both the Barkley East Formation (Wonderkop unit only) and the Lesotho Formation basalts have been correlated with xenoliths from the Kroonstad cluster, which are dominated by compositions similar to the upper Maloti-Senqu-Mothae units. A full sequence of Lesotho Formation basalts as well as the upper Barkley East Formation basalts is present as xenoliths within the Kroonstad cluster pipes. Evidence for more evolved type basalt at the Kroonstad cluster may indicate that the original extent of the basalt at the time of emplacement would have been greater than the current extent of the basalt, assuming little thinning of the basalt occurred to the north. Denudation rates above the escarpment are significantly lower than below. Dunlevey et al. (1993) gave an approximate value of 300-400m of erosion over 180Ma post-extrusion of the Karoo basalt. This gives a denudation rate

of 2m/Ma, which indicates approximately 100m of erosion at the Kroonstad area before emplacement of the kimberlite pipes.

The northern most borehole data from the Lesotho Formation in the Oxbow area shows thickness of the units of: Wonderkop-100m; Mafika Lisiu-400m; Maloti-140m; Lower Senqu-360m; Upper Senqu-150m and Mothae-220m (Marsh et al. 1997 and Duncan and Marsh, 2006). The thicknesses are relatively consistent for the boreholes from Oxbow, Mafika Lisiu Pass, Bushman's Pass and Semonkong (Marsh et al. 1997 and Duncan and Marsh, 2006) and are used as estimates for the thickness of basalt at the time of emplacement of the Kroonstad cluster. Furthermore the dolerite in the palaeo-stratigraphy needs to be considered as well. Hawthorne (1975) estimates approximately 200m of dolerite in his model of a kimberlite pipe. Winter and Venter (1970) calculate a ratio of dolerite/sedimentary rocks of 0.3. This is an area of uncertainty for any erosion estimate as the thickness of dolerite sills in the palaeo-stratigraphy is likely to vary widely. An estimate of 100m thickness is used here for the calculation of post-emplacement erosion at the Kroonstad cluster. Based on the thickness calculated for the sedimentary rocks at the time of emplacement, a dolerite thickness of 100m gives a dolerite/sedimentary ratio of approximately 0.3. A combined thickness of approximately 1470m for the dolerite sills, Barkley East and Lesotho Formations is calculated.

Combining the thicknesses of the Karoo sedimentary and volcanic sequences (basalt and dolerite) calculated at the time of emplacement gives an approximate estimate of post-emplacement erosion of 1805m. This estimate must be used with care as it is based largely on the presence of a Karoo basalt sequence, which is similar to that for the Lesotho remnant. This estimate does not take into account the potential thinning of the basalt into the north as possibly indicated by the Springbok Flats basalt (discussed below) This estimate of basalt thickness is a maximum estimate and assumes the thickness of Karoo basalt does not change from the current outcrops toward Kroonstad.

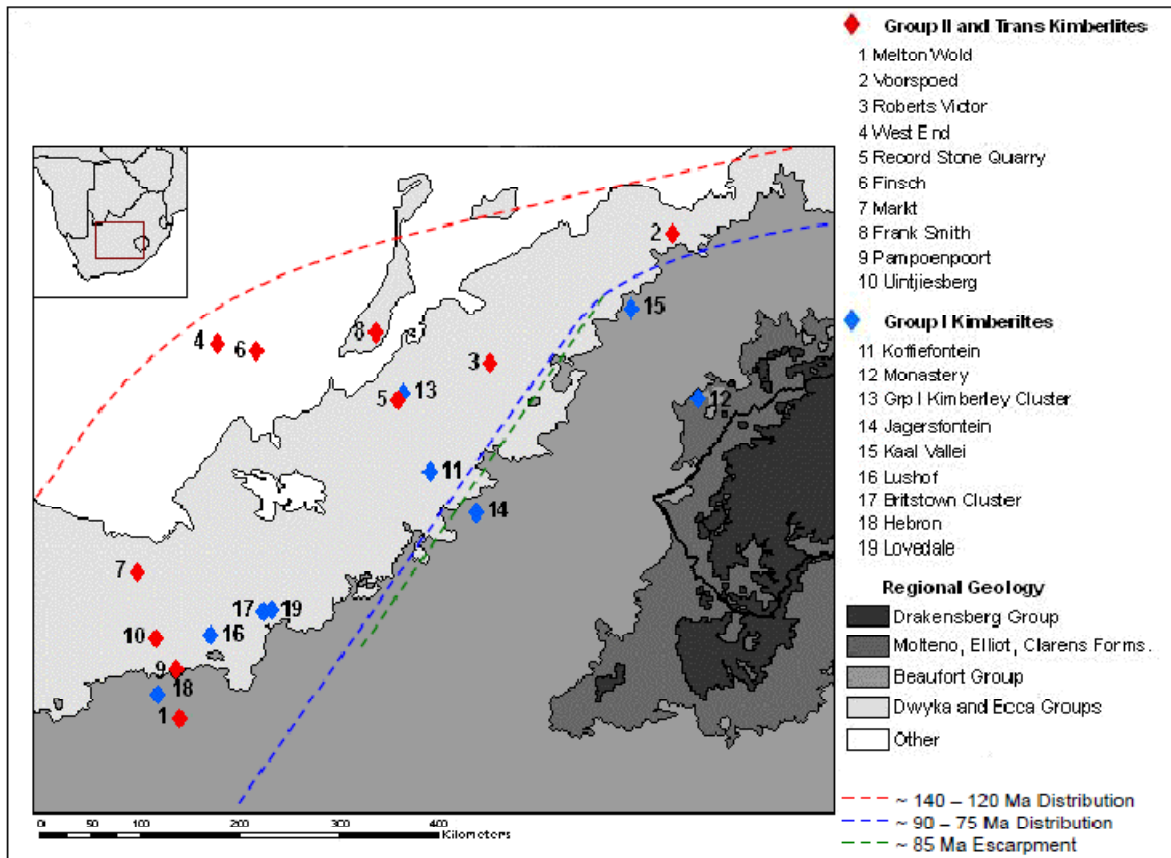


Figure 5.3 Palaeo-distribution of the Karoo basalt escarpment. Diagram from Hanson (2006). Note the Voorspoed pipe located between the 140-120 Ma and 90-75 Ma escarpments.

5.1.3.2 Method 2: Difference in Elevation

The current elevation at the Kroonstad cluster is 1410m meters above sea level (masl). The elevation of the contact of Stormberg Group sediments and basalt is at approximately 1900masl, which indicates a sedimentary/dolerite sequence of 490m. This is similar to the estimate of 435m for the total sedimentary/dolerite sequence in Method 1. The top of the basalt sequence is at approximately 3200masl given the thickness of the basalt at Oxbow (1270m, Marsh et al. 1997). The difference in height is 1790m. This simple method gives a very similar result to method 1.

5.1.3.3 Method 3: Denudation Rates Post-Emplacement

It is assumed that denudation rates in the Kroonstad area increased significantly subsequent to the emplacement of the Kroonstad kimberlites as the escarpment was just to the north of

the cluster at 140Ma and retreated to the south of the cluster by approximately 85Ma (Hanson, 2006), as shown in figure 5.3. Significant rates of denudation (16m/Ma) can be assumed to occur at the Kroonstad Cluster during this time. The denudation rate becomes less (10m/Ma) once the escarpment has retreated to the south. Denudation rates are based on the observations made by Hanson (2006). According to Hanson (2006) denudation rates changed slightly over the evolution of the South African landscape from approximately 16m/Ma between 140-85Ma to 10m/Ma from 85 Ma to present for the Kimberley area. A similar situation is occurring at the Kroonstad cluster and it is assumed that denudation rates would be similar. A simple calculation can be done to estimate the approximate amount of erosion, which would have occurred at the Kroonstad Cluster. An estimate of approximately 1620m is calculated.

5.1.4 Margin of Error Associated with Estimating Erosion

Analysis of the regional distribution of the Karoo Supergroup indicates that the Stormberg Group sediments may have been thicker than calculated above. Outliers of Molteno and Elliott Formation units to the north east of the current outcrop directly overlie the lower Beaufort Group (Adelaide Subgroup). The upper Beaufort Group (Tarkastad Subgroup) pinch out whereas the Stormberg Group does not, which indicates that the Stormberg Group onlaps directly onto the Adelaide Subgroup. However the margin of error associated with the Tarkastad Subgroup is negligible as thinning rates applied to the Kroonstad cluster give a thickness of only 20m. Furthermore the sandstone xenoliths analysed do not show definitive evidence for the occurrence of the Tarkastad Subgroup at the Kroonstad cluster. Figure 5.1 shows the xenoliths analysed with one possible xenolith showing compositions similar to the Tarkastad Subgroup, however the xenolith plots very close to the Stormberg/Tarkastad overlap. The important error margin here is the distribution of the Stormberg Group rocks. The xenolith suite analysed from the Kroonstad cluster are dominated by Stormberg Group compositions with lesser lower Beaufort and possible upper Beaufort Group rocks (Hanson, 2006 and Howarth, 2007). This indicates that the Stormberg Group sediments were more extensive in the area at the time of emplacement of the kimberlite pipes. The exact thickness is unknown but the current minimum thicknesses of the Stormberg Group can be used as maximum thicknesses for the Kroonstad cluster as it is unlikely that the rocks became thicker toward Kroonstad. The combined current minimum thickness in the northern outcrops for the

Molteno, Elliott and Clarens Formations is 210m (Johnson et al. 1996, Bordy et al. 2004 and Johnson et al. 2006). However some thinning of the Stormberg Group sediments is likely to occur toward Kroonstad but can not be speculated on as there is no data available. An error margin of underestimation of up to 210m can be inferred based on the current thickness of the Stormberg Group.

The thickness of Karoo basalt at the time of emplacement is very difficult to know and only estimates can be made based on the current outcrops. The estimate of 1370m used above is a maximum estimate for the basalt. The Springbok Flats basalts over 400km north of the Lesotho Formation basalts have stratigraphies geochemically similar to the Lesotho Formation; however it is unclear if they originated from the same source (Marsh et al. 1997). The Springbok Flats basalt is dominated by Fe-rich compositions similar to the Maloti-Senqu-Mothae (upper Lesotho Formation) units (Marsh et al. 1997). This is consistent with the distribution of basalt xenolith types observed at the Kroonstad kimberlites, which are dominated by Fe-rich compositions. Some thinning of the Mafika Lisiu unit may have occurred northward from the current Lesotho Formation outcrops based on the dominance of upper Lesotho Formation basalt xenoliths at the Kroonstad cluster. This possible thinning is unclear but may indicate a slight overestimation of the erosion using method 1. Calculating a thinning rate between the Lesotho Formation and the Springbok Flats basalts indicates that there may have been approximately 280m less basalt at the Kroonstad cluster relative to the current Lesotho Formation outcrops. This is assuming that the Lesotho Formation and Springbok Flats basalts originated from the same feeder, which is unclear.

From the above discussion it is clear that some margin of error exists with estimating erosion at the Kroonstad cluster using Method 1. This error margin indicates that the estimate of erosion can be constrained to 1525-2015m. An average value is used below to calculate the depth of the diatreme at the time of emplacement. Furthermore it must be noted that Methods 2 and 3 similarly contain assumptions, which may not be accurate. In method 2 it is assumed that no post-emplacement uplift has occurred. Partridge and Maud (1987) suggest that significant uplift has occurred, which is greater in the east compared to the west. If this is true the estimates for method 2 would be incorrect. Furthermore Method 2 assumes that the current elevation of the Lesotho Formation is similar to the time of emplacement of the

Kroonstad Cluster. However it is likely that some erosion has occurred, which indicates an underestimate using method 2. Method 3 uses denudation rates calculated by Hanson (2006) for the Kimberley area and may not apply to Kroonstad as denudation rates are likely to vary across South Africa. However the escarpment retreat at Kimberley is similar to that occurring at Kroonstad and provides a reasonable estimate for erosion.

5.1.5 Depth of Contact between Hypabyssal and Volcaniclastic Kimberlite at Kroonstad and Comparison with other South African Pipes

Previous estimates of the depth of the diatreme from various localities in southern Africa include 1900m and 1800m for Kimberley kimberlites (Hawthorne, 1975 and Field and Scott Smith, 1999 respectively), 2156m for Jagersfontein (Field and Scott Smith, 1999) and 1270m for Letseng (Field and Scott Smith, 1999). Skinner (2008) proposed a model for South African tuffisitic kimberlites, which shows the diatreme developing to 2000-2200m below the original land surface. The evidence from Hanson (2006) may indicate that far less erosion has occurred at the Kimberley kimberlites, which would have implications on the extent of the original diatreme. In the re-evaluated Hawthorne model of Hanson (2006) the erosion in Kimberley is lowered to 850m opposed to the 1400m of the Hawthorne model. This is based on the absence of Karoo basalt xenoliths in the area observed by Hanson (2006). This re-calculated erosion estimate applied to the De Beers, Wesselton and Dutoitspan pipes, where the diatreme is documented to 785m, 930m and 870m respectively (Clement, 1982), gives a depth of approximately 1635m, 1780m and 1720m respectively for the depth below the original land surface. These values are significantly lower than those calculated for the Kroonstad cluster. The maximum depth of the diatreme often varies within a kimberlite pipe. The diatreme often cross-cuts the earlier formed root zone, which is then preserved in the wall rocks along with earlier formed contact breccias. The De Beers pipe is a good example of this, the diatreme extends down to >785m from the surface and cross-cuts earlier formed root zone HK at 450m from the surface (Clement, 1982). One needs to take these variations into account when re-constructing the palaeo-depth of the diatreme. This is observed at the Voorspoed pipe where the VK in the centre of the pipe extends to greater depths than the hypabyssal transitional kimberlite breccia (HKtB) at the margin.

There is some variation in the hypabyssal kimberlite (HK)-volcaniclastic kimberlite (VK) contact at depth between the Voorspoed and Lace pipe. Refer to appendix 7 for a full list of abbreviations used in the text. The contact is not observed at the Lace pipe as the pipe has been mined out to 240m level. Both HK and VK is observed on the surrounding dumps indicating that the HK-VK contact must have been >240 from the current land surface. However at the Voorspoed pipe the contact is observed. The first occurrence of HK, in the form of HKtB, is at 290m below the current land surface. In the centre of the pipe VK is present to 350m. The depth to which the crater reaches varies within the Voorspoed pipe by 60m and is approximately 50-110m deeper than at Lace. An average post-emplacement erosion estimate for the Kroonstad cluster is calculated using the above three methods, which gives an average of 1750m of erosion. The depth of the diatreme from the original land surface at Lace is approximately 2000m whereas at Voorspoed it varies between 2040m and 2100m. Therefore the original depth of the diatreme at the Kroonstad cluster is approximately 300m deeper than the Kimberley kimberlites based on the erosion estimate of 850m at Kimberley from Hanson (2006).

5.2 Classification of Kimberlite Pipes

Kimberlite pipes can be broadly subdivided into three pipe types or classes (Skinner and Marsh, 2004 and Scott Smith, 2008a). This sub-division is based on Group I kimberlite pipes from around the world however as discussed in section 1 Group II kimberlites are kimberlite and not orangeites and therefore comparison of the KKC pipes with the typical kimberlite pipe classes is believed to be valid. Kimberlite pipes are divided primarily on three characteristics: 1) morphology, 2) pipe infill and 3) magmaclast characteristics. Class 1 or tuffisitic kimberlite pipes are based on South African kimberlite models first described by Hawthorne (1975) and Clement (1982). Class 2 pipes are based on Canadian pipes from the Prairies and Fort a la Corne (Carlson et al. 1999 and Field and Scott Smith, 1999). Lastly Class 3 pipes are based on kimberlite from Canada at Lac de Gras (Field and Scott Smith, 1999; Graham et al. 1999 and Doyle et al. 1999). Kimberlite pipes in South Africa are all currently classified as Class 1 tuffisitic kimberlite pipes. However observations from the Kroonstad kimberlites indicate that Voorspoed and Lace pipes are not Class 1 and are more similar to Class 3 pipes.

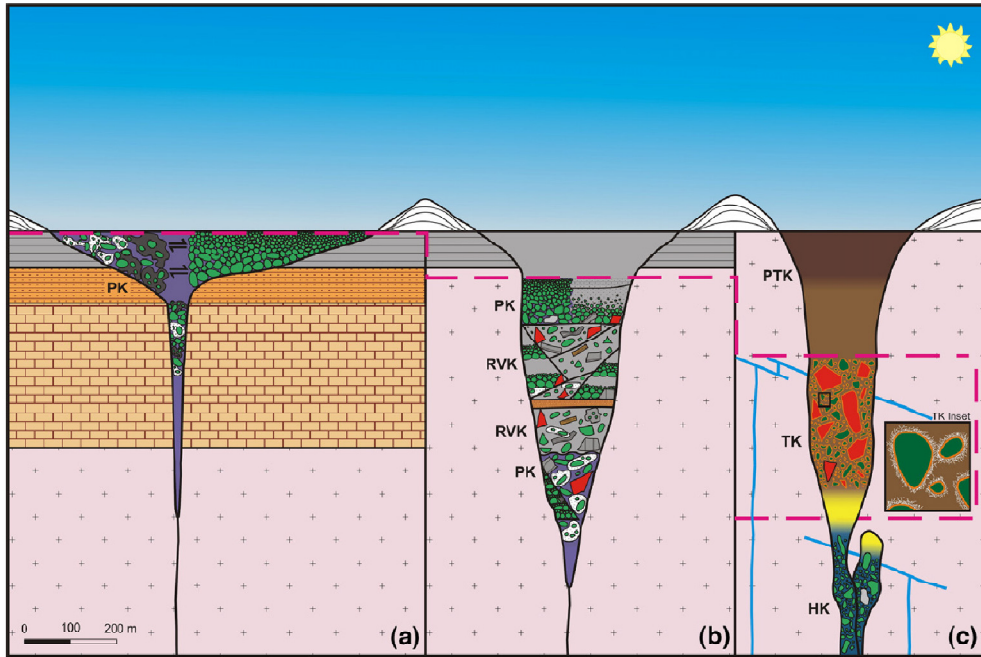


Figure 5.4 Schematic representations of the three pipe Class varieties. a) Class 2 Prairies Type Pipe; b) Class 3 Lac de Gras Type Pipe and c) Class 1 Tuffisitic Kimberlite Type Pipe. PK: Pyroclastic kimberlite; RVK: Resedimented volcanoclastic kimberlite; HK: Hypabyssal kimberlite; TK: Tuffisitic kimberlite and PTK: Pyroclastic equivalent of TK. Diagram from Scott Smith (2008a).

Class 1 pipes have also been described in Canada (Hetman et al. 2004; Hetman, 2008 and Fitzgerald et al. 2009), Brazil (Masun and Scott Smith, 2008), Lesotho and Botswana (Skinner, 2008) and West Africa (Skinner et al. 2004). Class 2 pipes are also documented in Angola and Siberia (Skinner and Marsh, 2004) and comparable pipes are noted in Attawapiskat in Canada (Kong et al. 1999). Class 3 pipes are also present at the Ekati cluster (Field and Scott Smith, 1999 and Nowicki et al. 2004), Nanavut Canada (Masun et al. 2004), Jwaneng Botswana (Machin, 2000 and Brown et al. 2008a), Siberia and several pipes in Angola (Skinner and Marsh, 2004).

5.2.1 Morphology

Pipe morphology is the most distinct feature of the pipes classes (figure 5.4). Class 1 and 3 pipes are very similar in terms of their pipe morphology however Class 2 pipes are easily distinguished from the former two classes. Class 2 pipes are characterised by shallow bowl-shaped craters and have sub-circular plan view shapes, which reach up to 80 ha in size (Scott

Smith, 2008b), as shown in figure 5.4. Berryman et al. (2004) note Class 2 pipes with surface areas up to 200 ha. The craters are typically <500m deep (Skinner and Marsh, 2004) and generally the base of the pipes are situated in prominent palaeo-aquifers (Field and Scott Smith, 1999 and Scott Smith, 2008b). Pipe margins range in dip from 0-60° (Scott Smith, 2008b). Class 1 kimberlite pipes have very consistent pipe margin dip of on average 82° (Clement, 1982 and Skinner, 2008). Graham et al. (1999) estimated a mean dip of Class 3 pipe margins of 78°-84°. Nowicki et al. (2004) also give Class 3 pipe margin dip angles of 75°-85°. Therefore the dip of Class 3 pipe margins is comparable to Class 1 kimberlites. Class 1 pipes extend down to approximately 2-3km from the palaeo-land surface. However Class 3 pipes are generally shallower and typical are >1km in depth (Skinner and Marsh, 2004). Rice (1999) showed that the dip of the pipe margin is related to the depth of eruption, where the steep 82° dip of Class 1 and 3 pipes is related to deep eruptions whereas the flared shallow dipping margins of Class 2 pipes is related to shallow eruptions. Therefore Class 1 and 3 pipe magmas are not likely to reach near the surface whereas Class 2 pipe magma may reach the surface.

5.2.2 Pipe Infill

Class 1 pipes contain the unique tuffisitic kimberlite infill, which is indicative of a Class 1 pipe (Skinner and Marsh, 2004). Class 1 pipes can be sub-divided into three distinct zones: 1) root zone, 2) diatreme zone and 3) crater zone (Skinner, 2008). Each zone is characterised by different kimberlite rock types. The root zone is irregular and filled with hypabyssal and transitional kimberlite (Hetman et al. 2004 and Skinner, 2008). The interpretation on the formation of the root zone is under much debate in the current literature, however observations made in this study indicate that the root zone must form through sub-volcanic processes similar to those proposed by Hetman et al. (2004) and Skinner and Marsh (2004). The diatreme zone is filled with tuffisitic kimberlite, which is also a much debated rock unit in the current literature (formation processes discussed below). The overlying crater zone is infilled with VK more similar to the Class 2 and 3 pipes. Class 2 and 3 pipes are infilled with a variety of pyroclastic kimberlite (PK) and resedimented volcanoclastic kimberlite (RVK) as shown in figure 5.4. PK in Class 2 pipes is typically well layered and sorting/grading is common (Kong et al. 1999 and Scott Smith, 2008b). Class 3 pipes generally contain PK at the base with RVK dominating the pipe infill (Scott Smith, 2008a). No underlying

hypabyssal root zone or transitional kimberlite has been noted in either of the Class 2 or 3 pipes. Furthermore tabular hypabyssal sheets have not been encountered in the country rock surrounding Class 2 pipes (Scott Smith, 2008b). In some cases Class 2 pipes may be completely filled with magmatic/coherent kimberlite (Field and Scott Smith, 1999), indicating hot magma at the surface. Therefore Class 2 and 3 pipes have been emptied prior to the deposition of the PK/RVK. This characteristic is also made clear by the common lack of xenolith material in the resultant VK deposits. Class 1 pipes are not emptied apart from the upper crater zone (Skinner, 2008).

5.2.3 Magmaclast Characteristics

Magmaclasts present within the VK infill of the pipes classes varies in terms of morphology and degree of crystallisation. Class 1 kimberlite contain pelletal lapilli, which have been interpreted to form in numerous processes in the literature. However pelletal lapilli are characterised by: spherical shape, typical cored by altered olivine and a mantle of crystalline kimberlite, which resembles typical hypabyssal kimberlite mineralogy and granularity (Skinner and Marsh, 2004). Numerous interpretations on the formation of Class 1 magmaclasts are present in the literature; however they are believed here to have formed in the transitional kimberlite and incorporated into the TK during fluidisation. Class 2 pipe magmaclasts are distinctly different from Class 1. The characteristic features include: amoeboid/curvilinear to ovoid shape, vesicles may be present, commonly fresh olivine grains and most groundmasses composed of typically isotropic serpentine or cryptocrystalline carbonate (Scott Smith, 2008b). These magmaclasts have undergone rapid cooling, which did not allow for the crystallisation of the groundmass minerals. Class 3 magmaclasts are similar to Class 1 in that they are typical crystalline and similar to typical hypabyssal kimberlite. However the magmaclasts are characterised by the often broken angular shape, altered olivine and abundant groundmass carbonate (Graham et al. 1999 and Skinner and Marsh, 2004). These magmaclasts are typical autoliths of earlier crystallised kimberlite.

Regardless of the interpretation of the formation of the various magmaclasts, the important characteristic to note is the crystalline hypabyssal nature of Class 1 and 3 magmaclasts, which must indicate that they were crystallised prior to eruption of the kimberlite.

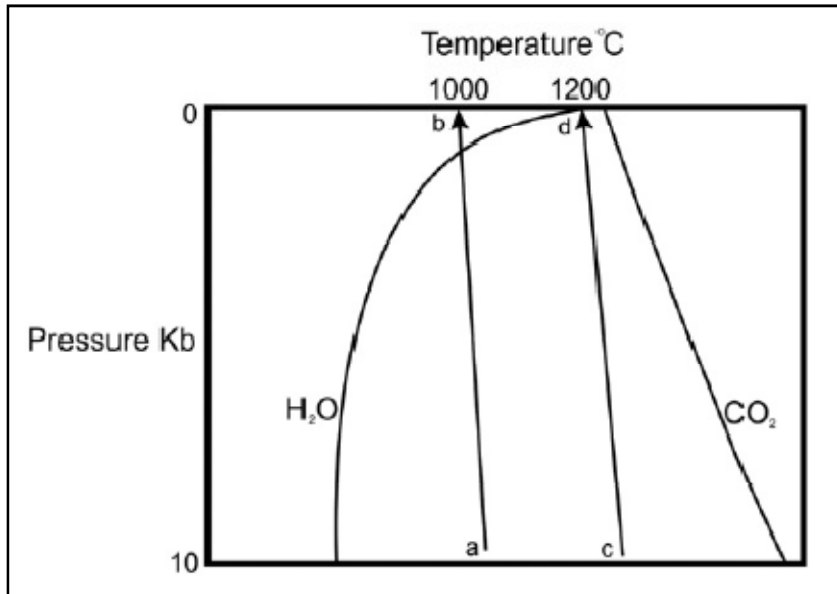


Figure 5.5 Simplified schematic illustration from Skinner (2008) showing the solidi ab for a water-saturated melt (i.e. Class 1 kimberlites) and cd for a CO₂ saturated melt (i.e. Class 2 kimberlites). Diagram based on experimental work on peridotite by Wyllie (1987).

Decompression eruption as proposed by Cas et al. (2008a) and Skinner (2008) would produce a rapid drop in temperature and the crystalline mantles would not be able to form as the temperature drop would result in much finer grained mantles. However the Class 2 magmaclasts, which contain common vesicles and cryptocrystalline mantles, must form during rapid cooling of hot kimberlite. Rapid cooling would produce the fine grained mantles as well as the vesicles. This is further evidence to suggest that Class 2 kimberlite reach near the surface as hot magmas whereas Class 1 and 3 kimberlites crystallise prior to eruption at depth.

5.2.4 Emplacement of Pipe Classes

A variety of emplacement mechanisms are proposed for the varies pipe classes although many of the current models for kimberlite emplacement do not distinguish between the different classes and simply propose one model to explain all kimberlite pipes. It is particularly important to note these very distinct pipe classes, which must form through different processes. In particular the Class 1 and 2 kimberlite pipes are very different in morphology, infill and magmaclast characteristics. Therefore it is very unlikely that they

formed through similar processes. Field and Scott Smith (1999) and Scott Smith (2008a) suggest that local country rock geology is the controlling factor on pipe morphology. However it is not uncommon to observe numerous pipe classes in the same geological setting (e.g. this study). Therefore it is unlikely that country rock geology has a major control on pipe morphology. Skinner and Marsh (2004) suggest that volatile composition of the kimberlite magma is the controlling factor for emplacement. Wyllie (1987) showed that CO₂-rich peridotite would cross the solidus near/at the surface whereas H₂O-rich peridotite would cross the solidus at depth, as shown in figure 5.5. The characteristic features of Class 2 pipes (shallow flared craters, amoeboid magmaclasts, common cryptocrystalline carbonate base, calcite filled vesicles) indicate that hot magma reached near the surface. Therefore the Class 2 magmas are likely to be similar to CO₂-rich peridotite in the experiments of Wyllie (1987). The CO₂-rich nature is also indicated by the abundant carbonate within the magmaclasts. Furthermore the eruptions of Class 2 pipes are shallow and related to aquifers, which indicate a phreatomagmatic eruption style. Shallow eruptions, as mentioned above, will form flared shallow dipping crater margins (Rice, 1999). The vent is cleared by the eruption with subsequent infilling occurring in an open vent.

Class 1 and 3 kimberlite pipes do not reach near the surface as indicated by crystalline hypabyssal-looking magmaclasts and the deep steep sided vents. Again it is important to note that deep explosions will form steep sided vents (Rice, 1999), which are typical of Class 1 and 3 pipes. Furthermore the crystalline nature of the magmaclasts must indicate that they were crystallised to near completion prior to eruption. This is also evident by the preservation of globular segregatory transitional kimberlites in many Class 1 pipes (Hetman et al. 2004 and Skinner and Marsh, 2004). Therefore the magma is likely to be at significantly lower temperatures at the onset of eruption. Class 1 transitional kimberlite is characterised by an increase in serpentine with subsequent decrease in calcite. This is interpreted by Skinner (2008) to indicate that H₂O is the controlling volatile phase during initial eruption as CO₂ has degassed and is no longer present in the magma. Therefore Class 1 kimberlite pipes are likely similar to H₂O-rich peridotite in the experiments of Wyllie (1987), which cross the solidus at depth. This is consistent with geological characteristics of Class 1 kimberlites. The deep steep vents indicate a deep explosion (Rice, 1999), abundant serpentine indicate the H₂O-rich nature of the kimberlite and the hypabyssal-looking magmaclasts indicate that they crystallise at depth prior to eruption. Class 1 eruptions are driven by juvenile volatile exsolution and not

phreatomagmatism (e.g. Sparks et al. 2006 and Skinner, 2008). The characteristic tuffisitic vent infill forms through fluidisation processes and is not deposited through pyroclastic airfall or flow processes in an open vent (Skinner, 2008). The formation of microlitic clinopyroxene, which is unique to Class 1 kimberlite, is discussed in detail in section 5.3 but it is important to note here that microlitic clinopyroxene increases in abundance from the base of the transitional kimberlite to the top in Class 1 kimberlites. It is interpreted in this study to be linked to the kimberlite magma through a deuteric processes and not a later stage secondary hydrothermal alteration processes.

Class 3 kimberlite pipes show characteristics similar to Class 1 and Class 2 pipes. The deep steep sided vents and crystalline hypabyssal-looking magmaclasts indicate that the initial emplacement is likely similar to Class 1 pipes. Steep sided vents indicate deep explosions and crystalline magmaclasts indicate the magma has crystallised to near completion. However the pipe infill is not similar to Class 1 pipes and is more similar to Class 2 pipes, in that the VK has been deposited into an open vent. Therefore it is unclear as to the exact controlling factors for Class 3 eruption although it is likely that subtle difference in the volatile composition is the controlling factor. Class 3 kimberlite pipes may fall somewhere between Class 1 and 2 pipes in terms of volatile composition.

5.2.5 Classification of the Kroonstad Kimberlite Pipes

Morphology

The Kroonstad pipes (Voorspoed and Lace) are steep sided with an average pipe margin dip of 82° (Clement, 1982). The pipes are also deep and extend to depths $>2.4\text{km}$ from the original land surface. The Lace and Voorspoed pipes have circular and sub-circular plan views respectively. The Voorspoed pipe is currently 12ha (490m by 350m) in size and the Lace pipe is 2ha (120m diameter). At the time of emplacement the Voorspoed pipe was approximately 980m by 700m and Lace was approximately 600m in diameter. This is based on the erosion estimate calculated above and using the average of 82° for the dip of the pipe margin. Therefore the Kroonstad pipe morphology is similar to Class 1 and 3 pipes and not similar to Class 2 pipes.

Pipe Infill

The pipe infill, at the Voorspoed pipe in particular, is complex and comprised of multiple horizontally layered volcanoclastic kimberlite deposits. Tuffisitic kimberlite is not observed. However a distinct root zone is noted, which contains globular segregatory hypabyssal transitional kimberlite (HKt). The Lace pipe also does not contain tuffisitic kimberlite (TK). The Lace pipe does contain distinct HKt, which is very similar to the HKt described for Class 1 pipes. Microlitic clinopyroxene gradually becomes more abundant and serpentine is present although calcite is also abundant. Only the HKt is observed and tuffisitic transitional kimberlite (TKt) is not present. Refer to appendix 7 for a full list of abbreviations used in the text. The Voorspoed HKt is not similar to typical Class 1 HKt as it does not contain microlitic clinopyroxene or serpentine. The base of the Kroonstad pipe infill (root zone) is similar to Class 1 kimberlites although Voorspoed is slightly different. The VK infill is not similar to Class 1 pipes and is more similar to Class 3 pipes. Therefore the initial development of the Kroonstad pipes is likely similar to Class 1 pipes however the latter pipe infilling is similar to Class 3 pipes.

Magmaclast Characteristics

The magmaclasts at the Kroonstad infill range from spherical to irregular/angular. The spherical variety is far more dominant. These spherical magmaclasts are characterised by common presence of central kernels, which are dominated by country rock xenoliths at Voorspoed and highly altered olivine at Lace. The kimberlite mantles are crystalline and look very similar to hypabyssal and HKt observed in the root zone of the pipes. These magmaclasts are similar to typical Class 1 and 3 kimberlite magmaclasts in that they have crystallised to near completion before eruption. If they had not crystallised to near completion one would expect a cryptocrystalline base similar to magmaclasts observed in Class 2 pipes.

Classification of the Voorspoed and Lace Pipes

The Voorspoed and Lace kimberlite have characteristics of both Class 1 and 3 pipes but show no similarities to Class 2 pipes. The morphology is typical of Class 1 and 3 pipes. The root zone at depth is more similar to Class 1 pipes although the Voorspoed HKt has distinct

differences, which are unique to Voorspoed (lack of microlitic clinopyroxene and serpentine). The VK infill is horizontally layered and is similar to Class 3 pipes, which indicates that the VK was deposited into an open vent. The magmaclasts are similar to Class 1 kimberlites in that they are dominated by spherical shapes, which contain crystalline kimberlite mantles. Therefore the Kroonstad pipes (Lace in particular) are characterised by the initial development similar to Class 1 pipes but the latter pipe infilling is similar to Class 3 pipes. The Voorspoed pipe may represent a typical Class 3 kimberlite as the HKt is not typical of Class 1 pipes. HKt has not been documented at Class 3 pipes before but this may be due to insufficient drilling or misinterpretation of the HKt as pyroclastic kimberlite.

5.3 Emplacement of the Root Zone at the Kroonstad Cluster

5.3.1 Root Zone/Embryonic Pipe Processes in Kimberlite Emplacement

Skinner (2008) divides the typical Class 1 kimberlite pipe into three zones, as discussed in section 5.2. As discussed above, the Kroonstad kimberlites (especially the Voorspoed pipe) are not typical of Class 1 South African pipes. However distinct root zones have not been described for Class 3 pipes in the literature, although this may be due to lack of exposure. It is interpreted in this section that the root zones observed at the Voorspoed and Lace pipes form in a similar way to typical Class 1 pipes as described by Clement (1982) and Skinner (2008). It must be noted that various other interpretations on the formation of the root zone are present in the literature, such as Lorenz and Kurszlaukis (2007) who propose phreatomagmatic process for the root zone. The following section discusses the development and typical features of the root zone. In particular the development and characteristic features of contact breccias and transitional kimberlite are discussed. Models for the near surface emplacement of kimberlites are briefly reviewed in terms of the hypabyssal kimberlite. The Voorspoed and Lace pipes are both interpreted to have formed through embryonic pipe development and the evidence for the sub-volcanic intrusive development of these pipes is presented below.

Root zones are typically present at depth within kimberlite pipes. The contact with the diatreme zone is variable across the pipes and typically occurs between 1.7-2.2 km from the

original land surface (Skinner, 2008). This zone forms by the intrusion of several pulses of magma (Hetman et al. 2004) and often >10 hypabyssal intrusions are observed (Skinner, 2008). Therefore the root zone is a complex array of hypabyssal intrusions. Root zones are typically highly irregular in shape relative to the diatreme zone, which is very consistent in shape all over the world. The upper contact of the hypabyssal kimberlite is often gradational within a single intrusive phase (Hetman et al. 2004). These gradational contacts are transitional kimberlites, which were not identified in the original model of Clement (1982) but have subsequently been added to the model by Skinner (2008). Detailed analysis of transitional kimberlite is fundamental in understanding the emplacement of kimberlite pipes. Numerous authors have interpreted transitional kimberlite to have formed by pyroclastic welding processes (e.g. Sparks et al. 2006 and Brown et al. 2008c) due to the theoretical calculations indicating a space problem with intrusive development and the common occurrence of welded pyroclastic rocks in other pyroclastic eruptions. However it is very clear from the development of transitional kimberlite in blind pipes that these distinct rocks must form in sub-volcanic environments, such as at Wesselton (Mitchell et al. 2009) and the 5034 kimberlite in Canada (Hetman et al. 2004).

5.3.1.1 Review of the Embryonic Pipe Model for Emplacement of Kimberlite Pipes – Clement (1982)

This model has essentially three stages in the emplacement of a kimberlite pipe. The model has been specifically developed for southern African kimberlite and therefore must be used with care when applying it to kimberlite pipes outside of southern Africa. The discussion below is based mostly on the initial model by Clement (1982) and Clement and Reid (1989). Further work on this model has been presented by Field and Scott Smith (1999), Skinner and Marsh (2004) and Skinner (2008).

Stage 1: The development of an embryonic pipe begins in the root zone prior to eruption. Kimberlite magma intrudes as dykes, sills and vertically extended embryonic pipes. Embryonic pipes are approximately >1.5km in height and up to 3-5ha in cross section (Skinner, 2009). Contact breccias form in the embryonic pipes as a result of the build up of pressure associated with volatile exsolution in the kimberlite magma. It is evident that contact breccias form prior to eruption for a number of reasons, which include: preservation under

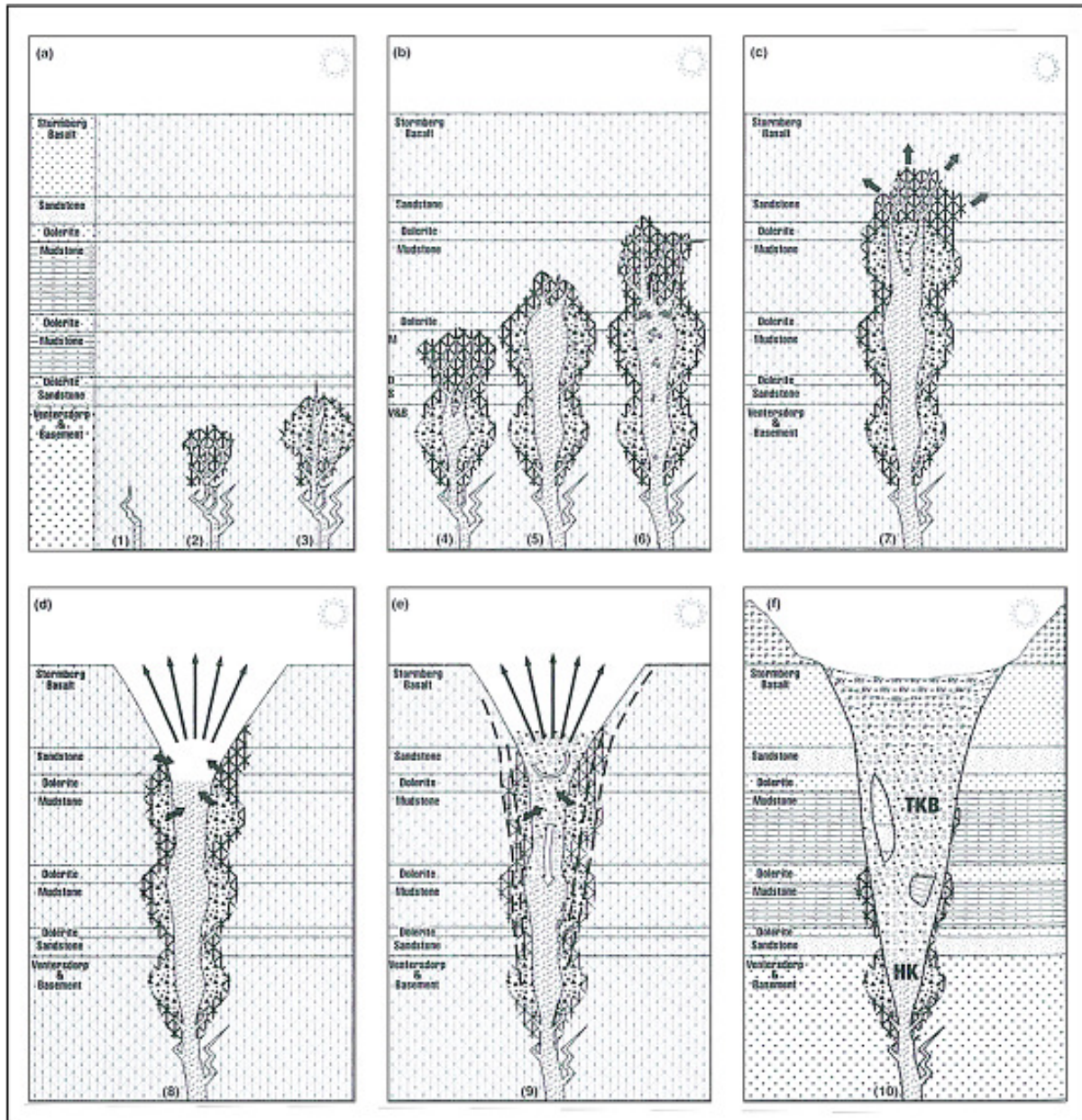


Figure 5.6 Schematic illustration of the Clement (1982) model for embryonic pipe development and near surface eruption of South African kimberlites. Note specifically the formation of contact breccias at the base of dolerite sills in the country rock. (Diagram from Field and Scott Smith, 1999).

country rock overhangs, local country rock lithologies, occurrence of these breccias in the roof rocks of blind pipes and the coring out of contact breccias by later intrusions (Clement, 1982). Contact breccias may become infilled by hypabyssal kimberlite but never tuffisitic kimberlite (TK) (Skinner, 2008), indicating concurrent formation with the hypabyssal kimberlite (HK) and not TK. The Clement (1982) model shows the formation of contact breccias in relation to more competent rock units within the local stratigraphy, in the case of South Africa these are Karoo dolerite sills. Magma ascent is temporarily halted at the base of

dolerite sills where volatiles then accumulate at the tip of the magma column until sufficient pressure has built up to overcome the more competent dolerite. Volatile exsolution also texturally modifies the HK as described by Skinner and Marsh (2004) and Hetman et al. (2004). This modification results in the formation of transitional kimberlite, which is characterised by the crystallisation of deuteric microlitic clinopyroxene, loss of calcite, serpentinization of olivine and the development of a globular segregatory texture (Skinner, 2008). These processes of contact breccia and transitional kimberlite formation may be repeated numerous times in a sub-volcanic environment during the ascent of the magma to the surface. Therefore the exsolution and accumulation of volatiles at the head of the magma column drives the ascent of the kimberlite magma by either infiltrating and dilating pre-existing fractures or creating new fractures in the roof country rock. This creates a weakened fractured zone known as the embryonic pipe. The genesis of these sub-volcanic pipes is the result of a complex and repetitive sequence of events.

Stage 2: Embryonic pipes develop upward to a point where the pressure in the vapour cap exceeds the lithostatic load and explosive breakthrough occurs. This increase in vapour pressure may also be related to en masse crystallisation of the groundmass mineralogy, which would induce volatile exsolution. Clement (1982) shows the final barrier to kimberlite ascent as the Karoo basalt sequence. Volatiles build up at the head of the column and fracture through the lava sequence. Upon breaching the surface the eruption would be driven by a major decompression related exsolution of the volatiles through the whole magma conduit. This would clear a vent to approximately 500-700m (Skinner, 2008).

Stage 3: Large volumes of exsolved volatiles induce fluidisation within the newly formed pipe or diatreme zone. Contact breccias and xenoliths from all stratigraphic levels as well as juvenile components are thoroughly mixed and overturned during this process. Most of the contact breccias formed during the development of the embryonic pipe are incorporated into the diatreme zone and only rare examples are preserved usually deep within the pipe as the root zone. Therefore the diatreme zone reflects the post-breakthrough modification of the embryonic pipe. Huge floating reef bodies represent down slumped masses of embryonic pipe side-wall material, such as those described at Kamfersdam (Skinner and Marsh, 2004). The resultant rock types are tuffisitic kimberlite. The diatreme zone extends from approximately 2.2km to 700 from the original land surface (Skinner, 2008). The crater zone

(<700m) is infilled by pyroclastic deposits associated with the major decompression related eruption as well as resedimented volcanoclastic kimberlite and tuff ring collapse deposits.

This model has been developed specifically for southern African Class 1 kimberlites but many of the initial mechanisms of formation are very relevant for the emplacement of the Voorspoed kimberlite, which is not a typical Class 1 tuffisitic kimberlite. The fundamental issue is the development of embryonic pipes in a sub-volcanic environment, which is characterised by the development of contact breccias and transitional kimberlite. Many of the recent models for kimberlite emplacement (Sparks et al. 2006; Wilson and Head, 2007 and Cas et al. 2008a) have not identified the importance of these distinct embryonic pipe processes.

5.3.1.2 Welding in Kimberlites: An Alternate Explanation for the Formation of Transitional Kimberlite

Numerous other models for the near surface emplacement of kimberlite pipes exist. These include magmatic juvenile driven models of Sparks et al. (2006), Wilson and Head (2007) and Cas et al. (2008a). A phreatomagmatic model was first proposed by Lorenz (1975) and more recently a phreatomagmatic model is used to interpret the formation of the diatreme at the Tuzo pipe, Gahcho Kue cluster Canada (Seghedi et al. 2009). Transitional kimberlite in the above models is interpreted to have formed by pyroclastic welding/agglutination processes. A detailed review of welding processes is beyond this study and the reader is referred to Brown et al. (2008b) for further discussion. Hayman et al. (2008) states that gradational contacts are more likely if both facies are fragmental, however ideas apparently worthy of consideration for gradational contact between coherent and fragmental include: 1) permeation of ultra low viscosity melt into the porosity of an unconsolidated fragmental rock, 2) contact was sharp but now overprinted by pervasive alteration and 3) thermal assimilation of fragmental facies by coherent kimberlite.

Sparks et al. (2006) prefer the interpretation of welding based on the common occurrence of welded rocks in other pyroclastic eruptions and the highly unlikely preservation of dynamic volcanic processes such as degassing fronts. Another interpretation of welding is based on gradational contacts between coherent kimberlite (CK) (called hypabyssal kimberlite in this

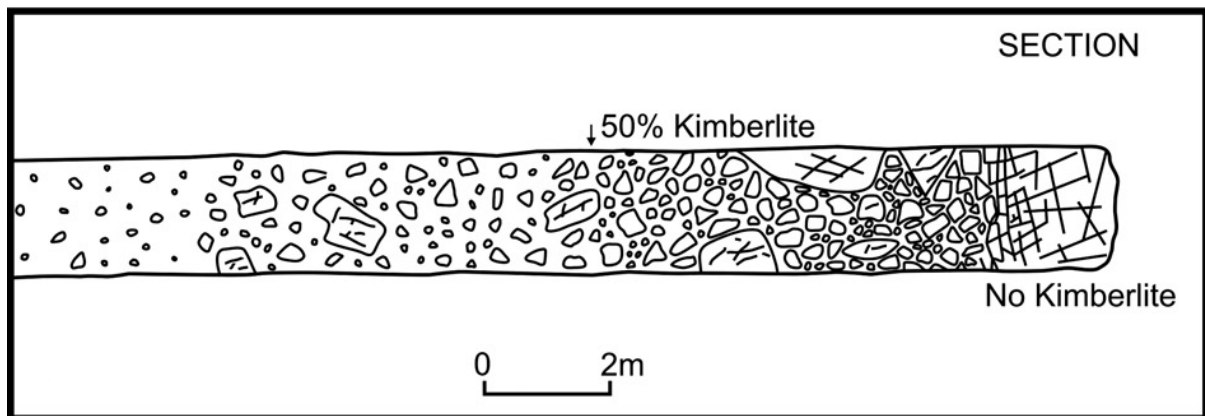


Figure 5.7 Schematic illustration of a tunnel developed through a contact breccia at the De Beers pipe. Note the variation in kimberlite percentage, which gradually becomes nothing toward the end of the tunnel (right hand side). Diagram from Skinner (2008) after Clement (1982).

study) in the root zone and MVK, which according to Brown et al. (2008b) is likely to indicate that a similar genetic process is responsible for forming both the CK and MVK. Brown et al. (2009) interpret welded rocks at the Venetia kimberlite based on 1) gradational contacts between CK/MVK and 2) the crystalline igneous groundmass. Nowicki et al. (2008) uses incompatible element variation to show that typical CK is depleted in incompatible elements, indicating that the fines component of the magma is lost during pyroclastic eruption. However an alternate interpretation is presented below where simple degassing of the magma may produce similar incompatible element variations. Cas et al. (2008a) state that; welding could occur but no convincing examples have yet been documented in kimberlites. Therefore the interpretations of welding in kimberlite pipes proposed by Sparks et al. (2006) and Brown et al. (2008b) are based on very little geological evidence and rather on theoretical calculations. Geological evidence from the Kroonstad kimberlites clearly indicates that the rocks could not have formed by pyroclastic process and therefore the interpretations of Skinner and Marsh (2004) and Hetman et al. (2004) for transitional kimberlite are much more likely. Armstrong et al. (2004) show that calcite forming in hypabyssal/coherent kimberlite is magmatic in origin and not meteoric, which indicates a hypabyssal origin rather than pyroclastic. Masun et al. (2004) state that the preservation of delicate atoll textured spinel in hypabyssal kimberlite at the Anuri kimberlite indicates a magmatic origin rather than pyroclastic. The most convincing evidence is the occurrence of globular segregatory transitional kimberlite in blind pipes, which are common throughout the world (e.g. Wesselton, Clement, 1982 and 5034 kimberlite Hetman et al. 2004). The

transitional kimberlite at the Kroonstad kimberlites are observed to have formed sub-volcanically and not by pyroclastic welding processes.

5.3.2 Contact Breccias and Hypabyssal Transitional Kimberlite (HKT): Review of Literature

Contact breccias and transitional kimberlite form at the same stage in the evolution of the embryonic pipe as a result of the exsolution of juvenile volatiles from the magma. This exsolution process is governed by second boiling produced by the en masse crystallisation of the magma (Skinner, 2008). Transitional kimberlite and contact breccias are often intimately associated at depth within the pipes. Transitional kimberlite often contains high proportions of country rock xenoliths (CRX), which is the result of the invasion and incorporation of contact breccias. The formation of contact breccias and transitional kimberlite is interpreted to be sub-volcanic as shown by Clement (1982), Skinner and Marsh (2004), Hetman et al. (2004), Skinner (2008) and Masun and Scott Smith (2008) and observed from evidence in this study. This process of sub-volcanic formation is discussed in detail in this section.

5.3.2.1 Contact Breccias

Clement (1982) was the first to provide detailed descriptions of contact breccia, which are present in the wall rocks of the De Beers and Wesselton kimberlites. Generally these breccias occur under country rock overhangs where the kimberlite dips outward at $<30^{\circ}$ and typically are $<30\text{m}$ wide. Monolithic contact breccias are also described at the head of blind intrusions, which are commonly underlain by transitional kimberlite. Field and Scott Smith (1999) describe an in situ highly brecciated sandstone and basalt with a central core of segregationary kimberlite at the A/K15 occurrence in Botswana. Hetman et al. (2004) describes a highly brecciated country rock zone (54m) above a blind intrusion at Gahcho Kue in Canada, figure 5.8. Clement (1982) observed contact breccias as caps to blind intrusions at the Wesselton and Monastery kimberlites. Furthermore contact breccias in these blind pipes are forming prior to explosive emplacement and a similar non-pyroclastic origin can be assumed for the contact breccias observed in the sidewalls of explosively formed kimberlite pipes. Contact breccias are typically highly variable in character but Clement (1982) described two consistent features, which have been repeatedly observed at other localities.

Firstly, the most important consistent feature of contact breccias is the local derivation of the fragments/blocks and generally monolithic character such as at the Wesselton kimberlite where a monolithic Ventersdorp Supergroup quartz porphyry breccia is present (Clement, 1982). There is very little relative movement of the fragments within contact breccias. Secondly a high degree of angularity is present within all contact breccias, although lesser sub-rounded to rounded fragments are also present (Clement, 1982). Sub-rounded fragments are present within the shale contact breccia at the Voorspoed pipe but the fragments are dominantly angular. Fragments may be densely to loosely packed. Densely packed breccias have the appearance of intense in situ shattering of the country rock whereas loosely packed breccias may have cavities >10cm in diameter, which are most commonly filled with calcite and/or pyrite (Clement, 1982). Fragments show a large range in size and are generally mm-<50cm in size although larger >1m blocks are commonly observed (Clement, 1982). Other examples of contact breccias with locally derived and angular fragments include for example: Clement and Reid (1989), Skinner and Marsh (2004), Lorenz and Kurslaukis (2007), Skinner (2008).

Furthermore contact breccias may be filled with kimberlite. In all cases this kimberlite is hypabyssal in character and never volcanoclastic (Skinner, 2008). In most cases the kimberlite is highly hydrated and altered to clay minerals (Clement, 1982). The percentage of kimberlite proportion in contact breccias generally increases inward into the pipe and CRX content gradually becomes insignificant as shown in figure 5.7. These inner areas show some degree of mixing of the fragments and numerous lithologies may be present (Clement, 1982). This is observed at the Kroonstad cluster where transitional kimberlite has infilled a contact breccia and subsequent mixing has occurred to produce HKtB. Numerous lithologies are observed at Voorspoed as fragments/xenoliths, which include local shale and dolerite with minor basement carbonates also present. There is an increasing degree of incorporation and dispersion of xenoliths by intruding kimberlite toward the inner margins when kimberlite is observed infilling the contact breccia. Lorenz et al. (2002) describe a process of fragmentation of the country rock in maar-diatreme volcanoes where shock waves associated with eruptions are thought to fracture and fragment the country rock. These zones of fragmented country rock collapse back into the magma chamber/conduit during eruption to form debris flow type deposits. Intruding coherent melt mingles with this debris flow deposit, which produces magma very rich in lithic fragments defined as peperite-like magma mixtures

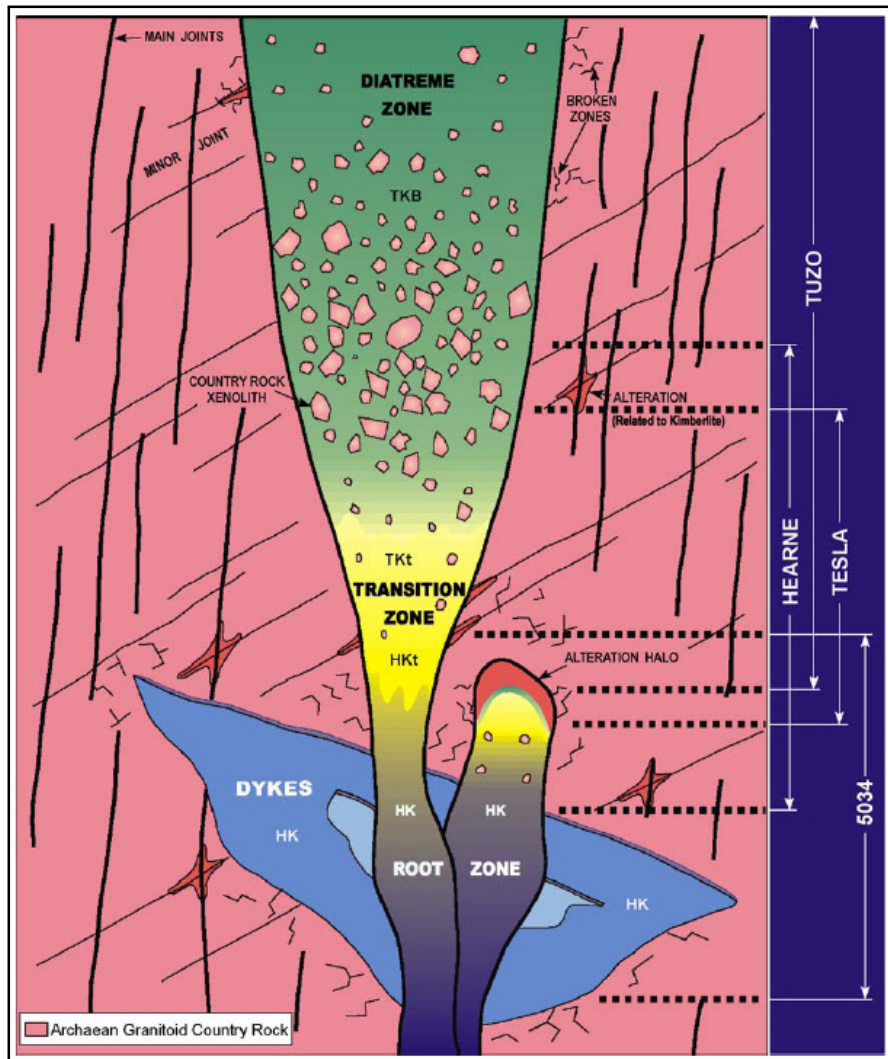


Figure 5.8 Composite model for the Gahcho Kue kimberlites. Diagram from Hetman et al. (2004).

(Lorenz et al. 2002). The following eruptions will produce pyroclasts with lithic clasts, which range in size from lapilli to bombs (Lorenz et al. 2002). This process of peperite-like magma mixtures has been used by Lorenz et al. (2002) to describe contact breccias in root zones of South African pipes. However the volatile phases driving kimberlite eruptions in South Africa are generally accepted to be juvenile rather than phreatomagmatic. This process of peperite-like magma mixtures is similar to the process of contact breccia formation described below, however contact breccias are interpreted to be sub-volcanic and not associated with explosive eruptions but rather hydraulic fracturing of the country rock.

5.3.2.2 Contact Breccia at the Voorspoed and Lace Pipes

Contact breccias are observed in the adjacent wall rocks at the Voorspoed kimberlite pipe. The pipe contacts at the Lace pipe were not observed in this study. However xenoliths of contact breccia devoid of kimberlite have been observed within the transitional kimberlite. The breccias at the Voorspoed pipe in particular have been logged in three boreholes. The eastern pipe, in borehole 10, shows typical contact breccias infilled with calcite only. This is an important feature to note and no serpentine is observed in any contact breccias observed. The wall rocks are shales and dolerite (intrusive dolerite sill part of Karoo volcanism). The contact breccias here are angular, monolithic and clast supported. The wall rocks become less fragmented further away from the pipe and eventually only calcite filled fractures are observed in the wall rock. It is particularly important to note here that no Karoo type basalt is observed in any contact breccias at the Kroonstad Cluster. The lack of any Karoo type basalt, which are the dominant country rock xenolith (CRX) in all the MVK varieties, as well as the presence of gradational contact into the wall rocks indicates that these breccias can not have formed by pyroclastic processes. The presence of relatively large voids (up to 6cm) filled with calcite indicate an increase in volume associated with the formation of the breccias. This space problem is noted in the original model by Clement (1982). Transitional kimberlite with a high proportion of CRX is intimately associated with the formation of contact breccias and is classified as hypabyssal transitional kimberlite breccia (HKtB). HKtB occurs at the same depth as the contact breccias at Voorspoed. The high CRX content of the HKtB is interpreted to be as a result of the incorporation of CRX fragments from the contact breccias. The incorporation of CRX into transitional kimberlite is a common feature noted at the Lace kimberlite where transitional kimberlite is observed with a high CRX proportion. The kimberlite component of these Lace rocks is highly altered by clay minerals, similar to that described by Clement (1982). This process is discussed in detail below.

5.3.2.3 Transitional Kimberlite

Transitional kimberlite rock types were first described by Clement (1982) as globular segregatory textured kimberlite although the significance of these rocks types has only been realised recently by Skinner and Marsh (2004) and Hetman et al. (2004). Field and Scott Smith (1999) also described globular segregatory kimberlite at the Kamfersdam pipe but specific genetic implications were not interpreted. Transitional rocks have been noted in the

literature for some time but have only recently been analysed in detail. The formation of these rocks is controversial in the current literature with many authors preferring an interpretation of pyroclastic welding/sintering origin (eg. Sparks et al. 2006 and Brown et al. 2009), rather than the in situ modification of hypabyssal kimberlite by processes developed in the embryonic kimberlite pipe as a consequence of second boiling (Skinner, 2008). Transitional kimberlite has been described in kimberlites from Canada (Hetman et al. 2004 and Scott Smith, 2008), South Africa, West Africa, Angola, (Skinner et al. 2004 and Skinner and Marsh, 2004) Botswana, Lesotho (Skinner, 2008) and Brazil (Masun and Scott Smith, 2008). This texturally distinct rock type has been repeated in time at a number of different localities. All the transitional kimberlite described in the current literature occurs in Class 1 tuffisitic kimberlites. The Kroonstad Cluster kimberlites contain the first transitional kimberlite zones to be documented, which are not Class 1 tuffisitic kimberlites.

Transitional kimberlites are present at depth as gradational contacts between hypabyssal kimberlite and the overlying tuffisitic kimberlite (TK). In Canada the Tuzo and Hearne kimberlites have transitional kimberlite zones of 73m and 115m in length respectively (Hetman et al. 2004) and in Brazil transitional zones have been documented at Cosmos-01 (50m) and Pepper-13 (60m) (Masun and Scott Smith, 2008). Hetman et al. (2004), Skinner and Marsh (2004) and Masun and Scott Smith (2008) show the clear spatial relationship of transitional kimberlite at the contact of HK and TK. The transitional kimberlite at the Voorspoed and Lace kimberlites are 90m and 350m in length respectively. The Lace transitional kimberlite is one of the most extensive transitional kimberlite columns documented to date. The Dark Piebald kimberlite at Premier extends to >600m, which is entirely transitional kimberlite (Skinner, 2008). The Voorspoed transitional kimberlite is expected to extend further with additional deep drilling. Globular segregatory textured transitional kimberlite has been observed at the top of blind intrusions, which have not achieved explosive breakthrough to the surface. The B/K44 occurrence in Botswana, located immediately below the Stormberg basalt, is characterised by well developed segregations of calcite and serpentine (Field and Scott Smith, 1999), indicating a juvenile volatile component of both H₂O and CO₂. The 5034 blind intrusion at Gahcho Kue in Canada is another example of transitional kimberlite forming at the head of a blind intrusion (figure 5.8), which is overlain by a 56m zone of altered brecciated country rock (Hetman et al. 2004). A/K15 is another example of a blind intrusion containing well developed globular segregatory

textures (Field and Scott Smith, 1999). Downes et al. (2007) noted distinct globular segregationary textures in intrusive kimberlitic dikes associated with the Aries kimberlite in Australia. This distinct globular segregationary texture at these kimberlites must have formed prior to explosive emplacement of the kimberlite. The presence of globular segregationary kimberlite in blind intrusions is particularly important in the understanding of the process in which they form and must indicate sub-volcanic origins.

The typical characteristics of transitional kimberlites are described by Hetman et al. (2004) and Skinner and Marsh (2004) in detail. Transitional kimberlites typically show a gradational change between two end member types; a hypabyssal transitional type (HKt) and a tuffisitic transitional type (TKt). The terminology of Hetman et al. (2004) has been adopted here to differentiate between the two textural varieties. The term TKt is used as a descriptive term, to describe transitional kimberlite which looks similar to TK but does not form in a similar process to the TK. TKt is part of the root zone, which is a hypabyssal environment, not the diatreme zone (Skinner, 2008). It may be useful to develop new terminology to avoid implying genetic connotations to the TKt. TKt is generally more competent than typical TK and show an inhomogeneous, patchy distribution of pelletal lapilli textures and hypabyssal textures (Hetman et al. 2004), which is dominated by the former. Hypabyssal patches are typically identified by a greater degree of crystallisation relative to the pelletal lapilli patches. Serpentine is the dominant component of the base in the TKt, which is interpreted to be the result of the dominance of H₂O exsolving from the magma (Skinner and Marsh, 2004). Hypabyssal transitional kimberlite shows a similar patchy distribution of the two distinct textures but the hypabyssal textures become more dominant. Hypabyssal patches become coarser grained with depth (Hetman et al. 2004). Segregationary textures are common in the tuffisitic transitional kimberlite (TKt) but become incipient with depth into the hypabyssal transitional kimberlite (HKt) (Skinner and Marsh, 2004). Calcite is absent in TKt but is present in the HKt (Hetman et al. 2004 and Skinner and Marsh, 2004). This is a particularly important characteristic as the loss of calcite is interpreted to indicate the loss of CO₂ from the system (Skinner and Marsh, 2004). Olivine is typically completely serpentinised in the TKt but becomes only partially altered in the HKt (Skinner and Marsh, 2004). Possibly the most important characteristic of the transitional zones is the appearance of microlitic clinopyroxene. Microlitic clinopyroxene in the HKt is typically patchily distributed and relatively coarser grained than in the TKt but microlitic clinopyroxene becomes particularly

abundant in the TKt and often becomes pervasive throughout the rock (Hetman et al. 2004 and Skinner and Marsh, 2004). Primary diopside is absent in typical hypabyssal kimberlite (with the exception of some Group II kimberlites e.g. Voorspoed) and the development of microlitic clinopyroxene is the first indication of a transitional kimberlite.

5.3.2.4 Transitional Kimberlite at the Kroonstad Cluster

The transitional kimberlites at the Voorspoed and Lace pipes do not show the complete gradation from hypabyssal type through to diatreme type as described by Skinner and Marsh (2004) and Hetman et al. (2004). However the transitional kimberlites at Lace show a gradational development of globular segregations and microlitic clinopyroxene. The HKt at Voorspoed show no gradational change and only show the development of incipient globular segregations. The diatreme type end member is not present at either pipe. The characteristic globular segregatory texture of the rock is always incipient although varying degrees of incipiently development textures are described at the Lace pipe (Section 3). Incipient globular segregatory textures are gradational and are described from a low degree of incipient development to a high degree of incipient development. This distinction is to clearly illustrate the varying degrees of development of the texture. Globular segregatory textures show a high degree of development with decreasing depth from the surface. Country rock xenolith as well as microlitic clinopyroxene content also increases with decreasing depth. Microlitic clinopyroxene is not observed at the Voorspoed pipe HKt however primary diopside phenocrysts are present. The gradational development of globular segregations in the HKt is only observed at the Lace pipe. Furthermore the xenolith population in the HKt is completely different from the overlying VK at both the Lace and Voorspoed occurrences. This is another particularly important characteristic discussed below.

It must be noted here that in the literature transitional kimberlite has only been described for Class 1 kimberlite and no transitional kimberlite has been observed outside of Class 1 examples. The Voorspoed and Lace kimberlite are not Class 1 pipes and therefore the observations made here are the first for transitional kimberlite outside of Class 1 kimberlites. Typical characteristics for Class 1 transitional kimberlite include: the appearance of microlitic clinopyroxene, the disappearance of calcite with subsequent abundant formation of

serpentine and the development of spherical, segregationary structures. The transitional kimberlite at the Voorspoed pipe is not similar to those described in the literature. The most obvious difference is the complete lack of serpentine at the Voorspoed kimberlite. Furthermore the Voorspoed pipe does not contain any microlitic clinopyroxene but does contain incipient globular segregationary textures and nucleated globules are abundant in the MVK. The HKt at Voorspoed is identified by the presence of an incipient globular segregationary texture only. The HKt at Lace is much more similar to that described by Skinner and Marsh (2004) and Hetman et al. (2004). The Lace HKt shows a gradational increase in the development of an incipient globular segregationary texture, microlitic clinopyroxene and the presence of serpentine.

5.3.3 Pre-development of the Embryonic Pipe

5.3.3.1 Magma Ascent to Near Surface

Kimberlite magma is derived from the asthenosphere and as it nears the surface consists of 25 vol.% olivine macrocrysts and 25 vol.% olivine phenocrysts (Mitchell, 2008). Again this figure of 50 vol. % olivine is for Group I kimberlites but as discussed in section 1 it is reasonable to compare Group I and II kimberlites. The high proportion of solids (olivine) indicates a relatively high effective viscosity of the magma as a whole. The silicate liquid portion will have a very low viscosity (Sparks et al. 2006). One would expect the magma ascent rates to be slow given the effective high viscosity of the magma. Sparks et al. (2006) postulate a high magma ascent rate of approximately 4m/s. This estimate is based on kimberlite magma having a very low viscosity. Wilson and Head (2007) suggest an ascent rate of up to 30-50 m/s. It seems more likely that the relatively high effective viscosity of the kimberlite magma created by the high proportion of solids would create slower magma ascent rates nearer the surface. The magma is more likely a slurry and ascent rates are unlikely to be very high (Mitchell, 1995). Possible fractional crystallisation (e.g. Harris et al. 2004) en route to the surface may further indicate a slower ascent rate than described by Sparks et al. (2006) and Wilson and Head (2007). The magma ascends through stoping and according to Barnett and Lorig (2007) the magma is passively emplaced in joints in the country rock.

5.3.3.2 Fractional Crystallisation, Differentiation and a Staging Chamber

The Voorspoed pipe HK is characterised by the absence of olivine macrocrysts. The Lace kimberlite is macrocrystic but olivine contents are slightly lower relative to the standard of approximately 50% as described by Mitchell (2008). This loss of olivine observed at the Voorspoed pipe in particular is interpreted to be the result of fractional crystallisation en route to the surface. Geochemical trends indicating fractional crystallisation are observed from the Voorspoed and Lace HK with decreasing Ni and MgO, as shown in section 4. The trends do not indicate a simple olivine fractionation as indicated by the increased Al₂O₃ and K₂O contents, as discussed in section 4. Fractional crystallisation of other hypabyssal kimberlites en route to the surface has been proposed by numerous authors (le Roex et al. 2003; Harris et al. 2004; Becker and le Roex, 2006 and Coe et al. 2008). This fractional crystallisation is likely to affect the magma composition (Mitchell, 1995 and Becker and le Roex, 2006), which is particularly evident at the Voorspoed pipe as it has a much more evolved chemistry relative to the Lace pipe. This compositional change may be due to the incorporation of lower crustal granulite xenoliths, which are common at both the Voorspoed and Lace pipes (Roberts, 1997 and Field et al. 2008) or through simple differentiation processes. Fractional crystallisation of the magma must further indicate that the magma could not ascend at the high rates, proposed by Sparks et al. (2006) and especially not the very high rate of Wilson and Head (2007), as it would have to stall for long enough to allow for fractionation to occur or have risen slow enough to allow for fractionation en route. The effective viscosity of the magma may be significantly lowered due to fractional crystallisation, which would remove the bulk of the solid content from the magma. However a detailed investigation of the magma ascent rate is outside the scope of this study and only assumptions can be made, although it does seem more likely that ascent rates were relatively low near surface due to the high solid content of the magma.

This fractionation process must also have affected the mantle xenolith content of the magmas. The Voorspoed pipe contains lower crustal granulite xenoliths but mantle xenoliths have not been reported in abundance (Roberts, 1997). The Lace pipe is characterised by the presence of garnet granulite xenoliths with lesser rare eclogite xenoliths also present (Field et al. 2008). Lower crustal xenoliths (granulite) may have been incorporated into the kimberlite magma during the process of fractional crystallisation in a staging chamber at depth.

Incorporation of significant proportions of these lower crustal xenoliths may account for the high SiO₂, Na₂O and Al₂O₃ observed at the Voorspoed evolved kimberlite. Further geochemical analysis of the Voorspoed HK and lower crustal xenoliths needs to be done to better understand this possible relationship. The presence of rare mantle xenoliths at Lace indicate that the magma did not undergo significant fractional crystallisation and only minor amounts of the solid content of the magma was lost.

Evolved Group II kimberlites show no simple relationship with the unevolved end member (Mitchell, 1995). However a number of features suggest that evolved Group II kimberlites are differentiates of the unevolved end member, which include: 1) absence of diamond, 2) scarcity of xenocrystal olivine, 3) primary mineral assemblage and 4) evolutionary trends of composition (Mitchell, 1995). Alternatively the evolved magmas form from different source rocks, although the evidence for fractional crystallisation favours differentiation. Fractional crystallisation and differentiation is envisaged to occur at depth in a magma staging chamber, which would allow for the fractionation of xenocrystal olivine, diamonds and any larger components within the magma such as mantle xenoliths. The presence of lower crustal granulite xenoliths at the Voorspoed and Lace kimberlites may indicate a possible location for a staging chamber. The granulite xenoliths may have been incorporated into the staging chamber from the sidewall. No evidence exists for the formation of staging chambers and further work needs to be done on Group II compositional trends to constrain these observations.

5.3.4 Embryonic Pipe Model for the Initial Development of the Kroonstad Kimberlite Pipes

5.3.4.1 Evidence for Sub-Volcanic Origin from the Kroonstad Cluster

The following section discusses the characteristic features of the Voorspoed and Lace transitional kimberlites and their genetic sub-volcanic connotations. The important characteristics discussed below include: 1) xenolith distribution, 2) gradational development of globular segregatory texture and microlitic clinopyroxene and 3) hypabyssal transitional kimberlite at the Lace blind pipe. Further features of the HKt relevant to the formation processes are also discussed below.

Xenolith Distribution relative to Volcaniclastic Infill

As described in section 3, the dominant country rock xenolith type in both the Voorspoed and Lace pipes volcaniclastic kimberlite (VK) is Karoo basalt. The xenolith population at the Voorspoed pipe VK contains abundant basalt xenoliths, which ranges between 60-80% of the CRX population and up to 60 vol. % of the rock. The Lace VK xenolith population is comprised of 50-90% basalt. Therefore Karoo basalt is the dominate xenolith observed in the VK infill at both the Voorspoed and Lace pipes. However the HKt at both the pipes do not contain any Karoo basalt xenoliths. The xenoliths in the HKt are all derived from local sidewall lithologies, which are dominated by shale. Dolerite xenoliths are observed at the Voorspoed HKt however a dolerite sill is located in the sidewall at the same depth. Dolomite xenoliths are also relatively abundant at the Lace transitional kimberlite, which would have been transported upwards in the magma from their original position in the country rock stratigraphy. The HKt must form sub-volcanically as no Karoo xenoliths are present. If the HKt formed through pyroclastic processes one would expect Karoo basalt xenoliths to be present, similar to the xenolith population in the overlying VK. The lack of basalt in the HKt clearly indicates a non-pyroclastic origin rather than a pyroclastic origin as suggested by Sparks et al. (2006) and Brown et al. (2008b) for other South African kimberlites. Analysis of the xenolith populations in the rock types at the cluster can provide an easy tool for the discrimination between sub-volcanic HKt and VK.

Gradational Development of Globular Segregationary Textures and Microlitic Clinopyroxene at the Lace HKt

The change observed in the hypabyssal transitional kimberlite (HKt) at the Lace pipe is characterised by two important gradational changes: 1) mineralogical change where microlitic clinopyroxene becomes evident with subsequent disappearance of monticellite and apatite and 2) development of an incipient globular segregationary texture. Primary diopside is not observed in the HK at the Lace pipe. Globular segregationary textures are always incipiently developed and do not become pervasive. The development of the globular segregationary textures varies from low to high degrees as described in section 3. Figure 5.9 shows the variation in globular segregationary texture observed and the patchy distribution of microlitic diopside.

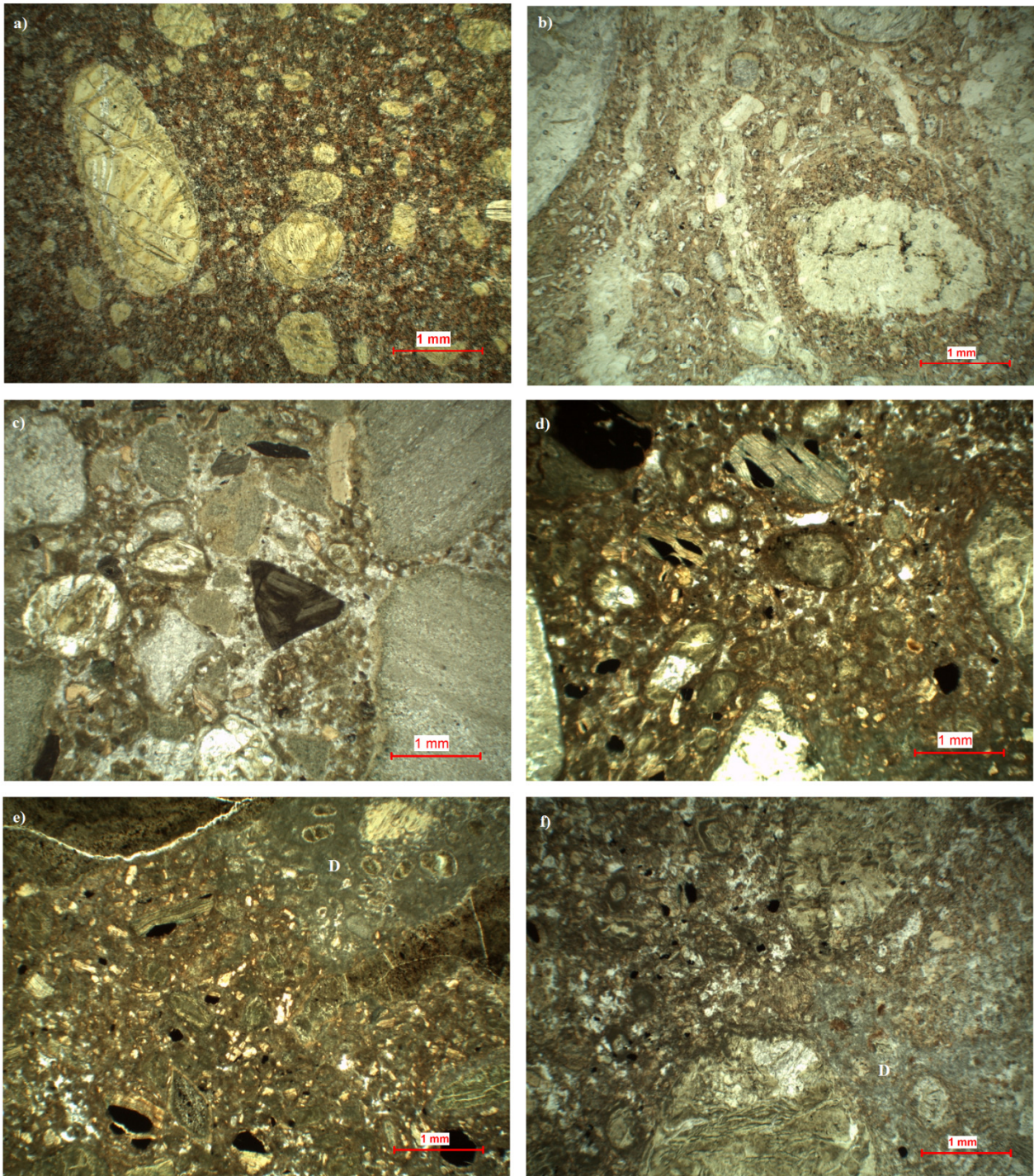


Figure 5.9 Photomicrographs from the Lace kimberlite HKt/HKtB. a) Sample C6-713; the base of the HKt with no globular segregatory texture, although microlitic clinopyroxene is abundant (too fine grained to see at this scale). b) Sample C6-706; First development of globular segregatory texture, note the distinct large globules cored by a serpentinised olivine macrocryst in the bottom right corner. The base of the rock is a combination of serpentine and calcite. c) C6-642; HKtB with abundant calcite in the base. Note the incipient development of globules cored by serpentinised olivine (centre left). d) Sample C6-630; Typical incipiently developed HKtB with an ultra fine base, which is often difficult to identify. e) Sample C6-630; Patchy distribution of ultra fine grey microlitic clinopyroxene in the HKtB. D: Microlitic clinopyroxene. f) Sample C6-706; Similar patchy distribution of ultra fine grey microlitic clinopyroxene indicated by D.

Microclitic clinopyroxene is believed to be indicative of a transitional kimberlite (Skinner and Marsh, 2004) where no globular textures are present. The deepest sample (C6-713) obtained from the Lace kimberlite is at approximately 620m below the current land surface. No HK sensu stricto has been observed in the borehole sampled, however HK sensu stricto samples have been obtained from the surrounding old mine dumps. This mining occurred in the early 1900's and HK must have reached close to the surface at some locality within the pipe. This is possible as the development of the hypabyssal transitional kimberlite (HKt) is patchy and later stage pulses of magma may easily have reached near the current land surface. The HK sensu stricto is classified as a macrocrystic melilite- and apatite-bearing, monticellite, phlogopite kimberlite and no primary diopside or microclitic clinopyroxene is present. Interlocking phlogopite plates reach up to 0.8mm in length. The maximum grain size of phlogopite from sample C6-713 at the base of the HKt is 0.2mm indicating a much shorter crystallisation period. Furthermore and most importantly microclitic clinopyroxene becomes evident and accounts for 11 vol. % of sample C6-713. However no globular segregatory texture is observed for C6-713. This sample shows evidence for the initial development of a transitional kimberlite by the finer grained nature and the first occurrence of microclitic clinopyroxene. Microclitic clinopyroxene replaces earlier formed minerals such as monticellite and apatite, which disappears in the transitional kimberlite. Microclitic clinopyroxene shows a gradational increase in content with decreasing depth as described in section 3 and becomes pervasive at 515m below the current land surface (sample C6-630), however the content does vary at this depth and may be completely absent in thin section samples. At this level the microclitic clinopyroxene content can reach up to 22 vol. %. Modal analyses are given in section 3 in table 3.1.

The first occurrence of an incipient globular segregatory texture is observed in sample C6-706, which shows a low degree of development. The texture is incipient, patchy and variable over the entire column of transitional kimberlite and ranges from moderate to high degrees of development as discussed in section 3. It must be noted that sample C7-338 from 280m below the current land surface is very similar to sample C6-713 in that it does not show the development of a globular segregatory texture. It is possible that numerous pulses of magma were intruded, all of which evolved differently in terms of the development of globular segregatory textures and microclitic clinopyroxene content. The lack of a globular segregatory texture in sample C7-338 is most likely due to a later pulse of magma, which

did not develop a segregationary texture. Multiple pulses of magma into a root zone are common in kimberlites throughout the world (Clement, 1982; Skinner and Marsh, 2004) and it is not unreasonable to assume that numerous pulses of magma have occurred at Lace.

Therefore there is a gradational change in the HKt, which is marked by the increase in microlitic clinopyroxene content, disappearance of monticellite and apatite, the development of globular segregationary textures and a decrease in grain size. These characteristics are similar to those described by Skinner and Marsh (2004) and Skinner (2008). Serpentine is present at the Lace pipe however is completely absent from the Voorspoed HKt. Serpentine becomes dominant in the tuffisitic transitional kimberlite (TKt) type kimberlite as described by Skinner and Marsh (2004). No gradational change is observed in the HKt at Voorspoed, which may indicate that the development of the transitional kimberlite was aborted prior to the development of serpentine or that the system did not contain abundant H₂O, after the crystallisation of phlogopite, required to crystallise serpentine. This gradational development of HKt is interpreted to be in situ and indicate a sub-volcanic origin for their formation.

Hypabyssal Transitional Kimberlite (HKt) at the Satellite Blind Pipe at Lace

The satellite pipe at the Lace kimberlite has been sampled at a depth of approximately 250m from the current surface. The kimberlite at this depth is hypabyssal transitional kimberlite breccia (HKtB) as described in section 3.1. The pipe does not reach the current land surface as it is directly overlain by shales. Therefore the rock types within the pipe can only have formed through sub-volcanic process as explosive breakthrough to the surface has not occurred. The xenolith lithologies within the sample obtained from the satellite pipe are the same as the xenolith content of the HKtB rock described for the main pipe with no Karoo xenoliths observed. Furthermore the HKtB at the satellite pipe has a very similar incipient globular segregationary texture to the main pipe. It is reasonable to assume that the two very similar rock types from the satellite and main pipes have formed by similar processes, which can only be sub-volcanic as the satellite pipe is blind. This is compelling evidence which supports the sub-volcanic origin of transitional kimberlites proposed by Skinner and Marsh (2004) and Hetman et al. (2004).

5.3.4.2 Discussion on the Term Nucleated Autolith/Magmaclast

The term nucleated autolith was first used to describe nucleated spheroids consisting of a xenolith or mineral fragment encased in fine grained kimberlitic material, occurring in diatreme zones (Ferguson et al. 1973 and Danchin et al. 1975). These magmaclasts were termed autoliths because kimberlite (nucleated autolith) is enclosed by kimberlite (diatreme zone kimberlite). Typical autoliths in kimberlites are angular to sub-rounded clasts formed by the fragmentation of pre-existing solidified material with textures the same as hypabyssal kimberlite in the root zone (Mitchell, 1995). These autoliths are not the same as nucleated autoliths and are generally accepted in the literature in terms of their formation. The term nucleated autolith has been thrown out of the current terminology (Cas et al. 2008b and Scott Smith et al. 2008c) and the non-genetic term nucleated globule was proposed by Mitchell (1995). However nucleated autolith may apply to the magmaclasts forming at the Kroonstad kimberlites.

Generally the term pelletal lapilli is used to describe spherical magmaclasts, which contain cores surrounded by very fine grained kimberlitic material in typical South African Class 1 kimberlites. The cores are dominated by olivine and xenoliths are very rarely observed (Mitchell, 1995). Clement (1982) interpreted coarse grained pelletal lapilli as originating from globular segregations in the hypabyssal environment. This is a similar interpretation for the nucleated magmaclasts at the Kroonstad kimberlites. The clear development of extensive globular segregations in the underlying HKt/HKtB, at both the Voorspoed and Lace kimberlites, which have mineralogies, textures and shapes identical to the nucleated magmaclasts found in the VK infill indicate that the magmaclasts are related to the globular segregations. Nucleated magmaclasts are interpreted in section 5.3.5 to have formed in the hypabyssal kimberlite during extensive exsolution of volatiles and the nucleation of crystallising magma around solid components already present within the magma, such as olivine or xenoliths. Therefore the term nucleated autolith may be relevant to the formation of the magmaclasts in the Kroonstad cluster. Regardless of the terminology these nucleated magmaclasts are forming in the hypabyssal environment as globular segregations and are not magma droplets crystallising after explosive eruption of the kimberlite. The following discussion deals with the characteristic of the nucleated magmaclasts, which have implications on the formation processes of the embryonic pipe.

5.3.4.3 Features of the Embryonic Pipe Transitional Kimberlite (HKt/HKtB) at the Kroonstad Cluster Relevant to Formation Processes

A number of characteristic features, which have relevant genetic connotations to the formation of the embryonic pipe, are discussed below. These include the 1) volatile content of the magma, 2) presence of basalt central kernels in nucleated globules, 3) presence of well developed nucleated magmaclasts within the massive volcanoclastic kimberlite (MVK) units, 4) sanidine and aegirine in nucleated magmaclasts and 5) geochemical variation.

Volatile Compositions of the HKt

Kimberlite magma is defined as being volatile-rich and contains both H₂O and CO₂. The proportion of the respective volatile phases is subject for much debate in the current literature. Wilson and Head (2007) believe CO₂ is the dominant volatile that drives the ascent and eruption of the magma whereas Skinner (2008) believes H₂O to be the dominant volatile phase driving Class 1 eruption. However it seems likely that volatile proportions vary widely between different kimberlite classes as discussed by Skinner and Marsh (2004). Transitional kimberlite in typical Class 1 tuffisitic kimberlite is characterised by the loss of calcite and the dominance of serpentine segregations, which is believed to be the result of the dominance of H₂O as the exsolved gas phase crystallising at a late stage. Therefore H₂O would be the more dominant volatile in these circumstances.

Voorspoed

The HKt at the Voorspoed pipe is not like any HKt described in the literature. The lack of the characteristic microlitic clinopyroxene as well as serpentine is unique to Voorspoed. The only indication of the transitional nature of the kimberlite is the moderate degree of incipient globular segregatory texture development. However the interesting characteristic of the Voorspoed HKt is in the base of the rock, which is comprised of abundant ultra fine grained (<0.01mm) phlogopite. This characteristic is not observed in the Lace transitional kimberlite. This feature indicates that H₂O was initially abundant in the magma and that much of the H₂O would have been locked up in the phlogopite crystal structure prior to exsolution of volatiles. This explains the complete lack of late stage serpentine and the dominance of late

stage calcite filling the interstitial spaces. In terms of emplacement process the magma would have originally been rich in both CO₂ and H₂O but, due to H₂O becoming locked into the phlogopite crystal structure, the dominant volatile phase during exsolution in the HKt must have been CO₂. As a result of this dominance of CO₂, calcite, which would crystallise from the supercritical fluid, is the only mineral filling the interstitial spaces between the globules. Furthermore CO₂ is likely to have been the dominant volatile phase driving the eruption of the Voorspoed pipe.

Lace

The Lace hypabyssal transitional kimberlite (HKt) is different from the Voorspoed HKt. The major differences are the presence of microlitic clinopyroxene (which becomes pervasive) and the presence of serpentine. The HKt generally contains an ultra fine grained base, which contains dominantly calcite. However serpentine is identified such as that shown in figure 5.9(b). The Lace HKt is very similar to typical transitional kimberlite described for Class 1 pipes (Skinner and Marsh, 2004 and Hetman et al. 2004). Although there is no complete gradation into tuffisitic transitional kimberlite (TKt) and the volcanoclastic kimberlite is not tuffisitic kimberlite (TK) as described in section 3. The initial processes of formation of the HKt must be similar to those described by Skinner (2008). The volatile composition is likely to be slightly different at Lace relative to Voorspoed as serpentine is present as a late stage mineral and free water is likely to be present at this stage. Calcite is also abundant in the HKt, which indicates CO₂ is also relatively abundant as a late stage volatile phase along with water. The presence of monticellite crystallising at an early stage indicates that CO₂ must be exsolving at this stage as well as monticellite crystallises as a consequence of degassing of CO₂ (Sparks et al. 2006). The Lace HKt is very similar to the HKt described by Skinner and Marsh (2004) and Hetman et al. (2004) and is likely to have formed in a similar process. However the process would be aborted at some stage as no tuffisitic kimberlite is observed at the Lace pipe.

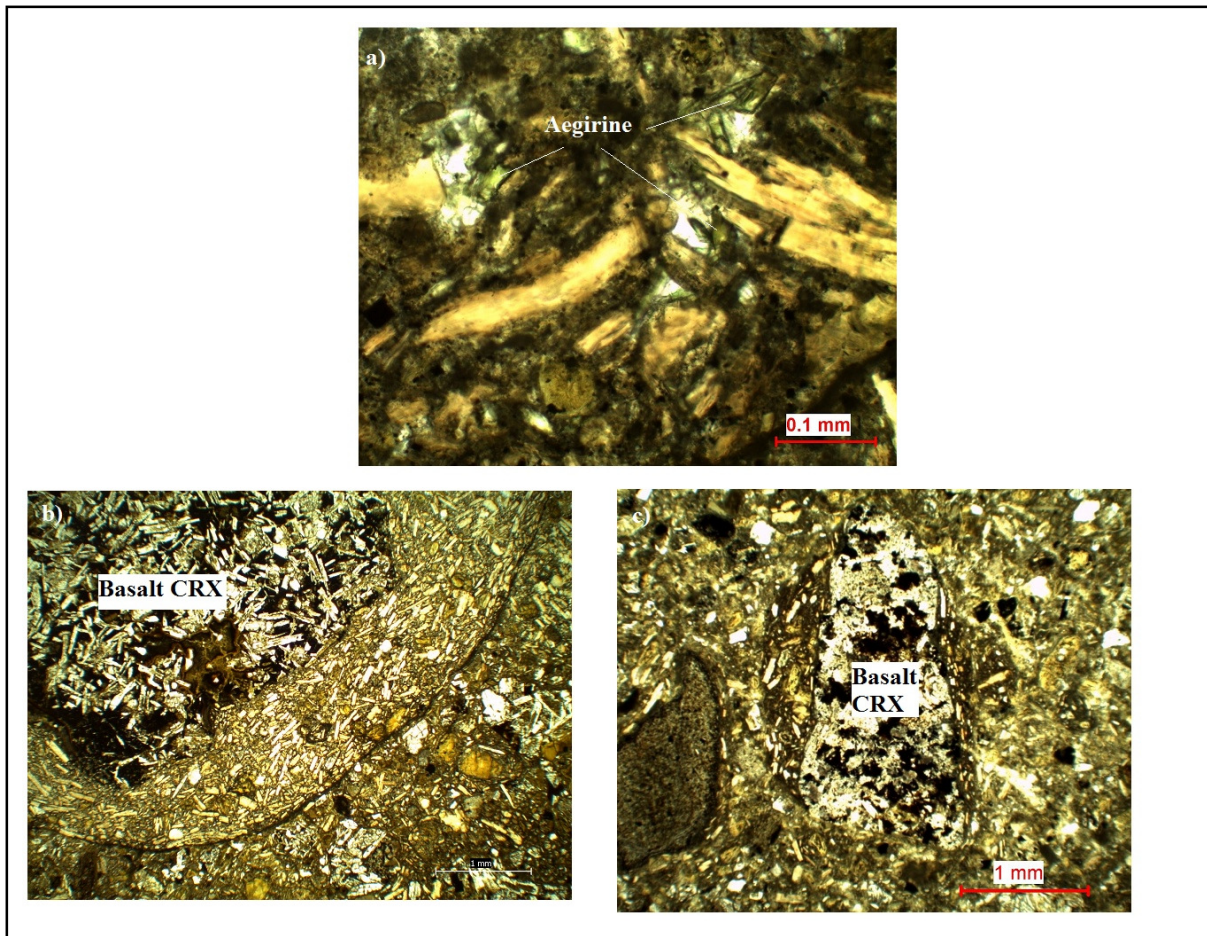


Figure 5.10 Photomicrographs of from the Voorspoed VK showing: a) aegirine laths within the nucleated globule shown in b). b) Nucleated globule with a basalt central kernel and coarse crystalline mantle. Aegirine is observed in the mantle as shown in a). c) Nucleated globule with basalt central kernel and relatively fine grained mantle with a dark brown turbid base. b) and c) show the two end member varieties as discussed in the text: section 5.3.4.2 below.

Extent of the Hypabyssal Transitional Kimberlite Column: Evidence from the presence of basalt CRX central kernels in nucleated magmaclasts and the volatile composition of the magma

Karoo type basalt xenoliths are commonly observed as central kernels within nucleated magmaclasts within the Voorspoed and Lace VK, as shown in figure 5.10. The basalt kernels are typically highly altered relative to the basalt xenoliths observed outside of the magmaclasts. Typically the basalt xenoliths in the VK deposits show a slight degree of alteration of the plagioclase however the clinopyroxene is almost always fresh. The basalt xenoliths as kernels within nucleated magmaclasts are highly altered with both the plagioclase and the clinopyroxene altered. The basalt forming central kernels must have been

incorporated into very hot kimberlite magma, which was able to alter the basalt. Furthermore the incorporation of the basalt must have been early in the crystallisation sequence as they must have formed sites for nucleated crystal growth. This would have occurred in a transitional kimberlite environment during the formation of the nucleated globules in the embryonic pipe, as discussed below.

The basalt central kernels most importantly provide evidence for the depth to which the kimberlite magma rises and the extent of the embryonic pipe. Karoo basalt is the upper lithological unit in the country rock stratigraphy and is approximately 1400m thick in the preserved outcrops (Marsh et al. 1997). Basalt xenoliths from both the Voorspoed and Lace pipes have been found to correlate with a full sequence of the Karoo basalt lava pile (Hanson, 2006 and Howarth, 2007) and the maximum thickness of the basalt at the time of emplacement of the Kroonstad Cluster is approximately 1400m as discussed in section 5.1. The kimberlite magma must have risen to at least <1400m below the surface in order to incorporate basalt xenoliths into the magma column. It is likely that the magma reached shallower levels as basalt CRX central kernels to magmaclasts are common in the volcanoclastic kimberlite (VK).

Skinner (2008) uses the solidus curve for an H₂O-rich and CO₂-rich peridotite (Wyllie, 1987) as an analogue for kimberlite magma as there are no experimental studies on kimberlite. As shown in figure 5.5 the volatile composition is directly related to the depth to which the magma can rise. The more CO₂-rich the magma; the closer to the surface the magma can reach. The Voorspoed and Lace kimberlite are interpreted to be initially H₂O-rich as discussed above and would be expected to crystallise at similar depths indicated by the H₂O-rich peridotite. This depth is approximately 3km from the original land surface, however breakthrough to the surface occur from approximately 1km (Skinner, 2008). Based on the above discussion of basalt CRX as central kernels in nucleated magmaclasts and interpretations from Skinner (2008) it can be confidently estimated that the kimberlite magma must reach at least 1000-1400m from the original land surface. It is likely that the estimate is closer to 1km as abundant basalt kernels are observed within magmaclasts in the MVK, which indicates the magma incorporated relatively abundant basalt country rock.

Crystallisation of the Nucleated Magmaclasts as Globular Segregations

The paragenesis and textural relationships of the mineralogy of the magmaclasts provides evidence to constrain the temperature evolution during their formation as globular segregations. Two nucleated magmaclasts end members exist, which indicate a range in temperature of formation. Firstly late stage aegirine-sanidine has been observed in rare occurrences (figure 5.10). Aegirine occurs as fine grained laths (+/- 0.05mm) protruding inward into irregular sanidine plates. The aegirine and sanidine is thought to have crystallised out of late stage evolved segregation in the magma and would be the last minerals to crystallise apart from calcite. Therefore this end member of formation must have crystallised to near completion at temperatures equivalent to the crystallisation of sanidine, which is approximately 600-700°C (Deer et al. 1992). Furthermore these nucleated magmaclasts are generally coarser grained, than those described below, indicating a longer crystallisation history with no quenching evident. These globules must have crystallised to near completion before explosive eruption, which would produce a rapid temperature drop and quench the remaining melt. No glass is observed in any nucleated magmaclasts and quenching is unlikely to have occurred.

The presence of late stage aegirine and sanidine within nucleated globules is particularly rare. The more dominant characteristic is a fine grained base component of ultra fine grained turbid brown material, which is identified as a combination of calcite and clay minerals. This is the second end member of the nucleated magmaclasts and these nucleated magmaclasts contain a finer grained mineralogy than the aegirine-sanidine end member and indicate a much shorter crystallisation history, however no glass is observed. These nucleated magmaclasts may have begun crystallisation at similar temperatures to the aegirine-sanidine end member but the temperature drop would have been much more sudden to produce the ultra fine grained base of the globules. These globules look very similar to typical HKt rather than HK proper. The temperature drop may have been faster, which would produce the finer grained base material.

Degree of Development of Globular Segregationary Texture in the Original Hypabyssal Transitional Kimberlite (HKt) Column: Evidence from the well developed nucleated magmaclasts in the Massive Volcaniclastic Kimberlite (MVK) units

At the current level of the HKt the globular segregationary texture is always incipiently developed and no gradation is observed into typical tuffisitic kimberlite, which is usually the case with transitional kimberlites (Skinner and Marsh, 2004 and Hetman et al. 2004). The Voorspoed pipe is unique in that the contact with the overlying MVK is sharp. The HKt at Voorspoed is expected to have developed for approximately another 1km above the current locality to approximately 1km below the original land surface, as described above. It would be expected to develop to pervasive globular segregationary textures such as those documented in the literature (Skinner, 2008 and Masun and Scott Smith, 2008). This is evident from the presence of well developed nucleated magmaclasts within the VK deposits at Voorspoed. The VK at Voorspoed is characterised by the presence of abundant nucleated magmaclasts, which have initially been formed in the HKt, as described below. The presence of abundant well formed nucleated magmaclasts in the VK must indicate that the globular segregationary texture within the HKt at higher levels must have been well developed in order to form abundant well developed nucleated magmaclasts.

Geochemical Variation of the Hypabyssal Transitional Kimberlite (HKt): Implications for emplacement processes

Analysis of xenolith-free HKt samples from the Lace pipe show trends of increasing Na₂O and SiO₂ with decreasing MgO. These trends are usually attributed to the contamination of the magma by country rock material (Clement, 1982 and le Roex et al. 2003). However these rocks contain insignificant proportions of country rock material. The trends have been linked petrographically to the increase in microlitic clinopyroxene proportion, which can account for both the increased SiO₂ and Na₂O as shown in section 4. Mitchell et al. (2009) show that microlitic clinopyroxene can form by either CO₂ degassing or xenolith contamination. Therefore in the case of the xenolith poor HKt from the Lace pipe, the microlitic clinopyroxene must have formed through CO₂ degassing. This is confirmed when comparing CO₂ contents between root zone hypabyssal kimberlite and dike/sill hypabyssal kimberlite, as shown in section 4. Therefore the geochemical variation observed at the Lace pipe is the result of CO₂ degassing from the magma. Furthermore trends of decreasing incompatible

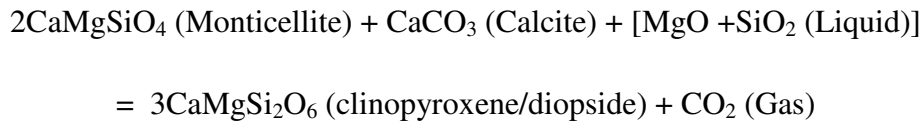
elements such as Nb is also observed, which is tentatively interpreted to result from incompatible elements being caught up in the fines material and possibly transported by degassing CO₂. However the only incompatible element showing these trends is Nb. Nowicki et al. (2008) shows similar trends with TiO₂ and V, which are not observed here. Further work needs to be conducted to better understand incompatible element variations in transitional kimberlites.

5.3.5 Formation of the Embryonic Pipe

5.3.5.1 Formation of Microlitic Clinopyroxene and Calcite in the Groundmass of the Lace Hypabyssal Transitional Kimberlite (HKt)

Microlitic clinopyroxene is a characteristic feature of transitional kimberlites and, when present in volcanoclastic kimberlite (VK), of tuffisitic kimberlite. Microlitic clinopyroxene is not observed in the VK at the Kroonstad Cluster apart from within the nucleated magmaclasts and therefore is not tuffisitic kimberlite. However microlitic clinopyroxene is observed in the transitional kimberlite at the Lace pipe. The formation of this clinopyroxene is particularly controversial in the current literature. Two schools of thought exist: 1) Post emplacement hydrothermal metamorphism, which does not relate to the kimberlite (Stripp et al. 2006, Sparks et al. 2006 and Hayman et al. 2009) and 2) clinopyroxene as a deuteric phase crystallising at a late stage out of an exsolved phase in an autometasomatic process (Skinner and Marsh, 2004 and Mitchell et al. 2009). The microlitic clinopyroxene at Kroonstad is accompanied by calcite and serpentine, although it is often difficult to identify these phases at Lace due to the often ultra fine grained nature of the base of the HKt.

Skinner and Marsh (2004) and Mitchell et al. (2009) present the only explanations to the formation of microlitic clinopyroxene as a deuteric mineral, which is at the expense of monticellite and CO₂ exsolution. This mineralogical change is very similar to that observed at the Lace pipe. Leaving aside the minerals common to both the HK and HKt (olivine and phlogopite) and the minor amounts of groundmass apatite, spinel, perovskite, melilite and serpentine at Lace the mineralogical change from the HK proper to HKt can be expressed as the following reaction as shown by Skinner and Marsh (2004):



This reaction fits perfectly with the Lace pipe, which shows the presence of clinopyroxene in the HKt. However the reaction does not fit with the Voorspoed pipe as no monticellite is present. This is confirmed by the complete absence of microlitic clinopyroxene at the Voorspoed pipe HKt. This reaction fits very well with the observations made at the Lace kimberlite and with the Voorspoed kimberlite. There is no mineralogical change observed at the Voorspoed pipe. The presence of primary diopside phenocrysts and the different late stage residual liquid composition at Voorspoed may inhibit the late stage crystallisation of microlitic clinopyroxene. Further work needs to be done on Group II kimberlites to confirm these initial observations as this is outside the scope of this study. However the reaction above clearly indicates the exsolution of CO₂ favours the formation of a clinopyroxene bearing assemblage.

Numerous authors (Sparks et al. 2006, Stripp et al. 2006 and Brown et al. 2009) have proposed a late stage hydrothermal process involving meteoric water for the formation of the characteristic assemblage of serpentine and diopside (microlitic clinopyroxene) in tuffisitic kimberlites and so called welded tuffs. These serpentine-diopside assemblages are interpreted to form at approximately 250-380°C from meteoric water (Stripp et al. 2006) and <370°C (Hayman et al. 2009). Sparks et al. (2006) gives two key lines of evidence to support a post emplacement hydrothermal origin: 1) the low CO₂ contents and 2) the sub-solidus temperatures calculated for the fluid that can form the common mineral assemblages (serpentine and diopside). Calcite is documented at the Venetia K2 pipe as a late stage hydrothermal mineral filling pore spaces in a welded pyroclastic rock (Brown et al. 2009), however an explanation of the origin of the CO₂ is not provided and it seems more likely that these rocks at Venetia are possibly HKt rather than welded tuffs.

Detailed investigations of carbonate compositions in kimberlites are rare in the literature. However it has been shown by Armstrong et al. (2004) and Wilson et al. (2007) that typical calcite compositions and stable isotopes respectively in coherent (hypabyssal) kimberlite from the Lac de Gras (Canada) kimberlites are indicative of a primary magmatic origin. Calcite segregations observed at the Lac de Gras kimberlites occur in both hypabyssal dikes (Anaconda, Rat, Rattler), which are not associated with VK, as well as from coherent kimberlite within kimberlite pipes (Grizzly and Leslie) (Armstrong et al. 2004). Furthermore similar calcite compositions are reported by Mitchell (1995) from hypabyssal dikes in South Africa (Bellsbank, Swartruggens). The calcite from both South Africa and Canada contains high Sr-Ba contents, which indicate a relatively high temperature of formation $>450^{\circ}\text{C}$ and more likely closer to 600°C (Chang, 1965). Furthermore stable isotope data on carbonates in South African kimberlites indicates a magmatic origin (Sheppard and Dawson, 1975 and Kobelski et al. 1979) similar to that described by Wilson et al. (2007) for the Lac de Gras kimberlites. Calcite analysis is outside the scope of this study but further investigation and comparison of calcite compositions from HK, HKt and VK may provide important evidence for the interpretation of the formation of transitional kimberlites.

Evidence for Deuteric Origin of Microlitic Clinopyroxene from the Lace Kimberlite

The Lace kimberlite contains abundant microlitic clinopyroxene in the HKt and HKtB. An important feature of the HKt is that the clinopyroxene does not occur as inclusions within the highly poikilitic phlogopite plates. If the clinopyroxene was primary it would be expected to crystallise before the phlogopite and therefore be present as inclusions within the phlogopite plates. Furthermore the clinopyroxene is observed replacing earlier formed minerals such as monticellite and apatite. The most important feature of the Lace kimberlite is from the VK where microlitic clinopyroxene is present in the nucleated magmaclasts but not within the interclast material of the VK. If the microlitic clinopyroxene formed through late stage secondary processes one would expect the whole rock to become altered and not just the kimberlite components. The nucleated magmaclasts are forming in the embryonic pipe where degassing magma crystallises clinopyroxene as a late stage mineral and therefore they are altered by microlitic clinopyroxene.

5.3.5.2 Stages in the Development of the Embryonic Pipe

Stage 1: Magma Crystallisation

The kimberlite magma ascends to the near surface where the depth of crystallisation will be controlled by the volatile composition and ratio within the magma (Skinner and Marsh, 2004 and Cas et al. 2008a). Based on theoretical observations using peridotite, Wyllie (1987) showed that a water-saturated peridotite would cross the solidus at approximately <3km from the surface whereas a CO₂-saturated peridotite would reach the surface. Due to the lack of experimental data for kimberlites it is assumed that kimberlite magma acts in a similar way to peridotite magma. Sparks et al. (2006) state that water is soluble in a carbonatitic melt and would effectively lower the liquidus, allowing the melt to reach the surface. Carbonatites are defined as containing >50% carbonate minerals (Winter, 2001). At the Kroonstad Cluster the Lace and Voorspoed HKs contain approximately 10% carbonates each and are not carbonatites by definition. Field and Scott Smith (1999) described three distinct varieties of kimberlite pipes, which were interpreted to be the result of differing local country rock geology. Skinner and Marsh (2004) showed that more than one variety often occurred in similar geological settings and therefore this could not be used to explain the variation of kimberlite pipes. Skinner and Marsh (2004) propose that the three distinct pipe classes are the result of the variation in the volatile composition of the magma. CO₂-rich magmas reach closer to the surface than water-rich magmas. Volatile composition of kimberlite magma is under much debate in the literature with numerous authors proposing CO₂ dominated magmas (Sparks et al. 2006 and Wilson and Head, 2007). However Sparks et al. (2006) does propose a proportion of water in the melt, which is indicated by the presence of phlogopite but the proposed emplacement model is governed by CO₂. Skinner and Marsh (2004) propose that the volatile composition can vary and is the most important factor governing kimberlite emplacement mechanisms. The volatile composition of the kimberlite magma will determine to what depth the magma is likely to rise.

In the case of the Voorspoed and Lace kimberlites the magma must have been initially water-rich, which is indicated by the high proportion of phlogopite (approximately 40% and 35% respectively) in the HK. However serpentine is notably absent from the Voorspoed pipe HK/HKt, which may indicate that water was not abundant at late stages in the kimberlite magma. Serpentine is present at the Lace HKt, which must indicate that free water was

present in the magma at a late stage to allow for the crystallisation of serpentine. Serpentine paragenesis is under much debate in the literature. Stripp et al. (2006) and Lorenz and Kurszlauskis (2007) interpret serpentine as a post emplacement replacement mineral. Mitchell (2008) interprets serpentine as a late stage deuteric mineral, which is directly related to the kimberlite. Furthermore monticellite is abundant at the Lace HK and is interpreted to be crystallising as a result of the exsolution of CO₂ (Sparks et al. 2006). Monticellite is a common mineral in typical Group I kimberlites. CO₂ must be exsolving at an early stage to induce the crystallisation of monticellite whereas H₂O may only exsolve at a later stage or not at all in the case of the Voorspoed kimberlite.

The presence of abundant phlogopite at the Voorspoed and Lace kimberlite indicates that the magma is likely to be water-rich and cross the solidus at <3km from the surface. This would induce en masse crystallisation of phlogopite at Voorspoed and both phlogopite and monticellite at Lace. The crystallisation of monticellite at Lace indicates that CO₂ must be exsolving at this stage. This en masse crystallisation of the magma would effectively render the Lace magma immobile as the solid content could be as high as 80% and further emplacement to the surface would be inhibited. However the Voorspoed magma may still be able to flow as the initial solid content was much lower than Lace as a result of fractionation processes. Furthermore the complete absence of serpentine and dominance of calcite as late stage deuteric minerals at Voorspoed indicates that CO₂ was the dominant volatile phase after the crystallisation of the phlogopite. Carbonate in kimberlites has been interpreted to be magmatic in origin from both compositional data (Armstrong et al. 2004) and from stable isotope studies on carbon (Sheppard and Dawson, 1975 and Kobelski et al. 1979). Cas et al. (2008a) observe carbonate filled veins in the country rock, which is interpreted to be a result of crystallisation from an exsolved gas phase. Contact breccias at the Kroonstad cluster show similar carbonate filled veins and voids in the country rock, which are interpreted similarly to Cas et al. (2008a). Geochemical data presented by Clement (1982) clearly indicates that CO₂ is degassing from hypabyssal dike/sill environments to root zone hypabyssal kimberlite. Therefore it is clear that CO₂ is degassing at this stage in the evolution of the pipe whereas water may be locked up in the phlogopite crystal structure. The magma at Voorspoed may have evolved to a more carbonatitic composition, which may have reached closer to the surface than the Lace kimberlite magma. Figure 5.11 shows the initial development of the Kroonstad pipes.

Stage 2: Nucleation of Crystallising Magma and Formation of Transitional Kimberlite

The kimberlite magma rises to a certain depth where en masse crystallisation occurs. The depth at which en masse crystallisation occurs is governed by the volatile content of the magma (Skinner and Marsh, 2004), as discussed above. The magma at the Kroonstad cluster reaches at least 1km from the surface as interpreted by the presence of basalt xenoliths as central kernels in nucleated magmaclasts. En masse crystallisation of the magma is likely to render it immobile due to the high solid content and therefore it is likely that en masse crystallisation is occurring at approximately 1km from the original land surface at Kroonstad. Initial crystallisation occurs through nucleation of the mineral phases around the larger solid components already present within the magma. These would form nuclei and include: olivine macro/phenocrysts, xenolithic material and mantle xenocrysts. Globular segregations form in the magma as a result of this nucleation. The spherical shape of the globular segregations is governed by surface tension effects (Sparks et al. 2006). Furthermore tangential alignment of the nucleating phases indicates rotation of the globular segregations during their formation as molten globules (Mitchell, 1995). The mantles of the nucleated magmaclasts in the VK deposits are generally coarse grained and have the appearance of typical HK or HKt. The preservation of the globular segregations in the HKt at the Voorspoed and Lace pipes at approximately 300m below the current land surface indicates that nucleation of crystallising magma and formation of globular segregations was occurring over a vertical distance of up to 1.2km in the embryonic pipe. Extensive exsolution of the volatiles at these depths would produce a continuous supercritical fluid with suspended globular segregations. Rotation of the globules would produce the tangential alignment of the minerals (phlogopite, melilite) observed in the nucleated magmaclasts. The globules crystallise to near completion at this stage prior to eruption. This is indicated by the generally coarse grained nature of the nucleated magmaclast mantles. Furthermore the presence of late stage aegirine and sanidine in nucleated magmaclasts indicates a very similar crystallisation history to the HK. Clement (1982) interpreted coarse grained spherical magmaclasts to have formed as globular segregations in the HK. A similar interpretation is made here for the formation of the nucleated magmaclasts. Therefore nucleated magmaclasts are interpreted to form in the sub-volcanic embryonic pipe during exsolution of the volatile phases prior to explosive emplacement of the VK.

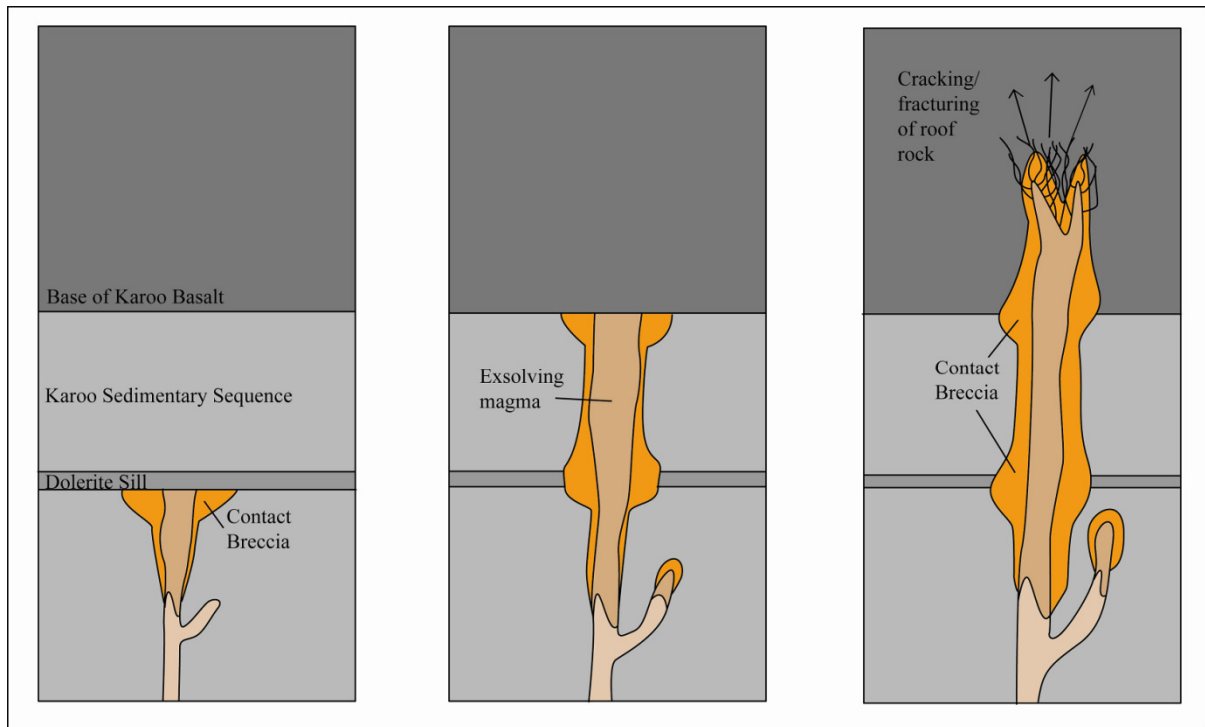


Figure 5.11 Simplified schematic illustrations showing the formation of the embryonic pipe at the Kroonstad kimberlite cluster. Contact breccias become more extensive in spatial relation to more competent rock units such as the dolerite sill observed at Voorspoed. The contact at the base of the exsolving magma shows the depth at which hypabyssal kimberlite with a coherent texture will be emplaced after eruption of the kimberlite pipe. The base of the Karoo basalt is at approximately 1400m from the original land surface and the base of the exsolving magma is at approximately 2000m.

Once the surface is breached through cracking/fracturing of the roof rock the embryonic pipe erupts due to decompression and the near fully crystallised globular segregations are incorporated into the resultant VK deposits as nucleated magmaclasts. Any partially molten globular segregations would crystallise the remaining melt phase very rapidly due to the temperature drop but does not quench as no glass is observed in the nucleated magmaclasts. Varying degrees of crystallisation of the nucleated magmaclasts is observed, as described above, and is interpreted to be the result of different degrees of crystallisation of the mantles at the time of eruption. Those globular segregations with partially molten margins would have fine grained bases relative to those fully crystallised prior to eruption. A very important observation which supports this interpretation is made at the Lace VK. Nucleated magmaclast at Lace are characterised by pervasive microlitic clinopyroxene. However microlitic clinopyroxene is completely absent from the interclast material of the VK. Therefore the microlitic clinopyroxene must have formed in the embryonic pipe during the exsolution of

volatiles, which is responsible for the crystallisation of the microlitic clinopyroxene (Mitchell et al. 2009). If the surface is not breached for any reason the embryonic pipe will stall at depth and crystallise to completion to form a blind pipe, such as that observed at the Lace satellite pipe. The reason for the embryonic system being aborted is unclear but does further indicate that kimberlite magma does not reach the surface as hot molten magma and rather crystallises or begins to crystallise at depth.

Stage 3: Exsolution of a Volatile Phase through Second Boiling and Resultant Pressure Increase in the Conduit

En masse crystallisation of the magma induces the exsolution of volatile phases through second boiling. The composition and ratio of the volatile phases at the Voorspoed and Lace pipes varies. The Voorspoed pipe is characterised by the absence of serpentine as a late stage groundmass phase whereas the Lace pipes contains both serpentine and calcite. The groundmass of Voorspoed HKt is dominated by ultra fine grained phlogopite, which locks up all the free H₂O in the crystal structure and indicates that the magma is initially water-rich. However, as discussed above in 5.3.4.2, the initial exsolution is likely dominated by CO₂. Exsolution becomes much more extensive than in Stage 2 described above. The resultant second boiling reaction is:



At this depth (approximately 1km) the exsolved phase is a supercritical fluid rather than a gas phase. The exsolution of a super critical fluid results in an increase in volume within the magma conduit and therefore creates an overpressure. The magnitude of the increase in volume is directly related to: 1) initial volatile content, 2) deformability of the country rock and 3) inversely dependent on depth (lithostatic load) (Burnham, 1985). During successive exsolution the volatile phase may become a continuous medium, which is evident in some highly developed transitional kimberlite described by Skinner (2008). This produces sufficient overpressure in the magma column to produce hydraulic fracturing of the sidewalls.

Stage 4: Hydraulic Fracturing of the Sidewall and Formation of Contact Breccias and Transitional Kimberlite Breccia

The second boiling reaction releases mechanical energy ($P\Delta V$) as a result of the volume increase and resultant overpressures in the magma conduit. This energy is expended in deforming the wall rocks to failure, which is commonly brittle fracturing at depths $<8\text{km}$ (Burnham, 1985). Upon failure the melt undergoes decompression, which is locally very rapid. Decompression induces further exsolution of volatiles and the volatiles already present also expand due to the phase change (Burnham, 1985). This leads to further volume increase and associated overpressure in the conduit. Mechanical energy is again released to relieve the overpressures. The mechanical energy released now may greatly exceed the energy expended, per unit mass of magma, in producing the initial failure (Burnham, 1985). This becomes a run away process with extensive brecciation occurring in the sidewall and roof rock of the embryonic pipe.

The resultant failure from overpressures in the magma column produces hydraulic fracturing of the country rock material. This fracturing is likely to be most extensive in the roof rock and adjacent to country rock overhangs, where contact breccias are most commonly preserved. The presence of contact breccias at the head of blind intrusions is further evidence to support this theory for extensive brecciation in the roof rock of the intrusion (e.g. Hetman et al. 2004). This also confirms their sub-volcanic origin. Contact breccias may be invaded by HKt, which forms concurrently. In these circumstances mixing of the fragments may occur to produce HKtB, which is evident at the Voorspoed and Lace kimberlites. Significant proportions of country rock xenoliths can be added to the magma during this process of brecciation. Contact breccias are never filled with VK (Skinner, 2008). This is a particularly important characteristic as it is further evidence for their sub-volcanic origin. Contact breccias are expected to form preferentially in less competent rocks. Clement (1982) illustrates the formation of extensive contact breccias below competent rock units such as dolerite sills and the base of the Karoo lava pile, as shown in figure 5.11. Contact brecciation is expected to be particularly extensive in the underlying sedimentary units associated with these competent horizons in the stratigraphy. This is noted at the Voorspoed pipe where the contact breccia has formed in direct spatial relation to a dolerite sill. Extensive contact

breccias are likely to have formed in the sedimentary sequence underlying the Karoo basalt at the Kroonstad cluster due to the competent nature of the basalt (Clement, 1982).

Contact breccias in the adjacent wall rocks of an embryonic pipe will form during the exsolution of volatiles due to initial second boiling followed by decompression. Decompression induced exsolution may occur numerous times as the system continuously exsolves volatiles during decompression of the conduit. Numerous generations of contact breccias should be evident at depth in the wall rock of any kimberlite pipe. As this process continues it will form an embryonic pipe as envisaged by Clement (1982). Most of the contact breccias forming during the development of the embryonic pipe will be incorporated into the resultant VK deposits during pyroclastic eruption.

During this process of contact breccia formation would be the possible time for the incorporation of an aqueous fluid as hypothesised in section 4.3.9. Sheppard and Dawson (1975) present stable isotope analytical work on phlogopite from the groundmass of a kimberlite as well as from phlogopite megacrysts (i.e. mantle xenocryst). The resultant isotopic signature obtained indicates a juvenile magmatic origin for the megacryst (xenocryst) while the phlogopite primary groundmass has a mixed juvenile magmatic-meteoric-metamorphic origin. If the groundmass isotopic signature is re-equilibrated in near surface meteoric/hydrothermal secondary conditions it would be expected that the megacryst would also be re-equilibrated. Therefore it is likely that the groundmass phlogopite has not been re-equilibrated but rather crystallises at a stage where the stable isotopes have undergone some mixing with external sources. The exact source can only be speculated on as very little work has been done on stable isotopes for kimberlites. The incorporation of an aqueous fluid at this stage during the formation of contact breccias would account for the increased SiO_2 and Na_2O contents of the HKt at Lace. However this process of the incorporation of an aqueous fluid is speculative and further work needs to be conducted.

Stage 5: Cracking through to the Surface

Successive formation of contact breccias and exsolution of volatiles produces cracking in the roof rock, which eventually breaks through to the surface. This is followed by a major decompression of the magma column to produce the crater/vent clearing eruption. This process of decompression is proposed by numerous authors for the formation of kimberlite pipes (e.g. Clement, 1982; Wilson and Head, 2007; Cas et al. 2008a and Skinner, 2008). The remaining volatiles within the magma column are exsolved to produce a major decompression related eruption. This eruption in the case of the Voorspoed pipe successfully clears a vent down to approximately 2km. Most of the earlier formed embryonic pipe becomes incorporated into this eruption and is destroyed. The remnants of the embryonic pipe are preserved at the very base of the original embryonic pipe and in sidewall overhangs, which are cross-cut by the vent. The process of pipe infilling now begins.

5.3.6 Summary of Emplacement

The stages in the development of the embryonic pipe at the Kroonstad cluster are shown in figure 5.11 and are by no means distinct and overlap greatly. It is likely that all of the first four stages may overlap and occur simultaneously. In particular the formation of contact breccias is constant and multiple generations are likely to form and be incorporated into subsequent rising magma. This is made evident by the presence of high level upper-crustal xenoliths, such as basalt, as central kernels within nucleated magmaclasts. The initial fragmenting of the basalt must have been through contact brecciation in the roof and sidewall with subsequent incorporation into the magma where they provided nucleation sites for crystallisation. It is likely that the stages outlined above occur numerous times during the evolution of the embryonic pipe, which is a complex array of multiple intrusions. Each of these intrusions is likely to evolve slightly differently in terms of the development of globular segregatory texture and microlitic clinopyroxene. This is evident at the Lace pipe where the development of transitional kimberlite characteristic varies in depth across the pipe. This may be due to slight variations in the volatile composition/content of each pulse of magma.

It is clear from the evidence presented above that the transitional kimberlite at the Kroonstad kimberlite forms in a sub-volcanic environment and can not be formed by pyroclastic

welding processes. The most incontrovertible evidence is the simple fact that typical transitional kimberlite commonly occurs in blind pipes, which have not achieved explosive breakthrough to the surface and therefore must have formed sub-volcanically.

5.4 Volcaniclastic Kimberlite (VK) at Voorspoed

The VK at the Kroonstad cluster is very different compared to typical South African pipe diatreme zones. The most important differences are: 1) lack of microlitic clinopyroxene, 2) complete absence of serpentine and 3) interclast material of abundant xenocrysts in fine grained unidentifiable material with very little pore space. A variety of VK types have been described in section 3, which are both horizontally layered and concentrically zoned within the pipe. The presence of the basalt megablock overlying horizontally layered VK is unique for South Africa and is not a typical floating reef, which is common at other localities in South Africa. This must indicate that the vent was open to this depth during the incorporation of the basalt megablock. A new mechanism for the formation of magmaclasts has been discussed above in section 5.3. It is interpreted that nucleated globules forming in the transitional kimberlite are incorporated into the resultant VK deposits and can be termed nucleated magmaclasts.

The typical model of fluidised emplacement of tuffisitic kimberlite (e.g. Skinner, 2008 and Gernon et al. 2009) can not be used to explain the emplacement of the Kroonstad VK as no tuffisitic kimberlite (TK) is observed infilling the pipe. Models proposed by Sparks et al. (2006) and Cas et al. (2008a) may be more relevant in the case of the Kroonstad cluster. Furthermore one can not ignore the possible influence of groundwater and phreatomagmatic processes must also be considered as a possible mechanism for emplacement at Kroonstad (e.g. Lorenz, 1975). There are two simplified stages of development of the VK infilling after the initial embryonic pipe formation: 1) crater excavation and 2) crater infilling.

5.4.1 Volcaniclastic Kimberlite Emplacement – Review of Models

The following models are based on papers presented by Skinner (2008), Sparks et al. (2006) and Cas et al. (2008a).

Classic South Africa Fluidisation Model

The typical model for the emplacement of South African kimberlites is described by Skinner (2008) and describes initial eruption due to major decompression of the magma column, which has formed as an embryonic pipe, as described by (Clement, 1982). The kimberlite magma reaches to within 1km from the surface where it becomes immobile due to en masse crystallisation of the magma. Cracking and fracturing of the roof rocks leads to fractures reaching the surface upon which, a major decompression of the magma column produces exsolution of the remaining volatiles within the magma down to a depth of approximately 2.2 km. This leads to a major explosion, which produces shock waves. These shock waves rebound from the surface to produce a cone of brecciation having a constant slope of 82° (Skinner, 2008). Considerable cap rock material spalls off and a crater approximately 500-700m deep is formed. However the explosion is mostly contained within the vent, which results in the formation of a distinct diatreme zone below the crater. The diatreme zone (originally the embryonic pipe) becomes fluidised by escaping gas exsolved from the magma, which results in the formation of typical tuffisitic kimberlite observed in Class 1 pipes. The complete lack of the characteristic tuffisitic kimberlite at the Kroonstad cluster indicates that the typical model for emplacement of Class 1 South African kimberlites is not relevant. However the initial stages of embryonic pipe development, as discussed in section 5.3 are very similar to this model. The original development of the root zones of the Kroonstad kimberlites follow the typical model for Class 1 South African kimberlite, however the later VK infilling is very different.

Episodic Model for Crater Excavation

The episodic model proposed by Sparks et al. (2006) shows kimberlite magma reaching near the surface where it disintegrates into explosive flows. The vent is widened from the top down by wall rock failures, rock-bursts, undermining, down-faulting and crater wall slumping as a result in underpressures within the vent. This model does not show development of an embryonic pipe or contact breccias prior to eruption. Therefore the initial stages of pipe formation are not relevant for the Kroonstad kimberlites. However the latter stages of pipe infilling may be relevant to the Kroonstad kimberlites. Once the exit conditions of the erupting magma reach one atmosphere gas velocities decline rapidly, which is aided by an increasing cross-sectional area of the vent during pipe formation process. Wall rock

failures and slumping material can no longer be cleared from the vent and pipe infilling begins. Breccia and layered VK are commonly preserved in the outer margins of the pipe. A fluidised bed is formed in the centre of the pipes, which acts as a major barrier and only gas and fines can pass through. Ultimately the magma supply rate decreases and magma loses its gas passively. The formation of a fluidised bed is not relevant to the Kroonstad cluster; however pipe infilling in this model is episodic as a result of numerous in vent explosive pyroclastic flows, which is very likely to be occurring at the Kroonstad kimberlites.

Column Collapse Model

This model has been proposed by Cas et al. (2008a) and the initial stages are relatively similar to Clement (1982). However the morphology of the pipe is expected to be controlled by the mechanical competency of the country rock, the volatile content of the magma, depth of exsolution and depth of fragmentation. Country rock has been shown to have little influence on kimberlite pipe morphology except possibly in the case of Class 2 pipes (Skinner and Marsh, 2004). Vent clearing is due to sudden decompression of the magma once the surface is breached by fractures. The result would be the formation of a buoyant eruption column dominated by a gas thrust zone immediately above the vent. A sustained period of gas jet driven erosion, abrasion, ablation and smoothing of the vent walls follows. Infilling of the vent will occur when the explosive eruption begins to wane. The gas-particulate eruption column quickly becomes too dense to remain buoyant and collapses rapidly back into the vent. Pyroclastic flows capable of flowing great distances away from the vent are created, however very little evidence for this is observed at any kimberlite. The resultant in vent deposit is poorly sorted and massive similar to a typical pyroclastic flow deposit. This model does not fit with the observations at the Kroonstad cluster as distinct horizontal layering can not be produced in this model of eruption column collapse. However numerous column collapses from episodic eruptions could result in the formation of horizontally layered massive volcanoclastic kimberlite (MVK) deposits, such as that observed at the Voorspoed pipe. Therefore with slight modification to this model it may be relevant to Voorspoed.

Phreatomagmatic Model

The phreatomagmatic model was first developed by Lorenz (1975) and subsequently been proposed for numerous other kimberlites around the world (e.g. Downes et al. 2007). This model relies on hot kimberlite magma reaching near the surface where interaction with groundwater drives the explosive eruptions. The initial stages of crater widening are controlled by spalling off of material, undermining, ring-faulting and crater wall slumping. Numerous pyroclastic eruptions are expected. Through continued eruption bedding is largely eliminated to produce the typical infill of South African kimberlites. It seems very unlikely that this model can apply to South African kimberlite but may be very relevant for Class 2 kimberlite crater excavation. Groundwater interaction is possible at the Kroonstad cluster in the latter stages of pipe emplacement; however there is little evidence to support a whole scale phreatomagmatic model of emplacement for the Kroonstad kimberlites.

Summary of Models

The models discussed above are largely based on observations made from typical Class 1 tuffisitic kimberlite. However the development of the embryonic pipe at the Kroonstad cluster is very similar to the typical development of the embryonic pipe described by Clement (1982) and Skinner (2008). The latter stages of pipe infilling are very different from typical Class 1 kimberlites. The above discussed models provide other possible mechanisms for the infilling of the Kroonstad pipes. Either through episodic in vent explosive pyroclastic flows (Sparks et al. 2006) or through column collapse (Cas et al. 2008a). The possible effect of phreatomagmatic activity is unknown as there is no evidence to support it. Initial observations indicate that column collapse is unlikely and episodic in vent flows are a far more likely process for the infilling of the Kroonstad kimberlite pipes.

5.4.2 Volcaniclastic Kimberlite Infill at the Voorspoed Pipe

5.4.2.1 Alteration of the Basalt Xenoliths in the Volcaniclastic Kimberlite (VK) Infill: Implications for Formation Temperatures

Low temperatures of formation for VK have been inferred by the lack of metamorphic effects on the entrained xenoliths. Skinner and Marsh (2004) suggest a rapid decrease in temperature

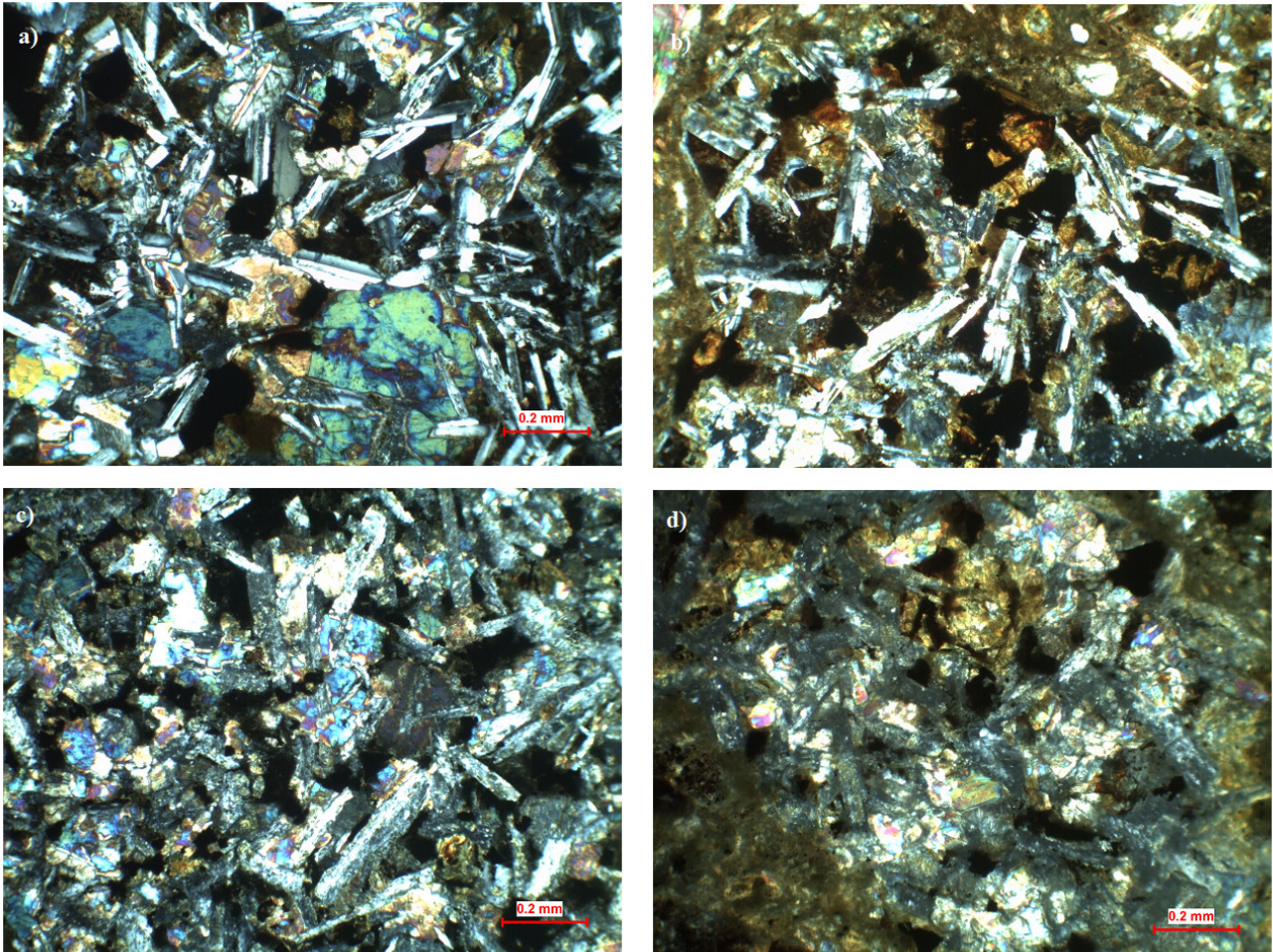


Figure 5.12 Photomicrographs of basalt xenoliths from a) MVBB showing no alteration; b) BVK showing some degree of alteration indicated by the partially altered plagioclase; c) and d) typical MVK xenoliths showing relatively high degrees of alteration.

from the transitional kimberlite to the diatreme zone, as a result of eruption, to approximately $<350^{\circ}\text{C}$. This estimate is based on the presence of coal in fragments in some kimberlites, which would ignite at temperatures $>350^{\circ}\text{C}$. Stasiuk et al. (1999) analysed organic matter within the Lac de Gras kimberlites and found a temperature of 150°C to 650°C for the emplacement of the VK. Wilson and Head (2007) have calculated a temperature of approximately 240°C for an eruption mixture of gas with equal proportions of magma droplets and country rock material. The temperature of approximately 240°C may be too low for the Kroonstad cluster as calcite crystallises at slightly higher temperatures. The calcite matrix of the VK is very fine grained, which indicates a relatively rapid drop in temperature. The exact temperature at the time of formation of the VK units at Voorspoed is unknown but must be relatively low as the upper crustal xenoliths show very little alteration.

The degree of alteration of the basalt xenoliths varies within the various VK units at the Voorspoed pipe. The basalt xenoliths within the six MVK varieties described in section 3.2 show a relatively higher degree of alteration when compared to the basalt xenoliths within the massive volcanoclastic basalt breccia (MVBB), massive volcanoclastic sandstone breccia (MVSb) and bedded volcanoclastic kimberlite (BVK) units. Refer to appendix 7 for a full table of abbreviations used in the text. Figure 5.12 shows the variation in degree of alteration between the different VK units. Typically in the MVBB, MVSb and BVK the basalt xenoliths are very fresh and show little to no alteration. The six MVK units show a much greater degree of alteration indicated by the replacement of plagioclase and less commonly clinopyroxene as well. Therefore this variation in alteration of the basalt xenoliths may indicate varying relative temperatures of formation for the different VK units.

Relative temperatures of formation for the MVKs and BVK/MVBB/MVSb can be based on the degree of alteration of the basalt xenoliths. The MVKs form at slightly higher temperatures relative to the other VK varieties as the basalt xenoliths show alteration. The BVK/MVBB/MVSb units will form at lower temperatures, indicated by the always fresh basalt xenoliths. The alteration affects on the basalt xenoliths fit well with petrographic analysis of the rock as a whole, as described below for formation processes.

5.4.2.2 Country Rock Xenolith Distribution Relative to the Original Stratigraphy

As discussed in section 5.1 a complete Karoo stratigraphy was present at the time of emplacement of the Kroonstad kimberlites. The VK infill is characterised by the high proportions of basalt as xenoliths, which account for 60-80% of the total xenolith population in the MVKs. The MVBB xenolith population is 100% basalt. The complete absence of sandstone xenoliths in almost all of the VK varieties is a particularly interesting characteristic as one would expect Karoo sandstone xenoliths to be relatively abundant or at least present in the VK. However sandstone xenoliths are very rare apart from the MVSb where they are very abundant and can constitute 100% of the xenolith population although basalt is commonly present in varying amounts. Sandstone fragments must have been cleared from the vent during initial eruption whereas basalt may have collapsed back into the pipe. This process is discussed in detail later for the model of emplacement.

There is a variation in the basalt xenolith content between the Initial Eruption Zone (IEZ) and the Central Eruption Zone (CEZ) as well. Basalt CRX content increases from 25 vol. % in the IEZ MVKs to 40 vol. % in the CEZ. The increase in basalt content can easily be explained by the presence of the basalt megablock. The CEZ is erupting through the basalt mega-block and a higher proportion of basalt xenoliths within the resultant deposits are expected relative to the IEZ.

5.4.2.3 Horizontal Layering and Nested Crater of the Volcaniclastic Kimberlite

The volcaniclastic rocks within the Voorspoed pipe are both horizontally layered and a distinct nested crater is observed in the centre of the pipe. Horizontal layering is particularly evident within the pipe, which indicates abundant ongoing pyroclastic eruptions depositing successive pyroclastic layers on top of one another. Horizontal beds can often be correlated across the length of the pipe such as the graded beds in boreholes 9 and 10. However beds often pinch out. Successive horizontal beds are best observed in the central eruption zone (CEZ) (borehole 3) between 210-250m. This zone contains alternating horizontally layered beds of the T2MVK and the intMVK. Refer to appendix 7 for a full list of the abbreviations used for the MVK units. Ten beds are present over the 40m interval, which range in thickness from 10m to <1m thick. This is the only example noted at the pipe with such small scale horizontal layering and in general the beds range in thickness between 30m and 100m. However it is only possible to distinguish these beds when there is a change in the nature of the MVK deposit, such as that described above where layering is made evident by the change between T2MVK and intMVK. Therefore the more extensive Type 1 MVK beds may be made up of multiple horizontally layered beds of the same characteristics. Grading within individual beds of MVK is not evident but grain size does vary between successive MVK beds. For example the T2MVK is generally coarser grained than the intMVK.

The VK rocks are also cross cut in the centre of the pipe by a later stage nested crater, which is called the central eruption zone (CEZ) in section 3. The presence of the nested crater is made evident by the complete lack of the very distinct T2MVK in the outer regions of the pipe. The T2MVK is restricted to the central zone. The VK rocks in the initial eruption zone (IEZ) have been cross-cut by the CEZ VK indicating a new vent has formed through the

original IEZ deposits. Nested craters are relatively common in Canadian kimberlites such as the Victor kimberlite (Webb et al. 2004) and 140/141 kimberlite at Fort a la Corne (Berryman et al. 2004). A relatively long period of inactivity of the pipe must have occurred, which would allow for the build up of pressure in a magma chamber beneath the IEZ MVK deposits. The sub-vertical walls of the CEZ vent suggests that the IEZ MVK was lithified at the time of the emplacement of the CEZ. This period of inactivity may have been caused by the collapse of the basalt mega xenolith from the wall rock. The basalt mega xenolith would have formed an effective plug within the pipe, which would have caused the temporary hiatus in pyroclastic deposition. Intruding magma would pond beneath the earlier formed pyroclastic kimberlite where the exsolution of volatiles would create overpressures in the chamber. Eventually explosive eruption would clear a vent through the basalt mega xenolith and pyroclastic deposition would continue. This later vent through the basalt mega xenolith is clearly evident in plan view as well as the distribution of the distinct T2MVK within the MVK deposits as shown in section 3.

5.4.3 Formation of the Pipe Infill

Interpretations of the VK deposits are limited due to the limited exposure of the rocks in open pits and the reliance on drill core; however this is a common problem in kimberlite geology. The VK at the Voorspoed pipe has been divided into four formation processes. The dominant process of formation of the VK at this depth within the pipe is through primary pyroclastic deposition. However it is likely that at high levels (now eroded parts of the pipe) resedimented volcanoclastic kimberlite may have become more dominant such as at the Class 3 Lac de Gras kimberlites in Canada.

5.4.3.1 Massive Volcanoclastic Kimberlite (MVK)

The overall similarity between the six MVK varieties (T1aMVK, T1bMVK, sMVK, intMVK, T2MVK, aMVK) leads to a similar interpretation on formation processes. As the name suggests the MVKs are massive, poorly sorted and matrix-supported, indicating a short-lived, high energy, mass emplacement of a high particle concentration mixture where the transport time does not allow for hydraulic sorting of the components (Porritt et al. 2008). Refer to appendix 7 for a full list of the abbreviations used for the MVK units. The MVK

dominates the pipe infill and therefore, at the current depth of erosion, represent the deposits of the dominant pipe infilling process. The horizontal layering of the various MVK deposits records the layer by layer filling of the pipe. Similar rocks are described by Moss et al. (2008), Pittari et al. (2008) and Porritt et al. (2008), which are interpreted to result from primary pyroclastic deposits from eruption column collapse. The rocks described by Moss et al. (2008) have lost their fines component, which is interpreted to indicate some degree of elutriation in an eruption column. However the model proposed by Cas et al. (2008a) shows that the texture of a typical in-vent column collapse deposit would be analogous to pyroclastic flow type deposits and may retain the fines component. The MVKs show some similarities to TK deposited in typical South African kimberlite diatreme zones, such as the massive, poorly sorted, matrix supported textures and presence of high proportions country rock xenoliths (Clement, 1982; Field and Scott Smith, 1999 and Skinner and Marsh, 2004). However several of the key characteristics of TK are not observed which includes: microlitic clinopyroxene, serpentine interclast material and retention of the fines component. Brown et al. (2008c) dispute the column collapse model on mass balance grounds but further state that column collapse might occur during the waning phase of an explosive flow. Brown et al. (2008c) show that between 100-400 column collapse events would have to occur to fill a 1km deep vent. Therefore the column collapse model is not applicable for typical Class 1 kimberlites where the typical diatreme deposits may reach these great vertical extents. However in the case of the Voorspoed pipe the MVK units are typically <100m thick and therefore the process of column collapse is believed to be viable in this case. However in vent explosive flows would produce primary pyroclastic deposits with very similar characteristic to typical column collapse deposits (Cas et al. 2008a). The depth of the current exposure of the Voorspoed pipe may favour this later model as the development of an eruption column from this depth may be difficult.

An important characteristic to note for the MVKs is the retention of the fines component in the interclast material. This further highlights the fact that no elutriation or hydraulic sorting of the deposits occurred, as the first components to be removed in these processes would be the fine ash material. The country rock xenoliths are typically angular and abundant within the MVK. The angular nature indicates that no milling and abrasion of the xenoliths has occurred. Rounded xenoliths are noted at both the Voorspoed and Lace pipe but are always from lithologies deeper in the crust such as Ventersdorp basalt. The rounding in these cases is

due to thermal and chemical effects and not abrasion/milling. Nucleated magmaclasts are typically spherical and broken fragments of nucleated magmaclasts are rare. Both these features indicate a short-lived eruption as one would expect milling and abrasion of the components in a sustained eruption column or explosive flow. The high abundance of country rock xenoliths is expected due to the extensive formation of contact breccias in the embryonic pipe system, which would be incorporated into the resultant deposits. Therefore country rock xenoliths added to the depositional processes have been fragmented in early processes and fragmentation is not necessarily related to explosive emplacement, although fragmentation of the roof rock is very likely during eruption. An important characteristic of the magmaclasts is the fact that they never show flattening or moulding, which would be expected if they were still partially molten during emplacement of the VK. Similar observations of the lack of flattening and moulding are made by Scott Smith (2008). The base of the magmaclasts is characterised by calcite only and serpentine is not observed. This is similar to typical Class 3 Lac de Gras Kimberlites (Scott Smith (2008)). Nucleated magmaclasts at the Kroonstad cluster are interpreted to have formed in the embryonic pipe and are solid when incorporated into the VK infill.

The complete lack of bedding structures, absence of rounding of xenoliths/xenocrysts, lack of quartz and location at the base of the vent indicates that the deposits are more likely the result of pyroclastic eruption rather than sedimentation processes. The MVKs at the Voorspoed pipe have formed through primary pyroclastic processes. The deposits have the typical characteristics of pyroclastic flow deposits, which could be formed through either column collapse or explosive in vent flows (Sparks et al. 2006 and Cas et al. 2008a). The eruptions are occurring deep within the vent (+/- 2km from surface) and may not clear the vent. Brown et al. (2008c) argue that in-vent column collapse is not possible. Large eruption columns extending high above the vent are not envisaged here however it is possible that eruption columns reached the surface. Furthermore the large diameter of the pipe created by the initial eruption and the high density of the eruption mixture would inhibit the development of prolonged eruption columns. Therefore it seems more likely that the MVKs were deposited through in-vent explosive pyroclastic flows rather than column collapse. This is based on the complete lack of bedding, the depth of the current deposits and the retention of the fines component. Column collapse deposits have characteristics which are very similar however it is likely that the fines component at least would be lost during this process of deposition

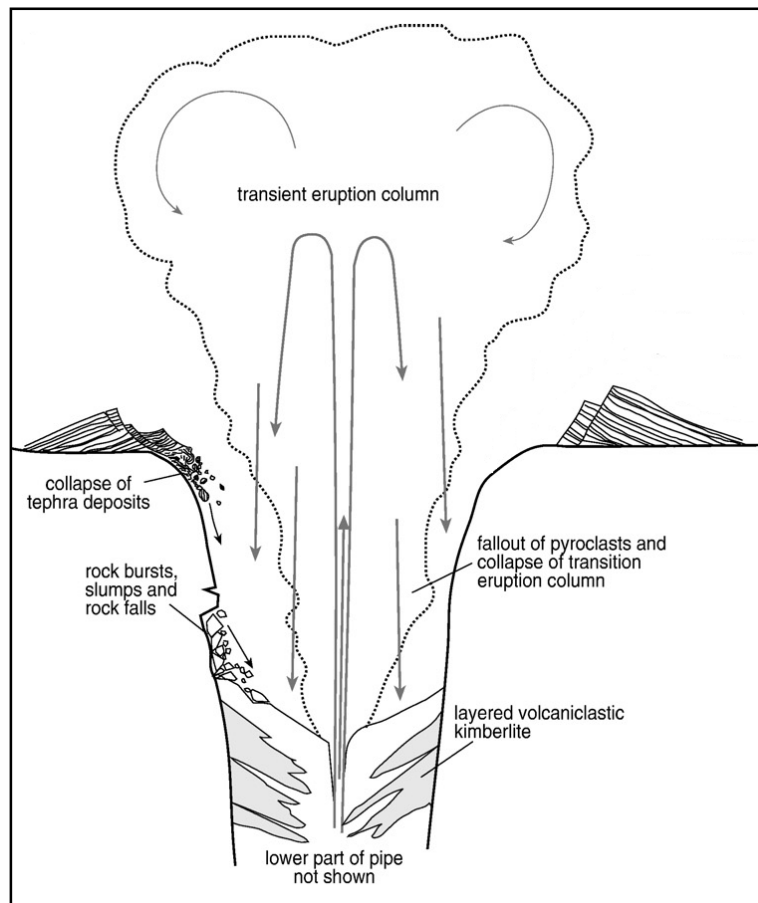


Figure 5.13 Illustration of mechanisms for infilling a kimberlite pipe. 1) collapse of surrounding extra crater deposits, 2) rock bursts/sidewall failure deep within the pipe and 3) deposition by primary pyroclastic process such as fall out from the column and column collapse. (Diagram from Brown et al. 2008c).

(Moss et al. 2008). Furthermore the MVKs are forming deep within the vent and Brown et al. (2008c) states that eruption columns must reach the atmosphere in order to collapse.

5.4.3.2 Massive Volcaniclastic Basalt Breccia (MVBB) and Massive Volcaniclastic Sandstone Breccia (MVSBB)

These massive, poorly sorted volcaniclastic kimberlites are characterised by similar features: 1) complete lack of basement xenoliths and 2) lack of juvenile component. Furthermore the basalt xenoliths are particularly fresh relative those in the pyroclastic MVK, indicating very low temperatures when incorporated relative to the MVKs. Based on the two characteristic features, the MVBB and MVSBB must have fallen back into the crater/vent from above. The complete lack of kimberlite magmaclasts indicates that they are not resedimented from extra

crater deposits as a higher proportion of juvenile material would be expected. Therefore these distinct units are interpreted to result from crater sidewall failure. The presence of abundant sandstone xenolith indicates that the sidewall failure must have occurred relatively deep within the pipe so as to incorporate significant proportions of sandstone material. This vent wall failure is interpreted to result simply from gravitational failure of the sidewall in a large open unstable vent. Alternatively the brecciated wall rock may be dislodged during eruption. Brecciation would have occurred in the embryonic pipe and therefore the eruption may easily incorporate/dislodge the brecciated wall rock. The complete lack of kimberlite magmaclasts indicates that the former mechanism is more likely as no kimberlite magmaclasts would necessarily be added. Further evidence for this interpretation is the complete lack of these distinct rock types in the central areas of the pipes and the presence only along the margins against the pipe walls, which would be expected through sidewall failure.

The MVBB and MVSBB are similar to the typical MVKs as they are all poorly sorted, massive and typically matrix-supported. However the complete lack of kimberlite magmaclasts and the presence of abundant quartz xenocrysts in the interclast material clearly indicate that the MVBB/MVSBB units were formed in a different style of deposition. The style is interpreted to be gravitational crater sidewall failure into an open vent due to the unstable nature of the crater walls. This process is shown in figure 5.13, although here it is interpreted to be through gravitational failure rather than rock bursting as a result of underpressures in the vent.

5.4.3.3 Bedded Volcaniclastic Kimberlite (BVK)

The BVK is characterised by the presence of numerous normally graded beds within each sequence. Individual beds are typically <3m and the whole BVK sequences are typically <10m. These rocks contain relatively abundant proportions of juvenile components and basement xenoliths are present. No lamination or imbrication is observed within the BVKs; however the BVK represents the only units within the Voorspoed infill to contain definite grading. The major components of the BVK are very similar to the typical MVKs dominating the pipe infill. The graded nature of the unit must indicate a different deposition style relative to the MVKs. The presence of abundant quartz xenocrysts as part of the interclast material is an important characteristic, which also indicates a change in depositional style relative to the

pyroclastic MVKs where quartz xenocrysts are not observed. Therefore the BVKs show features of both the MVKs (basement xenoliths, abundant kimberlite magmaclasts and kimberlite xenocrysts) and of the MVBB/MVSB units (quartz xenocrysts). The quartz grains are typically well rounded, which indicates a fluvial origin.

These deposits are interpreted to have formed through crater rim collapse or slumping from the top of the vent (figure 5.13), which re-incorporates tuff ring material into the pipe. Crater rim failures and incorporation of the tuff ring deposits would be expected due to the large volume of extra crater deposits which are likely to form during vent clearing eruptions, as described below. Furthermore the extra crater deposits would be expected to contain significant proportions of juvenile components incorporated by the vent clearing eruption. These crater rim failures are interpreted to have been deposited into possible crater lakes during periods of inactivity within the vent, which would account for the grading observed. Crater rim failures during periods of activity are likely to be re-cycled into the ongoing pyroclastic eruptions and no record of the failure would be preserved. Therefore the BVKs are interpreted to have formed by crater rim failure/slumping at the surface as a result of the weight of the overlying extra crater deposits produced during the initial vent clearing eruption. This would account for the similarity of the major components of the BVK with the MVKs. Quartz xenocrysts indicate that possible fluvial sedimentary processes are operating at the surface at this time, which would introduce rounded quartz into the extra crater deposits. Therefore these BVK units are resedimented volcanoclastic kimberlite from the tuff ring at the surface.

5.4.3.4 Fine grained Volcanoclastic Kimberlite Bands

These volumetrically insignificant units are very similar to the fine grained tops of the BVK units. The style of deposition is difficult to interpret due to the lack of exposure in the pit. The only observations were made in the core and individual bands are typically <5cm thick. Due to the similarity of these bands to the top of the BVK it may be interpreted that they form through similar processes, however far less extensive. Alternatively these fine grained units may represent pyroclastic airfall deposits, which were able to successfully sort the fines component of an earlier pyroclastic eruption. The pyroclastic MVKs typically contain their

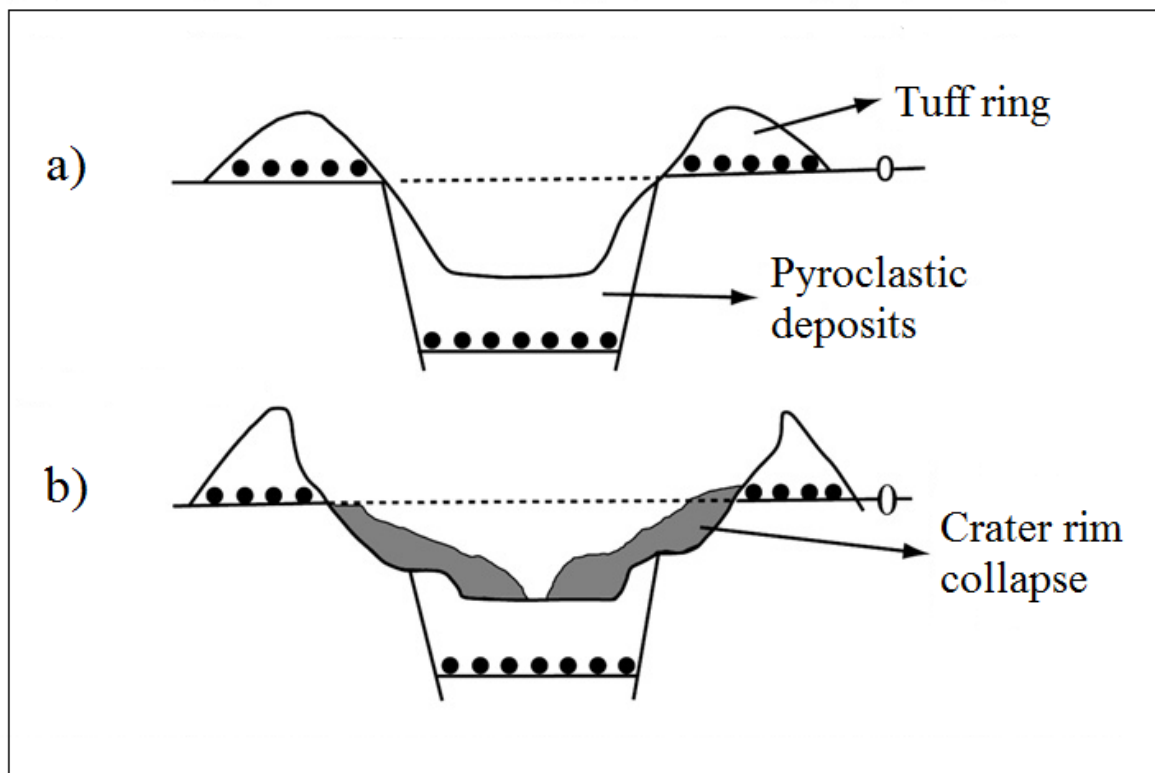


Figure 5.14 Illustration showing the failure of the crater rim and slumping of material back into an open vent. This model was developed for a 500-700m deep, cleared crater for Class 1 kimberlites. The tuff ring would be substantially bigger for the Kroonstad kimberlite where a +/-2km vent is cleared. Diagram after Skinner (2008).

finer component and therefore this interpretation may be unlikely. Regardless of the deposition style these bands must represent breaks in pyroclastic activity, which allow for their deposition as either resedimented volcanoclastic kimberlite into a crater lake or through pyroclastic airfall processes.

5.4.3.5 Basalt Megablock

The most distinctive feature of the Voorspoed pipe infill is the presence of a huge basalt megablock, which occupies approximately half the current surface area (6ha) and extends down to 300m at the southern margin of the pipe. The basalt megablock was analysed geochemically by Roberts (1997) and was correlated with the Mafika Lisiu formation. Re-analysis of the geochemical data presented by Roberts (1997) indicates that the basalt

megablock geochemistry is more similar to the upper Maloti-Senqu-Mothae units. This is based on the high Ti and Fe contents. The basalt megablock originated from near the original land surface at the time of emplacement. The timing of incorporation of the megablock is particularly interesting. The VK underlying the basalt is horizontally layered and three distinct MVK varieties and a BVK unit are observed. The presence of the bedded VK must indicate that the VK formed prior to the incorporation of the basalt. Therefore the initial vent clearing eruption was not responsible for the formation of this huge block as at least three successive periods of MVK deposition occurred prior to the incorporation of the basalt megablock.

The formation of the crater zone described by Skinner (2008) provides a possible mechanism for the incorporation of the basalt megablock. After the initial vent clearing eruption, extensive tuff ring deposits must have formed around the open crater at the surface, as shown in figure 5.14 (a). The weight of these deposits may produce crater wall collapse and slumping at the surface. Figure 5.14 (b) shows the collapse of the crater wall, which incorporates part of the upper country rock as well. This produces flaring and crater widening as envisaged by Skinner (2008). It is envisaged that the basalt megablock is incorporated at this stage as a huge block of Karoo country rock basalt produced by slumping of the crater. The basalt megablock would collapse back into the pipe and due to the size would reach the base much quicker than the tuff ring material, which would be re-incorporated into the pipe along with the basalt megablock. No record of possible overlying material is preserved due to extensive erosion at the pipe.

5.4.4 Role of Fluidisation in the Formation of the Massive Volcaniclastic Kimberlite (MVK)

Fluidisation has been invoked by numerous authors to explain typical tuffisitic kimberlite in South African pipes (e.g. Clement, 1982; Field and Scott Smith, 1999; Walter et al. 2006 Skinner, 2008 and Gernon et al. 2009). However in the case of Class 2 and Class 3 pipes major fluidisation of the MVK deposits is not observed. Fluidisation can also occur in typical pyroclastic flows, both during the flow as well as post-depositionally (Wilson, 1980). Fluidisation is likely to occur in the MVK deposits in the vent, however little is known about

the characteristics of these deposits or how much ash elutriation is occurring (Cas et al. 2008a). Fluidisation of the Voorspoed pipe MVK is likely but is not similar to fluidisation described for Class 1 kimberlites and is used here to describe a bed of particles, which develops fluid-like properties due to the flow of interstitial gas, similarly to Sparks et al. (2006). Fluidisation in this sense would only apply to the pyroclastic MVKs at the Voorspoed pipe and would not apply to the BVK, MVBB and MVSB units. Moss et al. (2008) interprets the absence of fines within a MVK unit at the A154N pipe at Diavik (Canada) to elutriation of the fines in a fully fluidised collapsing eruption column. Extensive fluidisation in this case removes the fines component and the resultant in vent deposit does not contain a fines component. However in the model presented by Cas et al. (2008a) the fines component is retained. Fine ash is trapped in the descending mass due to hydraulic coupling and interlocking of grains (Druitt, 1995) and Porritt et al. 2008). It seems likely that fluidisation with resultant elutriation of the fines component is likely to vary. The resultant MVK described by Moss et al. (2008) show grading on a mega-scale, which indicates a degree of sorting in the eruption column prior to collapse. In these prolonged fluidised systems it is more likely that the fines will be elutriated (Porritt et al. 2008). In systems where the eruption column collapses rapidly the fines component may be retained as elutriation would not have occurred prior to collapse. It is even more likely that in-vent explosive flows, such as those interpreted to have been depositing the MVK units at Voorspoed, will retain the fines material and the gas. In this case the resultant deposit may retain a large proportion of gas and form degassing structures such as those described by Gernon et al. (2008). Gas escape structures were not observed at the Voorspoed pipe; however the lack of pit exposure hinders these observations.

Fluidisation in typical South African kimberlites is believed to result in the formation of late stage deuteric microlitic clinopyroxene and serpentine in tuffisitic kimberlite (Mitchell et al. 2009). Microlitic clinopyroxene is observed rimming the larger components of the TK. In the case of the Voorspoed pipe ultra fine grained dark rims are rarely seen as rims around the larger components of the MVKs. This may indicate that minor fluidisation of the MVKs has occurred; however this is speculative as the ultra fine rims could not be identified optically as microlitic clinopyroxene. The presence of the fines component in the MVK deposits at the Voorspoed pipe indicates that extensive fluidisation and elutriation did not occur in the in-vent explosive pyroclastic flows, which supports the likely retention of the gas in the MVK.

Fluidisation does not play a big role in the deposition of the MVKs at Voorspoed as the well mixed nature of the deposits can easily be produced by the in-vent explosive flows. However it is likely that the in-vent flows were partially fluidised.

5.4.5 Stages in the Emplacement of the Volcaniclastic Kimberlite

Stage 1: Crater Excavation and Vent Clearing

This stage follows on directly from stage 5 (Cracking through to the surface) for the emplacement of the embryonic pipe in section 5.3.5.2. The embryonic pipe rises to a point where crystallisation of the magma renders it immobile. Cracking and fracturing of the roof rock occur due to the build of pressure as a result of exsolution through second boiling. Once the surface is breached a major decompression related eruption ensues. It must be noted here that the embryonic pipe does not always achieve this cracking through to the surface, as indicated by the presence of blind pipes such as the satellite pipe at Lace. In the case of the Lace blind pipe, the embryonic pipe only reached approximately 1800m from the original land surface (based on erosion estimate in section 5.1). This further indicates that kimberlite magma does not reach the surface but crystallises at depth. The proportion of volatiles within the magma drives the further development of the embryonic pipe. In the case of the Lace satellite blind pipe the volatile content may not have been high enough for further development of the pipe or alternatively the volatile content was dominated by water, which induces crystallisation at depth rather than nearer the surface as described by Skinner (2008).

Once the surface is breached, the pressure drop to atmospheric pressure creates a major eruption. Decompression related eruptions are also proposed by Wilson and Head (2007) and Cas et al. (2008a) and Skinner (2008). The depth at which the kimberlite magma has stalled and the volatile content will likely determine the size of the eruption. The deeper the kimberlite magma stalled the greater the pressure differential and the greater the eruption. However this is also greatly dependent on the remaining volatiles in the magma available for rapid expansion. To put the volume increase into perspective: 1gm of water at 1cm³ as a liquid expands to 4500cm³ as a gas at 1000°C (Holmes, 1965). Therefore the volatile phase's exsolved as supercritical fluid during the formation of the embryonic pipe may expand up to 4500 times when the surface is breached. The dramatic depressurisation produces a phase

change from a supercritical fluid to a gas phase and so increasing the volume by a factor of 4500. The resultant pressure increase drives the eruption.

In the case of the Voorspoed pipe the presence of BVK and sidewall rock failure deposits deep within the pipe indicate that this major eruption must have cleared the pipe to this depth. The pipe shape is thought to be the result of a rebounding shock wave produced by the eruption, which in turn produces a cone of brecciation having an 82° slope upward (Skinner, 2008). Numerous other models propose eruption nearer the surface with successive mining down to the current depth (e.g. Sparks et al. 2006 and Cas et al. 2008a). However the consistency of kimberlites within South Africa in terms of pipe morphology indicates that this is unlikely. The depth of the eruption governs the shape of the pipe: deep eruptions of steep sided pipes; whereas shallower eruption produce flared craters such as the Class 2 pipes (Rice, 1999).

The previously formed embryonic pipe is almost completely incorporated into the resultant eruption and only the base of the pipe is preserved. Minor preservation of contact breccias may occur in the sidewall. The complete lack of Karoo sandstone xenoliths as well as the lower Lesotho Formation (Mafika Lisiu) basalt may indicate that the contact breccias formed in the embryonic pipe were easily expelled from the pipe. The overlying upper Lesotho Formation basalt, which may not have been affected by contact brecciation could not be expelled as easily and large blocks collapsed back into the pipe, as shown in figure 5.15 (b). Therefore at the end of this stage of emplacement the vent has been mostly cleared to a depth of approximately 2km from the original land surface and only large blocks of dominantly upper Lesotho Formation basalt remain within the pipe. This interpretation is based on the Karoo basalt analysed from within the pipe, which are dominated by chemistry similar to the upper Lesotho Formation basalt (Hanson, 2006) These large basalt blocks plug the pipe and volcanic activity stops. The original eruption style due to decompression is likely to be Plinian; however the eruption style changes after plugging of the pipe to Vulcanian in style. The development of an eruption column at this initial vent clearing stage is unclear as there is no evidence of the original deposits from this eruption as they have either been eroded away or re-incorporated into the pipe infill. However it does seem likely that an eruption column would have been produced with extensive extra crater deposits forming around the crater.

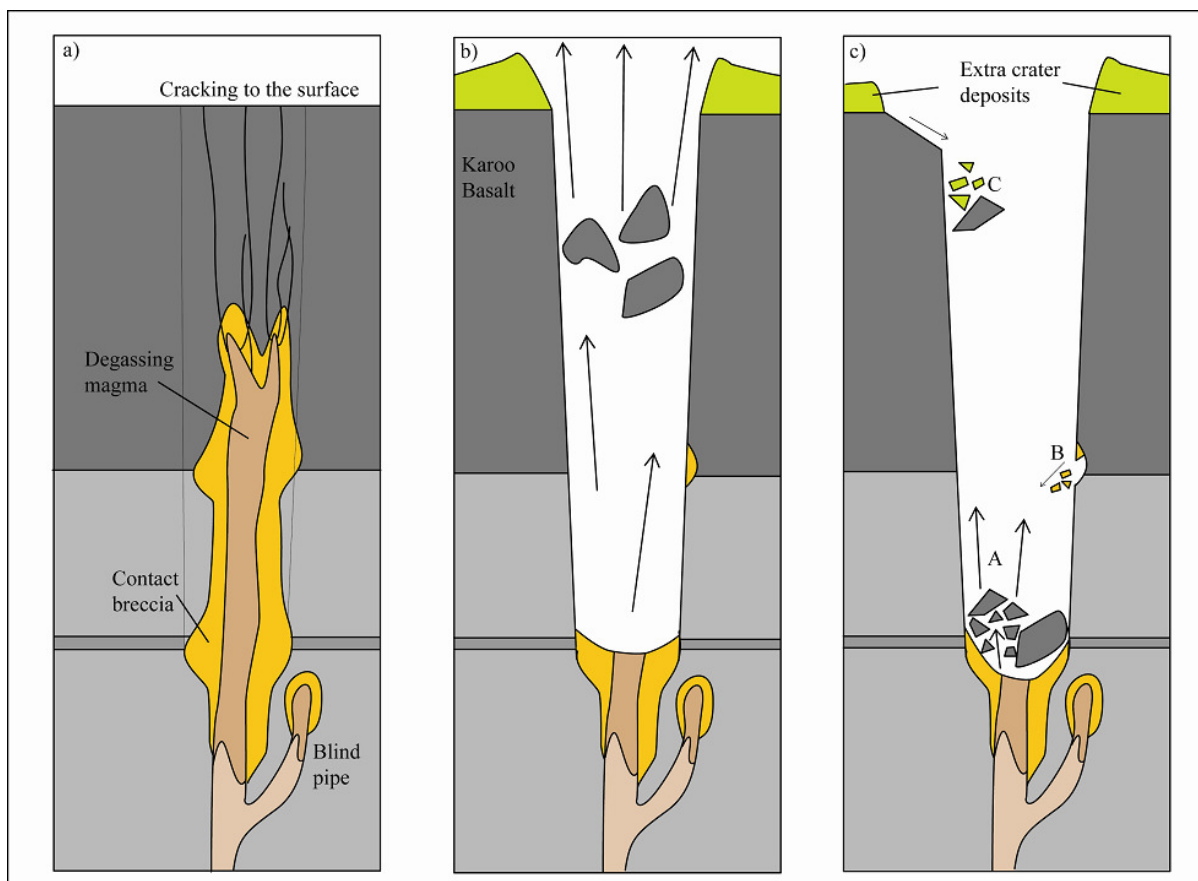


Figure 5.15 Illustration of the crater excavation and subsequent crater infilling proposed for the formation of the Kroonstad kimberlite pipes. a) exsolution in the embryonic pipe produces cracking through to the surface induces decompression of the magma column; b) decompression related eruption clears a vent and deposits extra crater tuff ring and c) infilling of the pipe by three processes (A) primary pyroclastic deposition through either column collapse or explosive in-vent flows, (B) gravitational sidewall failure and (C) crater rim collapse.

Stage 2: Crater Infilling

The eruption at the Voorspoed pipe successfully cleared a vent down to approximately 2km from the original land surface. However the pipe is plugged by large basalt blocks, as discussed above. This temporary hiatus in volcanic activity is very short and the build of volatiles beneath the plug quickly re-initiates activity. The stage of crater infilling now begins. Numerous depositional processes are occurring deep within the vent, which are shown in figure 5.15 (c) and include: 1) primary pyroclastic deposition, through in-vent explosive flows, of the MVKs, 2) sidewall failure through gravitational collapse deep within the vent and 3) collapse of the tuff ring deposits from the surface. These processes may all occur simultaneously. It is likely that crater rim failures/slump and sidewall gravitational failure deposits would be incorporated into pyroclastic eruptions if occurring at the same

time, although this depends on the size of the eruption forming the pyroclastic deposit. Brown et al. (2008c) shows the formation of crater rim failure and rock burst deposits along the margins of the pipe where pyroclastic eruptions do not re-incorporate the material (figure 5.13). Crater rim collapse may introduce new country rock from the surface along with the tuff ring deposits. This is likely to occur as the country rock would be upper Lesotho Formation basalt, which is the dominant xenolith observed within the pipe infill. Large blocks may collapse deep within the vent and may plug the vent again, as described above for the incorporation of the basalt megablock. It is clear that at least one stage of vent plugging has occurred, which is indicated by the huge basalt megablock occupying half the current surface area of the pipe. The resumed volcanic activity after the plugging of the vent by the basalt megablock decreases in intensity. This is indicated by the substantial decrease in the vent diameter observed cutting through the basalt plug. At the current depth of erosion the vent is 490m by 350m whereas the vent through the basalt plug is approximately 200m in diameter. Furthermore the sub-vertical walls of the smaller CEZ vent cross-cutting the IEZ/basalt block suggests that the IEZ MVKs were lithified by the time of emplacement of the CEZ. Numerous large blocks may have collapsed earlier in the evolution of the pipe as shown in figure 5.15 (b and c), however the volcanic activity would still have been able to fragment the blocks with subsequent deposition into the MVK deposits. The collapse of the later megablock would result from the weight of the tuff ring deposit, which would produce slumping of the crater margins and could not be fragmented. This further indicates that eruptions were becoming less intense. Along with the incorporation of the large basalt block would be significant amounts of the tuff ring deposit, which would be re-worked into the resultant MVK deposits. This stage is dominated by repetitive eruptions and deposition of primary pyroclastic deposits, which are interpreted to result from in-vent explosive flows. The variety of distinct MVK units and the lack of mega graded beds indicate that the deposits could not have been the result of a sustained eruption column.

Each MVK unit is characterised by distinct xenolith and nucleated magmaclasts contents indicating they must have formed by separate eruptions. This is further indicated by the presence of later MVK deposits cross-cutting earlier deposits, which can only occur in separate eruption phases. Crater infilling at this depth is dominated by continuous pyroclastic eruptions forming MVK deposits with minor gravitational collapses in the sidewall. Crater rim failure and incorporation of the tuff ring may have been significant. Therefore the pipe is

infilled by episodic volcanic events with periods of inactivity marked by deposits incorporated from the sidewall and crater rim. A similar episodic infilling with periods of quiescence is interpreted by Kjarsgaard et al. (2009 b) for the Orion South kimberlite, although this is a Class 2 pipe.

5.4.6 Deposits Overlying the Current Land Surface

It is impossible to determine the style of deposition of the now eroded portion of the pipe. However two important facts can help to speculate on the possible overlying VK deposits: 1) the similarity of the Voorspoed pipe to typical Class 3 kimberlites and 2) the observation of decreasing volcanic intensity within the pipe at depth. Class 3 pipe are typically infilled with dominantly RVK and primary pyroclastic kimberlite is typical only observed at the base of the pipe (Scott Smith, 2008). This is very similar to the current exposure of the Voorspoed pipe. The current depth of erosion exposes the base of the pipe and VK infilling the pipe is interpreted to be dominantly primary pyroclastic kimberlite. Furthermore the dramatically decreased volcanic intensity between the IEZ deposits and the CEZ deposits (indicated by the much smaller vent producing the CEZ) indicates that eruptions are waning. It is likely that the Voorspoed kimberlite volcano soon became extinct with much of the pipe still open. This would result in the rest of the pipe becoming infilled with RVK reworked from the extra crater deposits. The resultant pipe infill would be very similar to the Lac de Gras type kimberlites. This is speculative and there is no evidence of the rock types, however it does seem likely that with decreasing volcanic activity within the pipe, RVK type infilling would become dominant.

5.4.7 Volcaniclastic Kimberlite at the Lace Pipe

The VK at the Lace pipe is no longer present in situ but is abundant on the surrounding old mine dumps. Two varieties are identified as described in section 3. These rocks are very similar petrographically to the Voorspoed VK. In particular the basalt-rich VK at the Lace pipe is very similar to the MVBB at Voorspoed. The occurrence of a distinct transitional kimberlite with features very similar to transitional kimberlite described for Class 1 kimberlites indicates that the overlying VK at Lace is likely to be tuffisitic kimberlite. However the VK analysed from the old mine dumps is distinctly different from tuffisitic

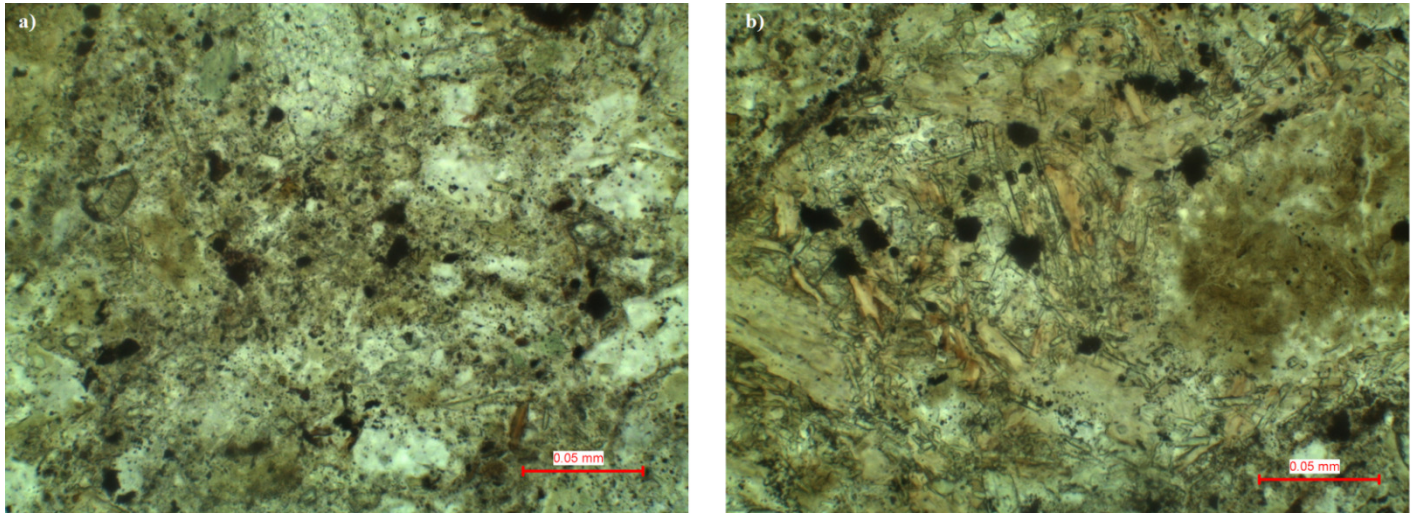


Figure 5.16 Photomicrographs of the basalt-rich VKB at the Lace pipe. a) interclast material; note the complete absence of microlitic clinopyroxene relative to photo b). b) nucleated magmaclast; note the abundant high relief microlitic clinopyroxene.

kimberlite. No serpentine or microlitic clinopyroxene is observed in the interclast material. Microlitic clinopyroxene is observed within the magmaclasts but the interclast material is very similar to that described for the Voorspoed pipe. The ultra fine grained nature of the interclast material may inhibit the identification of microlitic clinopyroxene. The abundant well rounded quartz xenocrysts, in the quartz-rich VK at Lace, are not observed anywhere else in the cluster. This abundance of quartz xenocrysts may indicate a resedimented origin for the VK unit. Furthermore reference by Merensky (1909) to kimberlitic sandstones within the pipe (not observed in this study) must indicate that sedimentary processes were operating at this depth during the emplacement of the pipe. This must indicate that the pipe was open to this depth in order for RVK deposits to form. The lack of in situ VK hinders these conclusions as clear horizontal layering such as that observed at the Voorspoed pipe would be expected.

Microlitic clinopyroxene is abundant in the magmaclasts observed at Lace but is not observed in the interclast material as shown in figure 5.16. This is a very important feature to note as it has specific genetic connotations. Microlitic clinopyroxene is interpreted to form as a late stage deuteric mineral in the HKt as discussed above on section 5.3. The complete lack of microlitic clinopyroxene in the interclast material at Lace indicates that the microlitic

clinopyroxene in the magmaclast must have formed prior to incorporation into the VK units. Therefore the magmaclasts are incorporated from the transitional kimberlite units where microlitic clinopyroxene is abundant. Globular segregations formed in the HKt/HKtB are incorporated into the VK where they are now classified as nucleated magmaclasts. The presence of microlitic clinopyroxene only in the nucleated magmaclasts at the Lace VK is further evidence to support the interpretation of their formation in sub-volcanic environments in the transitional kimberlite.

The interpretation for formation of the VK rocks at Lace is made difficult by the lack of in situ exposure. However the similarity to the Voorspoed VK and the presence of possible kimberlitic sandstone deep within the vent suggest that the VK units at Lace formed in a similar process to the Voorspoed VK. Therefore it is tentatively suggested that the quartz-rich VK at the Lace pipe forms through re-sedimentation of extra crater deposits similar to the BVK at Voorspoed. Secondly the basalt-rich VK is interpreted to form through rock bursts or wall rock failures deep within the pipe similarly to the MVBB/MVSB at the Voorspoed pipe. The evidence obtained in this study and from Merensky (1909) suggests that the Lace pipe infill forms in a deep open vent similar to that proposed for the Voorspoed pipe. However the lack of in situ VK creates large uncertainty and therefore the interpretations made here for the Lace VK are very tentative.

5.5 Economics of the Voorspoed and Lace Kimberlites

5.5.1 Petrographic Interest Rating of the Hypabyssal Kimberlite

Voorspoed

The Voorspoed HK has been classified as aphanitic diopside phlogopite kimberlite and where sanidine and aegirine is present, aphanitic sanidine and aegirine bearing diopside phlogopite kimberlite. Other rare HK varieties include melilite-bearing kimberlite and pure diopside kimberlite. However the bulk of the HK sampled and the HKt is diopside phlogopite kimberlite. The olivine contents in all the HKs are generally low (<10 vol. %) relative to the defined proportion of 50 vol. % by Mitchell (2008). Furthermore the olivine population is dominantly phenocrysts (<0.5mm) and macrocrysts are very rare. Therefore there has been

significant fractionation and loss of the olivine macrocrysts en route to the surface. This has negative implications for diamonds as the larger size fraction of the diamonds is likely to have also fractionated out with the olivine. Oxides at the Voorspoed pipe occur in relatively low abundance and are typically 0.01mm in size. Therefore resorption of the diamonds associated with oxidation is likely to be negligible. However the kimberlite magma is an evolved type indicated by the presence of aegirine and sanidine. This is also confirmed by the geochemistry by high SiO₂ and Na₂O contents. Diamonds are more prone to resorption in evolved magmas and significant resorption related to the unevolved magma may be observed.

All the above petrographic conclusions made on the diamonds at the Voorspoed mine are confirmed by Wagner (1914). Octahedral diamonds are rare at the Voorspoed pipe (Wagner, 1914). A large proportion of the diamonds recovered in the early 1900's were small stones. This fits with the petrology as the lack of olivine macrocrysts indicates fractionation of the magma en route to the surface. Therefore the large stones have been completely lost and it is unlikely that significant proportions of large stones will ever be recovered at the Voorspoed mine. The presence of relatively good diamond grades at the Voorspoed pipe indicates that the original magma must have been particularly rich in diamonds as large proportions of the diamonds would have been removed through fractional crystallisation.

Lace

The Lace hypabyssal kimberlite (HK) has been classified as macrocrystic phlogopite kimberlite with varying proportions of melilite and monticellite. Olivine contents are much higher than at the Voorspoed pipe and are generally 30 vol. %. Therefore with the preservation of the olivine macrocrysts it is likely that the larger diamonds have also been preserved and not fractionated out such as at the Voorspoed pipe. Oxides at the Lace HK are relatively abundant compared to Voorspoed however they are still very fine grained (<0.04mm) and therefore do not indicate any resorption of the diamonds. The Lace HK geochemistry and the mineralogy indicate it is an unevolved type Group II kimberlite magma, which has positive implications for diamond survival as diamonds are more likely to survive in the unevolved magma. SiO₂ and Na₂O contents are low and no evolved type minerals are observed in the HK. Monticellite is particularly abundant in some samples, which is most

commonly observed in Group I kimberlites and therefore the Lace kimberlite has some characteristics more similar to Group I kimberlite. This further indicates the unevolved nature. Therefore the diamonds at Lace are expected to show a typical size distribution.

This is confirmed by Wagner (1914) and by a visit to the mine during the course of this study. The bulk of the diamonds are octahedral in shape (Wagner, 1914) and this was confirmed during a visit to the mine in 2008. However the size distribution of the diamonds is unknown, although it seems likely that the Lace kimberlite will produce larger stones than the Voorspoed pipe based on the petrography and the diamond grades are likely to be significantly higher at the Lace pipe relative to the Voorspoed pipe.

Besterskraal North

The Besterskraal North kimberlite is a highly evolved aphanitic K-richterite bearing Group II kimberlite. The aphanitic nature of the kimberlite and the highly evolved magma compositions are indications that diamond survival is very low. The highly evolved nature of the kimberlite is clearly indicated by the presence of abundant evolved type minerals, which include: K-richterite, sanidine, aegirine and leucite. Therefore if any diamonds were present in the magma they were likely totally resorped by the magma during ascent to the surface. This has been confirmed by exploration programmes and the kimberlite has been determined to be sub-economic.

5.5.2 Diamond Distribution in the Voorspoed Volcaniclastic Deposits

Typical South African kimberlites have homogenous diamond distributions within the volcaniclastic kimberlite as a result of thorough mixing of the rock during their formation. However the Voorspoed kimberlite is not a typical South African kimberlite and the volcaniclastic kimberlite is likely to not have a homogenous diamond distribution. The diamond grades for each of the specific volcaniclastic rocks types identified are unknown as individual volcaniclastic units have never been sampled for diamond grades. However the proportion of kimberlite within each VK unit is easily obtained by point counting techniques. Therefore the VK units can be ranked using the relative proportion of kimberlite present

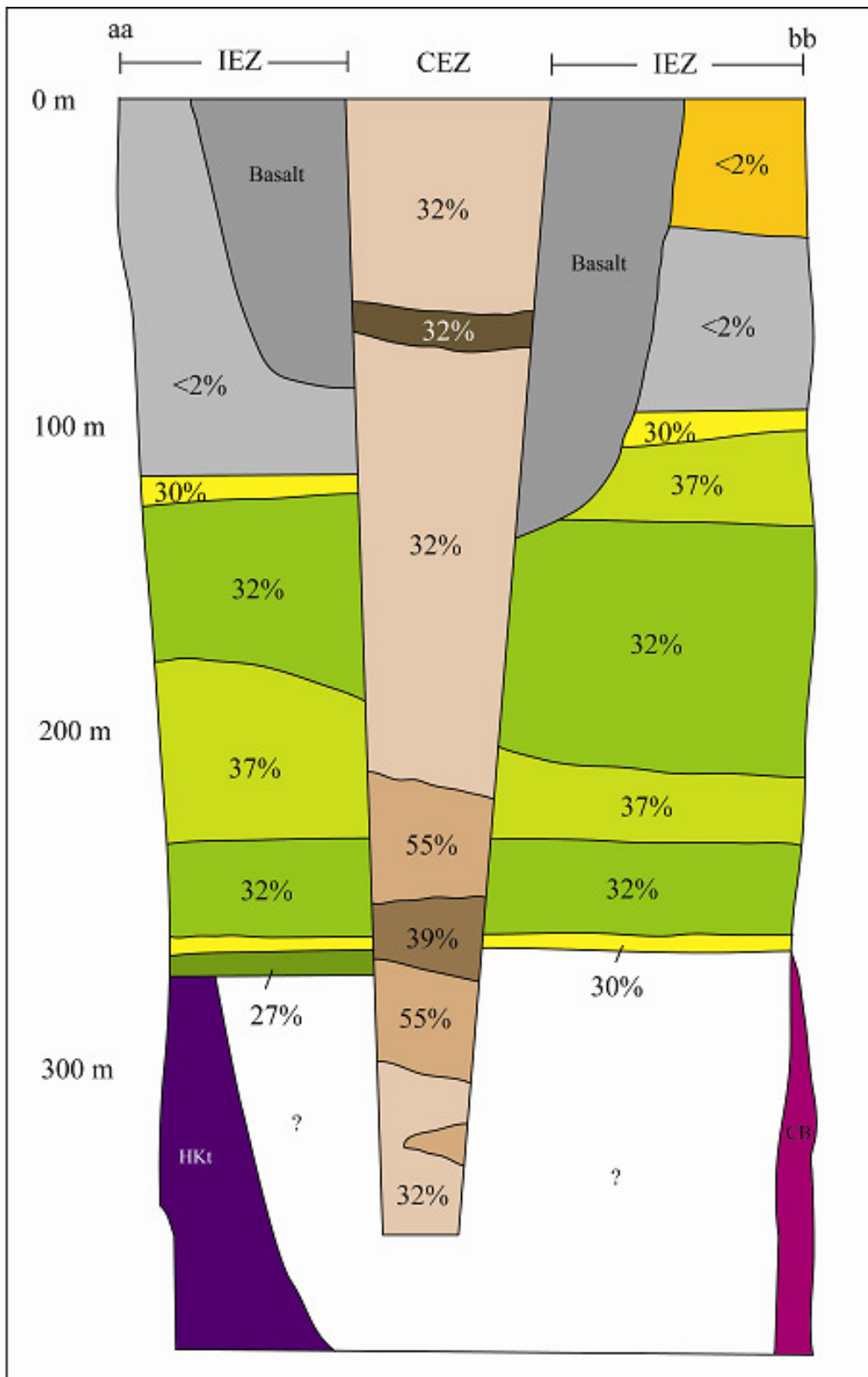


Figure 5.17 Cross-section aa-bb through the Voorspoed pipe, as shown in figure 3.14, showing the distribution of the volcaniclastic kimberlite. This figure shows the percentage of kimberlite present within each of the volcaniclastic units. Kimberlite components include magmaclasts and xenocrysts. HKt: transitional kimberlite and CB: contact breccia.

within the unit. The proportion of kimberlite within the infill at the Voorspoed pipe ranges from 0 vol. % to 55 vol. % as shown in figure 5.17. Therefore the VK units containing no kimberlite at all should not be treated as ore but rather dumped as waste. Furthermore these VK units with low kimberlite abundances need to be thoroughly mapped to avoid dilution and possibly regarded as waste. This is particularly important for the Voorspoed pipe as the petrographic interest rating indicates low to moderate interest and therefore the mine is likely to be marginal. The graded RVK beds and the fine-grained RVK layers are volumetrically insignificant in terms of mining operations and can be ignored from an economic perspective.

The olivine contents at the Voorspoed pipe are very low in abundance and olivine macrocrysts are generally very rare. Therefore the larger diamonds have likely fractionated out at the same stage as the olivine macrocrysts as discussed above. However the T2MVK does contain olivine macrocrysts albeit in relatively low abundance. This indicates that the larger diamond sizes may still be present to some degree and therefore this zone needs to be actively targeted by mining operations. The T2MVK has the highest kimberlite content as well as the containing olivine macrocrysts. This unit will contain by far the best grade of the pipe.

Therefore it is clearly evident from a detailed petrographic study that the upper basalt and sandstone breccia units should not be targeted by mining operations but rather treated as waste as the kimberlite component of the rock is very low. Furthermore it is clear that the highest grades within the pipe are in the CEZ at depth <200m where the T2MVK and intMVK are interbedded. Therefore this zone should be actively targeted by mining operations. The hypabyssal kimberlite sampled so far has mostly been from surrounding dike/sills in the country rock and as late stage internal dikes. These rocks are all of low to moderate interest and it seems very likely that the HK in the root zone of the Voorspoed pipe will have the same low to moderate interest. This is based on the HKt sampled at depth, which is very similar to the samples from surrounding intrusive kimberlite dike/sills.

Section 6. Summary and Conclusion

The Kroonstad kimberlite pipes are not like any other kimberlite pipes within South Africa. The unique characteristic is the volcanoclastic pipe infill, which is more similar to kimberlite pipes from Lac de Gras in Canada (Class 3 pipes). The initial stages of near-surface emplacement are similar to typical South African kimberlites and are likened to the development of an embryonic pipe (Clement, 1982). The formation of a vent is also similar to typical South African kimberlite as the vent shape is very consistent with the Class 1 pipe model proposed by Skinner (2008). The pipe margins have a typical dip of approximately 82° and the maximum depth of the volcanoclastic kimberlite is approximately 2km, both of which are typical characteristics of South African kimberlites.

The presence of abundant primary diopside, aegirine and sanidine in the Voorspoed hypabyssal kimberlite (HK) clearly indicates the evolved nature of the Group II kimberlite magma. The aegirine compositions show some solid solution with augite. The phlogopite analysed in this study does not show any trend toward an evolved Ti-rich mantle. Mitchell (1995) found similar results for the sample K1/110, however sample K1/111 clearly shows enrichment of Ti and a trend toward the phlogopite compositions of the highly evolved Besterskraal North and Sover North kimberlites. Therefore the Voorspoed kimberlite is intermediate in terms of the evolution of the magma, which is also indicated by the absence of the more highly evolved type minerals (K-richterite, leucite) and from the intermediate phlogopite compositions. The mineral chemistry of the Voorspoed pipe along with mineral chemistry done on the Voorspoed HK by Mitchell (1995) indicate that the magma evolved to a late stage residual fluid with a composition rich in SiO₂, Na₂O, Al₂O₃, FeO and depleted in MgO and CaO as indicated by the late stage aegirine and sanidine compositions. Furthermore it is likely that the residual fluids were CO₂-rich, indicated by the presence of calcite forming the segregations in the HKtB at Voorspoed. This composition is not typical of kimberlites worldwide, which generally have residual fluids rich in H₂O, K₂O, CaO, MgO, which contains some SiO₂ and is CO₂ poor (Mitchell et al. 2009). This difference in the residual fluid at Voorspoed is likely the reason for the complete lack of the formation of late stage deuteric microlitic clinopyroxene, which is likely also inhibited by the earlier primary crystallisation of diopside phenocrysts. This characteristic absence of microlitic

clinopyroxene may be true for all evolved Group II kimberlites and further work needs to be done on these very unique evolved types of kimberlite.

The geochemistry of the Lace and Voorspoed kimberlite clearly illustrates the difference in the evolution of the magma. The Lace kimberlite is a typical unevolved low SiO₂ and Na₂O Group II kimberlite whereas the Voorspoed kimberlite has high SiO₂ and Na₂O. Three possible conclusions can be made to explain the variation in the magma compositions: 1) crustal contamination at depth, 2) different source rocks or 3) differentiation in a staging chamber. Detailed investigation into the paragenesis of the magma is outside the scope of this study. However evidence of fractional crystallisation for the Voorspoed magma may indicate differentiation played a role in the evolution of the magma. Bulk rock geochemical analysis of the Lace kimberlite shows some very important trends, which have been linked to two processes: 1) crystal contamination and 2) CO₂ degassing. The first trend is characterised by an increase in SiO₂, Na₂O and Al₂O₃, which is typical of crustal contamination (e.g. Harris et al 2004 and Becker and le Roex, 2006). The latter trend is linked to a rise in microlitic clinopyroxene abundance in HKt, which contains insignificant proportions of country rock material. This trend is interpreted to result from the crystallisation of microlitic clinopyroxene due to CO₂ degassing. CO₂ degassing has been shown to be the mechanism for microlitic clinopyroxene crystallisation by both Skinner and Marsh (2004) and Mitchell et al. (2009). Furthermore similar trends to the Lace HKt are observed at the Wesselton and Dutoitspan HKs (data presented by Clement, 1982). These data also shows that CO₂ correlates with the geochemistry for the interpreted CO₂ degassing trend. Therefore the geochemistry of the hypabyssal transitional kimberlite (HKt) is controlled by CO₂ degassing, which induces crystallisation of microlitic clinopyroxene. Furthermore this must indicate that microlitic clinopyroxene is not a later secondary alteration phase (Stripp et al. 2006) but rather a late stage deuteric mineral.

Substantial erosion has occurred at the Kroonstad kimberlite cluster since their emplacement. Approximately 1750m of post-emplacement erosion has been calculated for the Kroonstad area based on an average of the three methodologies presented in section 5.1. Some margin for error exists although the average value obtained fits well with the model presented by Skinner (2008) for typical South African kimberlites. The Voorspoed kimberlite pipe is not

typical of South African pipes and is more similar to kimberlites from the Lac de Gras region in Canada. These pipes in Lac de Gras are classified as Class 3 pipes based on the VK infilling the pipe. Therefore the Voorspoed pipe is not a typical Class 1 South African pipe but rather something more similar to a Class 3 type pipe. The classification of the Lace pipe is hindered by the lack of in situ VK within the pipe. The in situ transitional kimberlite has characteristics of typical Class 1 kimberlites but the VK from the surrounding dumps does not show similarities to typical tuffisitic kimberlite, which is a characteristic feature of Class 1 pipes. Therefore classification of the Lace pipe is unclear, although based on the in situ kimberlite one would favour the interpretation of Class 1 over Class 3. The discussion on the root zone processes at the Kroonstad cluster is based mainly on observations from the Lace pipe as an extensive in situ root zone has not been intersected at the Voorspoed pipe, although the presence of contact breccias and the transitional kimberlite indicate that the Voorspoed pipe developed as an embryonic pipe. The processes of formation of the embryonic pipe are similar at both the Voorspoed and Lace pipe although some differences are noted. The development of microlitic clinopyroxene is restricted to Lace, which indicates that there are some subtle differences in the formation of the embryonic pipe. However in general the formation of contact breccias and transitional kimberlite is similar. The dominant process driving the formation of the embryonic pipe at both the Voorspoed and Lace kimberlite pipes is volatile exsolution. Volatile exsolution creates overpressure in the sub-volcanic embryonic pipe, which leads to the formation of extensive hydraulic fracturing of the sidewall and roof rock material. This process forms the distinct contact breccias preserved in the sidewall at the Voorspoed and Lace kimberlites. Globular segregatory textures are produced by nucleation of the early crystallising mineral phases around the solid components already present within the magma. The preservation of these textures results in the formation of the transitional kimberlite. The complete absence of microlitic clinopyroxene at the Voorspoed pipe is most likely related to two features: 1) abundant primary diopside at Voorspoed may hinder the later crystallisation of microlitic clinopyroxene and 2) the late stage residual liquid at the Voorspoed pipe is not similar to typical late stages liquids as described by Mitchell et al. (2009). Therefore the development of the root zones/embryonic pipes at the Voorspoed and Lace pipes are interpreted to be very similar with the major difference being the development of microlitic clinopyroxene at Lace.

The volcanoclastic kimberlite at the Voorspoed pipe is unique to South African kimberlites. The presence of horizontal layering has not been documented in any other South African kimberlite. The complete absence of tuffisitic kimberlite must indicate that the VK infill formed through a different process from typical tuffisitic Class 1 kimberlite. It is interpreted that the dominant variety of VK (the MVK units) at the Voorspoed pipe formed through repetitive pyroclastic eruption forming primary pyroclastic deposits through possible column collapse or in-vent explosive flows, the latter mechanism is favoured for the formation of the Voorspoed VK. Either way the deposits have characteristics of typical primary pyroclastic type deposits. The only difference is the lack of directional indications as the Voorspoed deposits would not have travelled anywhere. Other depositional processes operating at the Voorspoed pipe include: gravitational sidewall failure and crater rim failure/slumping. Interpretations of the formation of the VK at the Lace pipe are hindered by the complete lack of in situ exposures. However due to the similarity of the VK to the Voorspoed pipe and the reference by Merensky (1909) to kimberlitic sandstones within the pipe; similar depositional processes to the Voorspoed pipe VK are proposed. These processes include gravitational sidewall failure for the basalt-rich VK and crater rim failure/slumping for the quartz-rich VK.

The near surface emplacement of the Kroonstad kimberlites takes place in three broad stages; firstly through sub-volcanic intrusion of the embryonic with the formation of contact breccias in the sidewall. Secondly a major decompression driven eruption occurs when fractures/cracks reach the surface and thirdly the infilling of the pipe by repeated episodic primary pyroclastic deposition as well as resedimentation processes into a deep open vent. This process is not typical of South African kimberlites and is more similar to Lac de Gras Class 3 kimberlites. However distinct root zones have never been documented in Class 3 kimberlites and the presence of distinct root zones at the Kroonstad cluster may aid in the future understanding of the emplacement of Class 3 kimberlite pipes.

6.1 Further Work

The observations made in this study indicate that the interpretations of Skinner and Marsh (2004) and Hetman et al. (2004) for the formation of transitional kimberlite are correct. The sub-volcanic development of transitional kimberlite and contact breccias is made very clear

by the presence of these distinct rock types at the head of blind pipes, which have not reached the surface. Therefore it seems very important to study these blind pipes in detail as they have not formed through pyroclastic processes. In particular the geochemistry of xenolith poor HKt from within these pipes may prove valuable. Initial observations made in this study showing geochemical trends controlled by the abundance of microlitic clinopyroxene as a result of CO₂ degassing needs to be conducted at numerous other localities to constrain these subtle geochemical trends. The source of the increased SiO₂ and Na₂O has not been resolved in this study and therefore further work needs to be done to ascertain the source of the Si and Na.

The Voorspoed kimberlite is unique in terms of the VK infill and the characteristics of the HKt. Therefore further analysis of these evolved Group II kimberlite pipes needs to be done to fully understand the differences observed at Voorspoed. The complete lack of serpentine and microlitic clinopyroxene in the HKt is an intriguing characteristic, which indicates that the magma and volatile compositions are different from typical kimberlites. The Dokolwayo kimberlite is the only other kimberlite in southern Africa (Swaziland) to be documented to contain a crystallinoclastic interclast material in the VK (Clement, 1982). Further work needs to be done on this kimberlite to determine if it is similar to the Voorspoed VK infill. Therefore it may be likely that numerous pipes in South Africa may not be typical tuffisitic kimberlites. Future studies need to be careful not to simply classify VK infill as tuffisitic kimberlite before detailed macroscopic mapping and petrographic analysis has been done.

Hypothesis for the Incorporation of an Aqueous Fluid at Depth

The geochemical variation observed at the Lace HKt indicates that there has been a possible minor addition of SiO₂ and Na₂O. The increased Si and Na is observed petrographically in the form of an increased abundance of microlitic clinopyroxene. Microlitic clinopyroxene forms through either crustal contamination or CO₂ degassing (Mitchell et al. 2009). The lack of crustal xenoliths indicates that degassing is the more likely mechanism. However it is unclear whether degassing can cause differentiation and subsequent increase in Si and Na in the magma. Therefore an alternate process is proposed here as a relatively speculative hypothesis based on the stable isotope work of Shepard and Dawson (1975).

Sheppard and Dawson (1975) show that phlogopite megacrysts (mantle xenocrysts) have typical juvenile magmatic stable isotope signatures as would be expected. However the groundmass primary phlogopite had a mixed origin with juvenile magmatic-metamorphic characteristics. If this was a result of late stage secondary hydrothermal fluid circulation and re-equilibration one would expect the megacryst phlogopite to have a similar stable isotope signature to the groundmass. It is suggested here that the incorporation of an aqueous fluid at depth early in the evolution of the embryonic pipe during hydraulic fracturing of the country rock may have occurred. This would account for the increased Si and Na. Furthermore a fluid with elevated Na is likely to be a more evolved brine or connate fluid. The exsolution of a juvenile fluid from the kimberlite magma during embryonic pipe formation may have mixed with aqueous fluids present in the country rock at this depth and subsequent mixing of stable isotopes signatures. A possible convective cell may form where juvenile fluids circulate through the country rock and mix with aqueous fluids. This is highly speculative and further detailed work needs to be done to either confirm or discard these ideas.

Section 7. References

- Armstrong, J.P., Wilson, M., Barnett, R.L., Nowicki, T. and Kjarsgaard, B.A. 2004. Mineralogy of primary carbonate-bearing hypabyssal kimberlite, Lac de Gras, Slave province, Northwest Territories, Canada. *Lithos*, 76, 415–433.
- Barnett, W. P. and Lorig, L. 2007. A model for stress-controlled pipe growth. *Journal of Volcanology and Geothermal research*, 159, 108-125.
- Becker, M., and le Roex, A.P. 2006. Geochemistry of South African On- and Off craton, Group I and Group II Kimberlites: Petrogenesis and Source Region Evolution. *Journal of Petrology*, 47, 673-703.
- Becker, M., le Roex, A. and Class, C. 2007. Geochemistry and petrogenesis of South African transitional kimberlites located on and off the Kaapvaal Craton. *South African Journal of Geology*, 110, 631-646.
- Berryman, A.K., Scott Smith, B.H. and Jellicoe, B. 2004. Geology and diamond distribution of the 140/141 kimberlite, Fort á la Corne, central Saskatchewan, Canada. Proceedings of the 8th International Kimberlite Conference. *Lithos*, 76, 99–114.
- Bordy, E.M., Hancox, P.J. and Rubidge, B.S. 2004. Provenance study of the Late Triassic – Early Jurassic Elliot Formation, main Karoo Basin, South Africa. *South African Journal of Geology*, 107, 587-603.
- Brown, R. J., Gernon, T., Stiefenhofer, J. and Field, M. 2008 (a). Geological constraints on the eruption of the Jwaneng Centre kimberlite pipe, Botswana. *Journal of Volcanology and Geothermal Research*, 174, 195–208.
- Brown, R.J., Buse, B., Sparks, R.S.J. and Field, M., 2008 (b). On welding of pyroclasts from very low viscosity magmas: examples from kimberlite volcanoes. *Journal of Geology*, 116, 354–374.
- Brown, R. J., Field, M., Gernon, T., Gilbertson, M. and Sparks, R.S.J. 2008 (c). Problems with an in-vent column collapse model for the emplacement of massive volcanoclastic kimberlite. A discussion of 'In-vent column collapse as an alternative model for massive volcanoclastic kimberlite emplacement: An example from the Fox kimberlite, Ekati Diamond Mine, NWT, Canada' by Porritt et al. [J. Volcanol. Geotherm. Res. 174, 90-102]. *Journal of Volcanology and Geothermal Research*, 178, 847-850.
- Brown, R. J., Tait, M., Field, M. and Sparks R. S. J. 2009. Geology of a complex kimberlite pipe (K2 pipe, Venetia Mine, South Africa): insights into conduit processes during explosive ultrabasic eruptions. *Bulletin of Volcanology*, 71, 95–112.
- Burnham, C.W. 1985. Energy release in subvolcanic environments: implications for breccia formation. *Economic Geology*, 80, 1515–1522.
- Carlson, S.M., Hillier, W.D., Hood, C.T., Pryde, R.P. and Skelton, D.N., 1999. The Buffalo Hills kimberlites: a newly discovered diamondiferous kimberlite province in North-central Alberta, Canada. Proceedings of the 7th International Kimberlite Conference, Cape Town, South Africa, 1, 109–118.
- Cas, R.A.F., Hayman, P.C., Pittari, A. and Porritt, L.A. 2008(a). Some major problems with

- existing models and terminology associated with kimberlites from a volcanological perspective and some suggestions. *Journal of Volcanology and Geothermal Research*, 174, 209–225.
- Cas, R.A.F., Porritt, L., Pittari, A. and Hayman, P. 2008(b). A new approach to kimberlite facies terminology using a revised general approach to the nomenclature of all volcanic rocks and deposits: descriptive to genetic. *Journal of Volcanology and Geothermal Research*, 174, 226–240.
- Catuneanu, O., Wopfner, H., Eriksson, P.G., Cairncross, B., Rubidge, B. S., Smith, R. M. H. and Hancox, P. J. 2005. The Karoo basins of south-central Africa. *Journal of African Earth Sciences*, 43, 211-253.
- Chalapathi Rao, N. V. 2005. A petrological and geochemical reappraisal of the Mesoproterozoic diamondiferous Majhgawan pipe of central India: evidence for transitional kimberlite – orangeite (Group II kimberlite) – lamproite rock type. *Mineralogy and Petrology*, 84, 69-106.
- Chang, L.L.Y. 1965. Subsolidus phase relations in the system BaCO₃–SrCO₃, SrCO₃–CaCO₃, and BaCO₃–CaCO₃. *Journal of Geology*, 73, 346– 368.
- Clement, C.R. 1982. A comparative geological study of some major kimberlite pipes in the Northern Cape and Orange Free State. Ph.D thesis University of Cape Town.
- Clement, C.R. and Skinner, E.M.W. 1985. A textural-genetic classification of kimberlites. *Transactions Geological Society of South Africa*, 88, 403–409.
- Clement, C.R. and Reid, A.M. 1989. The origin of kimberlite pipes: an interpretation based on the synthesis of geological features displayed by southern African occurrences. *In*: Ross, J., Jaques, A.L., Ferguson, J., Green, D.H., O'Reilly, S.Y., Danchin, R.V. and Janse, A.J.A. (Eds.), *Kimberlites and Related Rocks*, *Geological Society of Australia*, 14, 632–646.
- Coe, N., le Roex, A., Gurney, J., Pearson, D. G. and Nowell, G. 2008. Petrogenesis of the Swartruggens and Star Group II kimberlite dyke swarms, South Africa: constraints from whole rock geochemistry. *Contributions to mineralogy and petrology*, 156, 627–652.
- Crow, C. and Condie, K.C. 1988. Geochemistry and origin of late Archean volcanics from the Ventersdorp Supergroup, South Africa. *Precambrian Research*, 42, 19-37.
- Danchin, R.V., Ferguson, J., MacIver, R. and Nixon, P.H. 1975. The composition of late stage kimberlite liquids as revealed by nucleated autoliths. *Physics and Chemistry of the Earth* 9, 235–246.
- Deer, W.A., Howie, R. A. and Zussman, J. 1992. An introduction to The Rock-Forming Minerals. Prentice Hall. pp687.
- Doyle, B.J., Kivi, K. and Scott Smith, B.H. 1999. The Tli Kwi Cho (DO27 and DO18) diamondiferous kimberlite complex, Northwest Territories, Canada. *Proceedings of the 7th International Kimberlite Conference*, 1, 194–204.
- Downes, P. J., Ferguson, D. and Griffin, B. J. 2007. Volcanology of the Aries micaceous kimberlite, central Kimberley Basin, Western Australia. *Journal of Volcanology and Geothermal Research*, 159, 85–107.

- Druitt, T.H. 1995. Settling behaviour of concentrated dispersions and some volcanological applications. *Journal of Volcanology and Geothermal Research*, 65 (1–2), 27.
- Duncan, A. R. and Marsh, J. S. 2006. The Karoo igneous province. In: Johnson, M. R., Anhaeusser, C.R. and Thomas, R. J. (Ed.) *The Geology of South Africa*. Geological Society of South Africa, Johannesburg/Council for Geoscience, Pretoria, 501-520.
- Dunlevey, J. N., Ramluckan, V. R. and Mitchell, A. A. 1993. Secondary mineral zonation in the Drakensberg Basalt Formation, South Africa. *South African Journal of Geology*, 96, 215-220.
- Eriksson, P. G., Schreiber, U. M., van der Neut, M., Labuschagne, H., van der Schyff, W. and Potgieter, G. 1993. Alternative marine and fluvial models for the non-fossiliferous quartzitic sandstones of the Early Proterozoic Daspoort Formation, Transvaal sequence of southern Africa. *Journal of African Earth Science*, 16, 355-366.
- Eriksson, P. G., Altermann, W. and Hartzler, F. J. 2006. The Transvaal Supergroup and its precursors. In: Johnson, M. R., Anhaeusser, C.R. and Thomas, R. J. (Ed.) *The Geology of South Africa*. Geological Society of South Africa, Johannesburg/Council for Geoscience, Pretoria, 237-260.
- Ferguson, J., Danchin, R.V. and Nixon, P.H. 1973. Petrochemistry of kimberlite autoliths. *Lesotho Kimberlites*, 285–293.
- Field, M. and Scott Smith, B.H. 1998. Textural and genetic classification schemes of kimberlites: new perspective. *Extended Abstracts of the Seventh International Kimberlite Conference*. Cape Town, South Africa, 214–216.
- Field, M. and Scott Smith, B.H. 1999. Contrasting geology and near-surface emplacement of kimberlite pipes in southern Africa and Canada, *Proceedings of the 7th International Kimberlite Conference*, 1, 217–237.
- Field, M., Stiefenhofer, J., Robey, J., Kurszlaukis, S. 2008. Kimberlite-hosted diamond deposits of southern Africa: A review. *Ore Geology Reviews*, 34, 33–75.
- Fitzgerald, C. E., Hetman, C. M., Lepine, I., Skelton, D. S. and McCandless, T. E. 2009. The internal geology and emplacement history of the Renard 2 kimberlite, Superior Province, Quebec, Canada. *Lithos*, doi:10.1016/j.lithos.2009.05.036.
- Fraser, K.J. and Hawkesworth, C.J. 1992. The petrogenesis of group 2 ultrapotassic kimberlites from Finsch Mine, South Africa. *Lithos* 28, 327–345.
- Gernon, T.M., Sparks, R.S.J. and Field, M. 2008. Degassing structures in volcanoclastic kimberlite: examples from southern African kimberlite pipes. *Journal of Volcanology and Geothermal Research*, 174 (1–3), 186–194.
- Gernon, T. M., Gilbertson, M. A., Sparks, R. S. J. and Field, M. 2009. The role of gas-fluidisation in the formation of massive volcanoclastic kimberlite. *Lithos*, doi:10.1016/j.lithos.2009.04.011
- Graham, I., Burgess, J.L., Bryan, D., Ravenscroft, P.J., Thomas, E., Doyle, B.J., Hopkins, R.

- and Armstrong, K.A. 1999. Exploration history and geology of the Diavik kimberlites, Lac de Gras, NWT, Canada. *Proceedings of the 7th International Kimberlite Conference*, 1, 262–279.
- Groenewald, G.H. 1989. Stratigrafie en sedimentologie van die Groep Beaufort in die Noordoos-Vrystaat. *Bulletin, Geological Survey of South Africa*, 96, 62.
- Hanson, E.K. 2006. Estimating erosion of cretaceous-aged kimberlites in the Republic of South Africa through the examination of upper-crustal xenoliths. M.Sc. thesis (unpubl.), Rhodes University, South Africa.
- Harris, M., le Roex, A. and Class, C. 2004. Geochemistry of the Uintjiesberg kimberlite, South Africa: petrogenesis of an off-craton, group 1, kimberlite. *Lithos* 74, 149–165.
- Hawthorne, J.B. 1975. Model of a kimberlite pipe, *Physics and Chemistry of the Earth*, 9, 1–15.
- Hawthorne, J. B., Carrington, A. J., Clement, C. R. and Skinner, E. M. W. 1979. Geology of the Dokolwayo kimberlite and associated palaeo-alluvial diamond deposits. In: Boyd, F. R. and Meyer, H. O. A. (Ed.) *Kimberlites, Diatremes and Diamonds: Their geology, petrology and geochemistry*. 59-70. Am. Geophys. Union, Washington.
- Hayman, P.C., Cas, R.A.F. and Johnson, M. 2008. The difficulties in distinguishing coherent from fragmental kimberlite: a case study of the Muskox pipe (Northern Slave Province, Nunavut, Canada). *Journal of Volcanology and Geothermal Research*, 174, 139–151.
- Hayman, P.C., Cas, R.A.F. and Johnson, M. 2009. Characteristics and alteration origins of matrix minerals in volcanoclastic kimberlite of the Muskox pipe (Nunavut, Canada), *Lithos*, doi:10.1016/j.lithos.2009.06.025
- Hetman, C.M., Scott Smith, B.H., Paul, J.L. and Winter, F. 2004. Geology of the Gahcho Kue kimberlite pipes, NWT, Canada: root to diatreme magmatic transition zone. *Lithos*, 76, 51–74.
- Hetman, C.M. 2008. Tuffisitic kimberlite (TK): a Canadian perspective on a distinctive textural variety of kimberlite. *Journal of Volcanology and Geothermal Research*, 174, 57–67.
- Holmes, A. 1965. *Principles of physical geology*. Thomas Nelson, London.
- Howarth, G. H. 2007. Estimating erosion of Group II kimberlite pipes and palaeo-distribution of the Karoo Supergroup, in the Free State province of South Africa, using upper-crustal xenoliths. BSc. Hon thesis (unpubl.), Rhodes University, South Africa.
- Johnson, M.R., Van Vuuren, C.J., Hegenberger, W.F., Key, R. and Shoko, U. 1996. Stratigraphy of the Karoo Supergroup in southern Africa: an overview. *Journal of African Earth Science*, 23 (1), 3–15.
- Johnson, M. R., van Vuuren, C. J., Visser, J. N. J., Cole, D. I., de V. Wickens, H., Christie, A. D. M., Roberts, D. L. And Brandl, G. 2006. Sedimentary rocks of the Karoo Supergroup. In: Johnson, M. R., Anhaeusser, C.R. and Thomas, R. J. (Ed.) *The Geology of South Africa*. Geological Society of South Africa, Johannesburg/Council for Geoscience, Pretoria, 461-499.

- Kjarsgaard, B. A., Pearson, D. G., Tappe, S., Nowell, G.M. and Dowall, D.P. 2009 (a). Geochemistry of hypabyssal kimberlites from Lac de Gras, Canada: Comparisons to a global database and applications to the parent magma problem. *Lithos*, doi:10.1016/j.lithos.2009.06.001
- Kjarsgaard, B. A., Harvey, S., McClintock, M., Zonneveld, J. P., Du Plessis, P., McNeil, D. and Heaman, L. 2009 (b). Geology of the Orion South kimberlite, Fort à la Corne, Canada, *Lithos*, doi:10.1016/j.lithos.2009.05.039.
- Kong, J.M., Boucher, D.R. and Scott Smith, B.H. 1999. Exploration and geology of the Attawapiskat kimberlites, James Bay Lowland, Northern Ontario, Canada. The J.B. Dawson Volume, Proceedings of the 7th International Kimberlite Conference, 1, 452–467.
- Le Roex, A.P., Bell, D.R. and Davis, P. 2003. Petrogenesis of group 1 kimberlites from Kimberley, South Africa: evidence from bulk rock chemistry. *Journal of Petrology*, 44, 2261–2286.
- Lorenz, V. 1975. Formation of phreatomagmatic maar–diatreme volcanoes and its relevance to kimberlite diatremes, *Physics and Chemistry of the Earth*, 9, 17–29.
- Lorenz, V., Zimanowski, B., Büttner, R., and Kurszlaukis, S. 1999. Formation of kimberlite diatremes by explosive interaction of kimberlite magma with groundwater: field and experimental aspects. Proceedings of the 7th International Kimberlite Conference, 2, 522–528.
- Lorenz, V., Zimanowski, B. and Büttner, R. 2002. On the formation of deep-seated subterranean peperite-like magma–sediment mixtures. *Journal of Volcanology and Geothermal Research*, 114, 107–118.
- Lorenz, V. and Kurszlaukis, S. 2007. Root zone processes in the phreatomagmatic pipe emplacement model and consequences for the evolution of maar– diatreme volcanoes. *Journal of Volcanology and Geothermal Research*, 159, 4–32.
- Machin, K. 2000. Processes and products in kimberlitic crater facies of the south lobe, Jwaneng Mine, Botswana. Unpublished M.Sc. thesis, Rhodes University, Grahamstown, 152 pp.
- Marsh, J.S., Hooper, P.R., Rehacek, J., Duncan, R.A. and Duncan, A.R. 1997. Stratigraphy and age of Karoo basalts of Lesotho and implications for correlations within the Karoo Igneous Province. In: Mahoney, J.J., Coffin, M.F. (Eds.), Large Igneous Provinces: Continental, Oceanic, and Planetary Flood Volcanism. *Geophysical Monograph 100*. American Geophysical Union, Washington DC, 247–272.
- Marsh, J.S. 1998. Geochemical stratigraphy in basalts of the Mohale Dam – Katse dam areas, Lesotho. Report on Contract LHDA 1009, Mohale Tunnel: Sampling and testing of cores. Lesotho Highlands Tunnel Partnership (Mohale) (unpubl.). Rhodes University, Grahamstown, 21pp.
- Masun, K., Doyle, B. J., Ball, S. and Walker, S. 2004. The geology and mineralogy of the Anuri kimberlite, Nunavut, Canada. *Lithos*, 76, 75-97.
- Masun, K. and Scott Smith, B.H. 2008. The Pimenta Buena kimberlite field, Rondonia, Brazil: tuffisitic kimberlite and transitional textures. *Journal of Volcanology and Geothermal Research*, 174, 81–89.

- Merensky, H. 1909. Geological observations in the Lace diamond mine. *Transactions of the Geological Society of South Africa*, 12, 203.
- Meyers, R. E., McCarthy, T. S., Bunyard, M., Cawthorn, R. G., Falatsa, T. M., Hewitt, T., Linton, P., Meyers, J.M, Palmer, K. J. and Spencer, R. 1990. Geochemical stratigraphy of the Klipriversberg Group volcanic rocks. *South African Journal of Geology*, 93, 224-238.
- Mitchell, R.H. and Meyer, H.O.A. 1989. Mineralogy of micaceous kimberlites from the New Elands and Star mines, Orange Free State, South Africa. In: Ross, J., Jaques, A.L., Fergusan, J., Green, D.H., O'Reilly, S.Y., Danchin, R.V. and Janse, A.J.A. (Eds.), *Kimberlites and Related Rocks*, *Geological Society of Australia*, 14, 83-96.
- Mitchell, R.H. 1995. *Kimberlite, Orangeites and Related Rocks*. Plenum Press, New York. 410pp.
- Mitchell, R.H. 2008. Petrology of hypabyssal kimberlites: relevance to primary magma compositions. *Journal of Volcanology and Geothermal Research*, 174, 1–8.
- Mitchell, R. H., Skinner, E. M. W and Scott Smith, B. H. 2009. Tuffisitic kimberlites from the Wessleton Mine, South Africa: Mineralogical characteristics relevant to their formation. *Lithos*, doi:10.1016/j.lithos.2009.06.018.
- Moss, S., Russell, J.K. and Andrews, G.D.M. 2008. Progressive infilling of a kimberlite pipe at Diavik, Northwest Territories, Canada: insights from volcanic facies architecture, textures and granulometry. *Journal of Volcanology and Geothermal Research*, 174, 103–116.
- Naidoo, P., Stiefenhofer, J., Field, M. and Dobbe, R. 2004. Recent advances in the geology of the Koffiefontein mine, Free State Province, South Africa. *Lithos*, 76, 161-182.
- Norrish, K. and Hutton. J.T. 1969. An accurate X-ray spectrographic method for the analysis of a wide range of geological samples. *Geochemica et Cosmochimica Acta*, 33, 431-453.
- Nowicki, T., Crawford, B., Dyck, D., Carlson, J., McElroy, R., Oshust, P. and Helmstaedt, H. 2004. The geology of kimberlite pipes of the Ekati property NWT, Canada. Proceedings of the 8th International Kimberlite Conference. *Lithos*, 76, 1–27.
- Nowicki, T., Porritt, L., Crawford, B. and Kjarsgaard, B.A. 2008. Geochemical trends in kimberlites of the Ekati property, Northwest Territories, Canada: insights on volcanic and resedimentation processes. *Journal of Volcanology and Geothermal Research*, 174, 117–127.
- Phillips, D., Machin, K.J., Kiviets, G.B., Fourie, L.F., Roberts, M.A. and Skinner, E.M.W. 1998. A petrographic and $^{40}\text{Ar}/^{39}\text{Ar}$ geochronological study of the Voorspoed kimberlite, South Africa: Implications for Group II kimberlite magmatism. *South African Journal of Geology*, 101, 299-306.
- Phillips, D., Kiviets, G.B., Barton, E.S., Smith, C.B., Viljoen, K.S. and Fourie, L.F. 1999. $^{40}\text{Ar}/^{39}\text{Ar}$ dating of kimberlites and related rocks: problems and solutions. Proceedings of the 7th International Kimberlite Conference, 2, 677-687.
- Partridge, T. C. and Maud, R. R. 1987. Geomorphic evolution of southern Africa since the Mesozoic. *South African Journal of Geology*, 90, 179-208.

- Pittari, A., Cas, R.A.F., Lefebvre, N., Robey, J., Kurszlaukis, S. and Webb, K. 2008. Eruption processes and facies architecture of the Orion Central kimberlite volcanic complex, Fort à la Corne, Saskatchewan; kimberlite mass flow deposits in a sedimentary basin. *Journal of Volcanology and Geothermal Research*, 174, 152–170.
- Porritt, L.A., Cas, R.A.F. and Crawford, B.B. 2008. In-vent column collapse as an alternative model for massive volcanoclastic kimberlite emplacement: an example from the Fox Kimberlite, Ekati Diamond Mine, NWT, Canada. *Journal of Volcanology and Geothermal Research*, 174 (1–3), 90–102.
- Reczko, B. F. F., Oberholzer, J. D., Res, M., Eriksson, P. G. and Schreiber, U. M. 1995. A re-evaluation of the volcanism of the early Proterozoic Pretoria Group (Kaapvaal Craton), and a hypothesis on basin development. *Journal of African Earth Science*, 21, 505-519.
- Rice, A. 1999. Can the blasting excavation engineering sciences provide insight into the processes of kimberlite emplacement and eruption? In: Gurney, et al. (Eds.), *Proceedings of the 7th International Kimberlite Conference*, 2, 699–708.
- Roberts, M.A. 1997. The geology of the Voorspoed kimberlite and its xenoliths. BSc Honours thesis (unpubl.), Rhodes University, South Africa, 105pp.
- Scott Smith, B.H. 2008(a). Canadian kimberlites: geological characteristics relevant to emplacement. *Journal of Volcanology and Geothermal Research*, 174, 9–19.
- Scott Smith, B.H. 2008(b). The Fort à la Corne kimberlites, Saskatchewan, Canada: Geology, emplacement and economics. *Journal of the Geological Society of India*, 71, 11–55.
- Scott Smith, B. H., Nowicki, T. E., Russell, J. K., Webb, K. J., Hetman, C. M., Harder, M. and Mitchell, R. H. 2008. Kimberlites: Descriptive Geological Nomenclature and Classification. 9th International Kimberlite Conference Extended Abstract No. 9IKC-A-00124.
- Seghedi, I., Maicher, D. and Kurzlauskis, S. 2009. Volcanology of the Tuzo pipe (Gahcho Kue cluster) - Root diatreme processes re-interpreted. *Lithos*, doi:10.1016/j.lithos.2009.04.027.
- Sheppard, S.M.F. and Dawson, J.B. 1975. Hydrogen, carbon and oxygen isotope studies of megacryst and matrix minerals from Lesothan and South African kimberlites. *Physics and Chemistry of the Earth* 9, 747–763.
- Skinner, E.M.W. and Clement, C.R. 1979. Mineralogical classification of southern African kimberlites. In: Boyd, F.R., Meyer, H.O.A. (Eds.), *Proceedings of 2nd International Kimberlite Conference*, Washington D.C. AGU, 129–139.
- Skinner, E.M.W. 1989. Contrasting Group 1 and Group 2 kimberlite petrology: towards a genetic model of kimberlites. In: Ross, J., Jaques, A.L., Ferguson, J., Green, D.H., O'Reilly, S.Y., Danchin, R.V., Janse, A.J.A. (Eds.), *Kimberlites and Related Rocks*, vol. 14. Geological Society of Australia, Sydney, 528–544.
- Skinner, E. M. W., Viljoen, K. S., Clark, T. C. and Smith, C. B. 1994 The petrography, tectonic setting and emplacement ages of kimberlites in the south western border region of the Kaapvaal craton, Prieska area. In Meyer and Leonardos. Vol. 1, 80-97.

- Skinner, E.M.W., Mahotkin, I.L. and Grutter, H.S. 1999. Melilite in Kimberlites. Proceedings of the 7th International Kimberlite Conference, 1, 788-794.
- Skinner, E.M.W., Apter, D.B., Morelli, C. and Smithson, N.K. 2004. Kimberlites of the Man craton, West Africa. *Lithos* 76 (1-4), 233-259.
- Skinner, E.M.W. and Marsh, J.S. 2004. Distinct kimberlite pipe classes with contrasting eruption processes. *Lithos*, 76, 183-200.
- Skinner, E.M.W. 2008. The emplacement of Class 1 kimberlite. *Journal of Volcanology and Geothermal Research*, 174, 40-48.
- Skinner, E. M. W. 2009. Developments in kimberlite emplacement theory. *The South African Institute of Mining and Metallurgy. Diamonds-Source to Use 2009*. In press.
- Smith, C.B., Gurney, J.J., Skinner, E.M.W., Clement, C.R. and Ebrahim, N. 1985. Geochemical character of southern African kimberlite: a new approach based on isotopic constraints. *Transactions Geological Society of South Africa*, 88, 267-280.
- Smith, R.M.H., Eriksson, P.G. and Botha, W.J. 1993. A review of the stratigraphy and sedimentary environments of the Karoo-aged basins of Southern Africa. *Journal of African Earth Science*, 16, 143-169.
- Smith, R.M.H. 1990. A review of the stratigraphy and sedimentary environments of the Karoo basin of South Africa. *Journal of African Earth Science*, 10, 117-137.
- Sparks, R.S.J., Baker, L., Brown, R.J., Field, M., Schumacher, J., Stripp, G. and Walters, A. 2006. Dynamical constraints on kimberlite volcanism. *Journal of Volcanology and Geothermal Research*, 155, 18-48.
- Stasiuk, L.D., Lockhart, G.D. and Nassichuk, W.W. 1999. Thermal maturity evaluation of dispersed organic matter inclusions from kimberlite pipes, Lac de Gras, Northwest Territories, Canada. *International Journal of Coal Geology* 40, 1-25.
- Stiefenhofer, J. and Farrow, D.J. 2004. Geology of the Mwadui kimberlite, Shinyanga district, Tanzania. *Lithos*, 76, 139-160.
- Stripp, G., Field, M., Schumacher, J., Sparks, R. and Cressey, G. 2006. Post-emplacement serpentinization and related hydrothermal metamorphism in a kimberlite from Venetia, South Africa. *Journal of Metamorphic Geology*, 24 (6), 515-534.
- Tavener-Smith, R. and Cooper, J.A.G. 1988. Depositional environments in the Volksrust Formation (Permian) in the Mhlatuze River, Zululand. *South African Journal of Geology*, 91, 198-206.
- Torab, F.M. and Lehmann, B. 2007. Magnetite-apatite deposits of the Bafq district, Central Iran: apatite geochemistry and monazite geochronology. *Mineralogical Magazine*, 71, 347-363.
- Van der Westhuizen, W. A., de Bruijn, H. and Meintjies, P. G. 2006. The Ventersdorp Supergroup. In: Johnson, M. R., Anhaeusser, C.R. and Thomas, R. J. (Ed.) *The Geology of South Africa*. Geological Society of South Africa, Johannesburg/Council for Geoscience, Pretoria, 187-208.
- Wagner, P.A. 1914. *The Diamond Fields of South Africa*. Transvaal Leader, Johannesburg.

- Walters, A.L., Phillips, J.C., Brown, R.J., Field, M., Gernon, T., Stripp, G. and Sparks, R.S.J. 2006. The role of fluidisation in the formation of volcanoclastic kimberlite: grain size observations and experimental investigation. *Journal of Volcanology and Geothermal Research*, 155, 119–137.
- Webb, K.J., Scott Smith, B.H., Paul, J.L. and Hetman, C.M. 2004. Geology of the Victor kimberlite, Attawapiskat, Northern Ontario, Canada: Cross-cutting and nested craters. Proceedings of the 8th International Kimberlite Conference. *Lithos*, 76, 29–50.
- Wilson L. and Head, J.W. 2007. An integrated model of kimberlite ascent and eruption. *Nature*, 447, 53-57.
- Winter, H. and Venter, J. J. 1970. Lithostratigraphic correlations of recent deep boreholes in the Karoo-Cape sequence. In: Haughton, S. H. (ed). Proceedings 2nd IUGS symposium on Gondwana Stratigraphy and Palaeontology. CSIR, Pretoria, 395-408.
- Winter, J.D. 2001. An introduction to Igneous and Metamorphic Petrology. Prentice Hall. 697pp.
- Wilson, M., R., Kjarsgaard, B., A. and Taylor, B. 2007. Stable isotope composition of magmatic and deuteric carbonate phases in the hypabyssal kimberlite, Lac de Gras field, Northwest Territories, Canada. *Chemical Geology*, 242, 435-454.
- Wyllie, P.J. 1987. Transfer of subcratonic carbon into kimberlites and rare earth carbonatites. In: Mysen, B.O. (Ed.), Magmatic processes: Physiochem. Principles. Special Publication of the Geochemistry Society, 1, 107–119.

Appendix 1. Major and Minor element geochemistry for the Lace Kimberlite. Samples K2-1 to K2-C are HK/HKt dump samples. Samples 713-338 are samples taken from the in situ core. Sample numbers 713-338 are the depths at which the pipe was sampled. Tex. in column 2 is an abbreviation for textural variety of kimberlite. See appendix 8 for a full list of samples collected in this study.

Sample No.	Tex.	SiO ₂	TiO ₂	Al ₂ O ₃	FeO	MnO	MgO	CaO	Na ₂ O	K ₂ O	P ₂ O ₅	LOI	Tot	CI
713	HKt	39.00	1.52	4.58	8.50	0.17	20.27	9.14	0.16	4.37	0.78	10.18	98.71	1.50
706	HKt	40.37	1.34	5.11	8.56	0.19	21.03	8.73	0.59	3.94	0.93	7.91	98.75	1.59
689	HKt	38.72	1.30	5.46	8.26	0.19	21.33	8.56	0.53	2.96	0.81	10.30	98.47	1.63
630	HKtB	39.84	1.22	6.89	8.20	0.15	20.89	7.26	0.70	3.19	0.79	8.48	97.66	1.73
626	HKtB	37.86	1.28	4.48	8.32	0.21	20.92	8.10	0.49	3.42	1.06	9.46	95.89	1.54
616	HKt	43.86	1.29	4.96	8.36	0.16	20.51	7.84	0.91	3.46	0.70	5.88	98.00	1.81
614	HKt	40.00	1.35	4.03	7.52	0.16	20.19	9.16	0.22	3.62	0.81	10.96	98.08	1.61
607	HKtB	30.30	0.86	3.98	5.13	0.37	11.63	21.90	0.64	1.20	0.51	21.47	98.09	2.49
599	HKtB	46.43	0.67	6.66	6.42	0.16	17.62	7.52	0.99	1.43	0.33	10.51	98.79	2.63
552	HKtB	24.94	0.57	4.71	4.04	0.41	6.62	28.27	0.11	0.85	0.30	26.97	97.83	3.57
540	HKtB	28.21	1.33	5.67	5.65	0.32	9.11	23.12	0.10	1.38	0.62	21.90	97.46	2.86
375	HKtB	24.46	1.35	3.85	7.37	0.35	12.81	22.07	0.41	0.99	0.90	21.61	96.20	1.94
338	HKtB	35.85	1.36	3.96	8.58	0.17	21.92	7.68	0.18	4.00	0.87	11.59	96.21	1.33
K2-1	HK	35.04	1.34	3.36	8.28	0.15	25.95	7.52	0.02	4.05	0.52	11.68	97.92	1.12
K2-2	HKt	33.47	1.37	3.02	8.34	0.16	23.16	9.93	0.07	4.32	0.98	13.96	98.79	1.14
K2-3	HKt	36.46	1.50	3.05	8.43	0.23	21.40	9.11	0.15	5.28	0.90	11.39	97.86	1.24
K2-4	HKt	35.63	1.38	3.13	8.43	0.22	22.35	8.42	0.12	4.62	0.77	12.29	97.35	1.23
K2-5	HKt	36.68	1.45	3.11	8.45	0.22	22.08	8.53	0.12	4.89	0.95	11.67	98.14	1.22
K2-6	HKt	35.53	1.28	2.88	8.12	0.20	24.44	8.20	0.10	3.78	0.74	12.90	98.19	1.20
K2-7	HKt	32.76	1.22	2.55	8.17	0.21	20.45	8.32	0.10	3.67	0.70	12.40	90.64	1.27
K2-C	HKt	34.90	1.18	3.11	8.00	0.19	27.74	7.12	nd	4.02	0.35	11.78	98.39	1.06

Appendix 2. Trace element geochemistry for the Lace kimberlite. See appendix 1 for sample number explanation.

Sample No.	Mo	Nb	Zr	Y	Sr	U	Rb	Th	Pb	Ce	Nd	La	Co	Cr	V
713	1.3	108.5	343.6	18	1158.3	3.2	191.9	19.9	12	245.6	99.3	135.5	77.6	1419.5	103.9
706	0.6	98	277.7	19.4	1449.9	3.3	159.6	17.6	20.9	236.8	96	127.4	61.5	1285.7	338.8
689	1.2	92.9	265.7	19.7	947.7	3.6	118.7	15.1	14.5	223.9	92.4	119.8	57.9	1129.8	162.2
630	0.9	88.5	264.3	20.1	1135.4	4.9	125.2	18.2	22.9	228.3	92.6	123.3	59.1	1039.2	167.9
626	0.5	100.7	285.7	22.5	1416	4.2	143.5	15.8	25	232.2	94.5	124.9	61.3	1235.6	143.2
616	1.1	90.7	280.7	20.3	1296	2.3	146.8	17.2	26.4	226.8	92	121.3	61.6	1152.3	154.1
614	1.4	95.7	246.5	15.5	1168.4	4.9	155.4	19.8	13.2	270.3	110	148.3	82.2	1420.4	126.9
607	1.2	56.1	148.7	13.2	498	2.5	44.4	13.3	17	151.5	63.9	79.3	52.2	785.6	107.7
599	1.7	36.1	135	14.1	386.7	0.8	51	11	19.6	85	35.9	44.1	31.8	447.6	92.8
552	2	31.4	122.6	12.6	263.3	1.9	33.4	9.7	12	98.3	42.4	50.5	36.4	404.2	72.6
540	1.8	77.7	200.6	17.2	332.2	2.4	61.3	15.5	15.1	195.7	80.3	104.5	67.2	1105.3	110.2
375	1.7	102.6	256.2	24.3	1401	3.9	47.1	16.9	28.2	237.7	98.6	132	108.3	1543.6	194.3
338	0.3	108.1	254.8	19.9	904.5	4.9	163.5	13.8	19.2	271	112.2	147.5	76.2	1354.8	133.9
	Mo	Nb	Zr	Y	Sr	U	Rb	Th	Pb		Zn	Cu	Ni		
K2-1	1.7	94.9	301.9	15.1	1042.8	2.3	172.5	20.8	-0.3		74.4	22.8	1406		
K2-2	1	125.6	291.2	14.7	1670.3	2.4	182.1	22.6	17.2		74.7	50.8	1114.1		
K2-3	2	118	366.2	17.1	1424	5.4	198.9	23.5	16.8		72.9	38.3	1177.3		
K2-4	0.7	120.9	269.9	16.1	1725.3	3.3	178.7	23.1	17.9		73.9	38.3	1259.9		
K2-5	1	120.8	308.5	17.1	1598.8	5.4	188.2	21.8	16.6		73.4	43.2	1268.5		
K2-6	1.6	116.4	300.9	15.3	1542.1	5.3	141.1	22.3	16.9		68.1	36.6	1299.6		
K2-7	1.2	115	295.2	15	1495.5	4.3	151.5	22.3	16.6		70	36.9	1360.1		
K2-C	1	89	252.2	14.9	1443.8	3.2	155.9	19.7	2.9		67.6	20.4	1238.5		

Appendix 3. Mineral Chemistry

Appendix 3a. Compositional data for Aegirine analysed for sample K1/114 from Voorspoed.

Analysis #	SiO ₂	TiO ₂	Al ₂ O ₃	Fe ₂ O ₃	FeO	MgO	CaO	Na ₂ O	Total
194	53.64	4.05	0.01	17.45	4.92	4.51	6.50	9.92	101.00
196	53.01	2.24	0.09	16.48	4.65	5.52	9.64	8.08	99.71
199	52.24	2.42	0.01	18.56	5.24	3.85	6.84	9.59	98.75
201	53.37	4.45	0.11	17.35	4.89	3.53	5.19	10.70	99.59
208	52.70	3.90	0.28	19.36	5.46	2.80	3.54	11.53	99.57
210	53.56	3.56	0.11	19.27	5.44	3.44	5.21	11.04	101.63
211	52.57	4.45	0.14	16.79	4.73	4.06	5.95	10.20	98.89
232	52.86	1.80	0.10	15.83	4.46	5.84	10.13	8.08	99.10
236	53.56	3.80	0.12	19.45	5.49	2.87	4.03	11.55	100.87
245	52.84	2.31	0.10	15.79	4.45	5.91	9.32	8.68	99.40

Appendix 3a. Aegirine structural formula on the basis of four cations and six oxygens

Analysis	194	196	199	201	208	210	211	232	236	245
Si	2.010	2.014	2.018	2.027	2.017	2.011	2.012	2.019	2.024	2.012
Fe ³⁺	0.441	0.423	0.484	0.445	0.500	0.489	0.434	0.408	0.496	0.406
Mg	0.252	0.312	0.222	0.200	0.160	0.192	0.231	0.332	0.162	0.336
Fe ²⁺	0.210	0.201	0.231	0.212	0.238	0.233	0.207	0.194	0.236	0.193
Ti	0.114	0.064	0.070	0.127	0.112	0.101	0.128	0.052	0.108	0.066
Al	0.004	0.004	0.001	0.005	0.012	0.005	0.006	0.004	0.005	0.004
Na	0.720	0.595	0.718	0.788	0.856	0.804	0.757	0.598	0.846	0.641
Ca	0.261	0.392	0.283	0.211	0.145	0.209	0.244	0.414	0.163	0.380

Appendix 3b. Compositional data for Diopside analysed from sample K1/114 from Voorspoed.

Analysis #:	SiO ₂	TiO ₂	Al ₂ O ₃	FeO	MgO	CaO	Na ₂ O	K ₂ O	Total
189	54.09	0.53	0.20	5.22	15.17	23.44	0.78	0.00	99.42
192	54.91	0.64	0.15	3.36	16.67	24.17	0.24	0.05	100.19
193	54.14	0.27	0.13	11.32	11.53	18.64	2.96	0.00	98.98
195	55.41	0.45	0.22	4.52	15.72	23.56	0.43	0.02	100.33
197	54.45	0.84	0.55	2.87	16.47	23.95	0.24	0.00	99.38
202	54.95	0.49	0.33	3.08	16.02	23.92	0.09	0.04	98.91
204	54.61	0.54	0.37	3.17	16.28	24.05	0.18	0.02	99.22
205	54.59	0.67	0.24	3.12	16.94	24.33	0.13	0.02	100.04
206	54.56	0.60	0.30	2.99	16.72	23.91	0.30	0.00	99.37
207	53.58	0.77	0.58	3.27	16.24	23.74	0.23	0.00	98.40
219	55.15	0.48	0.20	3.16	16.63	23.95	0.13	0.01	99.72
221	53.60	0.63	0.20	3.07	17.08	24.04	0.14	0.00	98.73
224	54.74	0.71	0.38	3.04	16.47	23.39	0.11	0.01	98.84
226	55.08	0.63	0.32	3.28	16.76	23.95	0.24	0.03	100.29
229	54.75	0.60	0.18	3.14	16.38	23.96	0.19	0.00	99.21
231	55.22	0.69	0.28	3.01	16.59	23.98	0.23	0.00	100.00
237	55.09	0.33	0.25	3.30	16.47	23.85	0.22	0.00	99.51
238	55.24	0.46	0.24	2.96	16.30	23.97	0.22	0.03	99.42
244	54.37	0.76	0.37	3.11	15.86	23.76	0.07	0.00	98.30
246	55.25	0.51	0.19	3.01	16.78	23.97	0.26	0.00	99.98
247	55.53	0.68	0.21	3.09	16.64	23.64	0.20	0.00	99.98
248	54.84	0.68	0.24	3.83	16.26	23.56	0.23	0.00	99.65
250	54.75	0.65	0.31	2.99	16.29	23.84	0.09	0.00	98.92

Appendix 3b. Structural formula on the basis of four cations and six oxygens

Analysis #:	Si	Ti	Al	Fe2+	Mg	Ca	Na	K
189	2.00	0.01	0.01	0.16	0.84	0.93	0.06	0.00
192	2.00	0.02	0.01	0.10	0.90	0.94	0.02	0.00
193	2.05	0.01	0.01	0.36	0.65	0.76	0.22	0.00
195	2.02	0.01	0.01	0.14	0.85	0.92	0.03	0.00
197	1.99	0.02	0.02	0.09	0.90	0.94	0.02	0.00
202	2.02	0.01	0.01	0.09	0.88	0.94	0.01	0.00
204	2.00	0.01	0.02	0.10	0.89	0.95	0.01	0.00
205	1.99	0.02	0.01	0.10	0.92	0.95	0.01	0.00
206	2.00	0.02	0.01	0.09	0.91	0.94	0.02	0.00
207	1.99	0.02	0.03	0.10	0.90	0.94	0.02	0.00
219	2.01	0.01	0.01	0.10	0.90	0.94	0.01	0.00
221	1.98	0.02	0.01	0.09	0.94	0.95	0.01	0.00
224	2.01	0.02	0.02	0.09	0.90	0.92	0.01	0.00
226	2.00	0.02	0.01	0.10	0.91	0.93	0.02	0.00
229	2.01	0.02	0.01	0.10	0.90	0.94	0.01	0.00
231	2.01	0.02	0.01	0.09	0.90	0.93	0.02	0.00
237	2.01	0.01	0.01	0.10	0.90	0.93	0.02	0.00
238	2.02	0.01	0.01	0.09	0.89	0.94	0.02	0.00
244	2.01	0.02	0.02	0.10	0.87	0.94	0.01	0.00
246	2.01	0.01	0.01	0.09	0.91	0.93	0.02	0.00
247	2.01	0.02	0.01	0.09	0.90	0.92	0.01	0.00
248	2.01	0.02	0.01	0.12	0.89	0.92	0.02	0.00
250	2.01	0.02	0.01	0.09	0.89	0.94	0.01	0.00

Appendix 3c. Compositional data for phlogopite analysed from sample K1/114 from Voorspoed.

Sample	SiO ₂	TiO ₂	Al ₂ O ₃	FeO	MgO	CaO	Na ₂ O	K ₂ O	SUM	H ₂ O
191	40.56	1.98	11.19	6.52	22.75	0.08	0.14	8.09	99.40	8.10
198	39.74	2.73	11.24	8.73	21.88	0.18	0.16	9.14	101.96	8.15
209	42.02	2.97	11.30	5.58	21.84	0.05	0.32	9.82	102.22	8.31
213	39.65	2.77	11.38	7.99	22.61	0.03	0.22	8.68	101.50	8.17
214	38.96	2.52	11.93	4.84	21.42	0.05	0.15	9.70	97.48	7.91
215	41.00	3.07	12.04	5.34	19.58	0.01	0.19	9.05	98.33	8.04
216	36.66	2.27	12.37	9.09	22.34	0.17	0.16	3.83	94.64	7.76
217	40.96	2.26	11.82	5.60	23.41	0.06	0.16	10.01	102.59	8.31
218	39.15	2.86	11.75	9.27	21.51	0.06	0.13	7.66	100.49	8.08
220	41.84	2.45	12.16	4.95	22.20	0.07	0.16	9.78	101.94	8.32
222	40.21	2.47	12.09	5.05	21.22	0.10	0.04	9.30	98.50	8.04
223	41.30	2.76	11.98	5.32	21.44	0.01	0.19	9.89	101.09	8.22
227	41.40	2.19	11.54	5.60	23.09	0.08	0.08	9.80	102.08	8.29
228	42.11	3.15	11.91	5.67	21.08	0.07	0.21	9.84	102.38	8.33
230	40.12	2.26	12.24	5.18	22.37	0.07	0.18	9.62	100.18	8.14
234	40.71	1.90	12.39	5.66	22.22	0.02	0.17	10.05	101.32	8.21
235	40.56	2.39	12.35	5.10	21.47	0.02	0.09	9.68	99.79	8.13
240	41.93	2.98	12.07	5.20	21.63	0.03	0.13	9.57	101.86	8.32
241	41.39	2.92	12.17	5.38	22.18	0.06	0.18	9.55	102.15	8.32
242	41.06	2.05	11.48	5.48	20.83	0.00	0.10	9.24	98.26	8.02
243	41.06	1.81	11.84	5.00	20.93	0.01	0.12	9.23	98.03	8.02
251	40.13	2.64	11.79	7.33	22.25	0.06	0.27	9.39	102.07	8.21

Appendix 3c. Structural formula based on 22 oxygens

Sample	Si	Ti	Al	Fe	Mg	Ca	Na	K
191	6.00	0.22	1.95	0.81	5.02	0.01	0.04	1.53
198	5.85	0.30	1.95	1.07	4.80	0.03	0.05	1.72
209	6.07	0.32	1.92	0.67	4.70	0.01	0.09	1.81
213	5.82	0.31	1.97	0.98	4.95	0.00	0.06	1.63
214	5.90	0.29	2.13	0.61	4.84	0.01	0.04	1.88
215	6.11	0.34	2.12	0.67	4.35	0.00	0.06	1.73
216	5.67	0.26	2.25	1.18	5.15	0.03	0.05	0.76
217	5.91	0.24	2.01	0.68	5.04	0.01	0.05	1.85
218	5.81	0.32	2.06	1.15	4.76	0.01	0.04	1.45
220	6.03	0.27	2.07	0.60	4.77	0.01	0.05	1.80
222	6.00	0.28	2.13	0.63	4.72	0.02	0.01	1.77
223	6.02	0.30	2.06	0.65	4.66	0.00	0.05	1.84
227	5.99	0.24	1.97	0.68	4.98	0.01	0.02	1.81
228	6.06	0.34	2.02	0.68	4.52	0.01	0.06	1.81
230	5.91	0.25	2.12	0.64	4.91	0.01	0.05	1.81
234	5.95	0.21	2.13	0.69	4.84	0.00	0.05	1.88
235	5.98	0.26	2.15	0.63	4.72	0.00	0.03	1.83
240	6.05	0.32	2.05	0.63	4.65	0.01	0.04	1.76
241	5.97	0.32	2.07	0.65	4.77	0.01	0.05	1.76
242	6.14	0.23	2.02	0.69	4.64	0.00	0.03	1.77
243	6.14	0.20	2.09	0.62	4.66	0.00	0.03	1.76
251	5.86	0.29	2.03	0.90	4.84	0.01	0.08	1.75

Appendix 3d. Mineral chemistry for the Lace kimberlite microlitic clinopyroxene from the HKt (Sample K2-5) and HKtB (Sample C7-713).

Analysis number 698-714 are for the HKtB. Analysis number 719-734 are for the HKt.

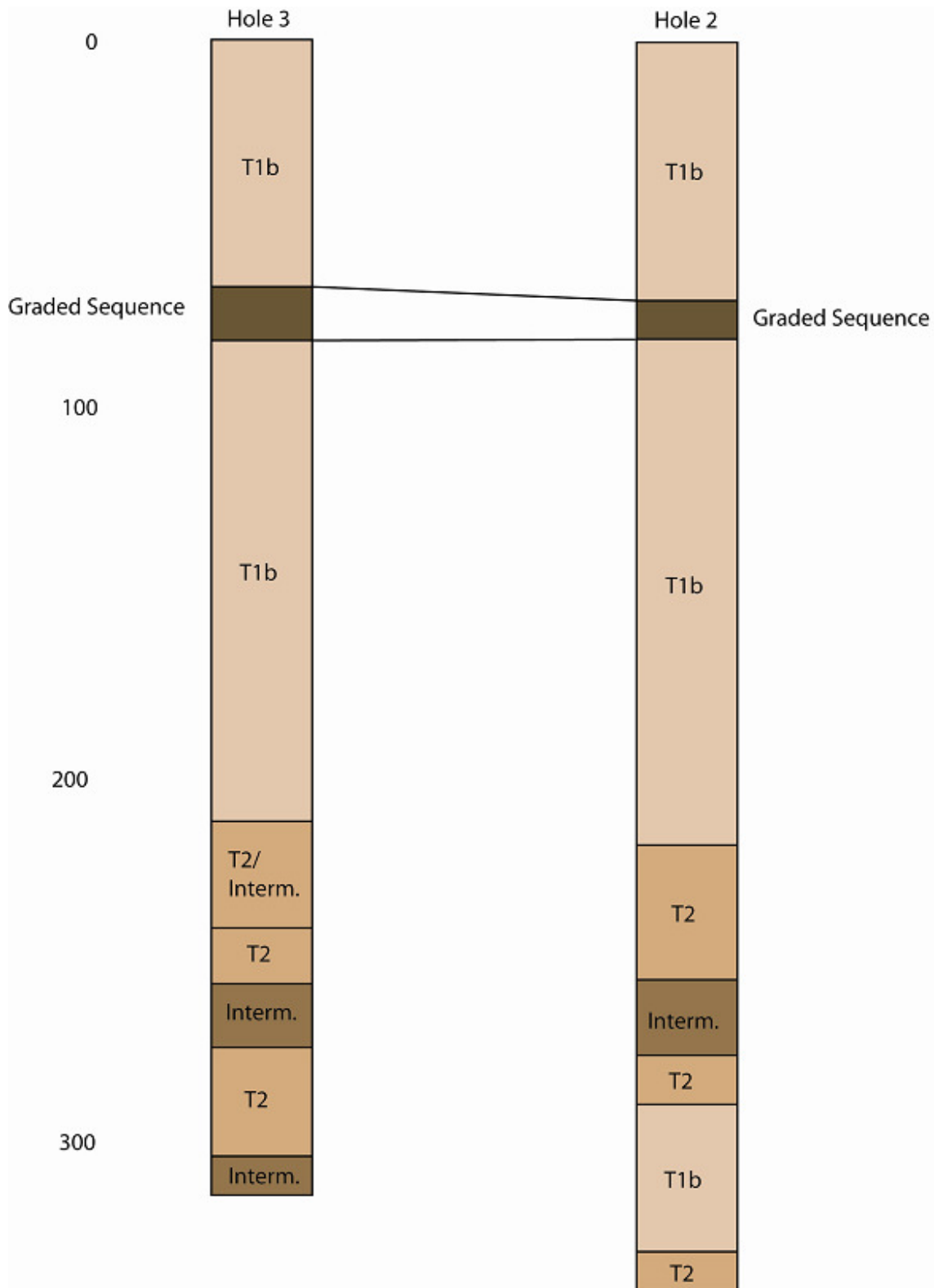
Analysis #	SiO ₂	TiO ₂	Al ₂ O ₃	FeO	MgO	CaO	Na ₂ O	Cr ₂ O ₃	MnO	Total
698 / 1 .	49.66	2.68	0.28	5.45	15.97	22.80	1.03	0.19	0.11	98.35
709 / 1 .	52.83	1.02	0.29	5.21	14.90	24.48	0.61	0.07	0.11	99.51
710 / 1 .	51.82	0.60	0.36	3.84	16.11	23.02	0.58	0.27	0.07	96.92
711 / 1 .	50.77	1.89	0.29	5.71	14.23	23.62	0.93	0.14	0.16	97.86
713 / 1 .	52.18	1.07	0.23	4.06	15.73	24.41	0.57	0.13	0.12	98.62
714 / 1 .	51.75	1.27	0.19	4.71	14.97	24.57	0.75	0.27	0.16	98.70
719 / 1 .	52.68	0.94	0.07	3.90	15.75	25.04	0.47	0.05	0.10	99.13
720 / 1 .	51.45	1.63	0.40	5.16	14.78	23.83	0.75	0.31	0.12	98.50
721 / 1 .	50.86	1.48	0.51	5.17	16.60	20.55	0.68	0.31	0.09	96.47
722 / 1 .	51.27	1.23	0.23	4.52	15.40	24.74	0.64	0.07	0.13	98.35
723 / 1 .	52.13	1.36	0.17	4.65	15.19	24.11	0.81	0.03	0.11	98.65
724 / 1 .	51.08	2.01	0.29	5.32	14.81	23.68	0.77	0.08	0.13	98.20
725 / 1 .	51.31	2.34	0.30	5.28	14.47	24.13	0.77	0.10	0.15	98.91
726 / 1 .	50.70	1.84	0.42	5.83	14.68	24.11	0.80	0.08	0.13	98.67
727 / 1 .	51.51	2.92	0.08	5.90	14.10	23.75	0.99	0.10	0.16	99.53
728 / 1 .	51.93	1.36	0.25	3.80	15.71	25.01	0.52	0.14	0.07	98.85
729 / 1 .	51.27	2.32	0.19	5.38	14.64	24.08	0.80	0.09	0.14	98.92
730 / 1 .	50.97	1.07	0.25	5.03	14.81	25.18	0.73	0.01	0.17	98.27
732 / 1 .	49.76	2.52	0.26	6.64	14.44	23.31	0.94	0.08	0.17	98.16
734 / 1 .	51.45	1.46	0.32	4.46	15.28	24.77	0.68	0.14	0.11	98.81

Appendix 4. Voorspoed Borehole logs

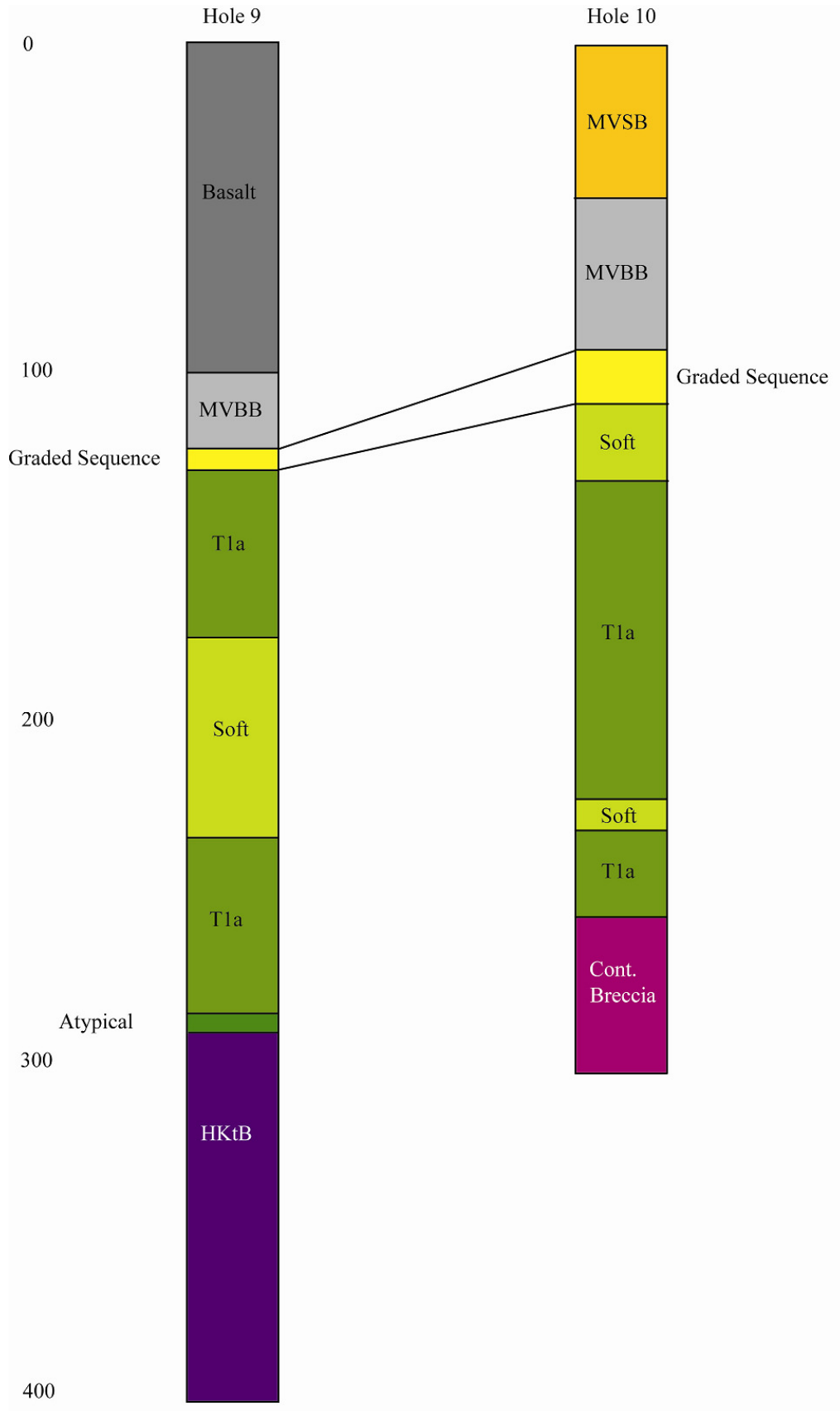
Appendix 4a. Criteria used during borehole logging of the Voorspoed Core. Characteristic features are highlighted.

	Colour	Relative Hardness	Mg.Clast Proportion	Xenolith Proportion	Xenolith Type	Average Grain Size	Sorting
T1a MVK	Brown – light brown		Rare visible mg. Clasts	High	Basalt dominated	Xenoliths: <10cm Mg.Clasts: <1cm	None
s MVK	Brown	Soft – pitted	Rare-moderate proportions of visible mg. Clasts	High	Basalt dominated	Xenoliths: <10cm Mg.Clasts: <1.5cm	None
a MVK	Dark Charcoal		Moderate – abundant visible mg. Clasts	Moderate – High	Sedimentary xenoliths dominate, basalt present	Xenoliths: <10cm Mg.Clasts: <1.5cm	None
T1b MVK	Brown – light brown		Rare visible mg.clasts	High	Basalt dominated	Xenoliths: <8cm Mg.Clasts: <1cm	None
T2 MVK	Tan - Grey		Abundant large mg. Clasts	Low – Moderate	Basalt dominated, common highly altered carbonate xenoliths	Xenoliths: <10cm Mg.Clasts: <15cm (olivine macrocrysts common)	None
int. MVK	Tan – Grey		Moderate – abundant visible mg. Clasts	Moderate – High	Basalt dominated	Xenoliths: <5cm Mg.Clasts: <1cm	Rare normal graded beds
BVK	Brown – light brown		Moderate proportions of visible mg. Clasts in coarse base	Moderate – High	Basalt and sedimentary dominated	Varies due to sorting: 6cm at base to <0.5cm at top	Normal graded beds characteristic
MVBB	Brown		Absent	Very High	Basalt dominated	Xenoliths: <15cm	None
MVSB	Light Brown		Absent	Very High	Sandstone dominated, basalt also present	Xenoliths: <15cm	None
HKtB	Brown		Globular structures rare to moderate in proportion	Moderate – High	Shale dominated – No basalt	Xenoliths: <10cm Globules: <2cm	None

Appendix 4b. Borehole logs for the CEZ boreholes 3 and 2. Depth given in meters from the current land surface. Hole 2 was drilled at 90° and hole 3 at 77°. Refer to figure 3.12 for the location of the boreholes within the Voorspoed pipe.



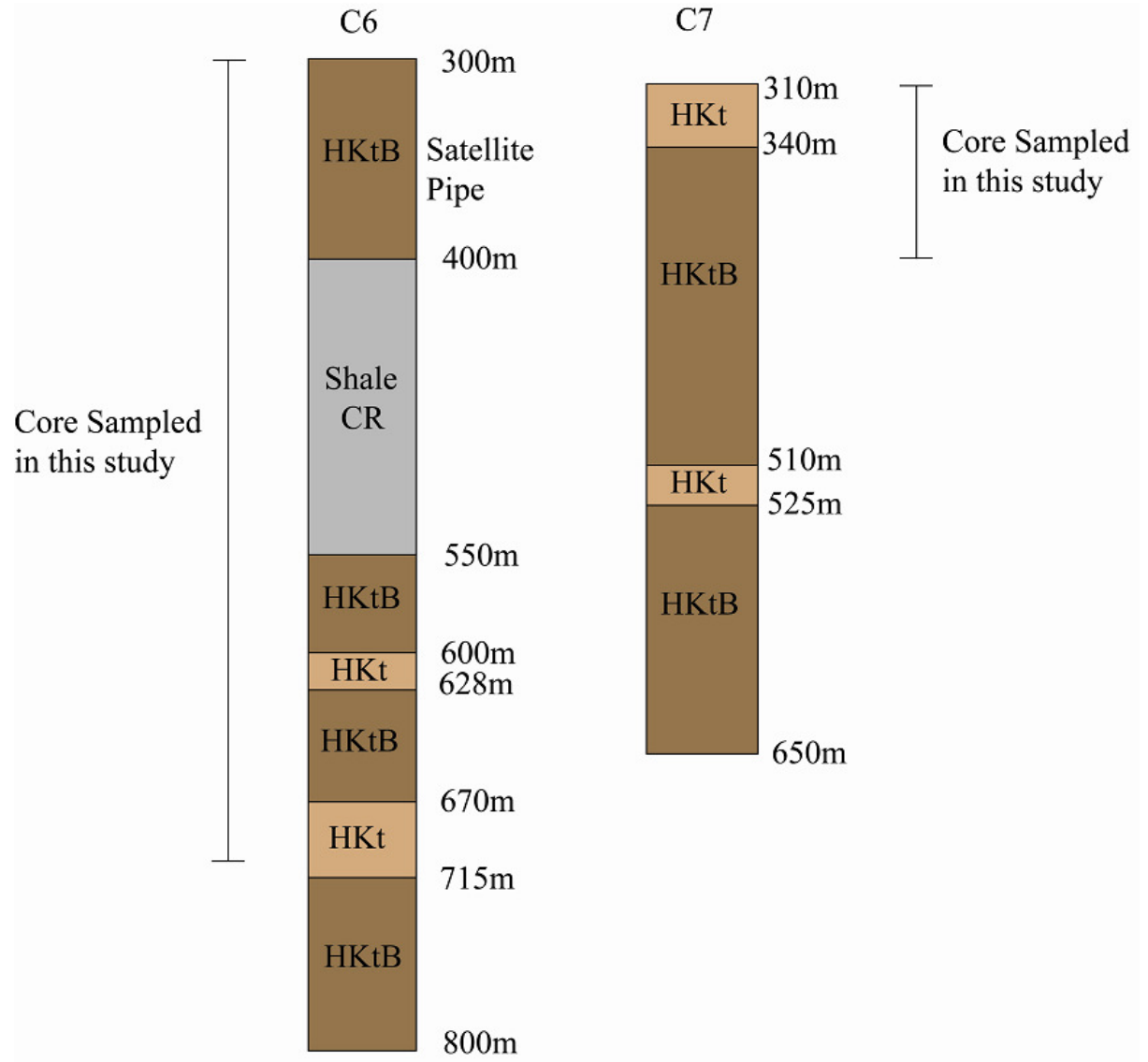
Appendix 4c. Borehole logs for the IEZ boreholes 9 and 10. Depth given in meters from the current land surface. Hole 9 was drilled at 85° and hole 10 at 90°.



Appendix 5. Correlation of Voorspoed Volcaniclastic kimberlite nomenclature from an internal De Beers report by Roger Clement in 1980; the current VK nomenclature used at the Voorspoed mine and the nomenclature used in this study. Note that the volcaniclastic kimberlite at Voorspoed has been misidentified as tuffisitic kimberlite breccia in the past; the phlogopite-rich TKB is not a fragmental rock; the granodiorite in the so called granodiorite-rich TKB is not granodiorite but rather coarse grained dolerite. (TKB: tuffisitic kimberlite breccia, MVK: massive volcaniclastic kimberlite, MVBB: massive volcaniclastic basalt breccia, MVSb: massive volcaniclastic sandstone breccia, HKt: hypabyssal transitional kimberlite).

This Study	Clement Int. Rep.	Current Mine Units
T1aMVK	Type 1	TKB; DarkTKB; Basalt-rich TKB; Granodiorite-rich TKB
T1bMVK	Type 1	
T2MVK	Type 2	Autolith-rich TKB
Intermediate MVK	Type 1	Transitional TKB
Soft MVK	Type 3	Soft TKB
Atypical MVK	Not noted	Not noted
MVBB	Not noted	Xenolith-rich TKB
MVSb	Not noted	Xenolith-rich TKB
BVK	Not noted	Not noted
HKt	Not noted	Phlogopite-rich TKB

Appendix 6. Borehole logs of the Lace kimberlite core sampled. (HKt – Hypabyssal transitional kimberlite; HKtB – Hypabyssal transitional kimberlite breccia; Shale CR – Shale country rock). See figure 3.2 for the inclination of the boreholes through the Lace pipe.



Appendix 7. Summary of Abbreviations used in the text.

Abbreviation	Long Hand Term
KKC	Kroonstad kimberlite cluster
Kimberlite Textures and related terms	
HK	Hypabyssal kimberlite
HKB	Hypabyssal kimberlite breccia
HKt	Hypabyssal transitional kimberlite
HKtB	Hypabyssal transitional kimberlite breccia
TK	Tuffisitic kimberlite
TKt	Tuffisitic transitional kimberlite
TKB	Tuffisitic kimberlite breccia
VK	Volcaniclastic kimberlite
VKB	Volcaniclastic kimberlite breccia
MVK	Massive volcaniclastic kimberlite
MVKB	Massive volcaniclastic kimberlite breccia
PK	Pyroclastic kimberlite
BVK	Bedded volcaniclastic kimberlite
RVK	Resedimented volcaniclastic kimberlite
CB	Contact breccia
CRX	Country rock xenolith
Lace Textural Rock Types	
bVK	Basalt rich volcaniclastic kimberlite
qVK	Quartz rich volcaniclastic kimberlite
Voorspoed Textural Rock Types	
T1aMVK	Type 1 a massive volcaniclastic kimberlite
sMVK	Soft massive volcaniclastic kimberlite
aMVK	Atypical massive volcaniclastic kimberlite
T1bMVK	Type 1 b massive volcaniclastic kimberlite
T2MVK	Type 2 massive volcaniclastic kimberlite
intMVK	Intermediate massive volcaniclastic kimberlite
MVBB	Massive volcaniclastic basalt breccia
MVSB	Massive volcaniclastic sandstone breccia
Voorspoed Volcaniclastic Zones	
IEZ	Initial eruption zone
CEZ	Central eruption zone

Appendix 8. Table of Samples List. Refer to appendix 6 for abbreviations used in the table. All samples collected in this study except for the Skinner collection samples labelled BH- and the 5 De Beers Collection samples listed at the end. It must be noted that 176 other samples from De Beers Collection were also analysed petrographically, however no information about their location within the pipe was available and therefore not included in this list. The Locations of the Voorspoed boreholes are given in figure 3.12 and shown in cross section in figure 3.14. The Lace boreholes are shown in figure 3.2.

Sample label	Location	Collected from:	Textural Variety	Comments
K2-1	Lace	Dump sites	Coherent HK	Collected in 2007
K2-2	Lace	Dump sites	Glob. Seg. HKt	Collected in 2007
K2-3	Lace	Dump sites	Coherent HKt	Collected in 2007
K2-4	Lace	Dump sites	Coherent HKt	Collected in 2007
K2-5	Lace	Dump sites	Coherent HKt	Collected in 2007
K2-6	Lace	Dump sites	Coherent HKt	Collected in 2007
K2-7	Lace	Dump sites	Coherent HKt	Collected in 2007
K2-8	Lace	Dump sites	Coherent HKt	Collected in 2007
K2-9	Lace	Dump sites	bVK	Collected in 2007
K2-10	Lace	Dump sites	bVK	Collected in 2007
K2-A	Lace	Dump sites	qVK	Collected in 2008
K2-B	Lace	Dump sites	qVK	Collected in 2008
K2-C	Lace	Dump sites	Coherent HKt	Collected in 2008
K2-D	Lace	Dump sites	bVK	Collected in 2008
C6-321	Lace Satellite	Borehole C6	Glob. Seg. HKtB	Satellite Pipe
C6-540	Lace	Borehole C6	Glob. Seg. HKtB	Main Pipe
C6-552	Lace	Borehole C6	Glob. Seg. HKtB	Main Pipe
C6-597	Lace	Borehole C6	Glob. Seg. HKtB	Main Pipe
C6-599	Lace	Borehole C6	Glob. Seg. HKtB	Main Pipe
C6-607	Lace	Borehole C6	Glob. Seg. HKtB	Main Pipe
C6-614	Lace	Borehole C6	Glob. Seg. HKt	Main Pipe
C6-616	Lace	Borehole C6	Glob. Seg. HKt	Main Pipe
C6-626	Lace	Borehole C6	Glob. Seg. HKt	Main Pipe
C6-629	Lace	Borehole C6	Glob. Seg. HKtB	Main Pipe
C6-630	Lace	Borehole C6	Glob. Seg. HKtB	Main Pipe
C6-642	Lace	Borehole C6	Glob. Seg. HKtB	Main Pipe
C6-689	Lace	Borehole C6	Glob Seg. HKt	Main Pipe
C6-706	Lace	Borehole C6	Glob Seg. HKt	Main Pipe
C6-713	Lace	Borehole C6	Coherent HKt	Main Pipe
C7-338	Lace	Borehole C7	Coherent HKt	Main Pipe
C7-372	Lace	Borehole C7	Glob. Seg. HKtB	Main Pipe
C7-375	Lace	Borehole C7	Coherent HKt Xenolith with HKtB	Main Pipe
2-45	Voorspoed Pipe	Borehole 2	Fine-grained VK layer	
2-123	Voorspoed Pipe	Borehole 2	T1b MVK	
2-202	Voorspoed Pipe	Borehole 2	T1b MVK	

2-262	Voorspoed Pipe	Borehole 2	T1b MVK	
2-270	Voorspoed Pipe	Borehole 2	T2 MVK	
2-280	Voorspoed Pipe	Borehole 2	Fine-grained VK layer	8cm thick
3-18	Voorspoed Pipe	Borehole 3	T1b MVK	
3-67.7	Voorspoed Pipe	Borehole 3	BVK	
3-112	Voorspoed Pipe	Borehole 3	HK internal dike	20cm thick
3-133	Voorspoed Pipe	Borehole 3	T1b MVK	
3-154	Voorspoed Pipe	Borehole 3	T1b MVK	
3-238	Voorspoed Pipe	Borehole 3	Int MVK	Graded layer
3-258	Voorspoed Pipe	Borehole 3	Int MVK	
3-311	Voorspoed Pipe	Borehole 3	Int MVK	
9-52	Voorspoed Pipe	Borehole 9	T1a MVK	Thin MVK zone within main basalt
9-95	Voorspoed Pipe	Borehole 9	T1a MVK	Thin MVK zone within main basalt
9-120	Voorspoed Pipe	Borehole 9	BVK	5m thick
9-145	Voorspoed Pipe	Borehole 9	T1a MVK	
9-168	Voorspoed Pipe	Borehole 9	T1a MVK	
9-256	Voorspoed Pipe	Borehole 9	T1a MVK	Minor sorting noted
9-288	Voorspoed Pipe	Borehole 9	a MVK	
9-296	Voorspoed Pipe	Borehole 9	Glob. Seg. HKtB	
9-338	Voorspoed Pipe	Borehole 9	Glob Seg. HKtB	
10-36	Voorspoed Pipe	Borehole 10	MVSB	
10-90	Voorspoed Pipe	Borehole 10	BVK	18m thick comprised of 4 graded beds
10-98	Voorspoed Pipe	Borehole 10	BVK	Fine grained sample
10-156	Voorspoed Pipe	Borehole 10	T1a MVK	
10-206	Voorspoed Pipe	Borehole 10	T1a MVK	
10-241	Voorspoed Pipe	Borehole 10	T1a MVK	
10-259	Voorspoed Pipe	Borehole 10	Contact Breccia	Dolerite country rock
10-277	Voorspoed Pipe	Borehole 10	Contact Breccia	Shale country rock
1-255	Voorspoed Pipe	Borehole 1	Contact Breccia	Shale country rock
BH2-55	Voorspoed Pipe	Borehole 2	T1b MVK	Skinner Collection
BH2-71	Voorspoed Pipe	Borehole 2	T1b MVK	Skinner Collection
BH2-109	Voorspoed Pipe	Borehole 2	T1b MVK	Skinner Collection
BH2-169	Voorspoed Pipe	Borehole 2	T1b MVK	Skinner Collection
BH2-219 (2/4 in text)	Voorspoed Pipe	Borehole 2	T2MVK	Skinner Collection
BH2-350	Voorspoed Pipe	Borehole 2	T1b MVK	Skinner Collection
BH3-31 (3/1 in	Voorspoed Pipe	Borehole 3	T1b MVK	Skinner

text)				Collection
BH3-169	Voorspoed Pipe	Borehole 3	T1b MVK	Skinner Collection
BH3-238 (3/3 in text)	Voorspoed Pipe	Borehole 3	T1b MVK	Skinner Collection
BH3-289	Voorspoed Pipe	Borehole 3	T2 MVK	Skinner Collection
BH4-230 (4/1, in text)	Voorspoed Pipe	Borehole 4	HK internal dike	Skinner Collection
BH5-28	Voorspoed Pipe	Borehole 5	T1b MVK	Skinner Collection
BH5-105	Voorspoed Pipe	Borehole 5	T2 MVK	Skinner Collection
BH5-249	Voorspoed Pipe	Borehole 5	T2 MVK	Skinner Collection
BH5-292	Voorspoed Pipe	Borehole 5	T1b MVK	Skinner Collection
BH5-307	Voorspoed Pipe	Borehole 5	T1b MVK	Skinner Collection
BH7-137 (7/1 in text)	Voorspoed Pipe	Borehole 7	Soft MVK	Skinner Collection
BH8-41	Voorspoed Pipe	Borehole 8	MVSB	Skinner Collection
BH8-94	Voorspoed Pipe	Borehole 8	Soft MVK	Skinner Collection
BH8-140	Voorspoed Pipe	Borehole 8	Soft MVK	Skinner Collection
BH9-216	Voorspoed Pipe	Borehole 9	T1a MVK	Skinner Collection
BH9-292 (9/2 in text)	Voorspoed Pipe	Borehole 9	Glob. Seg. HKtB	Skinner Collection
BH9-356	Voorspoed Pipe	Borehole 9	Glob. Seg. HKt	Skinner Collection
BH9-384	Voorspoed Pipe	Borehole 9	Coherent HK/HKt	Skinner Collection
BH10-36	Voorspoed Pipe	Borehole 10	MVSB	Skinner Collection
K1/110	Voorspoed Sill	Sill in country rock	Aegirine diopside phlogopite HK	De Beers Collection
K1/111	Voorspoed Sill	Sill in country rock	Aegirine diopside phlogopite HK	De Beers Collection
K1/114	Voorspoed Sill	Sill in country rock	Aegirine diopside phlogopite HK	De Beers Collection
K1/135	Voorspoed Unknown	Unknown	Melilite bearing HK	De Beers Collection
K1/151	Voorspoed Unknown	Unknown	Diopside HK	De Beers Collection
K5/9	Besterskraal North	Unknown	Type 2 HK	De Beers Collection
K5/34	Besterskraal North	Unknown	Type 1 HK	De Beers Collection
K5/35	Besterskraal North	Unknown	Type 1 HK	De Beers Collection

K5/30	Besterskraal North	Unknown	CRX-rich HK	De Beers Collection
K5/31	Besterskraal North	Unknown	CRX-rich HK	De Beers Collection
K5/32	Besterskraal North	Unknown	CRX-rich HK	De Beers Collection